A Structural and Economic Evaluation of Perpetual Pavements: A Canadian Perspective

by

Mohab El-Hakim

A thesis
presented to the University of Waterloo
in fulfillment of the
thesis requirement for the degree of
Doctor of Philosophy
in
Civil Engineering

Waterloo, Ontario, Canada, 2013

©Mohab El-Hakim 2013

AUTHOR'S DECLARATION

I hereby declare that I am the sole author of this thesis. This is a true copy of the thesis, including any required final revisions, as accepted by my examiners.

I understand that my thesis may be made electronically available to the public.

Abstract

Perpetual pavement design philosophy provides a long-life pavement design alternative. The ability of a pavement design to perform as long-life pavement is subjected to several technical constraints. Throughout the past 10 years, perpetual asphalt pavement designs have been under investigation in several parts of the world. The Canadian climate represents an additional challenge to the success of long-life pavement performance. This project investigated the construction and performance of three pavement test sections that were constructed on Highway 401 in Southern Ontario. The construction phase of this project was completed in 2010. The test sections were equipped with various sensors to monitor the structural performance. The test section included two perpetual pavement sections and one conventional pavement section. The two perpetual pavement designs were identical with the exception of the bottom asphalt layer, which was constructed as a Rich Bottom Mix (RBM) layer in one of the perpetual sections.

The three pavement sections were evaluated from a structural point of view through the analysis of the in-situ tensile strain collected from asphalt strain gauges installed at the bottom of asphalt layers under the wheel path. In addition, asphalt material laboratory characterization was undertaken by testing asphalt samples collected during construction of the three test sections. The laboratory testing was performed at the Centre for Pavement and Transportation Technology (CPATT) at the University of Waterloo. The laboratory experimental matrix in this research included dynamic modulus testing, resilient modulus testing and Thermal Stress Restrained Specimen Testing (TSRST). The correlation between various laboratory test results and the collected in-situ tensile strain was evaluated. Several

linear regression models were developed to correlate the laboratory test results and the field asphalt temperature with the in-situ tensile strain. Overall, it was found that the perpetual pavement with RBM section had the lowest tensile strain at the bottom of asphalt layers. Also, various models were developed that predict tensile strain at the bottom of asphalt layers by using laboratory test data.

An economic analysis was implemented to evaluate the perpetual and conventional pavement designs including a Life Cycle Cost Analysis (LCCA). Furthermore, a sustainability assessment for both design philosophies was executed to evaluate the environmental benefits of perpetual pavement designs.

The perpetual pavement designs were shown to provide many benefits over the conventional asphalt pavement designs for usage on Canadian Provincial and Interstate Highways in similar climatic zones with similar traffic loading. The advantages of perpetual pavement design philosophy are not limited to structural benefits, but also extended to economic and environmental benefits in the long term.

Acknowledgements

I would like to acknowledge the Natural Sciences and Engineering Research Council of Canada (NSERC), Ontario Hot Mix Producers Association (OHMPA) for funding this research project. Technical help and financial support was provided by Ministry of Transportation Ontario (MTO), the Centre for Pavement and Transportation Technology (CPATT), Stantec Ltd., McAsphalt Industries Lt. and Capital Paving Ltd.

I would like to thank my supervisor Professor Susan Tighe from the Civil and Environmental Engineering Department at the University of Waterloo as well as Dr. Khaled Galal from Stantec Ltd. for their guidance and encouragement throughout my research.

Several industry professional and colleagues assisted me with this research and I would like to extend my gratitude to them: Becca Lane, Joseph Ponniah and Warren Lee from the MTO, Mark Latyn from Capital Paving Ltd. for their guidance and assistance, Jodi Norris, Amin Hamdy, Andrew Northmore, Mohmed Hegazi, Doubra Ambaiowei, Vimy Henderson, Riyadh Ul-Islam, Shila Khanal, Rabiah Rizbi, Antonin Du Tertre and Peter Chan for their countless hours of assistance in the sensor installation at the test sections. Also special appreciation is extended to professors Ralph Haas, Carl Haas and Gerhard Kennepohl.

Dedication

I would like to dedicate this thesis to my parents and sister for supporting me throughout the years of my academic study and professional career. I would like to thank my adorable wife Manal and dear son Adam for their encouragement and reinforcement throughout my graduate studies. I wish to extend my dedication to my colleagues and friends in University of Waterloo and in Egypt for their endless support.

Table of Contents

AUTHOR'S DECLARATION ii
Abstract iii
Acknowledgements v
Dedication vi
Table of Contents vii
List of Figures x
List of Tables xiii
Chapter 1 Introduction 1
1.1 Background 1
1.2 Scope and Objective 2
1.3 Methodology 3
1.4 Organization of Thesis 4
Chapter 2 Literature Review 8
2.1 Introduction 8
2.2 Conventional Pavement Design 8
2.2.1 Empirical Pavement Design 9
2.2.2 Mechanistic Pavement Design 10
2.2.3 Mechanistic-Empirical Design Method 11
2.3 Perpetual Pavement Design 12
2.4 Tensile Strain in Flexible Pavement 18
2.5 Construction of Test Sections 24
2.5.1 Minnesota Road Research Project (Mn/Road) 25
2.5.2 Wisconsin Department of Transportation Pavement Testing 26
2.5.3 National Center for Asphalt Technology (NCAT) Test Track 28
2.5.4 Marquette Interchange Project 30
2.5.5 Shandong Province Test Section in China 33
2.5.6 Centre for Pavement and Transportation Technology (CPATT) Test Track 35
2.5.7 Highway 406 37
2.5.8 Red Hill Valley Parkway 37
2.6 Summary and Conclusion 39
Chapter 3 Construction and Instrumentation of the Test Section 41

3.1 Introduction 41
3.2 Location of the Test Sections 42
3.3 Pavement Sections 43
3.4 Location of the Sensors 46
3.5 Sensor Selection and Installation 49
3.5.1 Installation Infrastructure 50
3.6 Guelph Pavement Test Section 52
3.7 Summary and Conclusion 56
Chapter 4 Structural Evaluation 57
4.1 Introduction 57
4.2 In-Situ Tensile Strain 58
4.2.1 Guelph Test Section 67
4.3 Laboratory Testing Procedure, Results and Analysis 69
4.3.1 Resilient Modulus 71
4.3.2 Dynamic Modulus 74
4.3.3 Thermal Stress Restrained Specimen Test (TSRST) 87
4.4 Analysis of Fatigue Endurance Limit 91
4.5 Modeling of Field Strain and Laboratory Testing 92
4.5.1 Regression Analysis 94
4.5.2 Model for Perpetual Pavement with RBM 95
4.5.3 Model for Perpetual Pavement without RBM 103
4.5.4 Model for Conventional Pavement 107
4.5.5 Model for Both Perpetual Pavement Sections 112
4.5.6 Key Findings from Model Development 116
4.6 Summary and Conclusion 117
Chapter 5 Economic Evaluation and Sustainability Assessment 119
5.1 Introduction 119
5.2 Economic Analysis 119
5.2.1 Design of Maintenance Programs 121
5.2.2 Life-Cycle Cost Analysis 126
5.3 Sustainability Assessment 129
5.3.1 Greenroads 131

5.3.2 GreenPave 132
5.4 Summary and Conclusion 134
Chapter 6 Research Impact on Pavement Engineering 136
6.1 Pavement Engineering 136
6.2 Case Study - RAS 140
6.3 Case Study – Warm Mix 145
6.4 Case Study – In-Situ Strain Prediction 147
6.4.1 Calculation of the Correction Factor 148
6.5 Summary 154
Chapter 7 Conclusions and Recommendations 155
7.1 Conclusions 155
7.2 Recommendations 157
7.3 Major Contributions 159
References 161
Appendix A 174
Appendix B 175
Appendix C 205

List of Figures

Figure 1-1: Organization of the Thesis 7
Figure 2-1: Perpetual Pavement Design Concept [Newcomb, 2001] 16
Figure 2-2: Three-Layer System for Strain Calculation [Yoder, 1975] 19
Figure 2-3: Three Components of Strain for Burgers Model [Huang, 2004] 23
Figure 2-4: Mechanical Models for Viscoelastic/Viscoplastic Materials [Huang, 2004] 24
Figure 2-5: Mn/Road Site Map [MNDOT, 2001] 26
Figure 2-6: Wisconsin Perpetual Pavement Test Section 27
Figure 2-7: NCAT Test Track Layout [Pave Track, 2009] 29
Figure 2-8: NCAT Perpetual Pavement Cross-Section 30
Figure 2-9: HMA Perpetual Pavement Structure [Crovetti, 2008] 31
Figure 2-10: Marquette Interchange Instrumentation Layout [Hornyak, 2007] 31
Figure 2-11: Dynamic Modulus Master Curve for Marquette Interchange Section [Crovetti, 2008] .. 32
Figure 2-12: Perpetual Pavement Sections in China 34
Figure 2-13: Measured Strain Comparison for China Test Sections [Timm, 2011] 35
Figure 2-14: Flexible Pavement Portion of the CPATT Test Track after [Ul-Islam, 2010] 36
Figure 2-15: Perpetual and Deep Strength Conventional Sections of the Red Hill Valley Parkway Project [Uzarowski, 2008] 38
Figure 3-1: Project Location Overview [Google Earth, 2008] 43
Figure 3-2: Cross-Section of Perpetual Pavement with RBM 45
Figure 3-3: Cross-Section of Perpetual Pavement without RBM 45
Figure 3-4: Cross-Section of Conventional Pavement 46
Figure 3-5: Plan and Cross-Section for the Perpetual Pavement Section with RBM 47
Figure 3-6: Plan and Cross-Section for the Perpetual Pavement Section without RBM 48
Figure 3-7: Plan and Cross-Section for the Conventional Pavement Section 49
Figure 3-8: Steel Conduit Used for Cable Crossing. 50
Figure 3-9: Paving Marking Prior to Open Trench Excavation 51
Figure 3-10: Conduit Installation 51
Figure 3-11: PVC Tubes Inside the Steel Conduit 52
Figure 3-12: Plan of the Guelph Capital Paving Inc. Section 53
Figure 3-13: Longitudinal Cross-Section of the Guelph Test Section 53
Figure 3-14: Transverse Cross-Section of the Guelph Test Section 54

Figure 3-15: Opening the Trench to Construct the Perpetual Pavement Section 54
Figure 3-16: Preparation for ASG Installation on Top of Granular A 55
Figure 3-17: Installation of ASG at the Bottom of RBM Layer 55
Figure 4-1: Monthly 90th Percentile of Tensile Strain in Highway 401 Test Sections 60
Figure 4-2: 90th Percentile of Cumulative Tensile Strain in Perpetual Pavement Sections 64
Figure 4-3: 90th Percentile of Cumulative Tensile Strain in Conventional Pavement Section 66
Figure 4-4: Monthly 90th Percentile of Tensile Strain in Guelph Test Section 68
Figure 4-5: 90th Percentile of Cumulative Tensile Strain in Guelph Test Section 69
Figure 4-6: Master Curve Theory 76
Figure 4-7: Master Curve for all Four Mixes 77
Figure 4-8: Master Curve for Superpave 12.5 Mix 82
Figure 4-9: Master Curve for Superpave 19 Mix 82
Figure 4-10: Master Curve for Superpave 25 Mix 83
Figure 4-11: Master Curve for Superpave 25 RBM Mix 84
Figure 4-12: TSRST Result for SP 12.5 88
Figure 4-13: TSRST Result for SP 19 88
Figure 4-14: TSRST Result for SP 25 89
Figure 4-15: TSRST Result for SP 25 RBM 90
Figure 4-16: Interpolation to Determine the Dynamic Modulus Value at 15ºC 97
Figure 4-17: Residual Plot for Pavement Age 100
Figure 4-18: Residual Plot for Dynamic Modulus at the Construction Year 101
Figure 4-19: Residual Plot for Dynamic Modulus after One Year of Construction 101
Figure 4-20: Residual Plot for Temperature 101
Figure 4-21: Validation of the Perpetual Pavement with RBM Model 102
Figure 4-22: Residual Plot for Pavement Age 105
Figure 4-23: Residual Plot for Dynamic Modulus at the Construction Year 105
Figure 4-24: Residual Plot for Dynamic Modulus after One Year of Construction 106
Figure 4-25: Residual Plot for Temperature 106
Figure 4-26: Validation of the Perpetual Pavement without RBM Model 107
Figure 4-27: Residual Plot for Pavement Age 110
Figure 4-28: Residual Plot for Dynamic Modulus at the Construction Year 110
Figure 4-29: Residual Plot for Dynamic Modulus after One Year of Construction 110

Figure 4-30: Residual Plot for Temperature 111
Figure 4-31: Validation of the Conventional Pavement Model 111
Figure 4-32: Residual Plot for Pavement Age 114
Figure 4-33: Residual Plot for Dynamic Modulus at the Construction Year 114
Figure 4-34: Residual Plot for Dynamic Modulus after One Year of Construction 115
Figure 4-35: Residual Plot for Temperature 115
Figure 4-36: Residual Plot for TSRST Failure Temperature 115
Figure 4-37: Validation of Both Perpetual Pavement Models 116
Figure 5-1: Bottom-Up Cracking Damage 122
Figure 5-2: Rutting prediction in Conventional and Perpetual Design 123
Figure 5-3: International Roughness Index (IRI) Model Results 124
Figure 6-1: Flow Chart for the Application of Tensile Strain Models in Pavement Engineering 139
Figure 6-2: Pavement One: Perpetual Pavement Section with RBM 141
Figure 6-3: Pavement Two: Perpetual Pavement Section with RAS and RAP 141
Figure 6-4: Predicted Tensile Strain for the Original and Modified Perpetual Pavement Sections Using the Model 144
Figure 6-5: Tensile Strain in Perpetual Pavement with RBM and Perpetual Pavement with Warm Mix Asphalt and RBM 146
Figure 6-6: Pavement Section for the Case Study 147
Figure 6-7: Conventional Pavement Inputs for WESLEA 148
Figure 6-8: Load Configuration for the Mechanistic Calculation of Tensile Strain in Conventional Pavement 149
Figure 6-9: Output from WESLEA 150
Figure 6-10: Calculation of Mechanistic Strain in the Case Study 153
Figure 6-11: Output of WESLEA 153

List of Tables

Table 2-1: Dynamic Modulus Values for HMA Layers at 21ºC and 1 Hz 32
Table 2-2: Summary of Asphalt Mix Mechanistic Properties Testing 38
Table 4-1: Number of Laboratory Tested Samples and Sensors Installed on Site 57
Table 4-2: t-test comparing Monthly 90th Percentile of Tensile Strain in Perpetual Sections 61
Table 4-3: t-test Comparing Monthly 90th Percentile of Tensile Strain in Perpetual without RBM and Conventional Sections 62
Table 4-4: t-test Comparing Monthly 90th Percentile of Tensile Strain in Perpetual with RBM and Conventional Sections 63
Table 4-5: t-test for 90th Percentile of Cumulative Tensile Strain in Perpetual Designs 66
Table 4-6: Summary of Asphalt Mix Design 70
Table 4-7: Indirect Strength and Air Voids for Different Mixes 72
Table 4-8: Resilient Modulus Results (MPa) 73
Table 4-9: Summary of Resilient Modulus (MPa) 73
Table 4-10: Average Dynamic Modulus Results (MPa) at the Year of Construction 78
Table 4-11: Average Dynamic Modulus Results (MPa) after One Year of Construction 79
Table 4-12: t-test for Dynamic Modulus Average for SP 25 and SP 25 RBM at 37ºC and 54ºC 80
Table 4-13: Results of t-test Performed for Different Mixes 85
Table 4-14: Result of t-test Comparing SP 25 and SP 25 RBM 86
Table 4-15: Result of TSRST for Different Asphalt Mixes 90
Table 4-16: ANOVA Table for the Model of Perpetual Pavement with RBM 99
Table 4-17: P-Value for Various Parameters of the Perpetual Pavement with RBM Model 100
Table 4-18: ANOVA Table for the Model of Perpetual Pavement without RBM 104
Table 4-19: P-Value for Various Parameters of the Perpetual Pavement without RBM Model 104
Table 4-20: ANOVA Table for the Model of Conventional Pavement 109
Table 4-21: P-Value for Various Parameters of the Conventional Pavement Model 109
Table 4-22: ANOVA Table for the Model for Both Perpetual Pavements 113
Table 4-23: P-Value for Various Parameters for Both Perpetual Pavement Model 114
Table 5-1: Maintenance Schedule of Conventional Design 125
Table 5-2: Maintenance Schedule of Perpetual Design 126
Table 5-3: Construction Cost of Conventional Pavement Design 128
Table 5-4: Construction Cost of Perpetual Pavement Design 128

Table 5-5: Credit Distribution of Greenroads [Muench, 2010] 132
Table 5-6: Credit Distribution for GreenPave [Kazmierowski, 2012]..... 133
Table 5-7: Levels of Certification in GreenPave 133
Table 6-1: Dynamic Modulus Results for Alternative Surface and Intermediate Layers 143
Table 6-2: Dynamic Modulus Results for WMA..... 145
Table 6-3: Calculation of the 90^{th} Percentile of Tensile Strain Using the Developed Model 151
Table 6-4: Correction Factor Calculation 152

Chapter 1
Introduction

1.1 Background

The quality of the transportation network has a significant impact on a country's living standards and level of development. The construction of reliable, well-functioning transportation networks is essential for the achievement of a high standard of living and for the support of economic growth and social development. The greater part of the Canadian transportation system is comprised of ground transportation and road networks. According to Transport Canada, 73 % of Canadians commute to work in their vehicles, and another 7 % of employees use buses as their main mode of transportation. In addition, 41 % of Canadian freight is transported by truck over the Canadian highway and road system [Transport Canada, 2010]. Given this level of use, the condition of highway and road pavement plays a vital role in facilitating the social and economic development of Canada. According to a 2011 survey conducted by Statistics Canada, with 38 % of the total Canadian population, the province of Ontario has the highest population density [Statistics Canada, 2011], and its highways and roads serve more vehicles than do those of any other province. The associated heavy loads cause extensive deterioration of the pavement, especially on highways and freeways.

The expansion of the Canadian highway network has led to an increased consumption of high-quality aggregates and construction materials. Frequent highway maintenance and rehabilitation also create additional financial burdens and elevate pollution levels. These factors have the potential to compromise the ability of future generations to meet the

demands associated with the transportation network and have led to the exploration of long-life pavement designs. With the collaboration of active partners in the highway construction industry, this research project was undertaken in order to assess the possibility of improving pavement structure through the use of perpetual asphalt pavement designs and to evaluate the associated financial implications.

Canadian investment in highway maintenance and rehabilitation rose from $4.3 billion in 1998 to $7.3 billion in 2005 [Roy, 2008]. The trade-off between the cost of the initial construction of the roads and subsequent maintenance expenditures is a key element in the choice of an adequate alternative for road construction and management. This thesis focuses on the evaluation of perpetual asphalt pavement design, particularly in comparison with conventional asphalt pavement. This research focuses on the structural and economic evaluation of this design and will provide insight for decision makers and practicing engineers in the pavement industry.

1.2 Scope and Objective

The scope of this research project involves the evaluation of the perpetual pavement design in the Canadian context and its comparison with conventional pavement design. The research is based on a unique Canadian case study, which enables consideration of the severe impact of the year-round environmental conditions that affect pavements in Canada.

The Ministry of Transportation of Ontario (MTO), Ontario Hot Mix Producers Association (OHMPA), the Natural Science and Engineering Research Council of Canada (NSERC), Stantec Lt., McAsphalt Industries Ltd., Capital Paving, and Aecon collaborated with the

University of Waterloo Centre of Pavement and Transportation Technology (CPATT) in this research project. The methodology of assessment involved the development of a structural and economic assessment protocol for both conventional asphalt pavement design and perpetual pavement designs.

The structural evaluation involved interpretation and assessment of in-situ measurements of the structural parameters and performance indicators over time. For both the perpetual pavement and conventional designs, indicators of structural performance that reflect long-term structural deterioration were selected, and the economic evaluation was based on construction cost estimations and an assessment of maintenance and rehabilitation costs. To ensure the applicability of the economic evaluation, the cost estimations were based on local Ontario market prices.

1.3 Methodology

Based on the research scope and objectives, a scientific methodology was developed for the overall evaluation of the perpetual and conventional pavement designs. The methodology included the construction of three test sections on Highway 401 and their instrumentation with sensors in order to capture the parameters that would reflect the structural condition of the pavement. Two of these sections were perpetual pavement sections, designed and constructed as a means of determining the benefits of using a rich mix layer at the bottom of the perpetual pavement asphalt layers. A control mix was also designed and used to construct a conventional pavement section. All three test sections were equipped with asphalt strain gauges, earth pressure cells, thermistor strings, and moisture probes. The instrumentation of

a variety of sensors produced the data required for the completion of the structural evaluation and the development of regression models for calculating the tensile strain at the bottom of the asphalt layers. The tensile strain results were used as the key performance indicator reflecting the ability of the pavement design to resist fatigue cracking.

The economic aspects of the pavement designs were evaluated using the costs provided by the main contractor responsible for the construction of the test sections. A maintenance and rehabilitation program was also created for each pavement design so that a life-cycle cost analysis (LCCA) could be conducted. The maintenance and rehabilitation programs were based on a long-term model developed for the Mechanistic-Empirical Pavement Design Guide (MEPDG) and on the recommendations of the MTO regarding best practice maintenance and preservation programs for similar pavement designs. The costs associated with maintenance activities were determined based on both feedback from Ontario contractors or the provincial average costs of maintenance activities provided by the MTO.

1.4 Organization of Thesis

The thesis is comprised of seven chapters, with figures and tables supporting the information provided in the text. To demonstrate specific trends in the data, the figures provide visual representations of the data presented in the corresponding tables.

Chapter 1 explains the scope and objectives of the research project and summarizes the methodology applied in order to achieve the objectives.

Chapter 2 provides an extensive review of the literature related to the main thesis topics, with the intent of furnishing a solid background for readers from other majors or disciplines. This chapter covers the methods available for conventional pavement design and details the

assumptions and constraints associated with perpetual pavement design. Also included is an explanation of the methods and theories related to the calculation of tensile strain in pavement sections and a description of the best-known examples of research test sections that have been constructed both in North America and elsewhere.

Chapter 3 details the location of the three test sections, the cross-sections of the pavement, the construction stages, the infrastructure built for the instrumentation, and the types of sensors installed in the three sections. The construction of a fourth complementary test section as part of this research at the asphalt plant owned by Capital Paving Inc. in Guelph, Ontario, is also described.

Chapter 4 provides the results of the laboratory testing of the samples collected from the Highway 401 project. The tests were conducted at the Centre for Pavement and Transportation Technology (CPATT). The laboratory results were analyzed, and statistical analyses were then conducted in order to validate the comments and conclusions that stemmed from the test results. This chapter also contains a summary of the field data collected from the sensors installed in the Highway 401 sections along with an explanation of the development of regression models for correlating the laboratory test results with the in situ tensile strain field measurements.

Chapter 5 presents the economic evaluation of the perpetual and conventional pavement designs, including the determination of the construction cost of a unit length of each design. A long-term structural evaluation MEPDG model is introduced, the results of which formed the basis for the design of an appropriate maintenance and rehabilitation program. To perform an LCCA, the construction costs and the costs associated with the maintenance and

rehabilitation program were combined in order to calculate a net present value (NPV) for both the perpetual and the conventional designs. In addition, the sustainability of perpetual pavement designs is introduced in this chapter.

Chapter 6 represents some practical applications for the findings of this thesis. This chapter includes three practical examples for direct application of the findings in pavement engineering.

Chapter 7 contains the conclusions and recommendations based on the research conducted for this thesis and highlights the main contributions of this work.

Figure 1-1 presents an overflow chart explaining the relationship between various Chapters in this thesis.

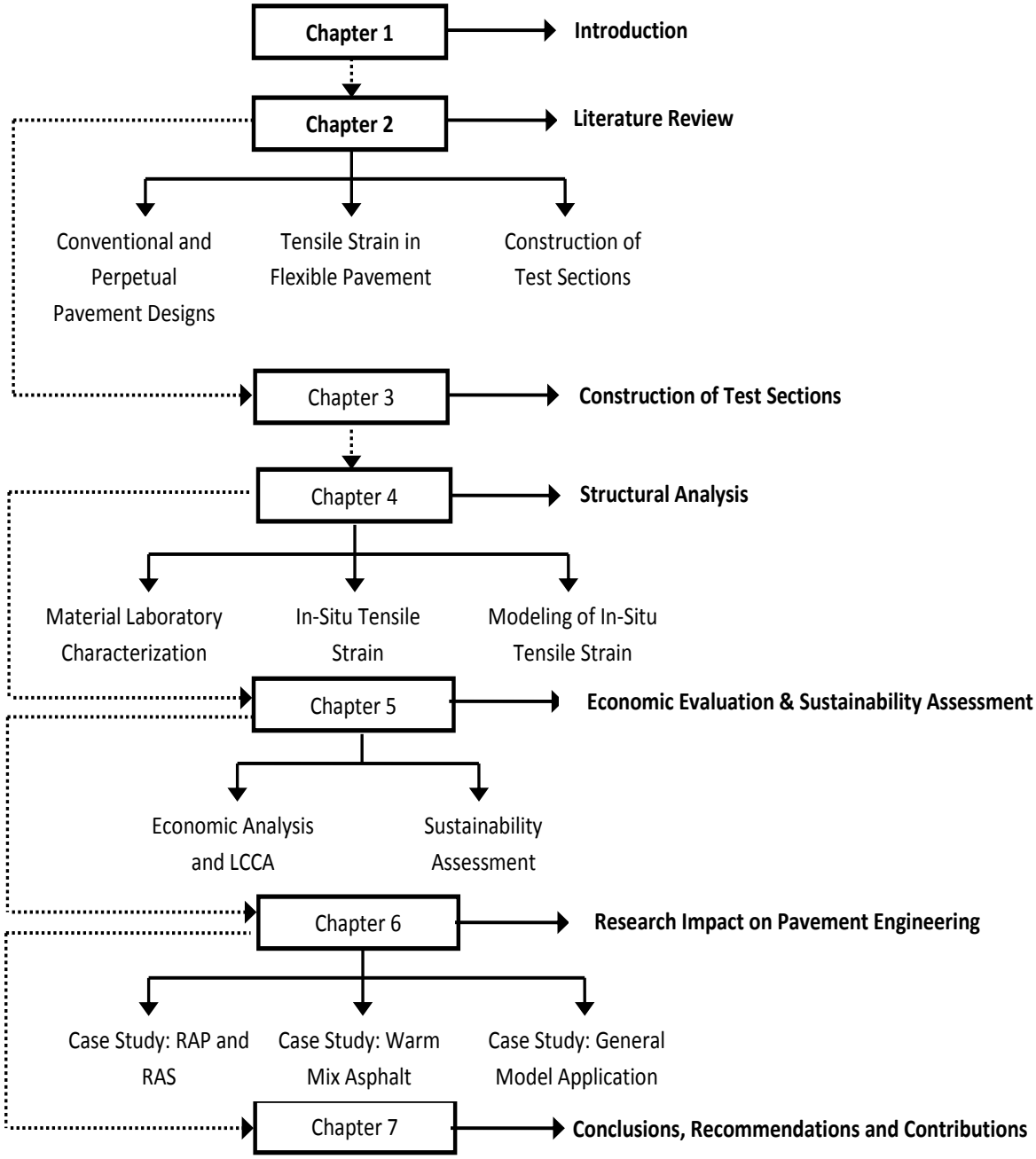

Figure 1-1: Organization of the Thesis

Chapter 2
Literature Review

2.1 Introduction

The research presented in this thesis involved the construction of test sections, the instrumentation and installation of sensors, laboratory testing, and the analysis of the laboratory testing results and the field data. Meeting the research objectives and ensuring that every stage of the project was implemented based on state-of-the-art technology required an extensive literature review, which is presented in the three main sections of this chapter. The first section introduces perpetual and conventional pavement design concepts and highlights the main points of difference. The second section covers methods of calculating strain in asphalt pavement, with an explanation of the theories and models that have been reported in the literature. The third section is an exploration of the construction of research-oriented test sections in North America and worldwide as well as a review of the methods of sensor selection, construction, and instrumentation that facilitated the construction of the test sections on Highway 401.

2.2 Conventional Pavement Design

This section presents historical background about theories and conventional methodologies of pavement design.

The history of pavement design comes back to the Roman Empire era. However, the modern asphalt pavement design based on scientific theories started in the mid 1800s [Hubbard, 1910]. Construction of an asphalt layer on top of a concrete base foundation was the popular

recipe during the mid 1800s. The typical wearing surface was constructed as 40 to 50 mm thick and composed of bitumen and sand. The typical binder layer consisted of broken stones and bitumen. The base layer was constructed as a cement concrete layer of 100 to 150 mm thick [Baker, 1903]. The main asphalt binder supplier in the late 1800's was Trinidad. The flexible pavement structural design was based on experience up to the 1920s. The reasons for depending on experience in asphalt pavement design could be illustrated as [Public Roads Administration, 1949]:

- Experience based method resulted in satisfactory results.
- Lack of basic scientific knowledge was a barrier from developing a more reliable structural design method.

The first attempt to develop an empirical structural flexible pavement design procedure was undertaken in 1939 [Gary, 1939]. Most of the empirical pavement design procedure, developed by Gary, was based on Boussinesq theory of load distribution.

2.2.1 Empirical Pavement Design

The development of empirical pavement design was initialized by the American Association of State Highways and Transportation Officials (AASHTO). The construction of the AASHTO Test Road in Illinois was accomplished in the 1950s. This test section was used to develop empirical equations to design the appropriate thickness of pavement layers. The disadvantages of this test section included the limited traffic loads as it was a closed-loop test section. In addition, the test section was subjected to the environmental impact of the climate

in Illinois only. Therefore, limitations existed when applying the empirical equations developed from this test section to design pavement thickness in other regions [Small, 1988].

The latest empirical pavement design guide was developed by the AASHTO in 1993. This design guide is used worldwide to implement flexible pavement designs. Several municipalities and Departments of Transportation (DOTs) are still following the AASHTO 1993 design guide to pursue pavement designs [Haas, 1997, Tighe 2012].

The empirical AASHTO 1993 design method introduced a way to calculate the structural number required to carry the traffic over the soil conditions. The structural number was then converted to layer thickness using empirical layer coefficients that reflected the material contribution to the structural strength of the pavement. The AASHTO 1993 design guide provided charts to determine the pavement thickness graphically and an equation to determine the structural number numerically.

2.2.2 Mechanistic Pavement Design

In the later portion of the 1900s, new materials and design philosophies were introduced in asphalt pavement structures. The noticeable advancement in basic scientific knowledge facilitated the development of new design criteria. The mechanistic design theory was based on calculating stress, strain and deflection using the linear elastic model. Several mechanistic pavement design methods were developed as Asphalt Institute method in 1982 and in 1991, and Shell Method in 1982 [Asphalt Institute 1982, Asphalt Institute 1991, Shook et al. 1982].

The mechanistic pavement design method depends on mechanical and physical characteristics to calculate performance indices. In addition, the mechanical properties of

visco-elastic/visco-plastic materials are sensitive to temperature change. Therefore, the mechanistic models for asphalt pavements are of high complexity.

2.2.3 Mechanistic-Empirical Design Method

The Mechanistic-Empirical design method was introduced to overcome the shortfalls of pure mechanistic and pure empirical design methods. It attempts to merge the best attributes of both design methods; the Mechanistic-Empirical method combines the two methods by calculating the tensile strain, stress and deflection using the mechanistic models. The calculated mechanistic properties are then converted to practical structural condition indices as the percentage of longitudinal cracking, percentage of alligator cracking, rutting depth and International Roughness Index (IRI). The process of transferring the mechanistic properties to the performance indices is executed using transfer functions. The transfer functions are determined using empirical methods. In addition, other empirical functions are developed to predict the future value for the structural condition indices (for example, longitudinal cracking, transverse cracking, fatigue cracking, rutting and IRI). The prediction of pavement structural deterioration in the future is a complicated process and depends on several factors as the traffic pattern and growth, climate impact, material deterioration and the accuracy of the transfer functions.

The first attempt to develop a Mechanistic-Empirical Pavement Design Guide (MEPDG) was successful in 2002. The software developed by the National Cooperative Highway Research Program (NCHRP) project 1-37A was investigated by several municipalities and DOTs in North America and worldwide [Schwartz, 2007]. The investigations executed by various

DOTs resulted in a local calibration for several states in order to develop MEPDG models that represent the actual structural deterioration in the states. However, several technical deficiencies were noted on the accuracy of transfer functions and specifically on the thermal cracking model [Zborowski, 2007]. Further research was implemented to update the MEPDG transfer functions and reach a more accurate and precise pavement design method. The second version of the Mechanistic-Empirical design guide was issued, in 2011, under the name of DARWin-ME. Although the MEPDG was offered for free on the Transportation Research Board (TRB) website, the new version entitled DARWin-ME was not offered as a free source. The investigation of the accuracy and precision of the DARWin-ME is currently underway in several Canadian Provinces and DOTs. The Transportation Association of Canada (TAC) has a working group to assess how it can be calibrated and implemented [Tighe, 2012]. The Mechanistic-Empirical design method is the state-of-the-art in the pavement design theories. However, further research and investigation is required to improve the accuracy of this method.

2.3 Perpetual Pavement Design

A perpetual pavement structure should have unique mechanical and physical characteristics that lead to long-term performance. The Washington State Department of Transportation defined several conditions that qualify a pavement for consideration as perpetual. It should be designed for a 50-year structural design life; its wearing course should be designed for 20 years design life; its layers should be specifically designed so that all distresses occur in the top surface course layer, with the result that the primary maintenance activity expected

throughout the design life would be mill and overlay rehabilitation [Mahoney, 2001, Newcomb, 2001].

The design theory behind perpetual pavement is that distresses are limited to top-down cracking in the top asphalt lift, which is designed as a high-quality Hot Mix Asphalt (HMA) layer [Thompson, 2006, Newcomb, 2006]. The pavement structural integrity is maintained throughout the service life by milling and overlaying, plus patching when surface cracks are observed. Cracks must be repaired in order to limit the roughness of the pavement, to increase skid resistance, to enhance tire-pavement interaction, and to reduce noise [Newcomb, 2001, Battaglia, 2010]. The lower HMA layers are designed to resist fatigue cracking and permanent deformation. The structural performance of perpetual pavement is a function of traffic loads, speed, climate, subgrade and pavement parameters, materials, quality of construction, pavement compaction, and the quality of maintenance [Von Quintus, 2001, Walubita, 2008]. Perpetual pavement is expected to provide long-life performance because the maximum tensile strains at the bottom of the HMA are limited, as is the vertical strain at the top of the subgrade [APA, 2002, Al-Qadi, 2008, Merrill, 2006].

A number of research projects have been implemented in order to estimate the maximum allowable strain at the bottom of the HMA while still avoiding fatigue cracking. The earliest investigation of the maximum tensile strain prior to fatigue cracking was performed by Monismith in the early 1970s. Monismith's initial estimation of the allowable tensile strain in asphalt was 70 με [Monismith, 1972]. Other research conducted by Nishizawa in Japan resulted in the conclusion that 200 με is the allowable limit without subjecting the asphalt pavement to fatigue cracking [Nishizawa, 1997]. This study was based on in-service

pavements. Strain levels of 96 to 158 με have also been predicted based on backcalculated stiffness data collected using Falling-Weight Deflectometer (FWD). This type of estimation was reported by Wu with respect to the bottom asphalt layer installed for a long-lasting asphalt project on the Kansas Turnpike [Wu, 2004]. Prowell predicted the maximum allowable tensile strain using a beam fatigue test in 2006; based on his observations, he concluded that 100 με would be a reasonable endurance limit. A test matrix was developed for Superpave (SP) designs with performance grade (PG) 64-22 binder material and optimum binder content [Prowell, 2006]. In short, for asphalt pavement, the determination of maximum allowable tensile strain to avoid fatigue cracking has been investigated through a number of research projects worldwide, but no accurate and definitive value has been proven to represent the maximum allowable strain. However, for design purposes, most scientists and practitioners experienced in the field of perpetual pavement agree on a value of 70 με as the maximum allowable tensile strain and a value of 200 με for the maximum vertical compressive strain on the top of the subgrade. The state-of-the-art perpetual pavement design software is PerRoad. This software utilizes Monte Carlo simulation to fulfill the design constrains of perpetual pavement design [Timm, 2006].

The concept of determining a thickness limit for asphalt pavement was analyzed by Nunn in 1997 [Nunn, 1997]. Nunn estimated an asphalt pavement thickness limit through a number of methods; his results were based on the properties of the material used in the research, the type of subgrade, and the environmental conditions. Nunn reported that 390 mm of asphalt pavement was sufficient for perpetual pavement performance in the United Kingdom and that fatigue cracking could be noticed on roads with less than 200 mm of asphalt thickness

within the 40-year design limit [Nunn, 2001]. Some states propose perpetual pavements as thick as 510 mm [Gierhart, 2008] while others have seen distress limited to surface cracking in pavements as thin as 160 mm [Walubita, 2008]. The conclusion seems to be that exceeding the asphalt pavement thickness limit has no significant effect on the structural performance or design life of the pavement.

Merrill reported that crack development and propagation would start to change from full-depth or fatigue cracking to top-down cracking within the range of 170 mm to 200 mm [Merrill, 2006]. Another investigation showed that 270 mm of thickness for asphalt pavement would provide a stiff structure capable of resisting fatigue cracking, while 180 mm structures would result in little deformation over time [Rolt, 2001]. Al-Qadi noticed a significant increase in strain when pavement thickness was reduced below 255 mm and recommended a 345 mm thickness for perpetual pavement designs [Al-Qadi, 2008].

Pavement thickness alone, however, is no guarantee of the long service life or perpetual performance of an asphalt pavement. The Washington State Department of Transportation determined that, in Washington, in many cases, pavements that exhibited shorter life cycles were thicker than conventional or traditional pavement designs [Mahoney, 2001]. Throughout the past decades, several studies have been conducted in order to prove that the magnitude of reduction in tensile strain at the bottom of HMA layers depends not only on an increase in HMA thickness, but also on the design of the asphalt mix [Romanoschi, 2008].

A common theme related to the design of a section of HMA perpetual pavement is that consideration should be given to designing each layer in the cross-section of the pavement in

a way that will fulfill the following conditions [Harm, 2001, Newcomb, 2001, Gierhart, 2008]:

1- Construct the pavement section over a sound subgrade. Soil stabilization and treatment can enhance the structural capacity of the subgrade.

2- Assemble a fatigue-resistant HMA base layer that will resist bottom-up fatigue cracking. This layer needs to be flexible enough to withstand freeze-thaw cycles without cracking.

3- Install a rut-resistant intermediate HMA layer that will keep rutting deterioration values within acceptable limits throughout the life of the pavement.

4- Apply a renewable surface course designed to maintain skid resistance, reduce tire-pavement interaction noise, and provide surface drainage over the slope of the road.

Figure 2-1 presents the perpetual pavement design concept and its applicability on the various pavement layers.

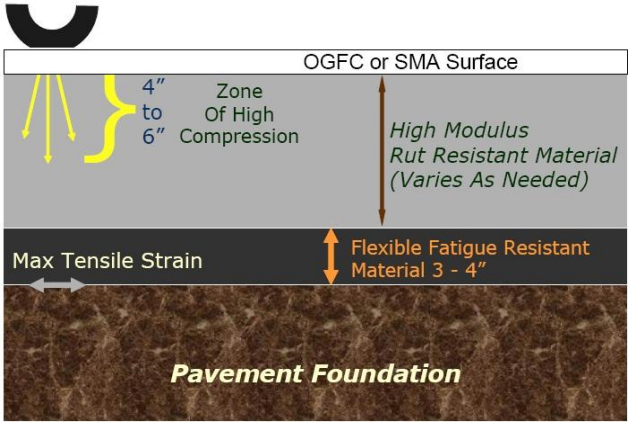

Figure 2-1: Perpetual Pavement Design Concept [Newcomb, 2001]

The design of a fatigue-resistant base layer should incorporate a soft binder, higher binder content, and a high-quality aggregate. This composition increases the flexibility of the asphalt and eliminates the development of cracks when the pavement is subjected to traffic loading and freeze-thaw cycles. Rich Bottom Mix (RBM) layers contain above-optimum binder content and have shown superior resistance to fatigue cracking [APA, 2002, Yang, 2005, Harm, 2001, Willis, 2009]. RBM layers also reduce susceptibility to moisture and enhance field compaction because they decrease in-place air voids in the field from 7.0 % to less than 6 % [Harm, 2001].

With the use of the new Superpave design methodology to produce a stable and durable layer, the intermediate layer is designed to be rut resistant. The stability of the asphalt mix is created by the stone-on-stone contact in the coarse aggregates. This layer should exhibit unique features: it is usually characterized by larger nominal maximum-sized aggregates to increase the internal friction of the mix [APA, 2002, Gierhart, 2008]. An appropriate high-temperature grade of asphalt binder enhances the durability of the asphalt mix and should be equivalent to a surface grade in order to prevent structural rutting.

The wearing surface layer is designed to withstand traffic and environmental conditions. It should be rut resistant and free of surface cracking while offering reliable surface drainage to reduce splash and spray. The surface course is designed as a dense-graded Superpave mix, a stone matrix asphalt (SMA), or an open-graded friction course (OGFC). OGFC is not recommended for the Canadian climate because the weather and freeze-thaw cycles limit its expected lifespan. SMA, however, is anticipated to provide enhanced long-term

performance, and a dense-graded Superpave mix is also an acceptable option [Harm, 2001, Uzarowski, 2012].

2.4 Tensile Strain in Flexible Pavement

Critical tensile strain prediction is a key element in perpetual pavement design. The methods of estimating tensile strain at certain depths of asphalt pavement vary in complexity and accuracy. The first theory to calculate tensile strain was introduced by Boussinesq in 1885 [Boussinesq, 1885]. The theory was based on concentrated load applied on an elastic space. In 1945, Burmister introduced the two-layer theory to calculate the stress, strain and deflection assuming the materials of each layer are homogeneous, isotropic, elastic and satisfy Hooke's law. In addition, the second layer is assumed to be of infinite thickness. Burmister's theory assumed no slippage and frictionless interface between the two layers [Mings, 1993]. An attempt to overcome the shortages in Burmister's theory was executed by Huang in the early 1970's. However, Huang neglected the viscoelastic properties of asphalt material. Charts for estimating tensile strain at the bottom of the asphalt layer in a 2-layer system were developed using Huang's model. The estimation of critical strain depended on a strain factor (F_e). The strain factor could be determined from Huang charts for single wheel loading [Huang, 1973]

$$e = \frac{q}{E_1} F_e \qquad (2\text{-}1)$$

where (e) is the maximum strain, (q) is the load intensity, E_1 is elastic modulus of top layer and F_e is a strain factor.

Huang also proposed charts to convert dual wheel loads to an equivalent single wheel load using the ratio between dual spacing (S_d) and tire-pavement contact radius (a). Also the ratio

between elastic modulus of the upper layer (E_1) and that of lower layer (E_2) affects conversion factors [Huang, 1973]. Similar charts were proposed by Huang for converting dual-tandem axle wheel loads to single wheel loads. Tandem spacing (S_t) is an additional factor that affects the conversion process [Huang, 1973].

A three-layer system to predict vertical and tangential strain values was explained by Yoder where [Yoder, 1975]:

$$\varepsilon_z = \frac{1}{E}(\sigma_z - \sigma_r) \tag{2-2}$$

$$\varepsilon_r = \frac{1}{2E}(\sigma_r - \sigma_z) \tag{2-3}$$

and ε_z and ε_r are the vertical and tangential strain values respectively. σ_z and σ_r are the vertical and tangential stresses, respectively, and E is the elastic modulus.

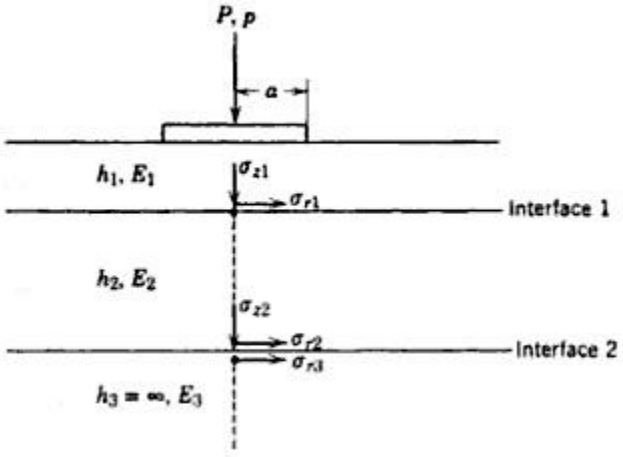

Figure 2-2: Three-Layer System for Strain Calculation [Yoder, 1975]

A series of tables and charts for determining the vertical and tangential stresses of the three-layer system were presented by Jones in 1962 [Jones, 1962].

Viscoelastic properties of asphalt material were considered in more recent strain calculation models.

Basic elastic materials obey Hooke's law which proves that stress is proportional to strain.

$$\sigma = E\varepsilon \qquad (2\text{-}4)$$

where σ is the stress in ton/m^2, ε is the strain and E is the elastic modulus in kPa.

Viscous materials follow Newton's law, which assumes that stress is proportional to the time rate of strain.

$$\sigma = \lambda \frac{\partial \varepsilon}{\partial t} \qquad (2\text{-}5)$$

where λ is the viscosity, σ is the stress and t is time. Under constant stress, the strain can be calculated as:

$$\varepsilon = \frac{\sigma t}{\lambda} \qquad (2\text{-}6)$$

where ε is the strain, λ is the viscosity, σ is the stress and t is time.

Since asphalt is a visco-elastic/ visco-plastic material, the strain calculation in asphalt is a combination of the strain in elastic materials (Hooke's law) and the strain in viscous materials (Newton's law). The simplest strain prediction model for visco-elastic materials was introduced by Maxwell's model. This model assumed the elastic and plastic strain occurring in series in asphalt pavement [Huang, 2004]:

$$\varepsilon = \frac{\sigma}{E_o} + \frac{\sigma t}{\lambda_o} = \frac{\sigma}{E_o}\left(1 + \frac{t}{T_o}\right) \qquad (2\text{-}7)$$

Here $T_o = \frac{\lambda_o}{E_o}$ = relaxation time, E_o is the instantaneous modulus of elasticity in Maxwell's model, λ_o is the viscosity in Maxwell's model, σ is the stress, ε is the strain and t is the loading time. If an initial stress is applied instantaneously to the model, an instantaneous strain ($\frac{\sigma_o}{E_o}$) will be applied to the model. If strain is kept constant, the stress will gradually decrease reaching a negligible value or zero. By integrating equation (2-7) with respect to time we can deduce:

$$\frac{\partial \varepsilon}{\partial t} = \frac{1}{E_o}\frac{\partial \sigma}{\partial t} + \frac{\sigma}{\lambda_o} \qquad (2\text{-}8)$$

If strain is constant over time, $\frac{\partial \varepsilon}{\partial t} = 0$, thus:

$$\sigma = \sigma_o \exp\left(-\frac{t}{T_o}\right) \qquad (2\text{-}9)$$

It can be deduced that at t=0, $\sigma = \sigma_o$ and when $t = \infty$, $\sigma = 0$. When $t = t_o$, $\sigma = 0.368\ \sigma_o$.

Thus the relaxation time (T_o) is the time needed to reduce strain to 36.8% of the original value.

A combination model of Hooke's and Newton's laws in parallel was introduced by Kelvin [Huang, 2004].

Kelvin assumes both models result in the same strain. Yet, the total stress is the sum of the two stresses obtained from both models.

$$\sigma = E_1\varepsilon + \lambda_1 \frac{\partial \varepsilon}{\partial t} \qquad (2\text{-}10)$$

E_1 is the modulus of elasticity in Kelvin's model, ε is the total strain, λ_1 is the instantaneous viscosity in Kelvin's model and $\frac{\partial \varepsilon}{\partial t}$ is the rate of change of strain.

If a constant stress is applied:

$$\int_0^{\varepsilon} \frac{d\varepsilon}{\sigma - E_1\varepsilon} = \int_0^{t} \frac{dt}{\lambda_1} \text{ or } \varepsilon = \frac{\sigma}{E_1}\left[1 - \exp\left(-\frac{t}{T_1}\right)\right] \qquad (2\text{-}11)$$

where $T_1 = \frac{\lambda_1}{E_1}$ = retardation time, it can be deduced that at t = 0, $\varepsilon = 0$ and at t = ∞, $\varepsilon = \frac{\sigma}{E_1}$ and at $t = T_1$, $\varepsilon = 0.632\frac{\sigma}{E_1}$. Thus, the retardation time in Kelvin's model is the time needed to reach 63.2% of the total retarded strain.

Burger presented a combination model for Maxwell and Kelvin models in series [Huang, 2004]. Under a constant stress, strain can be calculated as:

$$\varepsilon = \frac{\sigma}{E_o}\left(1 + \frac{t}{T_o}\right) + \frac{\sigma}{E_1}\left[1 - \exp\left(-\frac{t}{T_1}\right)\right] \qquad (2\text{-}12)$$

where σ is the stress, ε is the strain, t is the loading time, E_o is the instantaneous modulus of elasticity in Maxwell's model, $T_o = \frac{\lambda_o}{E_o}$ = relaxation time and λ_o is the viscosity in

Maxwell's model. E_1 is the modulus of elasticity in Kelvin's model, $T_1 = \frac{\lambda_1}{E_1}$ = retardation time and λ_1 is the instantaneous viscosity in Kelvin's model.

Burgers model calculated the strain as a composition of three portions: elastic strain, a viscous strain and a retarded elastic strain.

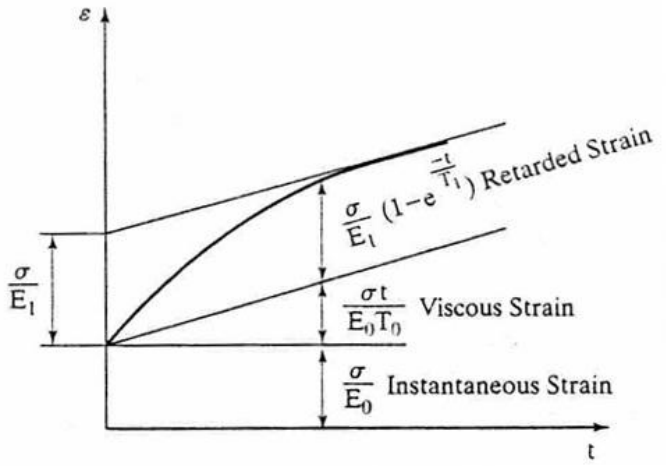

Figure 2-3: Three Components of Strain for Burgers Model [Huang, 2004]

Practically, a single Kelvin model is insufficient to cover the long strain retardation time (T_1). A general model provides superior accuracy using a number of Kelvin models:

$$\varepsilon = \frac{\sigma}{E_o}\left(1+\frac{t}{T_o}\right)+\sum_{i=1}^{n}\frac{\sigma}{E_i}\left[1-\exp\left(-\frac{t}{T_i}\right)\right] \qquad (2\text{-}13)$$

where n is the number of Kelvin models used in the general model. This model takes into account the effect of load duration on pavement responses. In case a single load is applied, instantaneous and retarded elastic strains are the main factors affecting the total strain, while viscous strains can be neglected. Applying large numbers of load repetitions, the accumulated viscous strains are the main factors causing permanent deformation.

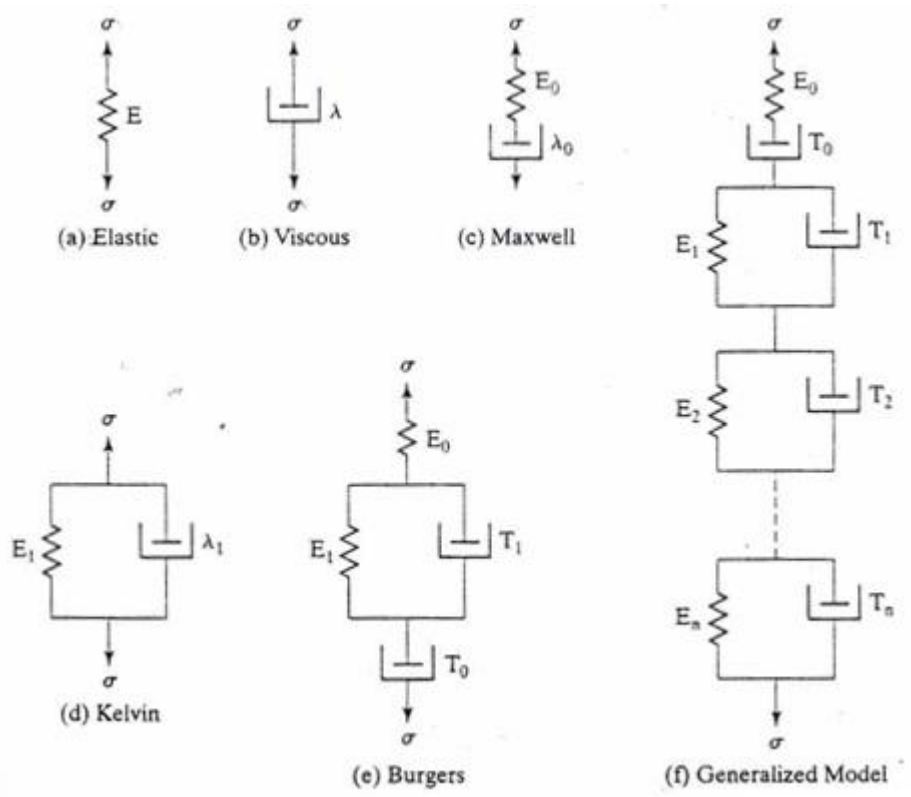

Figure 2-4: Mechanical Models for Viscoelastic/Viscoplastic Materials [Huang, 2004]

2.5 Construction of Test Sections

This research project included the design, instrumentation, and construction of three test sections on Highway 401. The Highway 401 test sections represent a unique case for the study and evaluation of perpetual pavement design because they were constructed on a heavily travelled controlled-access highway that connects major cities in southwestern Ontario. This section briefly describes the construction and instrumentation of other relevant North American and international pavement test sections.

2.5.1 Minnesota Road Research Project (Mn/Road)

Construction of the Minnesota Road Research Project (Mn/Road) began in 1990. Located in Otsego, Minnesota, Mn/ROAD is approximately 65 km on the west of the Minneapolis-St. Paul metropolitan area on westbound Interstate 94. A total of 40 test sections have been divided between two test roads. Part of the Mn/Road project has been constructed on the I-94 highway in order to provide researchers with data from a high-traffic-volume road. The other section has been constructed on a low-volume design test road in order to obtain data for known load conditions. Given the 4,572 sensors that have been installed in the 40 test sections, the Mn/Road research team has gained considerable experience related to investigating the construction and performance of pavement through the installation of sensors in both concrete and asphalt pavements [MNDOT, 2001]. The sensors can be divided into two categories: strain gauges and earth pressure cells used to collect dynamic data from the traffic loads passing over them; while moisture probes and thermocouples are used to monitor the environmental parameters that affect pavement performance. The strain gauges were installed in groups of three that span the wheel path. Some of the strain gauges were installed as a means of measuring the strain that occurs in the longitudinal direction while others capture the transverse strain. The data collected from the test track are downloaded from the data loggers via the internet. Current data can be accessed by researchers in the Minnesota Department of Transportation Materials Research and Engineering Laboratory in Maplewood, MN. Future plans for the Mn/Road project include enhancing accessibility to the data obtained from the Mn/Road so that they will be available for the public on the

internet, enabling all pavement researchers worldwide to benefit from this valuable source of information.

Several research projects are currently taking advantage of the Mn/Road test sections, including an evaluation of the relationships between the resilient modulus and drainage, thaw weakening and time, thaw weakening and moisture, and frost heave and drainage; a comparison of horizontal strain and deflection in bituminous pavements; and other miscellaneous projects [MNDOT, 2001]. Figure 2-5 shows the location of the Mn/Road site.

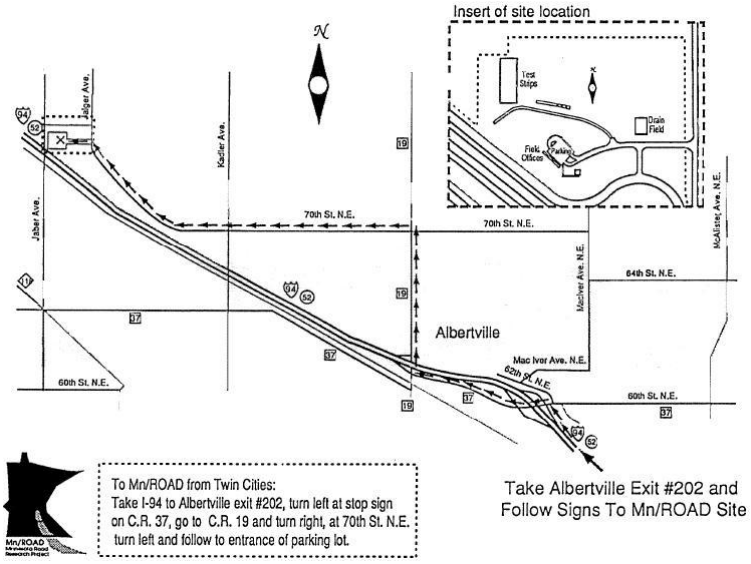

Figure 2-5: Mn/Road Site Map [MNDOT, 2001]

2.5.2 Wisconsin Department of Transportation Pavement Testing

In 2000, the Wisconsin Department of Transportation (WisDOT) constructed test sections on State Trunk Highway (STH) 50 in Kenosha and Walworth counties as a means of evaluating the performance of perpetual pavements. The test area was comprised of four perpetual pavement sections and two control sections. Pavement performance was monitored using a

falling weight deflectometer (FWD), and the strain at various asphalt layers was backcalculated. The results of the strain calculations showed that all perpetual sections were subjected to strain below 70 με [Battaglia, 2010].

In 2003, two perpetual pavement test sections were constructed on the westbound I-94 in southeastern Wisconsin. Figure 2-6 illustrates cross-sections for the two perpetual pavement designs [Battaglia, 2010].

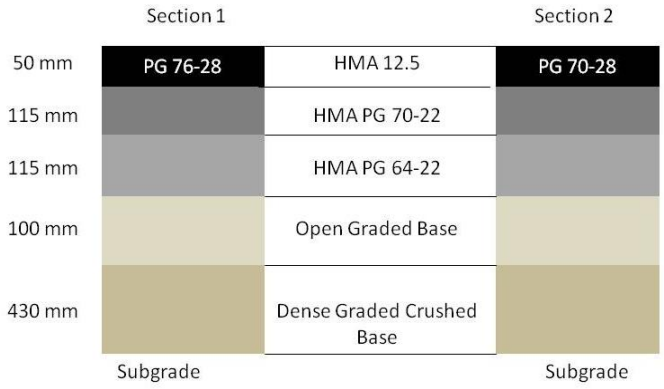

Figure 2-6: Wisconsin Perpetual Pavement Test Section

The two test sections were instrumented with 16 strain gauges oriented in both the longitudinal and transverse directions. Three strain gauges provided acceptable results, but the other 13 gauges were considered to be broken during the construction phase [Battaglia, 2010]. The maximum strain collected was 100 με, which occurred at 38 ºC and with slow traffic speeds.

To evaluate the quality of asphalt mixes, dynamic modulus testing was performed at three temperatures (16 ºC, 21 ºC, and 41 ºC). The results indicated superior performance in section one with respect to surface rutting. The middle and lower layers in both sections were

characterized by similar dynamic modulus results at different loading frequencies and temperatures.

2.5.3 National Center for Asphalt Technology (NCAT) Test Track

The National Center for Asphalt Technology (NCAT), located at Auburn University, Alabama in the United States, has constructed a 2.74 km (1.7 miles) test track in Opelika, Alabama. The test track consists of 45 flexible pavement sections, each approximately 60 m (200 ft), and was designed for 10 million Equivalent Single Axle Loads (ESALs) [NCAT, 2009]. The loading on the pavement sections is applied by means of heavy trucks driven over each section by professional truck drivers. The closed loop full-scale test track is operated five or six days a week, from 5:00 am to 10:45 pm. The application of the same traffic load on all the pavement sections allows structural comparisons between different sections. The test sections are equipped with a variety of sensors that monitor pavement performance, collect strain data in each of the asphalt layers, obtain vertical pressure readings from the top of the subgrade, and gather information about other environmental factors that impact pavement performance. Thermistor strings are installed in all test sections as a means of monitoring temperature variations in all pavement layers for all seasons, and a permanent weather station is installed in the test track. The response of the pavement to traffic loading is determined from installed strain gauges and pressure cells. Data is collected at high speeds and transferred using a wireless mesh network that is fitted along the entire length of the track [Pave Track, 2009]. Figure 2-7 shows the NCAT test track layout.

In 2003, sensors that monitor the dynamic pavement response were installed in eight NCAT test track sections, characterized by varying pavement cross-sections and mix designs. Also

installed in all of the eight sections were CTL-brand asphalt strain gauges, identical to one type of sensor used for the Highway 401 project. The installation of the sensors at NCAT was regarded as successful, with only a few strain gauges not surviving the installation and construction of the sections [Timm, 2004 b].

In 2006, two sections of perpetual pavement were constructed in the NCAT test track. Figure 2-8 illustrates the cross-section of the two perpetual pavement sections. Section N9 did not show signs of bottom-up fatigue cracking while fatigue cracking was observed in section N8 [Willis, 2009]. Laboratory test results obtained for these sections have not been reported in the literature currently available. The results for the other sections include dynamic modulus measurements and the establishment of the fatigue endurance limit based on fatigue beam testing [Willis, 2009].

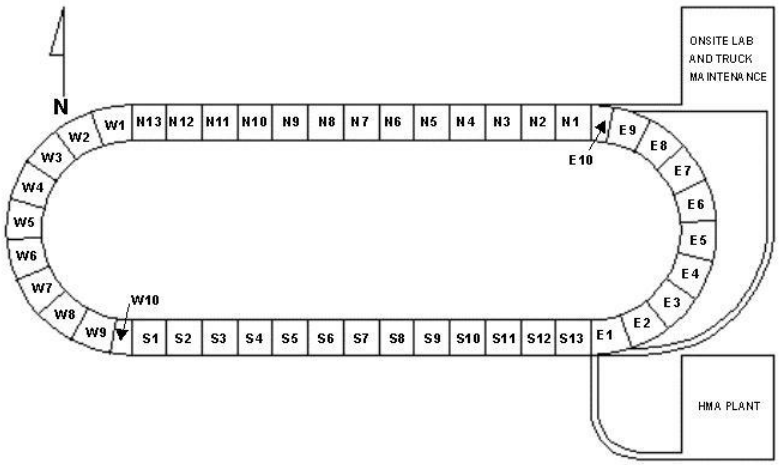

Figure 2-7: NCAT Test Track Layout [Pave Track, 2009]

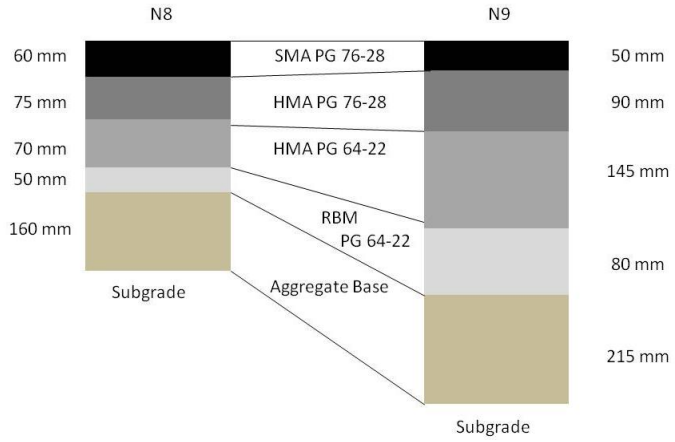

Figure 2-8: NCAT Perpetual Pavement Cross-Section

2.5.4 Marquette Interchange Project

In 2006, construction was completed on the Marquette Interchange Project, which the Wisconsin Highway Research Program had awarded to the Marquette University Transportation Research Center (MU-TRC) in 2005. The test section constructed for the project is located on highway I-43, between stations 385+00 and 385+50 in the extreme right-hand northbound lane. The perpetual pavement section is depicted in Figure 2-9 [Crovetti, 2008]. The instrumentation plan included the installation of 25 strain gauges, two earth pressure cells, and two temperature probes. Figure 2-10 indicates the layout of the test section and the location of the sensors [Hornyak, 2007]. The strain gauges that were installed as a means of monitoring the longitudinal and transverse strain values were manufactured and supplied by two different companies in order to compare their performance. Seventeen strain gauges were manufactured by CTL, and the remaining eight, by Dynatest. The CTL strain gauges used in the Marquette Interchange test sections are identical to those installed on Highway 401 for the research project presented in this thesis.

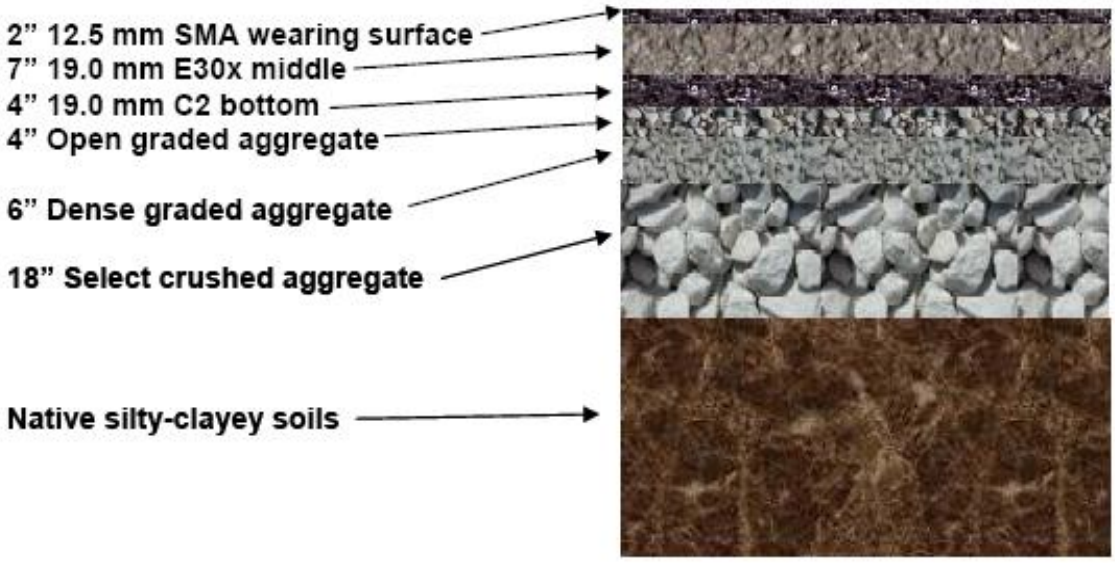

Figure 2-9: HMA Perpetual Pavement Structure [Crovetti, 2008]

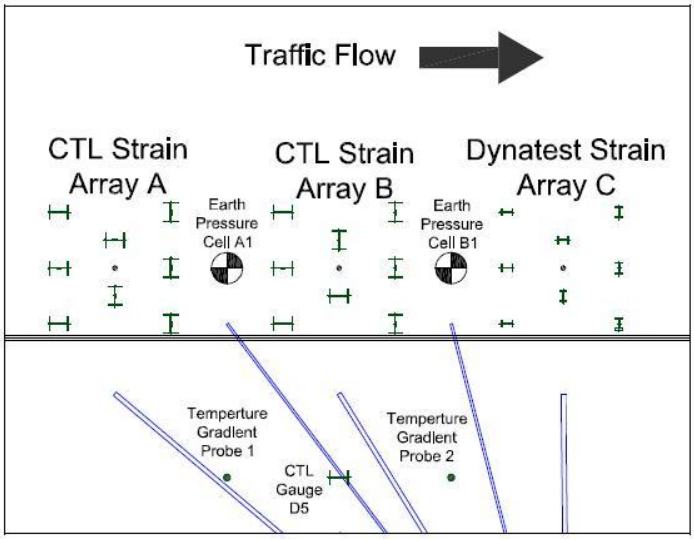

Figure 2-10: Marquette Interchange Instrumentation Layout [Hornyak, 2007]

Several laboratory tests were conducted in order to quantify the mechanical properties of the HMA used for the construction of the perpetual pavement test sections in the Marquette Interchange. Dynamic modulus testing was conducted for all HMA layers in accordance with

AASHTO TP 62. Five replicates that represented all layers were tested, and measurements were taken at three temperatures (4 ºC, 21 ºC, and 37 ºC), with nine frequencies for each temperature: 25 Hz, 15 Hz, 10 Hz, 5 Hz, 3 Hz, 1 Hz, 0.5 Hz, 0.3 Hz, and 0.1 Hz [Crovetti, 2008]. Table 2-1 lists the average dynamic modulus value for each layer of the HMA at a temperature of 21 ºC and a frequency of 1 Hz.

Table 2-1: Dynamic Modulus Values for HMA Layers at 21°C and 1 Hz

Mix Type	Dynamic Modulus (MPa)
SMA 12.5	2,640
Superpave 19 E30x	7,420
Superpave 19 C2	7,480
Superpave 19 RBM	3,200

Figure 2-11 presents the master curve of all HMA used in constructing the Marquette Interchange perpetual pavement test section.

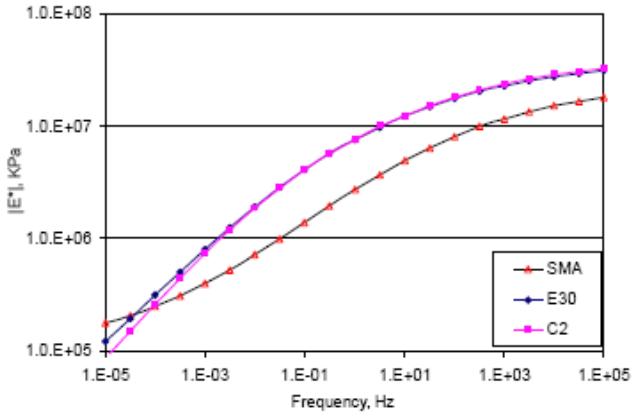

Figure 2-11: Dynamic Modulus Master Curve for Marquette Interchange Section [Crovetti, 2008]

As can be seen, the dynamic modulus results for the SMA are generally lower than those for either the SP 19 mm E30 or C2 mixes. However, in the low-frequency range, the SMA surface course was characterized by a higher dynamic modulus than that of the other two mixes (intermediate and bottom layers). The same phenomenon can be noted based on the analysis of the dynamic modulus data obtained for the Highway 401 perpetual pavement project. Further discussion of the dynamic modulus results is included in Chapter 4.

The laboratory test results for the Marquette Interchange pavement layers were modeled through the Mechanistic Empirical Pavement Design Guide (MEPDG), and the KENLAYER and EVERSTRESS analysis tools. The models confirmed the "perpetual" nature of the performance of this pavement section. The dominant distress predicted by the models is top-down cracking. The fatigue damage expected after 50 years of service is only 15 % of the total lane area [Crovetti, 2008].

2.5.5 Shandong Province Test Section in China

Beginning in 2005, three perpetual and two control test sections have been constructed on a new expressway in Shandong Province, China. The construction plan included the installation of weigh-in-motion (WIM) devices, earth pressure cells, temperature probes, and strain gauges for capturing strain measurements in the longitudinal and transverse directions [Yang, 2006]. The cross-sections of the three perpetual pavement designs are shown in Figure 2-12 [Timm, 2011]. The two control sections are 1050 mm in total thickness, with HMA thicknesses of 330 mm and 150 mm for S4 and S5, respectively.

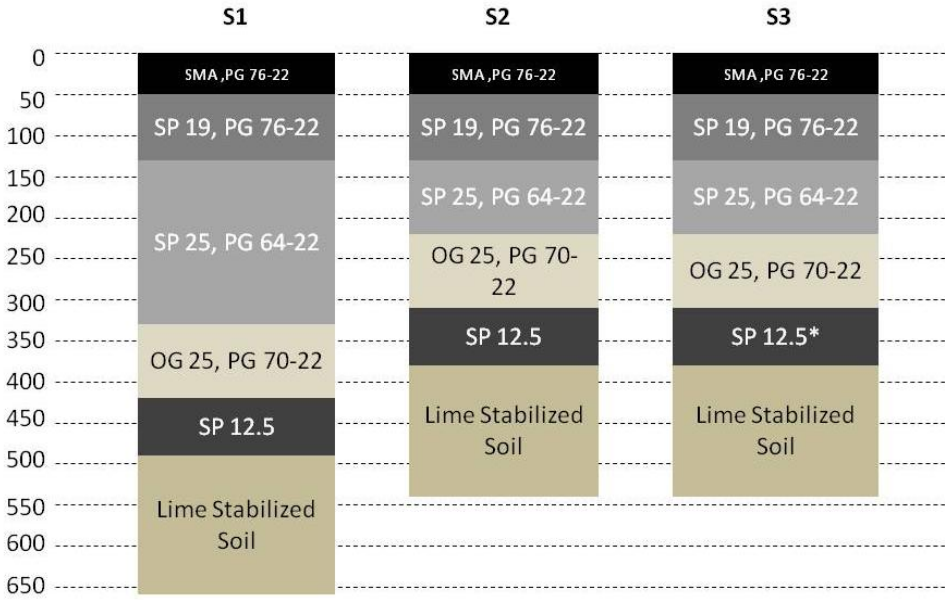

Figure 2-12: Perpetual Pavement Sections in China

Perpetual pavement section S1 was designed to withstand 70 με at the bottom of the HMA while sections S2 and S3 were designed for 125 με. The strain measurements for different test sections show that section S4 (a conventional full-depth section) is subjected to the lowest strain values because it is characterized by a 330 mm thickness of HMA overlaying 405 mm of lime-kiln dust-fly ash granular and stabilized soil in addition to 305 mm of lime stabilized soil [Timm, 2011]. The strain values at sections S1, S2, and S3 are also below the 70 με limit, indicating the effectiveness of the perpetual designs even though their total thickness is less than the total thickness of the S4 design [Timm, 2011]. Figure 2-13 shows the strain values for all of the pavement designs.

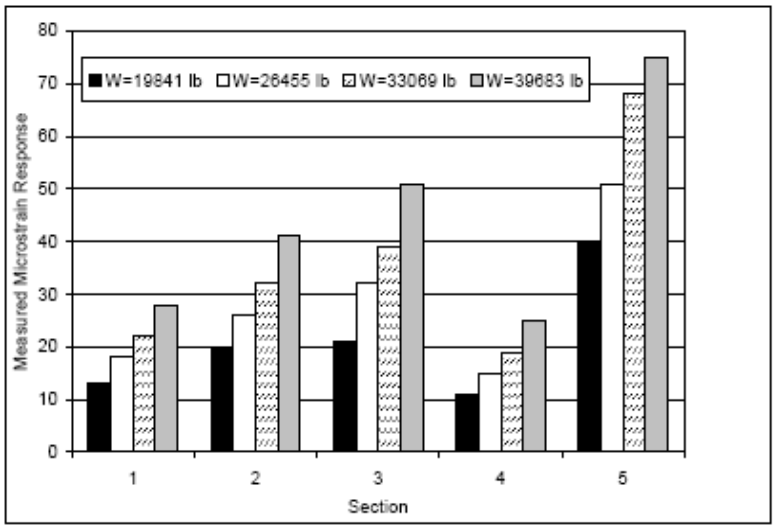

Figure 2-13: Measured Strain Comparison for China Test Sections [Timm, 2011]

2.5.6 Centre for Pavement and Transportation Technology (CPATT) Test Track

The Centre for Pavement and Transportation Technology (CPATT) test track was constructed by the University of Waterloo in cooperation with the Regional Municipality of Waterloo Waste Management Facility. The original section is 710 m long and contains a variety of pavement designs, such as standard Hot Laid 3 (HL 3), polymer-modified asphalt (PMA), SMA, and Superpave 12.5, as well as four interlocking concrete pavement crosswalks. The test sections are monitored using asphalt and concrete strain gauges, earth pressure cells, moisture probes, and thermocouples [Tighe, 2007]. A WIM has been installed in the test track along with a static scale located at the beginning of the test section. The location of the test section in the waste management facility provides unique features useful for the research projects implemented at this test track. The heavily weighted trucks passing over this test section represent 300,000 ESALs over a three-week period, and the traffic loads can be accurately measured using the station static scale and then compared with the

WIM records. Regular performance testing is also applied to different pavement sections, including visual distress surveys, roughness evaluations, FWD measurements, and skid and rutting evaluations. A number of sections have been added to the track since its inception. In 2007, four jointed plain concrete pavement sections containing 0 %, 15 %, 30 %, and 50 % recycled concrete aggregate were added as well as a section composed of recycled asphalt shingles in an HL3 mix. Other sections were added in 2010. Figure 2-14 shows a plan view of the test track [Ul-Islam, 2010]. CPATT has also implemented several satellite test sections located in the cities of Toronto, Vancouver, Dryden, and Chapleau. These sections include thermistor strings, moisture probes, and strain gauges. Although the satellite test sections do not contain any perpetual pavement sections, the experience gained in the construction and instrumentation of all of the test sections facilitated the construction of the Highway 401 perpetual pavement and conventional pavement sections.

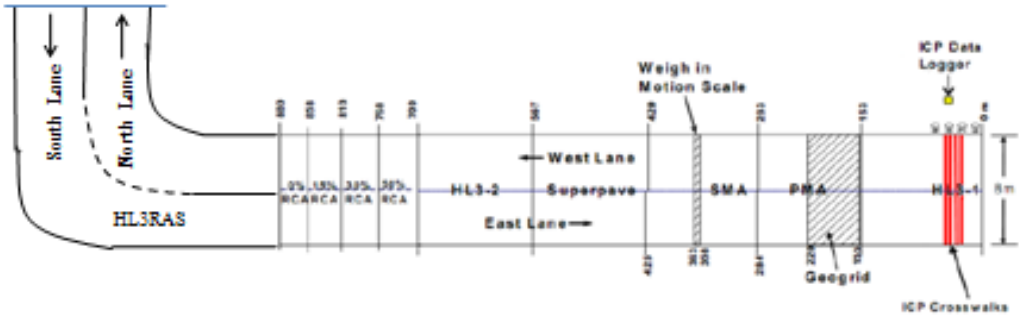

Figure 2-14: Flexible Pavement Portion of the CPATT Test Track after [Ul-Islam, 2010]

2.5.7 Highway 406

Constructed in the summer of 2004, the highway 406 project in Thorold, Ontario, was the first Canadian perpetual pavement trial [Ponniah, 2009]. This highway was originally constructed in 1969 as a rigid pavement highway and was then rehabilitated in 1998 and again in 2004. The most recent rehabilitation was first designed as a conventional deep-strength flexible pavement prior to the introduction of the perpetual pavement design concept. The pavement was then redesigned as a perpetual pavement section based on the design guide published by the American Association of State and Highway Transportation Officials (AASHTO 93) and on the Ontario Pavement Analysis of Costs (OPAC) 2000 program. This 50-year design life pavement was designed for 42 million ESALs. The HMA installed is 250 mm thick, including an 80 mm RBM layer of Superpave 25.0 [Ponniah, 2009]. This project does not include a monitoring plan that relies on sensors embedded in the pavement layers.

2.5.8 Red Hill Valley Parkway

The Red Hill Valley Parkway is the most heavily travelled urban highways in Hamilton, Ontario. It was constructed in 2007 using perpetual pavement. The designers estimated that the loading on this highway would reach 90 million ESALs by the end of the 50-year design period [Uzarowski, 2008]. The total thickness of the perpetual pavement is 760 mm, including 240 mm of asphalt layers. Like the Highway 406 project, this project was also initially designed as deep-strength conventional pavement and then redesigned as perpetual pavement. The total thickness of both the deep-strength and the perpetual designs were identical, but 80 mm of the granular material in the original subbase layer was changed to a

Superpave 19 HMA RBM. This layer has enhanced the fatigue resistance properties of the pavement [Uzarowski, 2008]. The two pavement designs are illustrated in Figure 2-15.

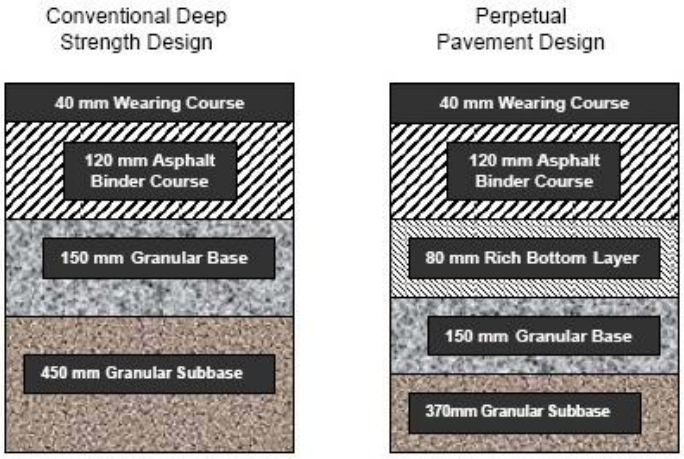

Figure 2-15: Perpetual and Deep Strength Conventional Sections of the Red Hill Valley Parkway Project [Uzarowski, 2008]

Several laboratory tests have been performed in order to determine the mechanistic properties of the pavement layers. Rutting resistance was tested using an asphalt pavement analyzer (APA), and dynamic modulus testing and fatigue testing were also carried out for each mix. The mechanistic properties of the mixes are listed in Table 2-2.

Table 2-2: Summary of Asphalt Mix Mechanistic Properties Testing

Mix Type	Dynamic Modulus (MPa)	Rutting Resistance (Depth) in APA (mm)
SMA 12.5	3,000	3.8
Superpave 19	5,100	4.9
Superpave 25	7,700	4.5
Superpave 19 RBM	3,200	4.6

The dynamic modulus results presented in this table were measured at a 1 Hz frequency and

21 ºC. PG 70-28 asphalt binder with high polymer content was used in the RBM layer in order to enhance the fatigue endurance of that layer.

This test section is instrumented with both pavement and traffic monitoring systems. The pavement response monitoring system includes pressure and moisture gauges installed in the subgrade as well as asphalt strain gauges in the RBM, SP 25, and SMA layers. In addition, temperature sensors are installed in the subgrade, granular, and HMA layers as a means of monitoring the temperature of each layer. The traffic monitoring system includes traffic loops and WIM sensors that collect and store traffic data (vehicle speeds, loading, and spacing) [Uzarowski, 2008]. These data can be accessed online and downloaded from the internet.

2.6 Summary and Conclusion

This chapter has provided a review of the literature relevant to the research presented in this thesis. The first section explained the concepts of perpetual and conventional pavement designs. The main research objective is to evaluate the tensile strain at the bottom of the asphalt layers in both perpetual and conventional pavement sections. Accordingly, the second section of the literature review introduced the models and theories used for mechanistic calculations of the tensile strain at the bottom of asphalt layers. Because the research project presented in this thesis included the construction of test sections on Highway 401, an examination of similar test sections that have been instrumented in North America and internationally was essential for an understanding of the selection and installation of sensors.

The third section of this chapter thus provided general background with respect to the construction of these well-known test sections.

The literature review presented the perpetual and conventional pavement design methods. The state-of-the-art design philosophy is the Mechanistic-Empirical pavement design. The literature showed the significance of tensile strain prediction as one of the main aspects in perpetual pavement design. Several research projects were executed to calculate the tensile strain at the bottom of asphalt layers using mechanistic and linear elastic models. The shortfall of these methods is the limited ability of accounting for the quality of construction and environmental impact of freeze-thaw cycles in the Canadian climate. The research project presented in this thesis, introduced empirical models to calculate tensile strain at the bottom of asphalt layers. The model will be based on a practical case study of a test section. The developed models are correlating laboratory tests evaluating the mechanistic characteristics of pavement layers with the tensile strain at the bottom of asphalt layers.

Chapter 3
Construction and Instrumentation of the Test Section

3.1 Introduction

The Ministry of Transportation in Ontario (MTO), the Ontario Hot Mix Producers Association (OHMPA), the Centre for Pavement and Transportation Technology (CPATT), the Natural Science and Engineering Research Council of Canada (NSERC), Stantec Inc., and McAsphalt Industries Limited partnered in order to evaluate three flexible pavement designs: two perpetual pavement designs and one conventional flexible pavement design. The goal of this research was to assist designers, researchers, contractors, and consultants working in pavement engineering to better understand how the perpetual pavement performs and deteriorates, with consideration of the impact of both the environment and traffic, especially under the effect of freeze-thaw cycles in southern Ontario region.

Three flexible pavement designs were designed, constructed, and equipped with sensors installed in each pavement layer: asphalt, granular base, and subbase. The design was provided by the MTO and was designed using the AASHTO 1993 design guide and [Hajek, 2008, Ponniah, 2009]. Located on Highway 401 between Woodstock and Waterloo in southwestern Ontario, the project included the construction of six monitoring stations in two stages. Stage one involved the preparation and instrumentation of three monitoring stations in the left lane. In stage two of the construction, the remaining three monitoring stations were constructed and instrumented in the right driving lane. A perpetual pavement section was also constructed and instrumented at the Capital Paving Inc. asphalt plant located in Guelph,

Ontario. The sensors installed are capable of collecting strain, vertical pressure, temperature, and moisture content data. The asphalt strain gauges (ASGs) were located so as to target the strain in the critical zones where crack initiation is expected. To study the rutting phenomenon, earth pressure cells (EPC) were installed under the wheel path in order to measure the vertical pressure on the top of the subgrade. Thermistor strings (TS) were positioned so that the temperature of various pavement layers could be monitored. The moisture content of the subgrade layer has an impact on the deterioration of the pavement, and the moisture probes were installed as a means of determining the moisture content in the subgrade layer. Weigh-In-Motion (WIM) sensors were also added in order to capture the axle loads of the vehicles. The WIM installation was part of a separate research study [Vaziri, 2011].

3.2 Location of the Test Sections

The test sections are located on the eastbound lanes of Highway 401 on the TransCanada Highways between Exits 238 and 250, as indicated on the map shown in Figure 3-1. An additional test section constructed at the Capital Paving Inc. asphalt plant in Guelph, Ontario, is described in section 3.6.

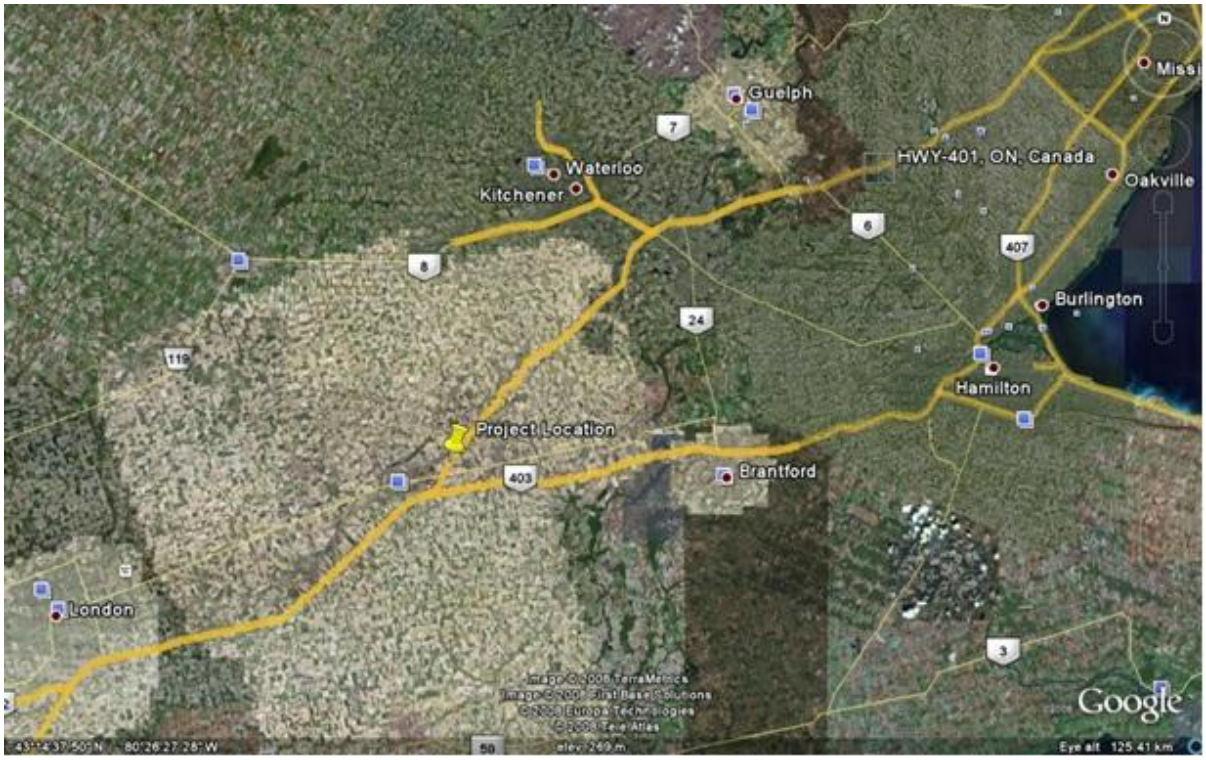

Figure 3-1: Project Location Overview [Google Earth, 2008]

3.3 Pavement Sections

Three different pavement designs were developed, but the same instrumentation was installed in each section. Station 12+230 is used for monitoring the perpetual pavement design, which includes a rich bottom mix (RBM) layer. The RBM contains a slightly higher percentage of asphalt binder and is designed to provide superior cracking endurance. The second test section was constructed with the same structural thickness but without the RBM, which adds an extra cost. These layers were varied so that a direct comparison of their impact could enable a determination of the cost-effectiveness of incorporating the RBM. The sensors installed at station 12+350 collected data from the perpetual pavement mix without the RBM layer, and station 13+067 monitored the conventional flexible pavement design, which was

the type of pavement that would normally be placed at this location and was thus the control section for comparison purposes. Figures 3-2, 3-3, and 3-4 illustrate cross-sections of the three pavement designs.

A preliminary analysis of the three pavement designs was conducted using the Multi-Layer Elastic Analysis (MLEA) program, ELSYM5, WESLEA, and MEPDG. The results obtained from the models revealed that the perpetual pavement is subjected to lower strains at the bottom of the hot mix asphalt (HMA) [El-Hakim, 2009 a, El-Hakim, 2009 b, El-Hakim, 2009 c]. This finding reflects the superior structural capacity of perpetual designs compared to that using conventional design methodology. An initial life cycle cost analysis (LCCA) demonstrated that, from an economic perspective, the perpetual design is also the optimum design methodology for heavily travelled highways. The LCCA was performed using a scheduled maintenance and rehabilitation program based on MTO recommendations [El-Hakim, 2009 a, El-Hakim, 2009 b, Tighe, 2010].

Figure 3-2: Cross-Section of Perpetual Pavement with RBM

Figure 3-3: Cross-Section of Perpetual Pavement without RBM

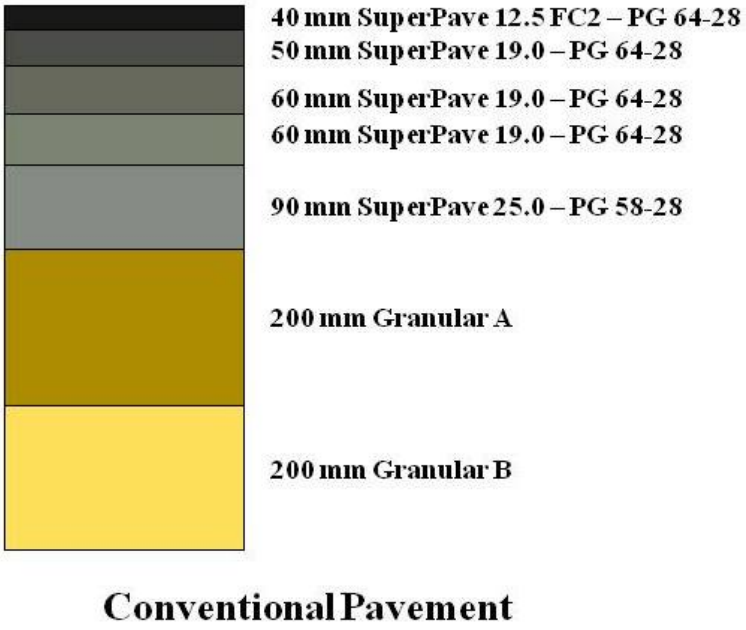

Figure 3-4: Cross-Section of Conventional Pavement

3.4 Location of the Sensors

The installation of the sensors was designed to provide the research team with the most accurate and pertinent engineering data for the modeling and predicting long-term changes in tensile strain at the bottom of asphalt layers. The specific position of each sensor in the pavement layers plays a vital role in the validation of the real-time pavement monitoring. Detailed drawings showing the plan and the cross-sections of the road are presented in Figures 3-5, 3-6, and 3-7.

The fatigue cracking is initiated at the bottom of asphalt layers or the top of Granular A as this is the part subjected to the highest tension level. On the other hand, structural rutting of the entire pavement is expected to be predicted through monitoring the vertical pressure at the top of subgrade material [Timm, 2003]. The asphalt strain gauges were placed under the

left and right wheel paths where the vehicles would drive over them and were installed so that the strain values could be measured in both the longitudinal direction and the transverse direction (μ_x and μ_y, respectively). The vertical location of the asphalt strain gauges was at the top and bottom of the lowest asphalt layer overlying the top of the uppermost granular layer. Because this location is subjected to the highest tension, crack initiation is expected to begin at the bottom of the asphalt layers directly under the wheel paths. These gauges thus provided the strain information necessary for a determination of the likelihood of cracking.

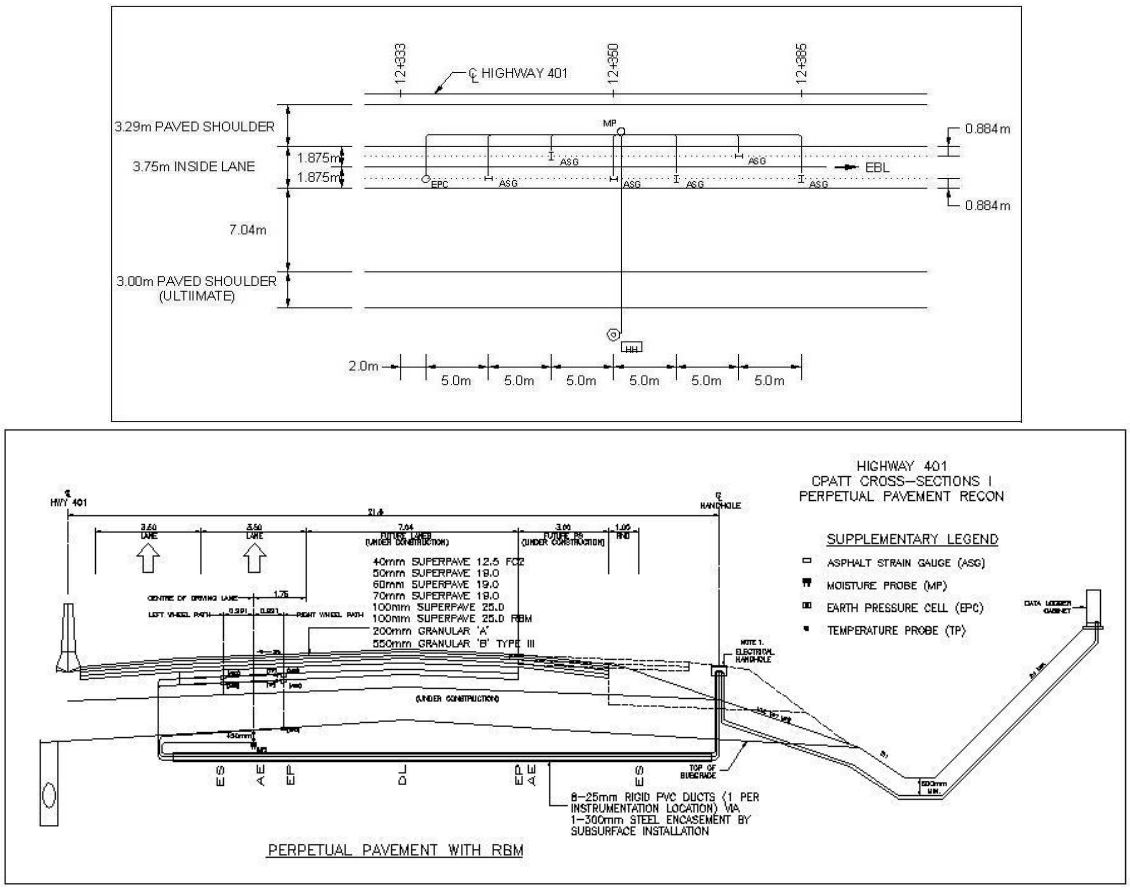

Figure 3-5: Plan and Cross-Section for the Perpetual Pavement Section with RBM

The project instrumentation plan also included the installation of thermistor strings at three monitoring stations. Thermistor strings indicate the temperature profile because they measure the temperature every 10 cm from the surface of the pavement through to the subgrade layer. Due to construction constraints, the installation of thermistor strings in lane number 3 was cancelled. The other alternative was to install thermistor strings in the paved shoulder, which would protect them from damage caused by winter maintenance and snow removal. The thermistor strings were the last sensor type to be installed on site and were successfully positioned in October 2010.

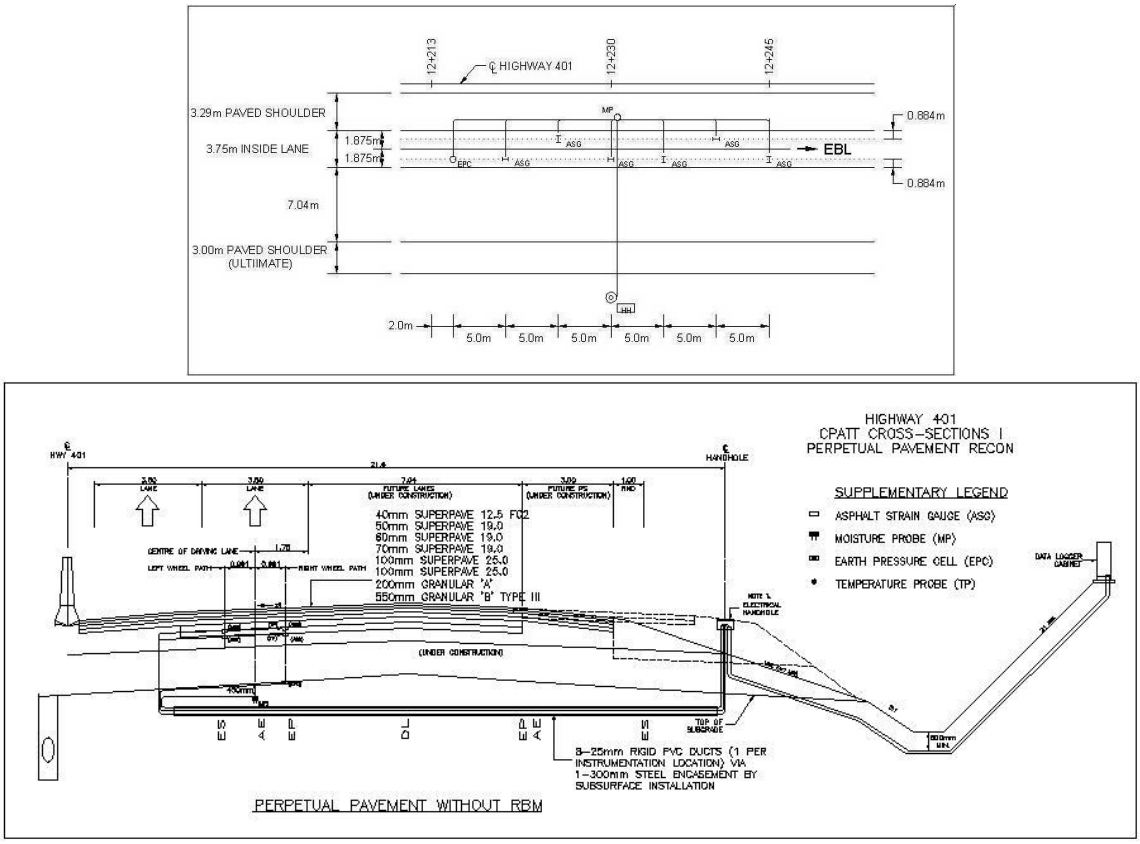

Figure 3-6: Plan and Cross-Section for the Perpetual Pavement Section without RBM

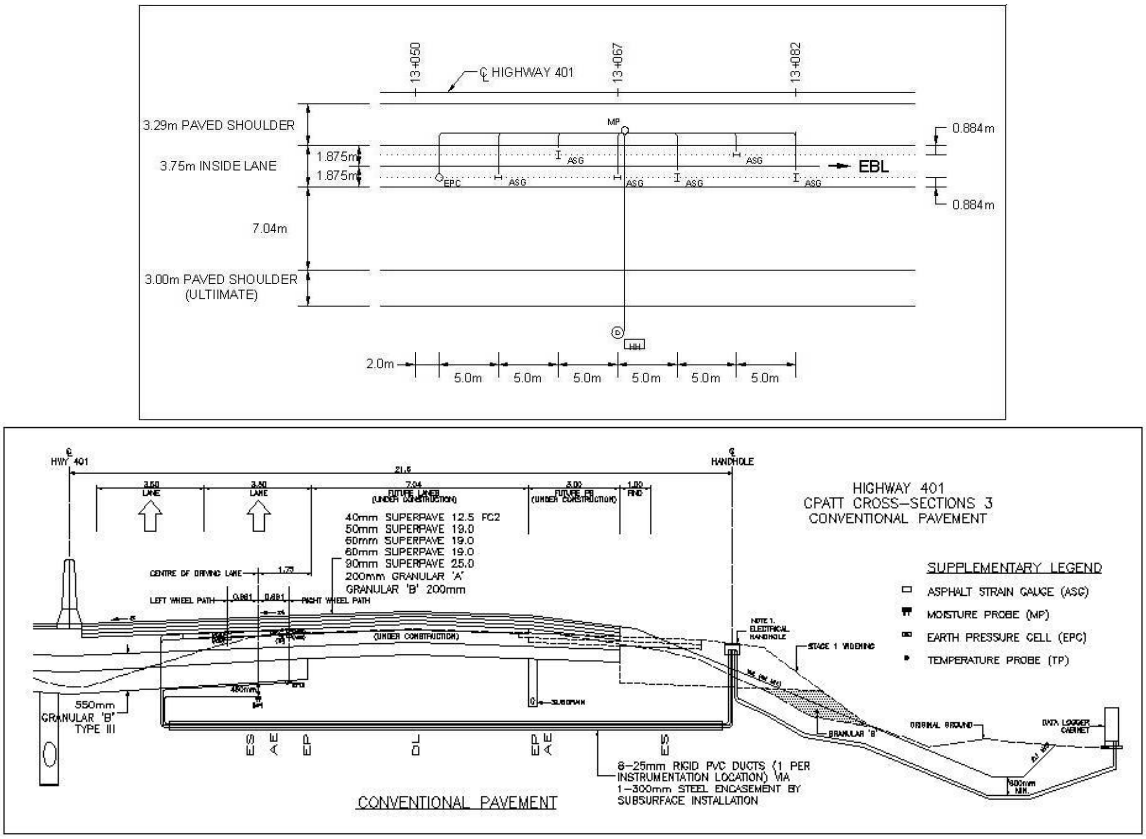

Figure 3-7: Plan and Cross-Section for the Conventional Pavement Section

3.5 Sensor Selection and Installation

Prior to the selection and installation of the sensors for the CPATT perpetual pavement experiment, the instrumentation plans for similar projects were reviewed. Projects such as the Minnesota Road Research Project (Mn/Road) [Baker, 1994], the Virginia SmartRoad [Louliz, 2007], and the National Center for Asphalt Technology (NCAT) test track [Timm, 2004 a] had produced reports that included valuable detailed information regarding their experience in constructing and installing a variety of sensors for their pavement test sections.

3.5.1 Installation Infrastructure

Site preparation, the opening of trenches, conduit installation, and the construction of concrete foundations for the three monitoring station cabinets constituted the main activities during the pre-installation phase. The location of the data loggers and solar panels on the right-hand shoulder of the highway provided all-season safe access to facilitate the data collection procedure for the CPATT research team. Experience with a previous instrumentation plan had shown that the installation of a conduit crossing through the subgrade material was essential so that the cable could pass from lane number 3 (left lane) to the shoulder where the data logger cabinet was located. An open trench technique was used for the construction of the conduit. A steel pipe 31 cm in diameter was positioned at a depth of 1.5 m in the subgrade, and eight PVC tubes 5 cm in diameter were installed inside the steel pipe. The photographs in Figures 3-8, 3-9, 3-10, and 3-11 show the construction of the infrastructure for the sensor installation.

Figure 3-8: Steel Conduit Used for Cable Crossing

Figure 3-9: Paving Marking Prior to Open Trench Excavation

Figure 3-10: Conduit Installation

Figure 3-11: PVC Tubes Inside the Steel Conduit

3.6 Guelph Pavement Test Section

A supplementary perpetual pavement test section that was constructed at the Capital Paving Inc. asphalt plant yard located in Guelph, Ontario is similar to the Highway 401 section that contains the RBM layer. The construction took place in July 2009, and this test section was equipped with eight ASGs and one EPC. Figure 3-12 is a detailed drawing that indicates the dimensions of the test section and the locations of the sensors. Sketches of the longitudinal and transverse cross-sections of the test section are presented in Figures 3-13 and 3-14, respectively. This was constructed as it provides supplemental information for the Highway 401 site. Also, it is easier to access.

The construction of this test section was accomplished with the support of the CPATT partners: Capital Paving, OHMPA, McAsphalt, MTO, and Stantec. This test section has

unique characteristics because of its location directly adjacent to the weigh station in the asphalt plant yard. All of the traffic on this test section is controlled and measured. However, the traffic is all slow moving compared to that using the Highway 401 sections, and the section is subjected to truck loading, mainly during the construction season, when the asphalt plant is open. The site can also function as an important facility for educating engineers about perpetual pavement technology. Figures 3-15, 3-16, and 3-17 show the construction of the Guelph test section.

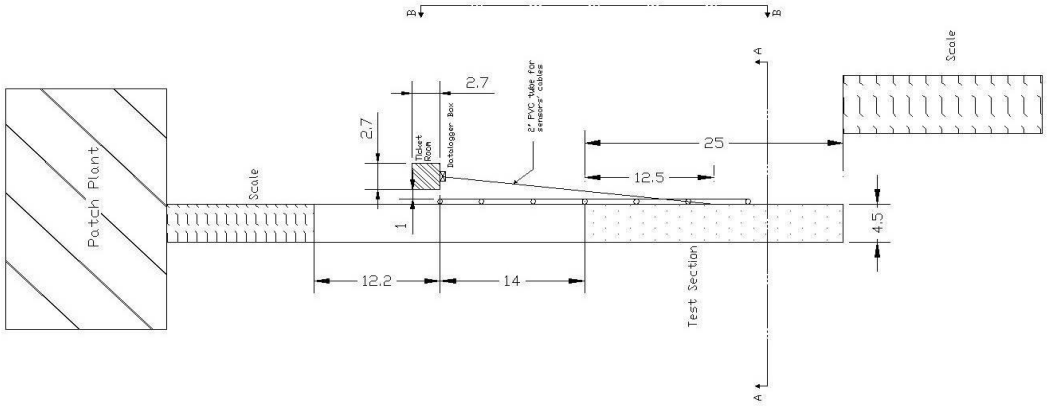

Figure 3-12: Plan of the Guelph Capital Paving Inc. Section

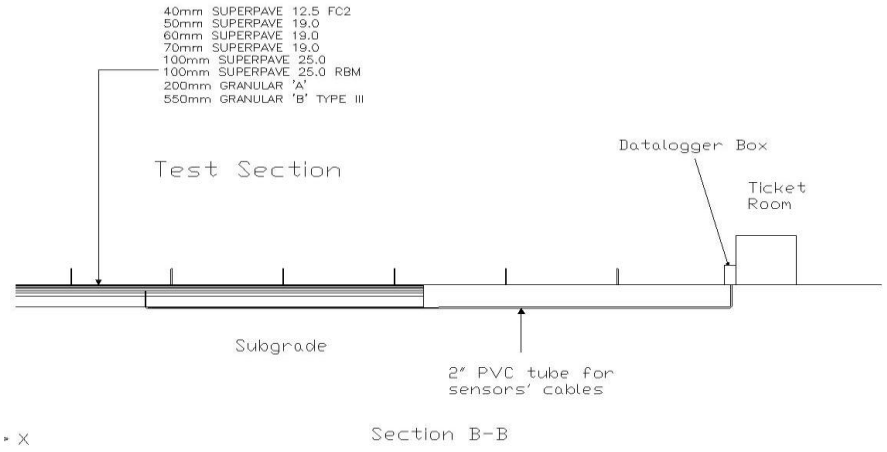

Figure 3-13: Longitudinal Cross-Section of the Guelph Test Section

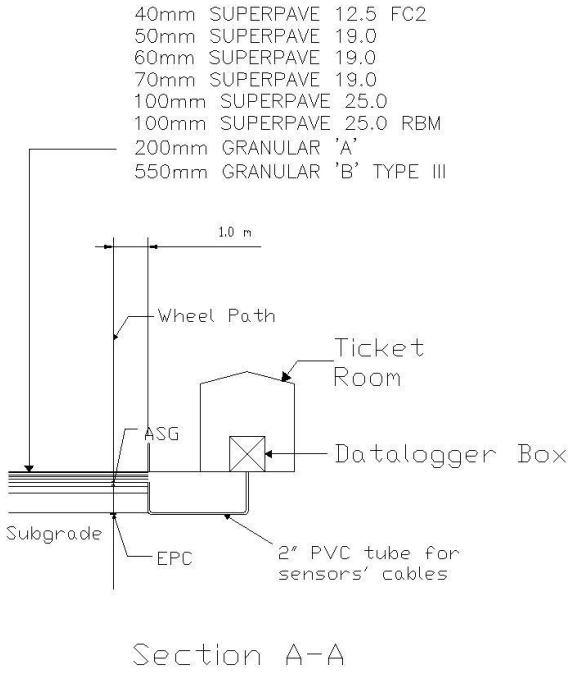

Figure 3-14: Transverse Cross-Section of the Guelph Test Section

Figure 3-15: Opening the Trench to Construct the Perpetual Pavement Section

Figure 3-16: Preparation for ASG Installation on Top of Granular A

Figure 3-17: Installation of ASG at the Bottom of RBM Layer

3.7 Summary and Conclusion

This section has described the fieldwork associated with the construction of the test sections and the installation of the sensors for this research project. Because they enabled the collection of real-world field data, the construction and instrumentation of the Highway 401 and the Guelph test sections were key elements in this research. The details provided in this chapter may benefit other researchers who wish to construct test sections on high speed and heavy trafficked highways.

Chapter 4
Structural Evaluation

4.1 Introduction

This chapter presents a structural evaluation of the two perpetual sections, the conventional section constructed on Highway 401 and the perpetual section in Capital Paving Inc.-Guelph. The structural evaluation includes all the asphalt material characterization laboratory test results from this research and evaluation of the in-situ strain measurements collected throughout the research period. Table 4-1 presents the number of laboratory tested samples and the number of sensors installed on site. The results of the material characterization laboratory tests were analyzed assess both the conventional and two perpetual pavement designs. A numerical model was developed so that the strain data collected from the test sections could be correlated with the laboratory test results. This model will enable researchers, designers, and practitioners to design perpetual and conventional asphalt pavement sections for both provincial highways and highways for heavy traffic volumes.

Table 4-1: Number of Laboratory Tested Samples and Sensors Installed on Site

	Material Characterization Data			
	Dynamic Modulus	**Resilient Modulus**	**TSRST**	
Number of Tested Samples	16	16	16	
	Instrumentation in Test Sections			
	Strain Gauges	**Earth Pressure Cells**	**Thermistor Strings**	**Moisture Probes**
Number of Installed Sensors	36	3	3	3

4.2 In-Situ Tensile Strain

The in-situ collection of strain data for the Highway 401 project began in December 2010. Strain gauges were installed at the bottom of the asphalt layers in all three test sections on Highway 401. The strain data collection frequency was initially set at one scan per second at the initiation of the data collection period. This collection frequency later was increased in May 2011 to ten scans per second, which is the maximum frequency that can be provided by the data acquisition sensors that had been installed. The modification produced a sound and meaningful database. A significant difference could be observed between the data sets collected prior to and following the change in the scan rate, so the data presented herein is from May 2011 to October 2012 inclusive.

A quality control check was carried out on the in-situ strain data collected starting in May 2011 to eliminate errors and unrealistic measurements. During construction, about 10 % of the strain gauges were damaged as no electric power was received from them, and over the next two years of data collection, seventeen strain gauges were also damaged for reasons that could not be identified. The data included in the final analysis were extracted from the six strain gauges that produced consistent data throughout the entire data collection period. Although it is recognized that more strain data would be desirable, the fact that these gauges generated realistic results was deemed to be the most important factor for further analysis in this research. This is further complicated by the limited access to the site during construction. The project was constructed in several stages which likely further contributed to strain gauge damage.

The in-situ strain database was divided into smaller data sets, each of which represents the strain data collected during a two-week period. Every calendar month of the test period is thus represented by two data sets.

The collected in-situ tensile strain was processed and filtered using Matlab codes. The steps of data processing could be explained in the following steps:

1- Create a moving window of 40 consecutive readings representing the data collected in 4 seconds.

2- Determine the minimum and maximum tensile strain within the 40 scans.

3- If the difference between the minimum and maximum tensile strain of the 40 consecutive readings is less than 2 με, calculate the average of the 40 readings and save it as "Reference".

4- Subtract all the reading from the "Reference" value.

5- Keep updating the "Reference" value every time the computer determines 40 consecutive readings meeting the condition stated in step 3.

The Matlab code used to process the data and determine the value of tensile strain corresponding to passage of a vehicle is presented in Appendix A. Figure 4-1 presents the individual 90^{th} percentile for each month, starting in May 2011. It can be seen that the tensile strain at the bottom of the asphalt layers was significantly affected by the environment. This behavior is the result of the visco-elastic/visco-plastic properties of the asphalt material as it changes as a function of the season. Also, it is noted that the perpetual pavement sections show much lower levels of strain as compared to the conventional design. It is also notable that the trend lines for all three sections show similar trend.

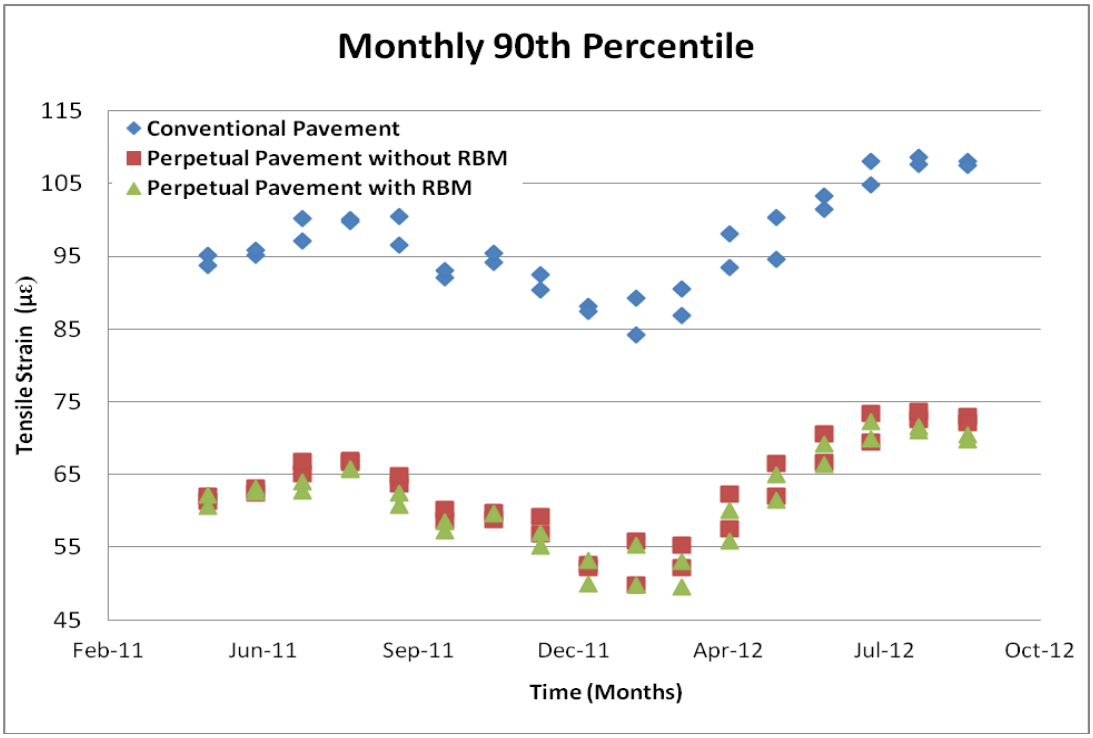

Figure 4-1: Monthly 90th Percentile of Tensile Strain in Highway 401 Test Sections

To evaluate the mean of the monthly 90th percentile of the three sections, a statistical t-test was performed three times to compare all the means of the 90th percentile of the two perpetual sections both with each other and with the means of the conventional section. The t-tests were implemented at a significance level (α) = 95 %. Table 4-2 lists the results of the paired t-tests that compared the mean 90th percentile of strain in the perpetual pavement section containing the RBM and that of the perpetual pavement section without the RBM.

Table 4-2: t-test comparing Monthly 90th Percentile of Tensile Strain in Perpetual Sections

H0: MEAN (Monthly 90th percentile of Perpetual Pavement with RBM) - MEAN((Monthly 90th percentile of Perpetual Pavement without RBM) = 0		
H1: MEAN (Monthly 90th percentile of Perpetual Pavement with RBM) - MEAN((Monthly 90th percentile of Perpetual Pavement without RBM) < 0		
	Perpetual Pavement with RBM	**Perpetual Pavement without RBM**
Mean Strain	61.48	62.76
Variance	42.17	43.66
Number of Observations	34	34
Hypothesized Mean Difference	0	
Degree of Freedom	33	
t Stat	-6.29	
P(T<=t) one-tail	2.03E-07	
t Critical one-tail	1.69	

For a P-value (2.03E-7) with a significance level of (0.05), there is strong statistical evidence to reject the null hypothesis. The physical interpretation of the results reveals a significant difference between the average mean of the monthly 90th percentile for the perpetual pavement with the RBM compared to that of the perpetual pavement without the RBM. The results of the one-tailed test show that the mean strain value for the Superpave (SP) 25 with the RBM is less than that for conventional SP 25. The decrease in tensile strain is attributed to the additional 0.8 % asphalt binder content above the optimum. The use of the RBM layer to date at the bottom of the asphalt layers is therefore showing reduced tensile strain at that location.

Another paired t-test was conducted in order to compare the monthly 90th percentile for the tensile strain in the perpetual section without the RBM and the data collected from the conventional section. Table 4-3 summarizes the results of this comparison.

Table 4-3: t-test Comparing Monthly 90th Percentile of Tensile Strain in Perpetual without RBM and Conventional Sections

H0: MEAN (Monthly 90th percentile of Perpetual Pavement without RBM) - MEAN((Monthly 90th percentile of Conventional Pavement) = 0		
H1: MEAN (Monthly 90th percentile of Perpetual Pavement without RBM) - MEAN((Monthly 90th percentile of Conventional Pavement) < 0		
	Perpetual Pavement without RBM	**Conventional Pavement**
Mean Strain	62.76	96.88
Variance	43.66	44.37
Number of Observations	34	34
Hypothesized Mean Difference	0	
Degree of Freedomf	33	
t Stat	-162.29	
P(T<=t) one-tail	8.82E-50	
t Critical one-tail	1.69	

The P-value (8.82E-50) associated with this test also indicates statistical evidence for the rejection of the null hypothesis. The statistical analysis therefore shows that the average mean of the monthly 90th percentile of the tensile strain for the conventional pavement is higher than that for the perpetual pavement without RBM. This conclusion can be supported based on a simple interpretation of Figure 4-1.

A similar paired t-test was performed in order to compare the monthly 90th percentile of the tensile strain data collected for the perpetual pavement section with the RBM to the data for the conventional pavement section. The results of this statistical test are summarized in Table 4-4.

Table 4-4: t-test Comparing Monthly 90th Percentile of Tensile Strain in Perpetual with RBM and Conventional Sections

H0: MEAN (Monthly 90th percentile of Perpetual Pavement with RBM) - MEAN((Monthly 90th percentile of Conventional Pavement) = 0		
H1: MEAN (Monthly 90th percentile of Perpetual Pavement with RBM) - MEAN((Monthly 90th percentile of Conventional Pavement) < 0		
	Perpetual Pavement with RBM	**Conventional Pavement**
Mean Strain	61.47	96.88
Variance	42.16	44.37
Number of Observations	34	34
Hypothesized Mean Difference	0	
Degree of Freedom	33	
t Stat	-118.45	
P(T<=t) one-tail	2.82E-45	
t Critical one-tail	1.69	

Based on the P-value (2.82E-45) and a direct interpretation of Figure 4-1, the results of this statistical test are clear. The mean tensile strain of the monthly 90th percentile for the perpetual section with the RBM is less than that for the conventional section and the difference between the two sections is statistically significant with a confidence level of 95%.

These statistical t-tests were executed in order to illustrate the monthly tensile strain occurring at the bottom of the asphalt layers. The results lead to a clear expectation with respect to the future tensile strain at the bottom of asphalt layers in the three test sections. However, the monthly tensile strain by itself is insufficient for an overall evaluation of the structure and long-term change in tensile strain in the pavement sections. Recent literature has reported the use of the cumulative 90th percentile for each test section as a means of evaluating the tensile strain of the sections [Timm, 2011]. The cumulative tensile strain throughout the service life of the pavement section indicates deterioration and the

development and propagation of cracks over the long term. The primary factor monitored for this research project involved the determination of the 90th percentile for the cumulative tensile strain at the bottom of the asphalt layers. The analysis and modeling of the in-situ tensile strain were conducted with the goal of developing criteria for predicting the value of the cumulative 90th percentile based on laboratory testing and other environmental factors. Figures 4-2 and 4-3 depict the cumulative 90th percentile for the two perpetual pavement sections and for the conventional pavement section.

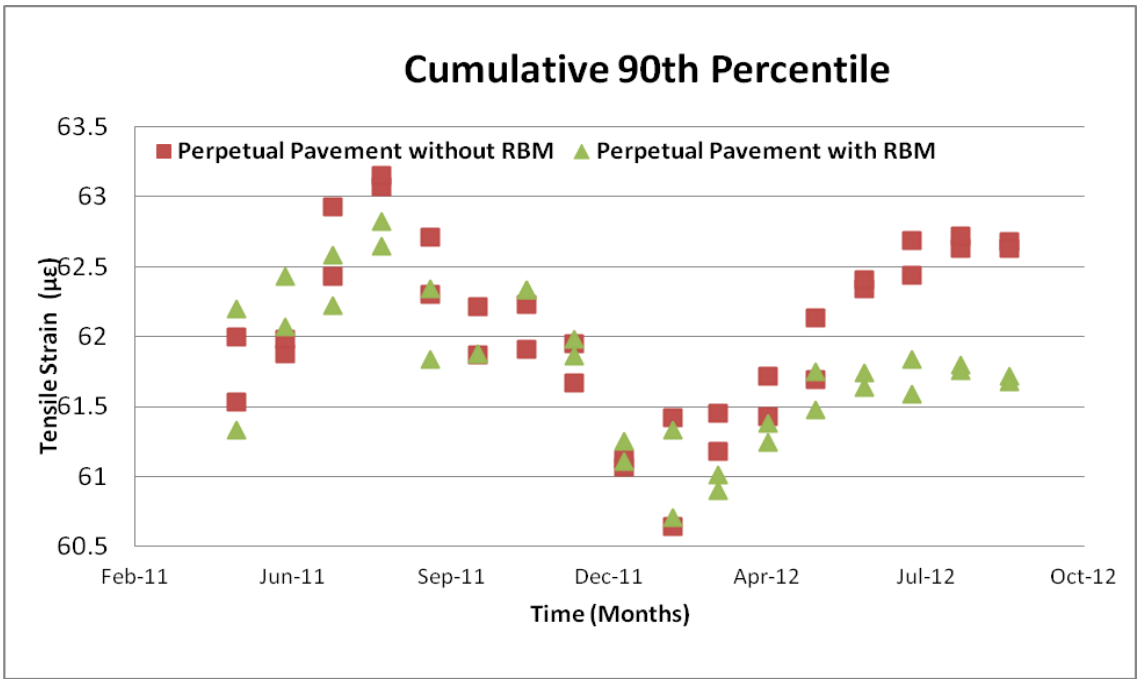

Figure 4-2: 90th Percentile of Cumulative Tensile Strain in Perpetual Pavement Sections

The cumulative data set was developed by totalling the previously collected in-situ strain measurements that were taken from May 2011 to the latest data collection date. The difference between **t**his data set and the previous one is that this set exhibits the aging effect and long-term deterioration of the pavement while the monthly 90th percentile is primarly

influenced by temperature variation and will not show the long term deterioration of tensile strain. The changes that can be seen in the cumulative 90^{th} percentile are relatively large and might be affected by temperature changes at the beginning of the lifetime of the pavement. This shift could be the result of the addition of one month of data to a set of data accumulated over only three or four months so that the effect of the new data would then be noticeable when the two data sets are combined. However, this effect decreased as the pavement aged because 20 months of data did not have a significant impact on the cumulative 90^{th} percentile for the total period. When the pavement reaches a specific end of life servicebility level, the 90^{th} percentile of the cumulative data becomes almost a constant value, increasing only marginally with increased age until the end of its service life. The perpetual pavement design is considered successful when the value of the cumulative tensile strain is below the 70 με limit and the vertical compressive strain on top of the subgrade is below 200 με. However, this study focused on the tensile strain constraint only as a means of accurately predicting how changes in its levels affect highways characterized by a traffic pattern similar to that of Highway 401.

The quantity of strain data collected per month was inconsistent due to changes in the traffic pattern and due to technical difficulties, such as the loss of electric power provided by the solar panels. The effect of adding recent data to the previously collected database therefore depends on the specific quantity and quality of the data collected.

A paired t-test was performed in order to compare the mean of the 90^{th} percentiles of the cumulative tensile strain for the perpetual section with the RBM and the data collected from

the perpetual pavement section without the RBM. Table 4-5 summarizes the results of this comparison.

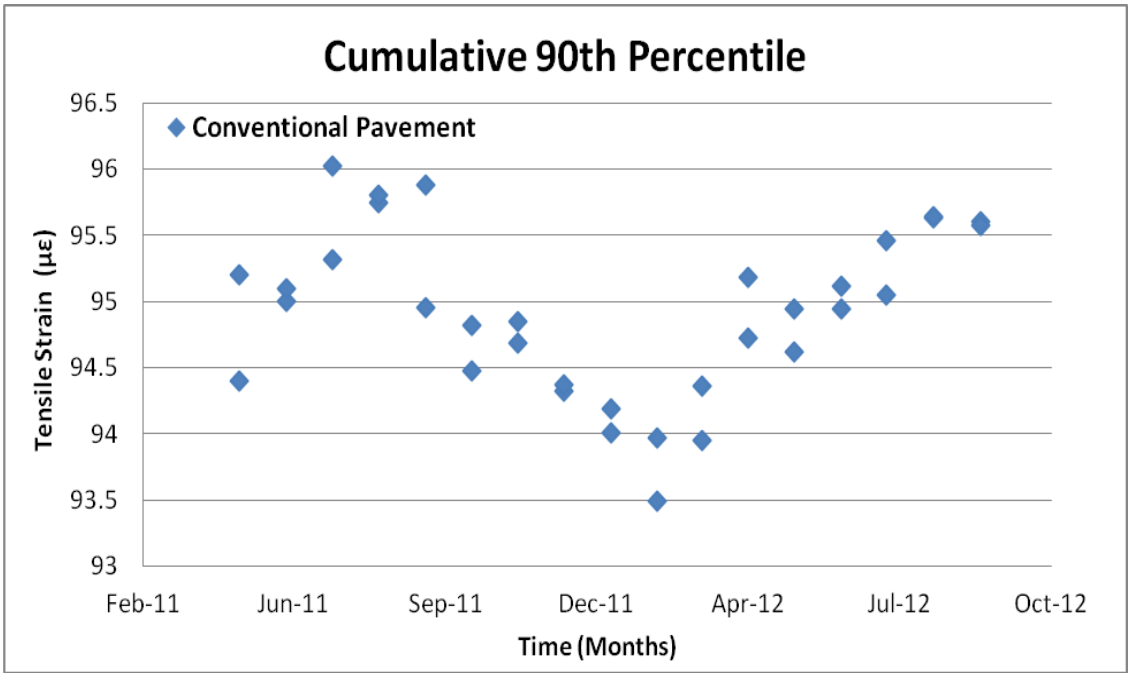

Figure 4-3: 90th Percentile of Cumulative Tensile Strain in Conventional Pavement Section

Table 4-5: t-test for 90th Percentile of Cumulative Tensile Strain in Perpetual Designs

H0: MEAN (Cumulative 90th percentile of Perpetual Pavement with RBM) - MEAN(Cumulative 90th percentile of Perpetual Pavement without RBM) = 0		
H1: MEAN (Cumulative 90th percentile of Perpetual Pavement with RBM) - MEAN((Cumulative 90th percentile of Perpetual Pavement without RBM) < 0		
	Perpetual Pavement with RBM	**Perpetual Pavement without RBM**
Mean Strain	61.78	62.06
Variance	0.26	0.38
Number of Observations	34	34
Hypothesized Mean Difference	0	
Degree of Freedom	33	
t Stat	-4.07	
P(T<=t) one-tail	0.000138	
t Critical one-tail	1.69	

The P-value (0.000138) of this test shows statistical evidence for the rejection of the null hypothesis. The statistical analysis therefore reveals that the average mean of the 90th percentile of the cumulative tensile strain for the perpetual pavement without the RBM is higher than that for the perpetual pavement with the RBM. However, for this comparison, the P-value is much larger than that resulting from the previous tests, which indicates that the two sections have just begun to exhibit a diverging pattern with respect to the tensile strain values. This effect can be observed in Figure 4-2, which shows divergence in May 2012. Further details related to the analysis of the in-situ tensile strain data collected and the regression models are presented in section 4.4.

4.2.1 Guelph Test Section

The in-situ tensile strain data collected from the perpetual pavement with RBM test section in Guelph is summarized in this section. The construction of the test section was completed in July 2009. The data collection started in August 2009. This test section is only exposed to traffic during the paving season, normally April to November, due to the construction winter shutdown. This test section was constructed adjacent to the weigh scale in the asphalt plant. Therefore, the traffic passing on this section is characterized by slow speed as the trucks pass over it directly following being weighed using a static weight scale. In addition, it should be noted that all the vehicles passing on this test section are loaded asphalt trucks. This would explain the small variation in the collected in-situ strain as the 90th percentile of in-situ strain was very close to the 80th percentile. However, the 90th percentile of the tensile strain data is presented in this section for consistency of the data summarization in this thesis.

Figure 4-4 presents the monthly 90th percentile of the tensile strain in the perpetual pavement section in Guelph. It is noted that the discontinuity of data collection took place from December to March in every year.

Figure 4-5 presents the 90th percentile of the cumulative tensile strain in the perpetual pavement section in Guelph. The 90th percentile of the cumulative tensile strain remains constant during the period from December to March as no data is added to the cumulative data set. The amplitude of change in Figure 4-5 decreases along with the increase of pavement age. It is interesting to note that the tensile strain appears to have leveled out although continued monitoring should be carried out.

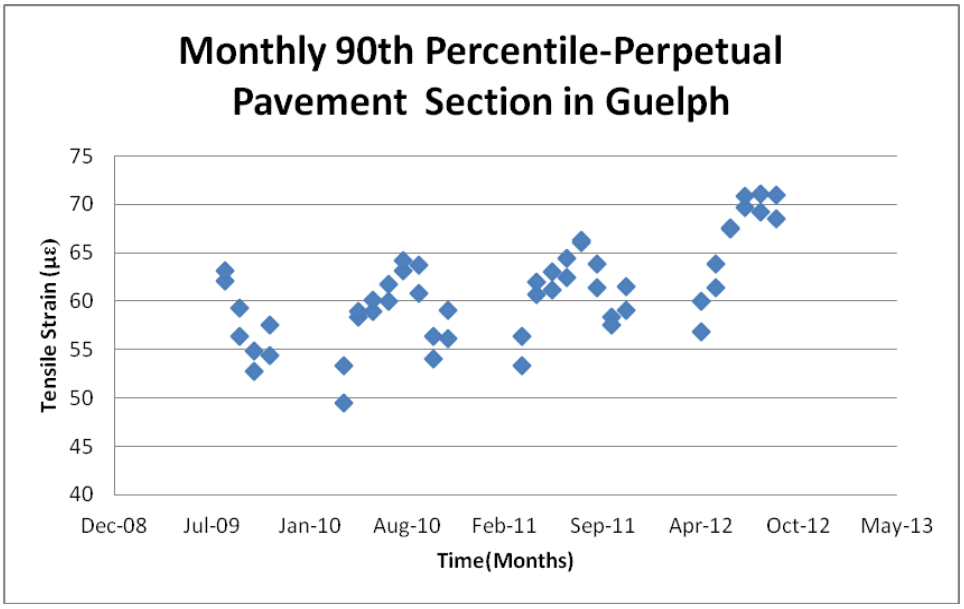

Figure 4-4: Monthly 90th Percentile of Tensile Strain in Guelph Test Section

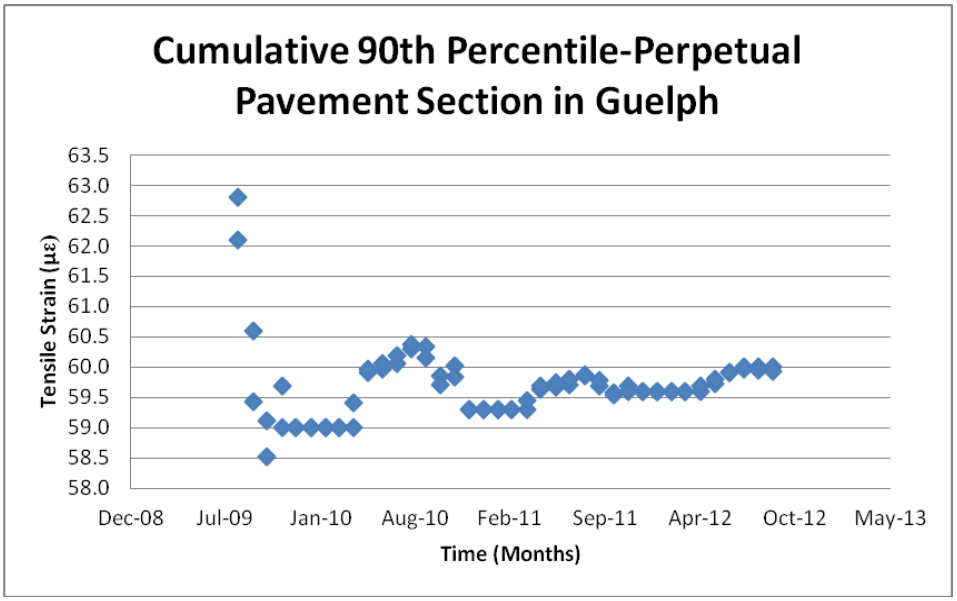

Figure 4-5: 90th Percentile of Cumulative Tensile Strain in Guelph Test Section

4.3 Laboratory Testing Procedure, Results and Analysis

This section describes the laboratory testing executed throughout this research project. The tests took place in the CPATT laboratory at the University of Waterloo. The asphalt samples were provided during construction by Capital Paving Inc.; the asphalt pavement contractor was a subcontractor on the project and they were responsible for the construction of the test section on Highway 401. The prime contractor was Aecon Group Inc. The experimental matrix for this research project included the advanced testing of the asphalt materials. The experiments conducted included the resilient modulus test, the dynamic modulus test and the Thermal Stress Restrained Specimen Test (TSRST). The samples were prepared in the CPATT laboratory according to the American Association of State Highway and Transportation Officials (AASHTO) and the American Society for Testing and Materials (ASTM) specifications [AASHTO, 2010, ASTM, 2009 b].

A gyratory compactor and an asphalt vibratory compactor (AVC) were used to prepare the specimens for a variety of tests. The AASHTO and ASTM standards specify a 6 % to 8 % range for an acceptable percentage of air voids in laboratory-prepared specimens, and the specimens were compacted accordingly [AASHTO, 2010] [ASTM, 2009 b]. The preparation of proper specimens was a long and complicated process that included the preparation of more than 50 asphalt beams and 40 asphalt cylinders in order to determine the proper compaction force, time, and temperature required to meet the appropriate mix properties.

Table 4-6 presents the Job Mix Formula (JMF) for all asphalt mixes used in different layers of the construction of the test sections. The mix designs of the various asphalt mixes used in the construction of the test sections are presented in Appendix B.

The following subsections explain the laboratory testing procedure and present the results for each of the material characterization tests.

Table 4-6: Summary of Asphalt Mix Design

	Job Mix Formula													
	Gradation Percentage Passing												**AC% - Binder**	**RAP %**
	25	**19**	**16**	**12.5**	**9.5**	**4.75**	**2.36**	**1.18**	**600**	**300**	**150**	**75**		
SP 12.5		100	100	99.9	85.6	53	35.6	26.1	17.9	10.1	5.4	3.2	4.5% 64-28	-
SP 19	100	96.9	89.3	78.7	66.3	49.6	45.2	28.9	16.7	10.1	6.3	4.4	4.7% 64-28	-
SP 25	97.1	89.2	80.9	71.5	62.1	47.3	37.8	23.8	14.2	8.9	5.7	4	4.3% 58-28	15%
SP 25 RBM	97	89.3	79.7	68.7	58.4	46.4	42.4	27.2	15.8	9.6	6.1	4.3	5.1% 58-28	-

4.3.1 Resilient Modulus

The resilient modulus test provides an indication of the fatigue and thermal cracking potential of the HMA. The resilient modulus of the samples was tested according to ASTM D7369-09 standards [ASTM, 2009 a]. Samples were prepared using the gyratory compactor in the CPATT laboratory at the University of Waterloo. The cylinders produced by the gyratory compactor were sawed to obtain samples within the dimensions recommended in ASTM standards [ASTM, 2009 a]. In addition, the air voids of each sample were checked prior to testing. The ASTM standard recommends air void percentage for laboratory prepared samples to be in the range from 6% to 8%. The samples that were out of range were excluded from the resilient modulus testing procedure and other samples were prepared to replace them.

The Indirect Tensile Strength (ITS) test was performed prior to concluding the resilient modulus test. This was conducted on different samples to determine the preconditioning for the applied loading. The ITS test was conducted in accordance with the ASTM D6931-07 [ASTM, 2007]. The air void ratio was also determined for the ITS samples and the tested samples were all within the acceptable air voids. Table 4-7 presents the results of the Indirect Tensile Strength test.

Table 4-7: Indirect Strength and Air Voids for Different Mixes

Sample Number	Superpave 12.5	Superpave 19	Superpave 25	Superpave 25 RBM
1	887 (6.3%)	807 (7.3%)	854 (7.2%)	993 (7.3%)
2	871 (6.5%)	835 (6.8%)	871 (6.8%)	1009 (6.8%)
3	841 (7.4%)	819 (7.0%)	885 (6.7%)	974 (7.4%)
4	857 (7.2%)	791 (7.5%)	902 (6.4%)	1028 (6.1%)
Average ITS (KPa)	864	813	878	1001
Standard Deviation	19.8	18.6	20.1	22.9

Note: ITS is Indirect Tensile Strength RBM is Rich Bottom Mix
RAP is Reclaimed Asphalt Pavement (Air Voids) %

The ASTM D6931-07 standard [ASTM, 2007] details the ITS testing procedure based on field cores from several pavement sections. For this research, the results obtained from the ITS laboratory samples were somewhat lower than the ITS results reported in the ASTM standards because of the discrepancies between the percentage of air voids in the laboratory-prepared samples and that in the field core samples. The air void percentages for the laboratory samples were between 6.1 % and 7.5 % while the results reported in the ASTM standard were for field samples characterized by lower air void ratios.

The additional 0.8 % of asphalt binder (AC) in the SP 25 RBM mix compared to the SP 25 with the RAP significantly improved the ITS and thus is expected to improve the resistance of the bottom asphalt layer to moisture and fatigue damage over the pavement life cycle.

The resilient modulus results for the four replicates are listed in Table 4-8.

Table 4-8: Resilient Modulus Results (MPa)

Sample Number	Superpave 12.5		Superpave 19		Superpave 25 RAP		Superpave 25 RBM	
1	2315	AV	2119	AV	3014	AV	2636	AV
	2091	8.0%	2424	7.3%	2998	7.5%	2340	8.2%
2	2109	AV	1928	AV	2457	AV	3063	AV
	1887	7.5%	2029	7.6%	2417	8.2%	2844	7.4%
3	2306	AV	2183	AV	2921	AV	2506	AV
	2490	7.8%	2316	7.2%	2916	7.6%	2315	8.4%
4	2125	AV	2292	AV	2257	AV	2824	AV
	2073	8.2%	2117	7.2%	2405	8.3%	2740	7.8%

Note: The samples highlighted were excluded from the calculation of the average resilient modulus due to unacceptable air void ratios. Although its air void ratio was acceptable, sample number 2 of SP 12.5 was also excluded due to noticeable segregation.

The resilient modulus results were filtered and analyzed following the ASTM D7369-09 standard [ASTM, 2009 a]. Some samples were observed to be outside the air void limit recommended for laboratory-prepared samples. These specimens were not considered in the structural analysis. Overall, four or more consistent resilient modulus results were determined for each mix. Table 4-9 summarizes the average resilient modulus value for each mix, along with the standard deviation.

Table 4-9: Summary of Resilient Modulus (MPa)

	SP 12.5	SP 19	SP 25	SP 25 RBM
Average Resilient Modulus (MPa)	2300	2176	2962	2867
Standard Deviation	163	162	50	137

4.3.2 Dynamic Modulus

The dynamic modulus test is used to measure the visco-elastic properties of the asphalt mixture. This test is an indicator of how the HMA will perform over a range of loading and temperature scenarios. An understanding of dynamic modulus test results can provide insight into evaluating the stiffness of the layers that contribute to the perpetual pavement design. The dynamic modulus is generally expressed as stress divided by strain. For testing purposes, the stress applied on the samples representing different mixes is constant because the testing load is unchanged, as are the cross-sections of the samples. An increase in the dynamic modulus value thus reflects a decrease in the strain corresponding to the same load, which can also be interpreted as an increase in the stiffness of the asphalt mix. Similarly, a decrease in the dynamic modulus results indicates an increase in strain and can be interpreted as decrease in the stiffness of the asphalt mix.

For this study, the dynamic modulus testing was performed according to the AASHTO TP62-07 specifications [AASHTO, 2007], and four replicates were tested for each asphalt mix. Although the air void ratios of some specimens were observed to be outside the specified range, all of the specimens prepared were tested. The tests were conducted at the following six loading frequencies (0.1 Hz, 0.5 Hz, 1 Hz, 5 Hz, 10 Hz, and 25 Hz) and five temperatures: -10 ºC, 4 ºC, 21 ºC, 37 ºC, and 54 ºC. The average dynamic modulus value for each mix was calculated from samples that generated results with no more than a 10 % discrepancy. Certain samples were eliminated because of sample production where inconsistent results were also observed and subsequently traced segregation in the samples or air void ratios that were beyond acceptable limits [El-Hakim, 2010].

The dynamic modulus results were used to obtain master curves for the asphalt mixes based on the AASHTO PP62-09 specification [AASHTO, 2009]. Table 4-10 summarizes the average dynamic modulus results of the samples obtained during construction. At this point, the samples had not been subjected to environmental conditions, freeze-thaw cycles, or aging. They were retested after exposure to one season of typical freeze-thaw cycling for Southern Ontario, and the results after conditioning are presented in Table 4-11. Each sample was exposed to 45 freeze-thaw cycles in the laboratory.

The methodology of developing master curves relies on the conversion of the results obtained at different temperatures into a specific reference temperature. This converted temperature is usually 21 ºC (70 ºF) [AASHTO, 2009]. The shifting process results in the calculation of a reduced frequency, leading to a corresponding shift in the |E*| results [AASHTO, 2009]. The master curve is then developed using the shift factors. In the master curve, a low reduced frequency represents high-temperature testing, whereas a high modified frequency on the master curve represents the low-temperature testing of the dynamic modulus samples.

Asphalt material is characterized as a visco-elastic material, which means that the temperature of the specimen has a significant impact on the strain developed and on the dynamic modulus results. Permanent deformation of viscoelastic materials, such as rutting, is expected to occur at high temperatures (37 ºC and 54 ºC) [Shenoy, 2002, Witczak, 2007]. Figure 4-6 shows the dynamic modulus test results for the various testing temperatures and loading frequencies. As noted, the line represents the master curve for that asphalt mix for

which all the shift factors have been used in order to develop the curve. The master curves representing the dynamic modulus results for all the mixes are shown in Figure 4-7.

The absolute value of the complex modulus (|E*|) is defined as the dynamic modulus and is calculated based on the following [Pellinen, 2002]:

$$|E^*| = \frac{\sigma_0}{\varepsilon_0} \qquad (4\text{-}1)$$

where:

|E*| is the Dynamic Modulus

σ_0 is the peak stress amplitude (applied load / sample cross sectional area)

ε_0 is the peak amplitude of recoverable axial strain (ΔL/L)

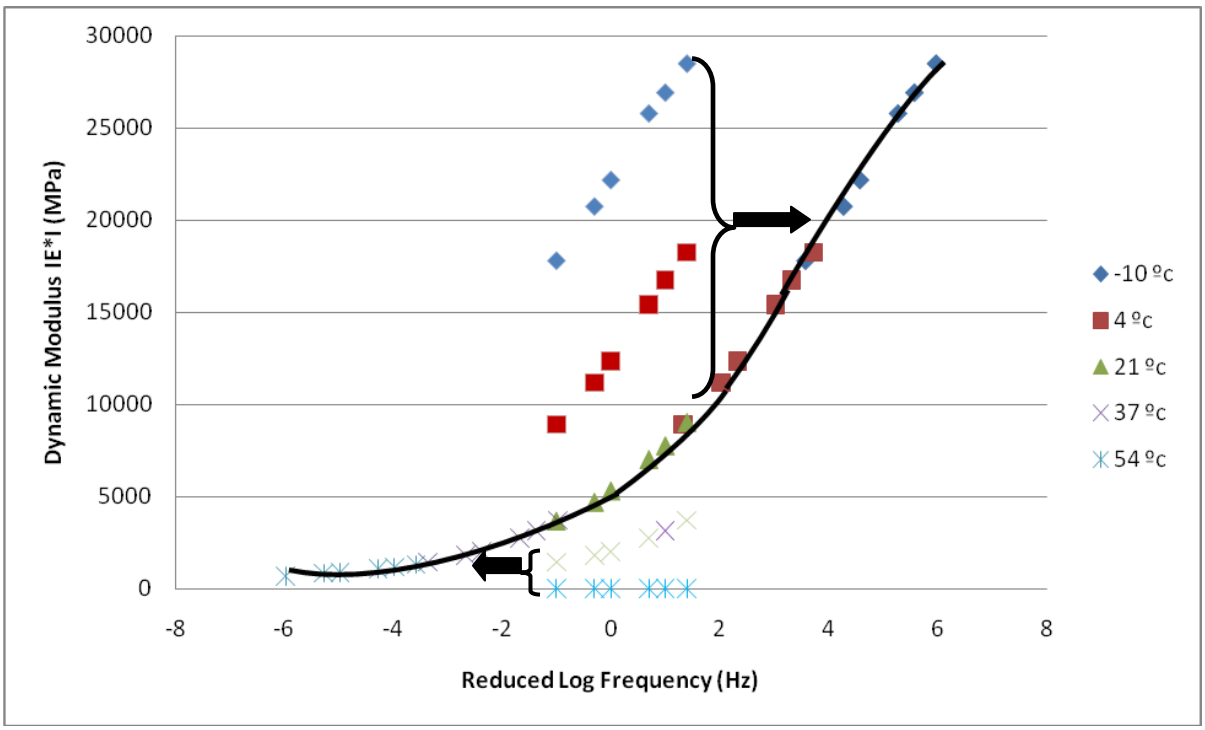

Figure 4-6: Master Curve Theory

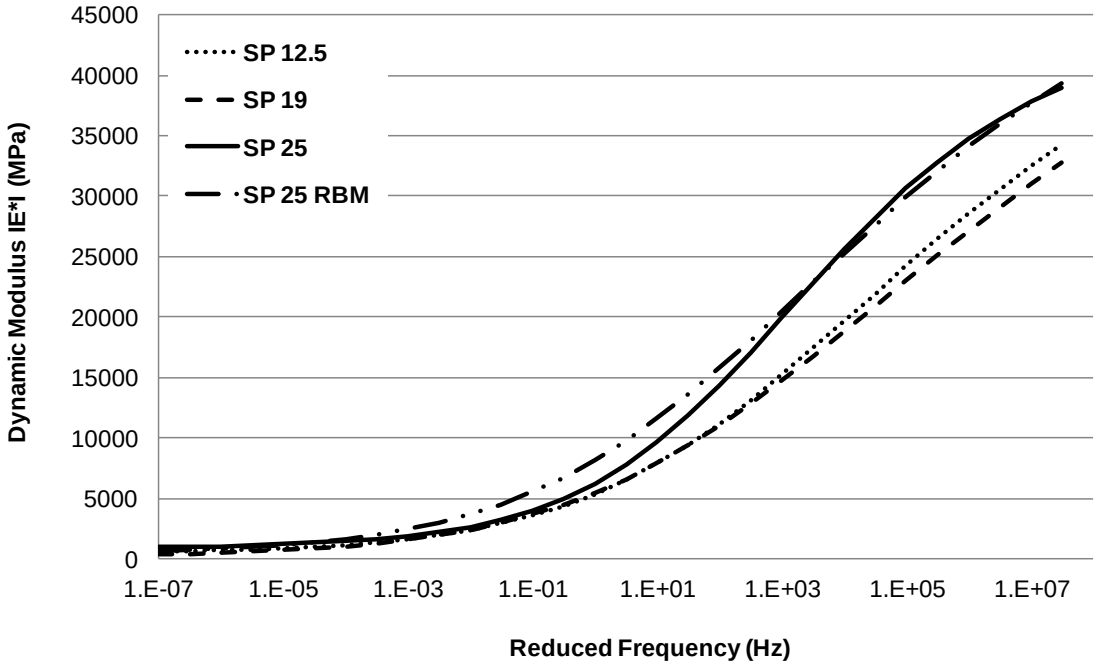

Figure 4-7: Master Curve for all Four Mixes

Table 4-10: Average Dynamic Modulus Results (MPa) at the Year of Construction

Temp (°C)	Frequency (Hz)	SP 12.5	SP 19	SP 25	SP 25 RBM
-10	**25**	28472	26582	34705	33985
	10	26903	25600	33230	32382
	5	25778	24568	31504	31685
	1	22178	21367	27732	28454
	0.5	20746	19897	26412	26897
	0.1	17813	16920	22506	23160
4	**25**	18235	16880	22762	23188
	10	16726	16117	21342	21676
	5	15429	15131	19603	20377
	1	12333	12156	15694	16650
	0.5	11189	11069	14001	15219
	0.1	8900	8795	10835	12566
21	**25**	9014	9287	11351	13264
	10	7757	8085	9625	11473
	5	7017	7088	8497	10391
	1	5317	5292	6098	8040
	0.5	4706	4799	5417	7217
	0.1	3688	3697	4149	5688
37	**25**	3711	3491	5462	6944
	10	3147	2857	4388	5803
	5	2750	2466	3784	5201
	1	2008	1833	2745	3789
	0.5	1812	1642	2424	3376
	0.1	1440	1330	2052	2597
54	**25**	1310	988	1543	2275
	10	1187	775	1344	1834
	5	1078	670	1271	1647
	1	875	513	1156	1257
	0.5	830	473	1105	1132
	0.1	681	403	1028	940

Table 4-11: Average Dynamic Modulus Results (MPa) after One Year of Construction

Temp (°C)	Frequency (Hz)	SP 12.5	SP 19	SP 25	SP 25 RBM
-10	**25**	23073	25367	23490	25842
	10	22386	24749	23246	25318
	5	21603	23985	22769	24512
	1	19089	20950	20578	21700
	0.5	18109	19850	19904	20622
	0.1	16691	17321	17726	18239
4	**25**	14555	16004	19093	17834
	10	13922	15188	18341	17981
	5	13067	13961	16702	16835
	1	10774	11457	14224	14193
	0.5	9984	10418	13029	13116
	0.1	8039	8619	10681	10962
21	**25**	9324	9835	10986	10944
	10	8370	8585	9687	9840
	5	7603	7547	8558	9402
	1	5797	5838	6283	7401
	0.5	5167	5254	5601	6666
	0.1	4057	4169	4375	5299
37	**25**	4034	3696	3485	5262
	10	3348	3117	2853	4563
	5	2920	2714	2449	3989
	1	2174	2064	1791	3023
	0.5	1961	1861	1610	2706
	0.1	1556	1527	1344	2178
54	**25**	1179	1061	1007	1523
	10	959	863	787	1269
	5	826	757	666	1091
	1	614	605	521	829
	0.5	545	565	486	752
	0.1	448	495	429	634

The analysis of the dynamic modulus results at high temperatures (37 ºC and 54 ºC) shows that the mean dynamic modulus of SP 25 with the RBM is higher than the average |E*| of regular SP 25 with the RAP. The increase in the average |E*| reflects the benefit expected because of the additional binder in the SP 25 RBM mix. This increase signifies the enhanced elasticity of the asphalt mix. The SP 25 RBM mix exhibits high resistance to fatigue cracking because of its ability to recover from elastic strain [El-Hakim, 2012 a]. Table 4-12 summarizes the t-test results between the mean of the dynamic modulus results for the SP 25 with the RBM, on the one hand, and the mean of the dynamic modulus results for the SP 25 at 37 ºC and 54 ºC. The P-value resulting from the t-test indicates very strong evidence for the rejection of the null hypothesis. Thus, the mean dynamic modulus value for SP 25 with the RBM is greater than that for SP 25, with a significance level of 95 %.

Table 4-12: t-test for Dynamic Modulus Average for SP 25 and SP 25 RBM at 37ºC and 54ºC

H0: MEAN (SP 25 RBM) - MEAN(SP 25) = 0		
H1: MEAN(SP 25 RBM) - MEAN(SP 25) > 0		
	SP 25	**SP 25 RBM**
Mean Dynamic Modulus	2359	3066
Variance	2,154,059	3,965,168
Observations	12	12
Hypothesized Mean Difference	0	
Degree of Freedom	11	
t Stat	-4.39	
P(T<=t) one-tail	0.0005	
t Critical one-tail	1.8	

The stress applied on the samples for the testing during the year of construction was identical to that applied in the second round of testing after the freeze-thaw conditioning. The change in the |E*| results is thus inversely proportional to the strain in the asphalt sample that is

produced by the same stress. If the |E*| value is observed to decrease after the sample has been subjected to the equivalent of one year freeze-thaw cycles, this change would indicate that the strain resulting from the same stress has increased. Therefore, the tendency of the samples to deform has increased; which is an indication of deterioration due to environmental conditioning. It should be noted that this experimental matrix simulates the impact of environmental condition and aging without consideration of variations in traffic loading applied on the pavement throughout the seasons.

The impact of the freeze-thaw cycling is evident in the SP 12.5 evaluation. Regardless of the loading frequency, the freeze-thaw cycles caused deterioration in the stiffness of the mix, particularly at low temperatures. It can be seen that the deterioration in the |E*| results occurs mainly at temperatures of -10 ºC and 4 ºC. The variations in the |E*| results decreased with higher temperatures, such as 21ºC, 37 ºC, and 54 ºC. The surface layer of the perpetual pavement is designed primarily as a rut-resistant layer that is milled and overlayed during the life cycle to eliminate top-down cracking. The results of this layer at high temperatures did not indicate rapid deterioration, but instead, showed that it maintained its structural capacity with respect to rutting resistance after one season of freeze-thaw cycles. Figure 4-8 depicts the dynamic modulus master curve for SP 12.5 for the year of construction and after one year of freeze-thaw cycles.

The freeze-thaw cycling resulted in observations of limited deterioration in the value of |E*|. The partial deterioration occurred mainly for a temperature of -10 ºC and with a high loading frequency of 25 Hz. The small amount of deterioration is a reflection of the fatigue-resistant intermediate asphalt layer, a component that is essential for increasing the life of the

pavement, a prerequisite for a pavement design to be designated perpetual. Figure 4-9 presents the dynamic modulus master curves for SP 19 both for the year of construction and after one year of freeze-thaw cycles.

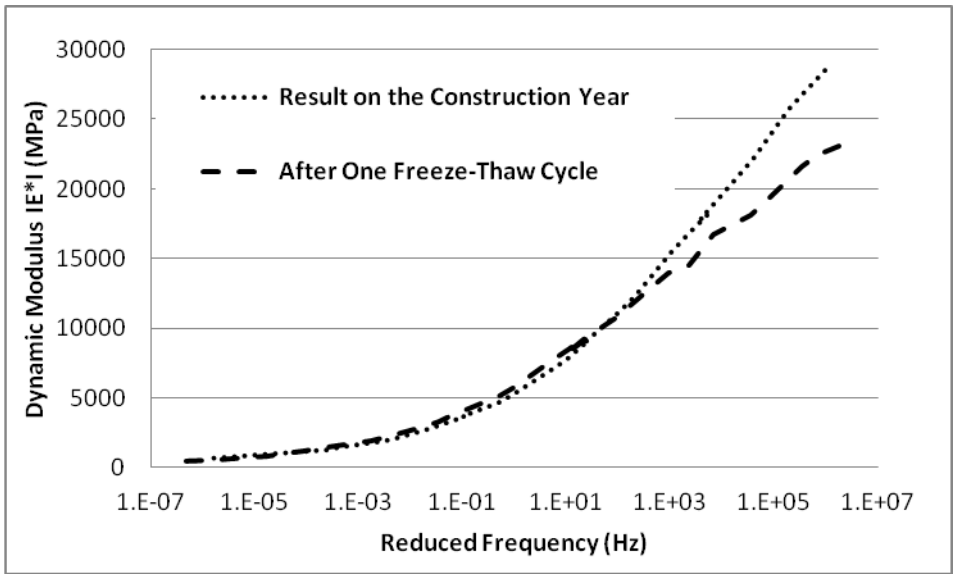

Figure 4-8: Master Curve for Superpave 12.5 Mix

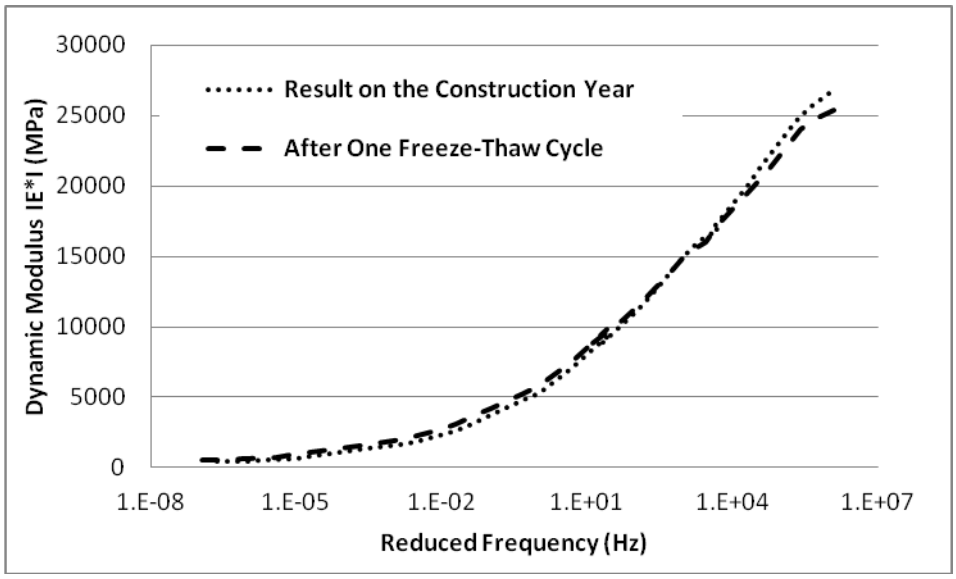

Figure 4-9: Master Curve for Superpave 19 Mix

The lower asphalt layer is an important factor in resistance to bottom-up fatigue cracking. The ability of this layer to resist such cracking is critical for extending the life of the pavement because its main purpose in the design is to provide sufficient structural capacity to resist fatigue cracking. This layer must also be sufficiently flexible to withstand the expansion and contraction caused by seasonal temperature variations. The two alternative mixes used as bottom asphalt layers in the perpetual pavement sections with and without RBM were SP 25 and SP 25 RBM, respectively.

The results produced with SP 25 revealed noticeable deterioration in the stiffness of the mix and a decrease in the |E*| results, primarily with temperatures of -10 ºC and 4 ºC. Figure 4-10 shows the dynamic modulus master curves for SP 25 for the year of construction and after one year of freeze-thaw cycles.

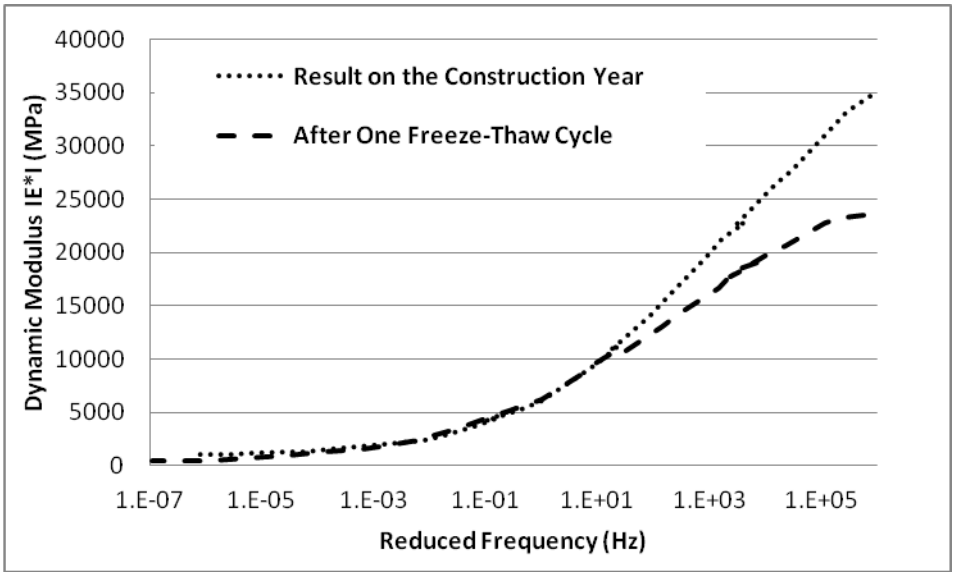

Figure 4-10: Master Curve for Superpave 25 Mix

The deterioration indicated in the results for the SP 25 RBM mix was limited to its stiffness in tests at -10 ºC, 4 ºC, and 21 ºC. At high temperatures, this mix maintained a high level of structural ability to resist rutting. The SP 25 RBM mix also demonstrated superior stiffness at low temperatures compared to the conventional SP 25 mix. This finding indicates that the additional 0.8 % of asphalt binder content increased the ability to withstand freeze-thaw cycles with less deterioration. At -10 ºC and a frequency of 25 Hz, the average |E*| of SP 25 RBM was less than that of SP 25 by 10 % although the |E*| value of mixes differed only slightly in the year of construction. Figure 4-11 shows the dynamic modulus master curves for SP 25 RBM at the year of construction and after one year of freeze-thaw cycles.

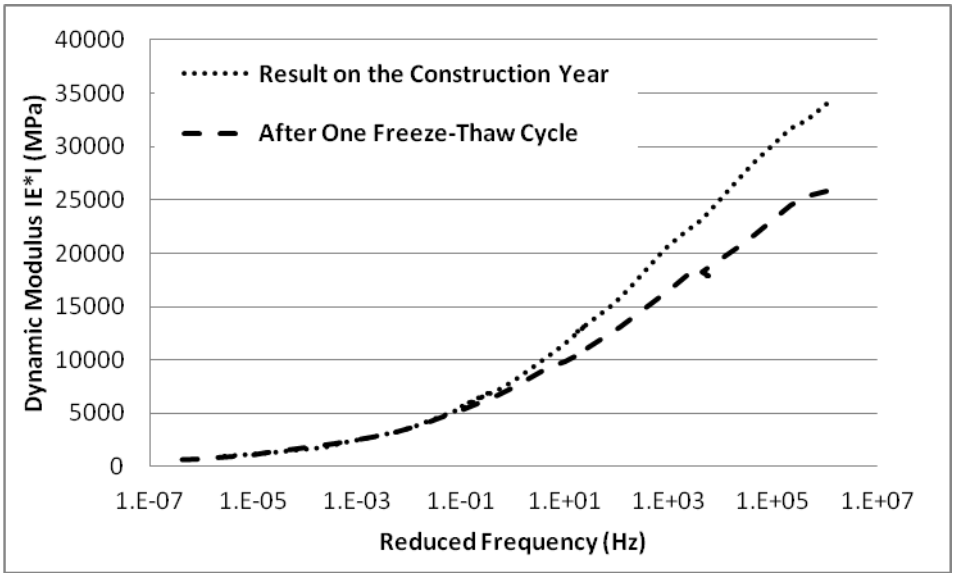

Figure 4-11: Master Curve for Superpave 25 RBM Mix

The deterioration of the pavement mixes was tested for statistical significance and showed that using a t-test, the means of the pairs of samples verified that the decrease in the |E*| results at low temperature were statistically significant. The confidence level assumed in all

t-tests was 95 %. Table 4-13 summarizes the results of the t-tests performed on the |E*| data for all of the asphalt mixes at -10ºC [El-Hakim, 2012 a].

Table 4-13: Results of t-test Performed for Different Mixes

	SP 12.5		SP 19		SP 25		SP 25 RBM	
	Year 0*	**Year 1**	**Year 0**	**Year 1**	**Year 0**	**Year 1**	**Year 0**	**Year 1**
Null Hypothesis	H_o: μ_0- μ_1=0		H_o: μ_0- μ_1=0		H_o: μ_0- μ_1=0		H_o: μ_0- μ_1=0	
Alternate Hypothesis	H_1: μ_0- μ_1>0		H_1: μ_0- μ_1>0		H_1: μ_0- μ_1>0		H_1: μ_0- μ_1>0	
Mean	23648	20866	22489	22037	29348	21286	29427	22705
Variance	1.6E+7	7.0E+6	1.4E+7	1.1E+7	2.0E+7	5.2E+6	1.7E+7	8.3E+6
t_{Stat}	5.95		2.18		11.55		11.44	
P(T<=t) one-tail	4.82E-05		0.03		8.58E-08		9.5E-08	
$t_{Critical}$ one-tail	1.80		1.80		1.80		1.80	
Conclusion	Reject Null Hypothesis		Reject Null** Hypothesis		Reject Null Hypothesis		Reject Null Hypothesis	

* The initial |E*| in the year of construction is presented as "Year 0," and the |E*| after one season of environmental conditioning is presented as "Year 1."

** The P-value in the case of SP 19 is less than the 0.05 (the assumed alpha value based on a 95 % confidence interval). The null hypothesis is rejected with weak evidence.

Based on the statistical testing, there is strong evidence that the freeze-thaw cycling resulted in a decrease of the mean value of |E*| at -10 ºC for mixes SP 12.5, SP 25, and SP 25 RBM. This conclusion was based on a confidence level of 95 %. Weak statistical evidence also indicates that the SP 19 mix exhibits a slight decrease in the |E*| values at -10 ºC [El-Hakim, 2012 a].

A statistical t-test was conducted in order to investigate the benefits gained by the additional 0.8 % asphalt binder content to the SP 25. The data for the year of construction and for one year of freeze-thaw conditioning were compared. The t-test of the means of the pairs of samples was performed using the results for SP 25 and SP 25 RBM samples at -10 ºC and 4 ºC. Table 4-14 summarizes the t-test results for the year of construction and after one year of environmental conditioning [El-Hakim, 2012 a].

Table 4-14: Result of t-test Comparing SP 25 and SP 25 RBM

	Year 0		**Year 1**	
	SP 25	**SP 25 RBM**	**SP 25**	**SP 25 RBM**
Null Hypothesis	H_o: μ_{25}- $\mu_{25\ RBM}$=0		H_o: μ_{25}- $\mu_{25\ RBM}$=0	
Alternate Hypothesis	H_1: μ_{25}- $\mu_{25\ RBM}$>0		H_1: μ_{25}- $\mu_{25\ RBM}$<0	
Mean	23360	23853	18315	18930
Variance	5.6E+7	5.0E+7	1.7E+7	2.2E+7
t_{Stat}	-1.41		-1.94	
P(T<=t) one-tail	0.09		0.03	
$t_{Critical}$ one-tail	1.71		1.71	
Conclusion	Fail to Reject Null Hypothesis		Reject Null Hypothesis	

The t-test results indicate no significant statistical difference between the average |E*| of the conventional SP 25 and that of SP 25 RBM at temperatures of -10 ºC and 4 ºC in the year of construction. The two mixes exhibited comparable strain values given the same stress was applied at different frequencies. These results were disappointing with respect to the year of construction because they failed to demonstrate the structural benefits of adding the additional 0.8 % binder content to the regular SP 25 mix. However, the statistical t-test for the two mixes at temperatures of -10 ºC and 4 ºC proved that weak evidence exists that the average |E*| value of SP 25 RBM is higher than that of SP 25.

This finding can be interpreted as meaning that the strain that occurs in SP 25 RBM is significantly less than that occurring in regular SP 25 based on the same loading frequency. In contrast, the t-tests conducted after one year of freeze-thaw cycling showed differences, and the benefits of the additional 0.8% asphalt binder were statistically significant after exposure to one year of freeze-thaw cycles [El-Hakim, 2012a].

4.3.3 Thermal Stress Restrained Specimen Test (TSRST)

The Thermal Stress Restrained Specimen Test (TSRST) was developed through the Strategic Highway Research Program (SHRP) and has been identified as an accelerated performance test that simulates low-temperature cracking potential of asphalt mixes. TSRST results represent the ability of asphalt mixes to resist thermal cracking. The failure of a specimen at low temperatures indicates the lack of ability of the asphalt mix to resist thermal cracking. For this research, TSRST testing was performed in the CPATT laboratory. The tests were based on the AASHTO TP 10-93 standard, using an MTS-810 environmental chamber [AASHTO, 1993].

Specimens were prepared using the Asphalt Vibratory Compactor (AVC) machine at the CPATT laboratory and a 390 mm x125 mm x 78 mm mould. The AVC machine applied vibration in order to compact the samples with 120 kPa. The compaction temperatures and times varied from one asphalt mix to another based on the hardness and stiffness of each mix. The compaction time ranged from 3 minutes to 6 minutes, depending on the type of asphalt mix. Several trials were conducted before air voids within the range of 6 % to 8 % could be achieved. The test samples were then saw-cut to the correct dimensions for testing: 250 mm x

50 mm x 50 mm. Figure 4-12 depicts the results of three SP 12.5 surface mix specimens. The failure temperature of the three specimens ranged from -21.2 ºC to -22.4 ºC.

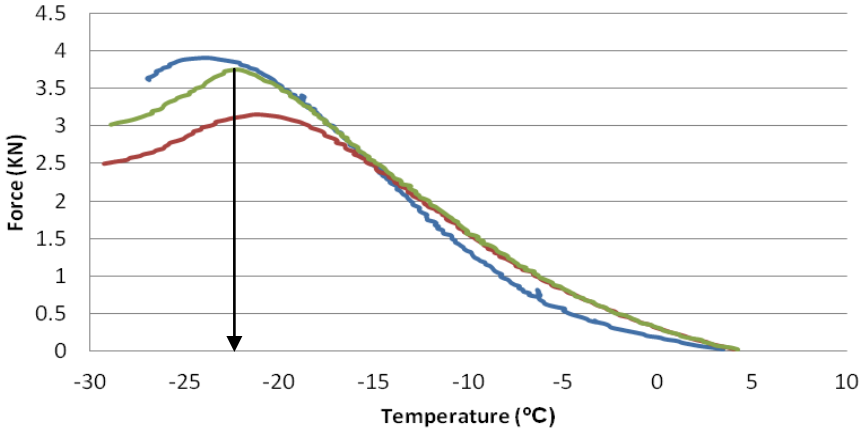

Figure 4-12: TSRST Result for SP 12.5

Figure 4-13 shows the results for the three SP 19 mix specimens. The failure temperature ranged from -26.2 ºC to -27.9 ºC. Variations in the failure temperature or force may occur as a result of changes in the air void ratios of the specimens or because of stone-to-stone contact within the specimens.

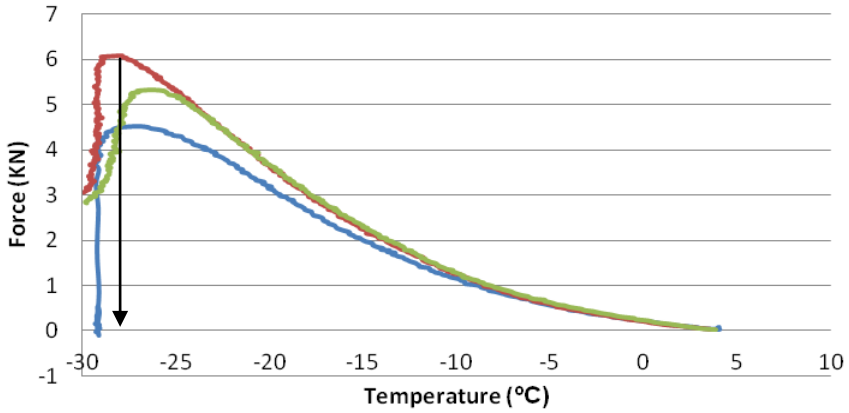

Figure 4-13: TSRST Result for SP 19

Figure 4-14 illustrates the results of the TSRST testing for the three SP 25 mix specimens. It can be observed that the failure temperature for all three specimens is close to -25 ºC. Small variations in failure temperatures can also be observed for this mix as noted by the standard deviation.

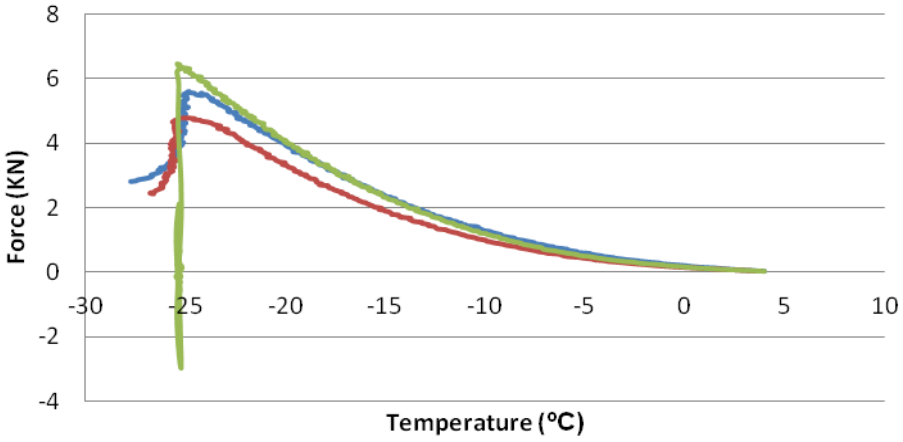

Figure 4-14: TSRST Result for SP 25

Figure 4-15 shows the results for SP 25 RBM. Differences in failure criteria between the SP 25 mix and the SP 25 mix RBM are observable. The conventional SP 25 mix exhibited sudden failure, as illustrated in Figure 4-14. In contrast, the SP 25 mix RBM was characterized by gradual failure attributable to the major elasticity of that asphalt mix. However, the failure load for the SP 25 RBM is lower than that for regular SP 25, a finding that was expected because the additional binder content decreases the stiffness of the asphalt mix.

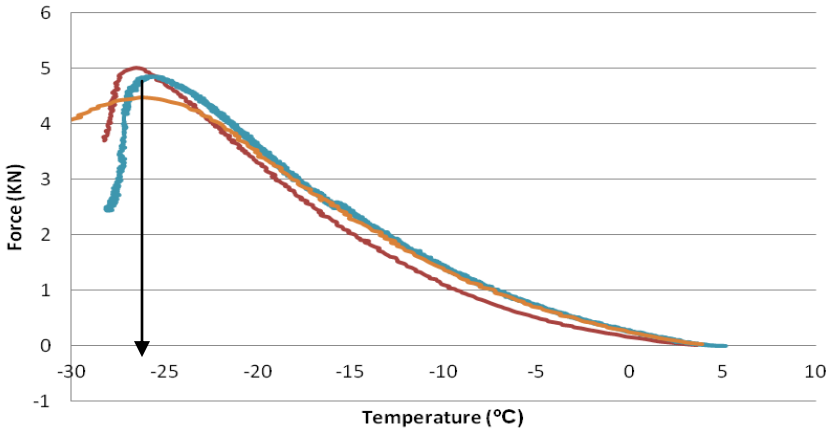

Figure 4-15: TSRST Result for SP 25 RBM

The TSRST failure temperature for each asphalt mix was used for the development of a regression model, which is presented in section 4.4. The average failure temperature for each asphalt mix and the corresponding standard deviation are listed in Table 4-15.

Table 4-15: Result of TSRST for Different Asphalt Mixes

Sample Number	SP 12.5		SP 19	
	Maximum Load (KN)	Minimum Temp (°C)	Maximum Load (KN)	Minimum Temp (°C)
1	3.75	-22.2	4.53	-27
2	3.16	-21.2	6.08	-27.9
3	3.91	-23.8	5.33	-26.2
Average	3.61	-22.4	5.31	-27
St. Dev.	0.39	1.32	0.78	0.85
Sample Number	**SP 25**		**SP 25 RBM**	
	Maximum Load (KN)	Minimum Temp (°C)	Maximum Load (KN)	Minimum Temp (°C)
1	5.62	-24.8	4.85	-25.9
2	4.79	-25	5.01	-26.6
3	6.47	-25.4	4.48	-26.2
Average	5.63	-25.1	4.78	-26.2
St. Dev.	0.84	0.31	0.32	0.32

4.4 Analysis of Fatigue Endurance Limit

The fatigue endurance was estimated for the SP 25 and SP 25 RBM mixes using the MEPDG model. Number of load repetitions to failure was estimated using the following equation [Baus, 2010]:

$$N_{f-HMA} = k_{f1}(C)(C_H)\beta_{f1}(\varepsilon_t)^{k_{f2}\beta_{f2}}(E_{HMA})^{k_{f3}\beta_{f3}} \quad (4\text{-}2)$$

Where:

N_{f-HMA} is the Allowable number of Axle-load applications for a flexible pavement before fatigue cracking is expected.

ε_t is the tensile strain at critical locations. The latest 90th percentile of the cumulative strain was assumed to be ε_t.

E_{HMA} is the Dynamic modulus of the HMA measured in compression (psi). The Dynamic modulus result used in this modeling was the one measured at 21 ºC and frequency 25 Hz.

k_{f1}, k_{f2}, k_{f3} are global filed calibration parameters (From NCHRP 1-40D). Assumptions for this model are $k_{f1} = 0.007566$, $k_{f2} = -3.9492$, $k_{f3} = -1.281$

$\beta_{f1}, \beta_{f2}, \beta_{f3}$ are local or mixture specific field calibration constants; for the global calibration effort, these constants were set to 1.0.

C A constant where $C = 10^M$

$$M = 4.84\left(\frac{V_{be}}{V_a + V_{be}} - 0.69\right) \quad (4\text{-}3)$$

Where:

V_{be} is the percentage of effective asphalt content by volume.

V_a is the percentage of air voids in the HMA mixture.

C_H is the thickness correction term.

$$C_H = \frac{1}{0.000398 + \frac{0.003602}{1 + e^{(11.02 - 3.49H_{HMA})}}} \quad (4\text{-}4)$$

where H_{HMA} is the total HMA thickness in inch.

The percentage of effective binder (V_{be}) for SP 25 and SP 25 RBM mixes were determined from the HMA mix design presented in Appendix B. The V_{be} for SP 25 and SP 25 RBM was 3.4125% and 3.685% respectively. The percentage of air voids in the HMA (V_a) was also determined from the HMA mix design and the result was 4% and 2.4% for the SP 25 and SP 25 RBM respectively.

The calculation of the number of load repetitions to achieve fatigue failure showed superior fatigue resistance for the SP 25 RBM mix compared to that of the SP 25. The number of load repetitions (N_{f-HMA}) is 7,174 and 31,595 cycles for the SP 25 and SP 25 RBM respectively. The additional 0.8% binder content resulted in increasing the number of load repetitions till fatigue cracking by 440%. The implementation of MEPDG fatigue model shows the significant improvement in fatigue resistance by using SP 25 RBM compared to using SP 25 asphalt mix.

4.5 Modeling of Field Strain and Laboratory Testing

One research objective was to develop a model capable of predicting field strain for highways characterized by traffic patterns and climatic conditions similar to those that occur on Highway 401 in Southern Ontario. The model was intended to be as simple as possible; however, accuracy and precision are essential for ensuring the applicability of a model. The models developed in this project are based on the collection of in situ field strain data during the first two years of the life of a pavement. The models developed are thus valid for the prediction of changes in field strain over the short and medium term.

The model created for this analysis was based on linear regression. To develop an accurate model using linear regression, trials were conducted for a number of pavement sections. If the accuracy of the linear regression was unacceptable and the residual plot indicated non-linear relation between one of the parameters and the tensile strain, a transformation for the linear regression model was developed.

The general regression formula can be expressed as follows:

$$Y = \beta_0 + \beta_1 f_1(X) + \beta_2 f_2(X) + \beta_3 f_3(X) + ... + \beta_n f_n(X) + \varepsilon \qquad (4\text{-}5)$$

The Y factor is the dependent variable, and X_1, $X_2 \ldots X_n$ are the independent variables. The Y-axis intercept is denoted by β_0. The parameters $\beta_1, \beta_2 ..... \beta_n$ are the coefficients of the independent variables. A linear regression is applied when the relation between the dependent variable and all of the parameters involved is linear. This relationship can be checked by determining the first derivative of Y with respect to X_1, $X_2 \ldots X_n$. The determination of parameters is explained in section 4.4.1.

For the analysis conducted in this research, the 90th percentile of cumulative tensile strain was considered to be the dependent variable (Y). The independent variables (X_1, $X_2 \ldots X_n$) were assigned to the age of the pavement section; the temperature; and the results of the laboratory testing with respect to the dynamic modulus, resilient modulus, and TSRST.

Four regression models were developed and were valid for the following cases:

1- To determine the 90th percentile of the cumulative tensile strain in the perpetual pavement section with the RBM.

2- To determine the 90th percentile of the cumulative tensile strain in the perpetual pavement section without the RBM.

3- To determine the 90th percentile of the cumulative tensile strain in the conventional pavement design.

4- To determine the 90th percentile of the cumulative tensile strain in the two perpetual pavement sections.

The independent variables vary from one model to the next. The models that represent a single pavement section are characterized by structural and mechanical pavement properties and the resilient modulus and the TSRST for every month. The following sections provide a detailed explanation of the model development.

4.5.1 Regression Analysis

The development of the regression model is executed by sorting the data in matrices of the form

$$y = \begin{bmatrix} y_1 \\ y_2 \\ . \\ . \\ y_n \end{bmatrix} \quad \text{and} \quad x = \begin{bmatrix} x_{1,1} & x_{2,1} & x_{3,1} & . & . & x_{m,1} \\ x_{1,2} & x_{2,2} & . & . & . & x_{m,2} \\ x_{1,3} & . & . & . & . & x_{m,3} \\ . & . & . & . & . & . \\ . & . & . & . & . & . \\ x_{1,n} & x_{2,n} & x_{3,n} & . & . & x_{m,n} \end{bmatrix}$$

where n represents the number of strain data collected throughout the research period. The data collected is considered the dependent variable. The 90th percentile of cumulative tensile strain is the dependent variable in the models developed in this project. The number of independent variables is represented by m. Examples for the independent variables include the pavement age, pavement temperature, dynamic modulus value and TSRST.

Regression analysis is executed to determine the parameters relating the different independent variables to the dependent variables.

$$Y = \beta_0 + \beta_1 f(X_1) + \beta_2 f(X_2) + \beta_3 f(X_3) + ... + \beta_n f(X_n) + \varepsilon \quad (4\text{-}6)$$

where ε is the error in the measurements. The parameters $\beta_0, \beta_1, \beta_2 ..... \beta_n$ are the maximum likelihood estimates if the errors are normally distributed. The coefficients $\beta_0, \beta_1, \beta_2 ..... \beta_n$ are calculated using the matrix equation, if the model is linear.

$$\beta = (X^{'} X)^{-1} X^{'} y \quad (4\text{-}7)$$

Models presented in the subsequent sections will vary in the number of data points (n). However, the models were developed using the procedure explained in this section. In addition, a F-Test is executed to test the overall significance of regression. The final models are presented herein. However, it should be noted that this is only a summary of the best results. Several trials were executed to determine the $f(X_i)$ resulting in the best perameter estimates.

4.5.2 Model for Perpetual Pavement with RBM

The first model was developed in order to calculate the 90th percentile for the cumulative tensile strain in the perpetual pavement section with the RBM. The dependent variable for this model is presented in Figure 4-2. Since all the dependent variables belong to the same structure (perpetual pavement with RBM), the values for the resilient modulus, the failure temperature during the TSRST, and the pavement thickness do not vary. In this model, the following independent variables are the only ones that affect the 90^{th} percentile of the cumulative tensile strain:

1- Age of the pavement structure in months

2- Temperature in degrees Kelvin

3- Dynamic modulus at the construction year (E^*_0) in MPa

4- Dynamic modulus after one year from construction (E^*_1) in MPa

The temperature considered in this model was the average temperature of the asphalt measured at a depth of 70 mm below the surface of the road. To avoid negative temperature values, the temperature was transferred into the Kelvin scale. The use of degrees Celsius in regression analysis will result in positive and negative values of temperature within the same data set. The calculation of the temperature parameter is thus considered inadequate in this condition as the temperature coefficient in the model will be ranging between a positive and negative value. The avoidance of having positive and negative values within the same independent variable is recommended in regression analysis. Therefore, degrees Kelvin are used as the temperature unit throughout the data analysis and developing regression models.

The dynamic modulus was measured at six loading frequencies and five temperatures. The values corresponding to the highest frequency (25 Hz) were considered in this regression analysis. The values corresponding to the highest frequency constitute a reasonable representation of the vehicles moving at high speeds on Highway 401. The dynamic modulus was measured at five temperatures (-10 ºC, 4 ºC, 21 ºC, 37 ºC, and 54ºC) and was calculated using linear interpolation between the values of E* at different temperatures in order to determine the E* value at the average temperature at a depth of 70 mm below the surface of the asphalt. This method of calculating E* for each layer was based on the assumption of a

linear relation between the values of E* at different temperatures. Once the value of E* at every temperature had been calculated, a weighted average for the whole pavement section was calculated using the ratio of the thickness of the layers.

The calculation of the average value of E* can be illustrated using the perpetual pavement with the RBM at 15 ºC as an example. The 15 ºC falls within the range of 4 ºC to 21 ºC, the values of E* at a frequency of 25 Hz and at temperatures of 4 ºC and 21 ºC are used in the calculation. Figure 4-16 depicts the calculation method for determining the value of E* at 15 ºC for the SP 12.5 mix. The values of E* for the SP 12.5 mix at 4 ºC and 21 ºC are 18 235 MPa and 9014 MPa, respectively. The estimated E* at 15 ºC is therefore 12 268.5 MPa.

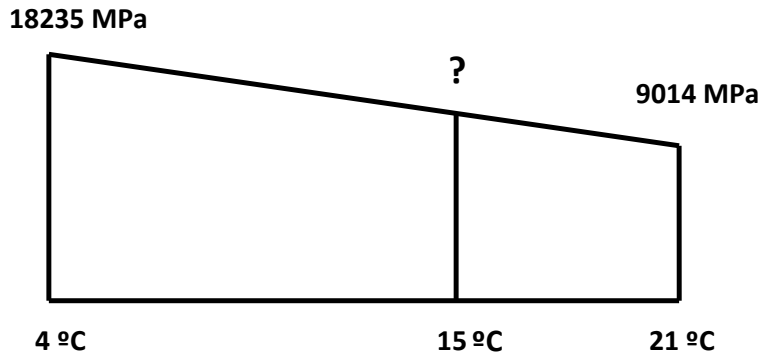

Figure 4-16: Interpolation to Determine the Dynamic Modulus Value at 15ºC

The calculation of the value of E* for all of the mixes at 15 ºC and 25 Hz is performed in the same way and produces the following respective E* values for the SP 19, SP 25, and SP 25 RBM: 11,967; 15,378; and 16,767.

A weighted average is then calculated for the average E* value for the entire section of perpetual pavement with the RBM at 15 ºC. The determination of the weighted average is based on the thickness of each layer in the cross-section of the pavement.

$$\text{Average E* perpetual pavement with RBM} = \frac{[(E^* \text{ for Layer i}) \text{ x (Thickness of Layer i)}]}{\text{Total Thickness of Pavement Cross-Section}} \quad (4\text{-}8)$$

Therefore, average E* for perpetual pavement with RBM at 15 ºC

$$= \frac{(12269 \times 40) + (11967 \times 180) + (15378 \times 100) + (16767 \times 100)}{40 + 180 + 100 + 100} = 13950.7 MPa$$

A similar methodology was employed for the estimation of an average E* value for the perpetual pavement section at a variety of temperatures.

In addition to calculating the average value of E^*_0 using the dynamic modulus results for the year of construction, E^*_1 values were also calculated using the dynamic modulus data for the one year of exposure to environmental conditions and freeze-thaw cycles.

The total number of observations for all the models was 34, which represents the number of two-week periods from May 2011 to September 2012. Twenty-eight of these observations were actually used in modeling, with six points being eliminated from the regression analysis so that they could be used later for the validation of the final models.

The best fit equation that was developed in this research after 54 trials with linear regression and various variables is as follows:

$$y = -46.77 - 0.048 \times age - 0.13 \times \frac{1000}{\left(E_0^*\right)^{1/5}} + 0.099 \times \frac{1000}{\left(E_1^*\right)^{0.215}} + 20.57 \times \ln(Temperature) \quad (4\text{-}9).$$

where Y is the 90th percentile of the cumulative tensile strain in the perpetual pavement section with the RBM, in με;

Age is the age of the pavement section from the beginning of the service life up to the time when y must be calculated, in months;

E^*_0 is the weighted average dynamic modulus for a sample tested in the year of construction for the perpetual pavement section at a frequency of 25 Hz and an average pavement temperature at a depth of 7 cm below the surface, with E^*_0 expressed in MPa;

E^*_1 is the weighted average dynamic modulus for a sample tested after one year of freeze-thaw cycles following the year of construction, and E^*_1 is at a frequency of 25 Hz and an average pavement temperature at a depth of 7 cm below the surface, with E^*_0 expressed in MPa.

Temperature is the average temperature of the asphalt in the road at a depth of 7 cm below the surface of the asphalt, in Kelvin.

The model is characterized by $R^2 = 86.5$ % and the adjusted $R^2 = 84.1$ %. Table 4-16 lists the ANOVA results for this model.

Table 4-16: ANOVA Table for the Model of Perpetual Pavement with RBM

ANOVA					
	Degrees of Freedom	SS	MS	F	Significance F
Regression	4	4.35	1.087	36.7	1.13E-09
Residual	23	0.68	0.030		
Total	27	5.03			

The P-values for the intercept and independent variables are presented in Table 4-17.

Table 4-17: P-Value for Various Parameters of the Perpetual Pavement with RBM Model

	P-value
Intercept	0.127
Age	2.29E-07
E*_0	0.016
E*_1	0.026
Temperature	0.001

Analysis of the P-values demonstrates that age and temperature have the greatest effect on the 90th percentile of cumulative tensile strain in the perpetual pavement with the RBM within the first two years of its service life. However, the dynamic modulus also has a significant effect on the value of the 90th percentile of the cumulative strain. Age is the only independent variable that has a linear relationship with the strain. The residual plots for the four independent variables are shown in Figures 4-17 to 4-20.

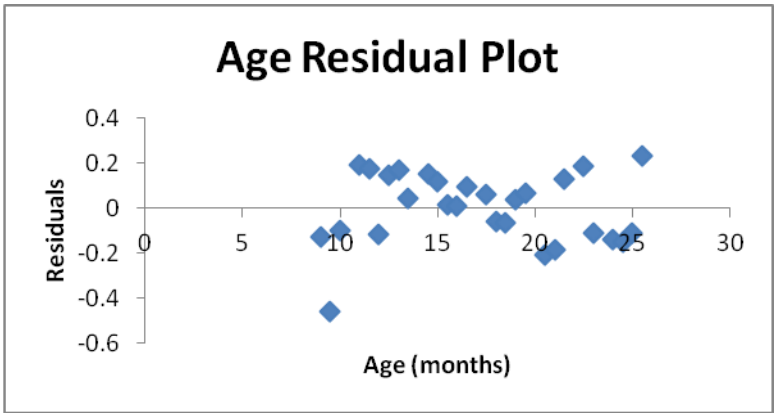

Figure 4-17: Residual Plot for Pavement Age

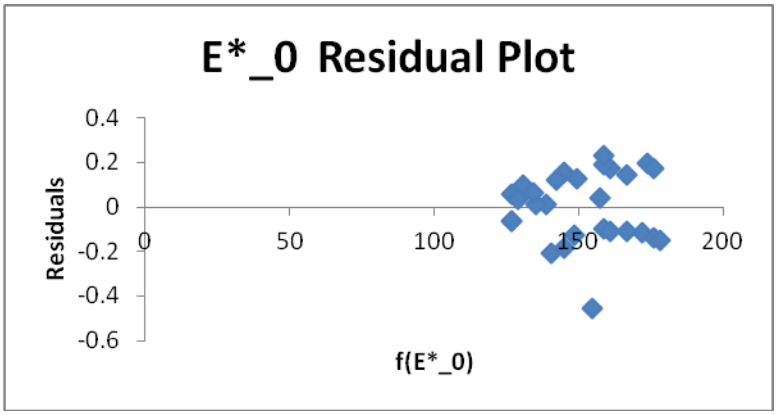

Figure 4-18: Residual Plot for Dynamic Modulus at the Construction Year

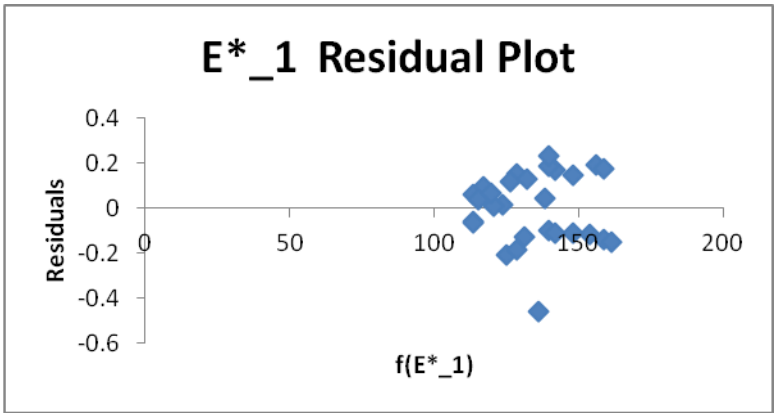

Figure 4-19: Residual Plot for Dynamic Modulus after One Year of Construction

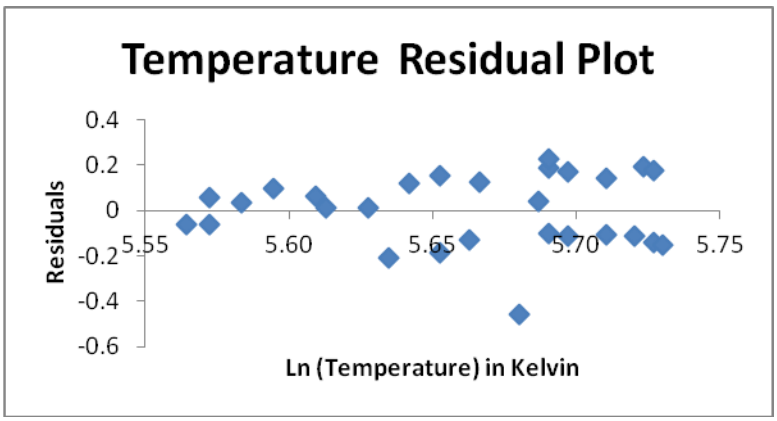

Figure 4-20: Residual Plot for Temperature

The model was validated through the application of six sets of trials in order to determine ($\hat{Y}$). To evaluate the accuracy of the model, the strain values calculated using the model was compared with those determined based on the field data. Figure 4-21 shows the plot that represents the validation of the model. It can be noted that the errors in strain prediction are randomly distributed above and below the line of balance. The model is therefore considered to be neither overpredicting nor underestimating the value of the 90^{th} percentile of the cumulative tensile strain and is therefore a good model.

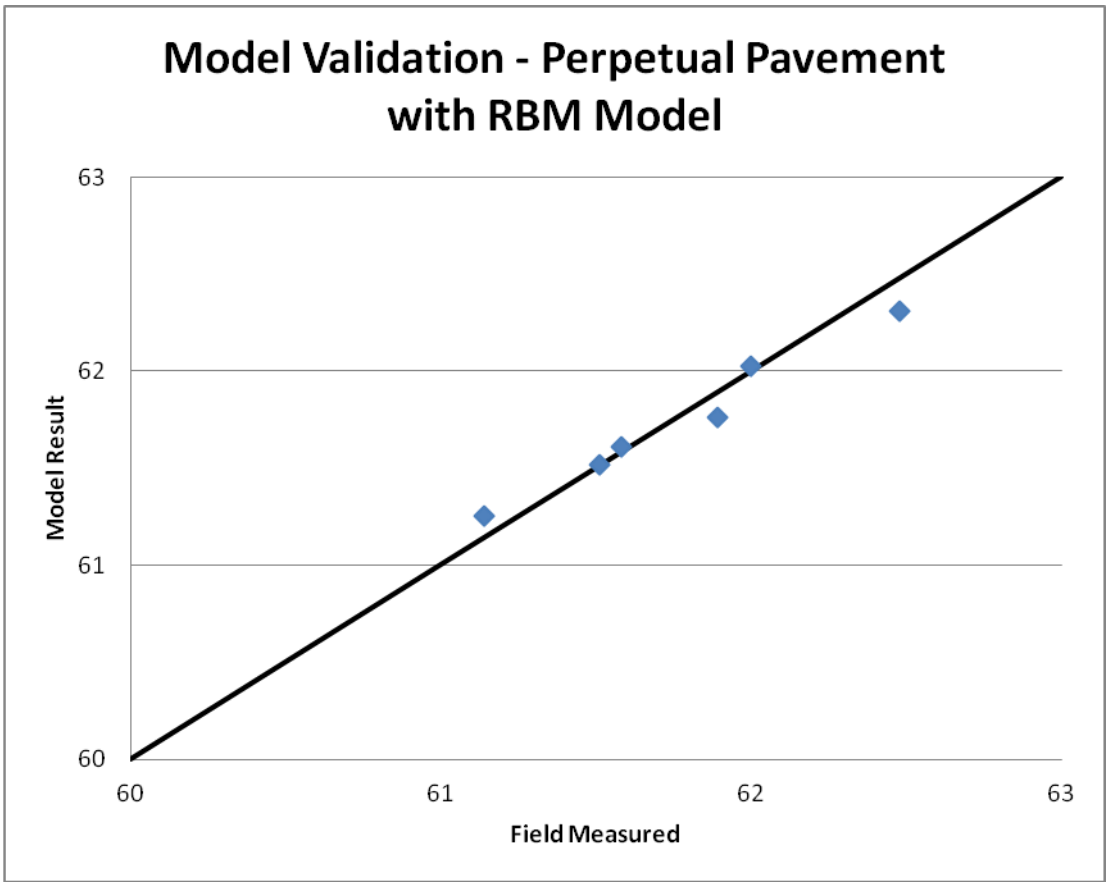

Figure 4-21: Validation of the Perpetual Pavement with RBM Model

4.5.3 Model for Perpetual Pavement without RBM

The second model was developed using the in-situ strain data collected from the perpetual pavement without the RBM. The independent variables used in this model were similar to those employed in the model for the perpetual pavement with the RBM. For models one and two, the trends for the two sets of dependent variables appear to be relatively comparable, as shown in Figure 4-2. At the completion of the trials, the final model that was developed for this pavement section can be expressed as follows:

$$y = -53.81 + 0.014 \times age - 0.1 \times \frac{1000}{\left(E_0^*\right)^{1/5}} + 0.077 \times \frac{1000}{\left(E_1^*\right)^{0.215}} + 21.27 \times \ln(Temperature) \quad (4\text{-}10)$$

where Y is the 90th percentile of the cumulative tensile strain in the perpetual pavement section without the RBM, in με;

Age is the age of the pavement section from the beginning of its service life up to the time when y must be calculated, in months;

E^*_0 is the weighted average dynamic modulus for a sample tested in the year of construction for the perpetual pavement section at a frequency of 25 Hz and an average pavement temperature at a depth of 7 cm below the surface, with E^*_0 expressed in MPa;

E^*_1 is the weighted average dynamic modulus for a sample tested after one year of freeze-thaw cycles following the year of construction, and E^*_1 is at a frequency of 25 Hz and an average pavement temperature at a depth of 7 cm below the surface, with E^*_0 expressed in MPa;

Temperature is the average temperature of the asphalt in the road at a depth of 7 cm below the surface of the asphalt, in K.

The model is characterized by R^2 = 87.5 % and the adjusted R^2 = 85.4 %. Table 4-18 lists the ANOVA results for this model.

Table 4-18: ANOVA Table for the Model of Perpetual Pavement without RBM

ANOVA					
	Degrees of Freedom	SS	MS	F	Significance F
Regression	4	8.07	2.016	40.35	4.44E-10
Residual	23	1.15	0.05		
Total	27	9.22			

The P-values for the intercept and independent variables are indicated in Table 4-19.

Table 4-19: P-Value for Various Parameters of the Perpetual Pavement without RBM Model

	P-value
Intercept	0.201
Age	0.062
E*_0	0.088
E*_1	0.063
Temperature	0.012

Temperature is the independent variable that has the greatest effect on the value of the 90th percentile of the cumulative tensile strain in the perpetual pavement without the RBM. However, with the exception of the intercept, the other independent variables have a P-value of less than 0.1, which indicates that these factors offer a positive contribution to the accuracy of the model. A number of trials were conducted in an attempt to develop other

models with a higher level of accuracy. However, the model presented here was found to be the most accurate. The residual plots for the four independent variables are shown in Figures 4-22 to 4-25.

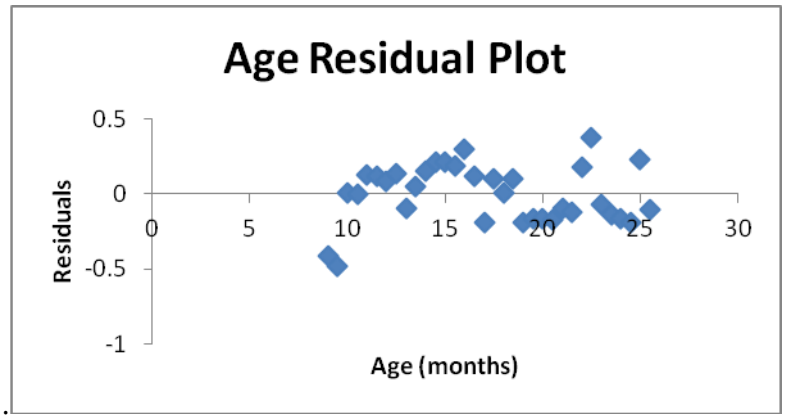

Figure 4-22: Residual Plot for Pavement Age

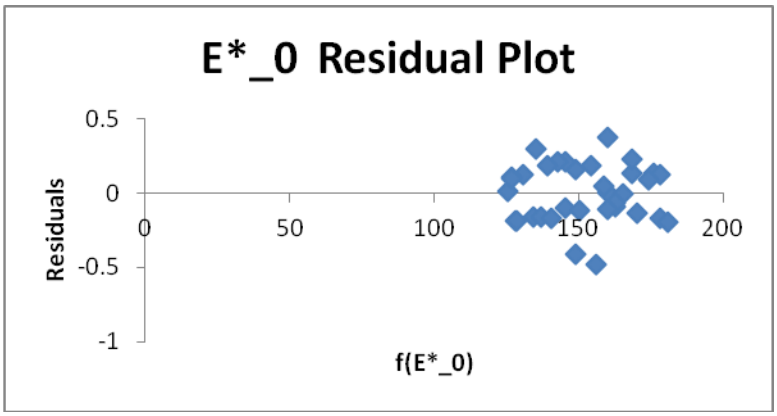

Figure 4-23: Residual Plot for Dynamic Modulus at the Construction Year

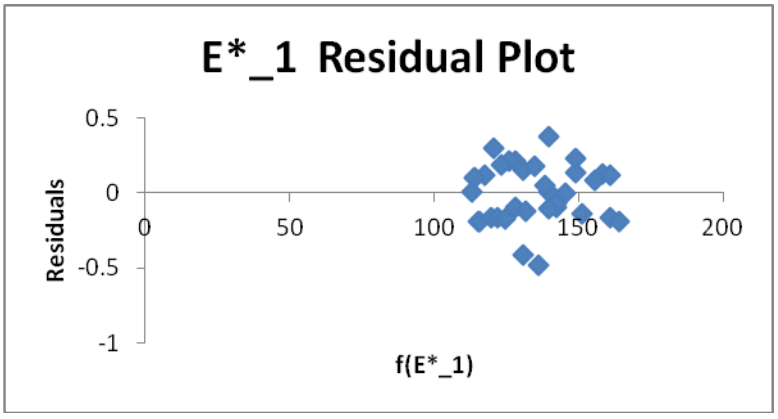

Figure 4-24: Residual Plot for Dynamic Modulus after One Year of Construction

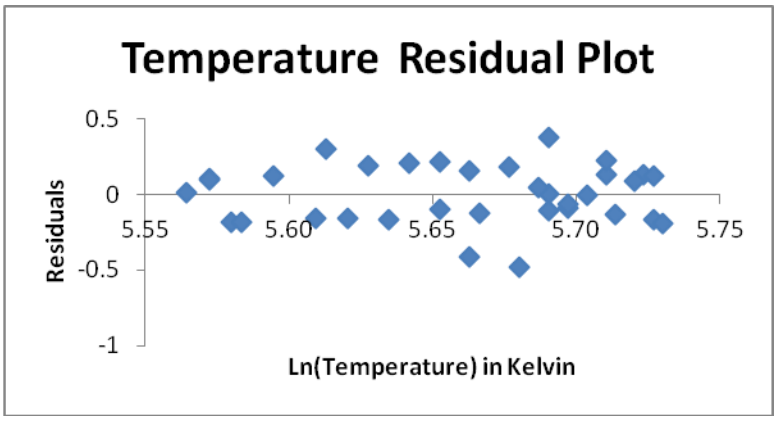

Figure 4-25: Residual Plot for Temperature

The model was validated through the application of six sets of trials in order to determine ($\hat{Y}$). To evaluate the accuracy of the model, the strain values calculated using the model were compared with those determined from the field data. Figure 4-26 shows the plot that represents the validation of the model. It can be noted that the errors in strain prediction are randomly distributed above and below the line of balance. The model is therefore considered to be neither overpredicting nor underestimating the value of the 90^{th} percentile of the cumulative tensile strain and is thus a good model.

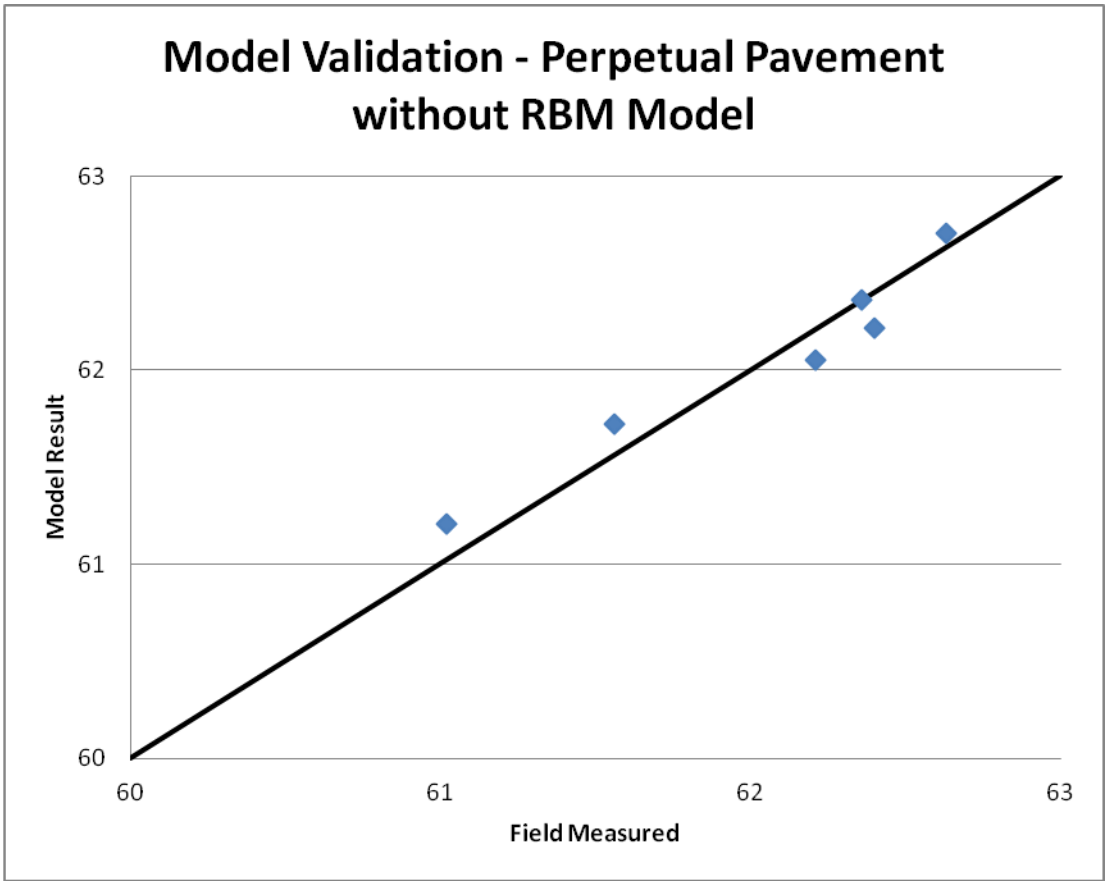

Figure 4-26: Validation of the Perpetual Pavement without RBM Model

4.5.4 Model for Conventional Pavement

The third model was developed using the in-situ strain data collected from the conventional pavement. The independent variables used in this model were similar to those used in the first two models. The dependent variables for this model also indicate the same increasing trend as that noted in the previous models. However, the value of the in-situ strain is much higher for the conventional pavement, as shown in Figure 4-3. The final model that was developed after the completion of the trials for this pavement section can be expressed as follows:

$$y = -18.75 + 0.018 \times age - 0.92 \times \frac{1000}{\sqrt{(E_0^*)}} + 0.767 \times \frac{1000}{\sqrt{(E_1^*)}} + 20.24 \times \ln(Temperature) \quad (4\text{-}11)$$

where Y is the 90th percentile of the cumulative tensile strain in the conventional pavement section, in με;

Age is the age of the pavement section from the beginning of its service life up to the time when y must be calculated, in months;

E^*_0 is the weighted average dynamic modulus for a sample tested in the year of construction for the conventional pavement section at a frequency of 25 Hz and an average pavement temperature at a depth of 7 cm below the surface, with the E^*_0 expressed in MPa;

E^*_1 is the weighted average dynamic modulus for a sample tested after one year of freeze-thaw cycles following the year of construction and E^*_1 is at a frequency of 25 Hz and an average pavement temperature at a depth of 7 cm below the surface, with E^*_0 expressed in MPa;

Temperature is the average temperature of the asphalt in the road at a depth of 7 cm below the surface of the asphalt, in K.

The model is characterized by R^2 = 82.2 % and the adjusted R^2 = 79.1%. Table 4-20 lists the ANOVA results for this model.

Table 4-20: ANOVA Table for the Model of Conventional Pavement

ANOVA					
	Degree of Freedom	SS	MS	F	Significance F
Regression	4	8.51	2.13	26.52	2.54E-08
Residual	23	1.84	0.08		
Total	27	10.36			

The P-values for the intercept and independent variables are indicated in Table 4-21.

Table 4-21: P-Value for Various Parameters of the Conventional Pavement Model

	P-value
Intercept	0.59
Age	0.12
E*_0	0.06
E*_1	0.06
Temperature	0.003

The effect of temperature on the 90^{th} percentile of cumulative strain in the conventional pavement section is significant. The remaining factors exhibit a moderate to weak impact on the dependent variable. However, the residual plots of the model show a random distribution of the errors when plotted against all of the independent variables. The residual plots are shown in Figures 4-27 to 4-30.

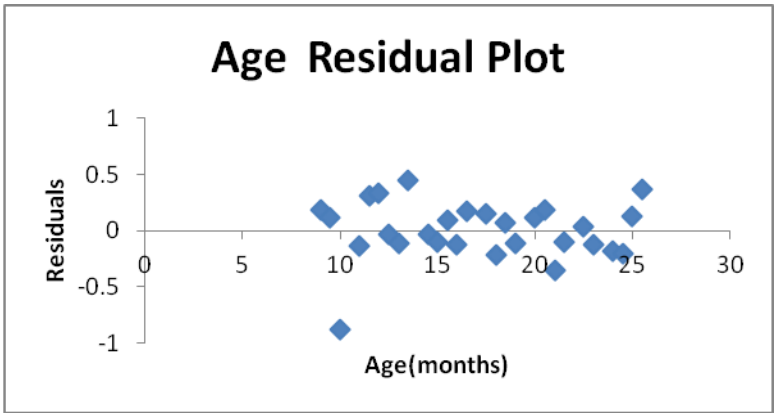

Figure 4-27: Residual Plot for Pavement Age

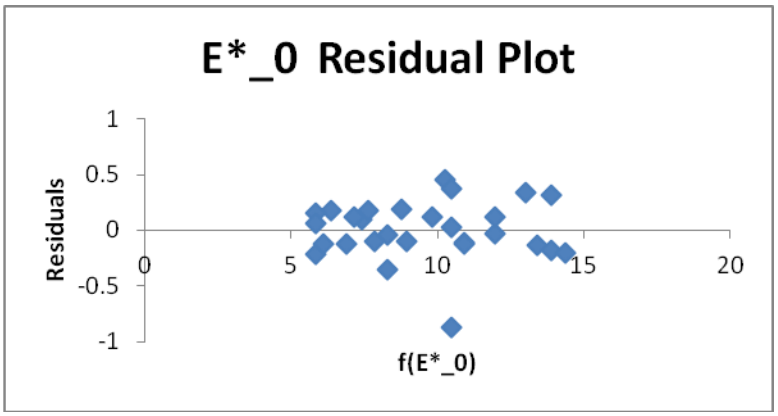

Figure 4-28: Residual Plot for Dynamic Modulus at the Construction Year

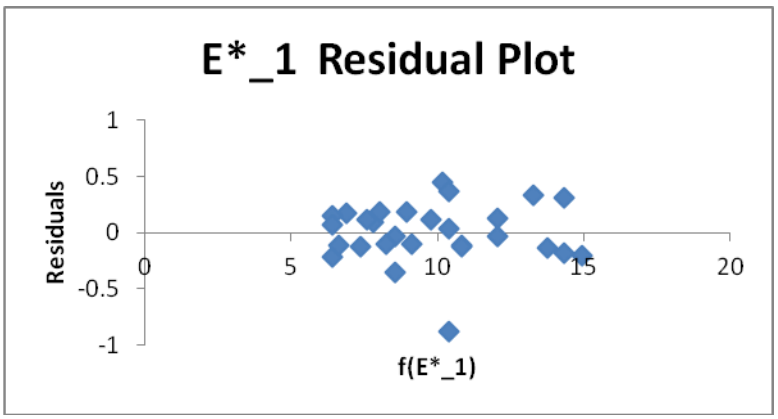

Figure 4-29: Residual Plot for Dynamic Modulus after One Year of Construction

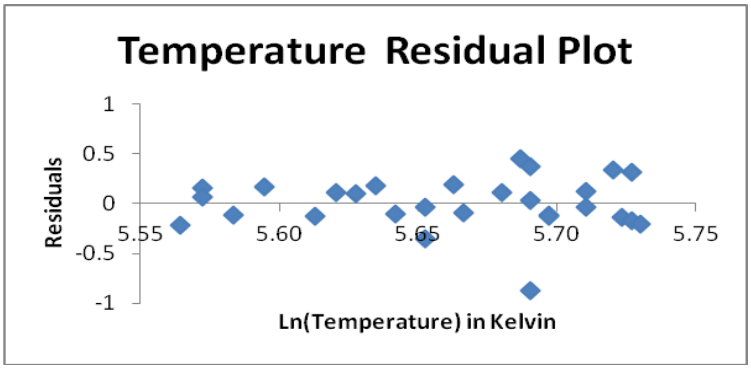

Figure 4-30: Residual Plot for Temperature

The model was validated through the application of six sets of trials in order to determine ($\hat{Y}$). To evaluate the accuracy of the model, the strain values calculated using the model were compared with those determined from the field data. Figure 4-31 shows the plot that represents the validation of the model. It can be observed that the errors in strain prediction are randomly distributed above and below the line of balance. The model is therefore considered to be neither overpredicting nor underestimating the value of the 90th percentile of the cumulative tensile strain. Thus, this is a good model.

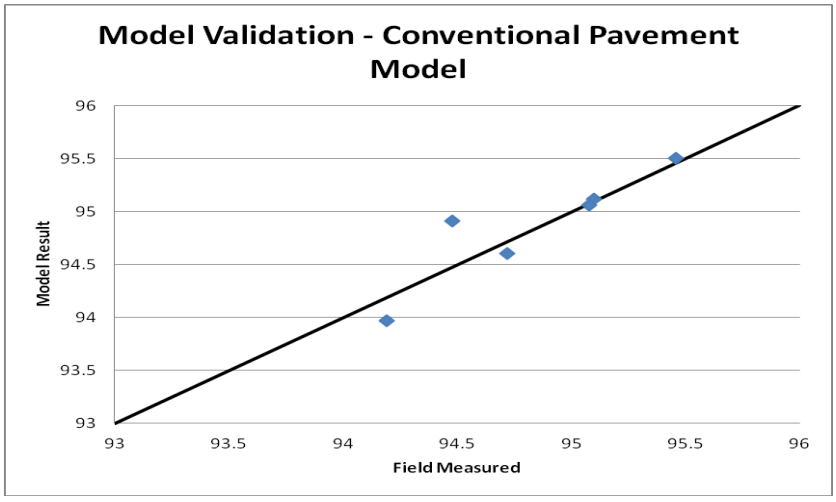

Figure 4-31: Validation of the Conventional Pavement Model

4.5.5 Model for Both Perpetual Pavement Sections

The fourth model was developed using the in situ strain data collected from both perpetual pavement test sections. The goal of developing this model was to create a general model for the determination of the 90th percentile of the cumulative tensile strain in perpetual pavements that are comprised of 420 mm of asphalt layers whether an RBM layer is used at the bottom or not. The independent variables used in this model are similar to those used in the previously presented perpetual pavement models with an additional independent variable that represents the TSRST failure temperature of the bottom asphalt layer. The regression model can be expressed as follows:

$$y = 8.81 - 0.017 \times age - 0.051 \times \frac{1000}{\left(E_0^*\right)^{1/5}} + 0.049 \times \frac{1000}{\left(E_1^*\right)^{0.215}} + 8.79 \times \ln(Temperature) + 0.0096 \times \frac{(TSRST_{Bottom_Layer})^4}{1000} \quad (4\text{-}12)$$

where Y is the 90th percentile of the cumulative tensile strain in the perpetual pavement sections, in με.

Age is the age of the pavement sections from the beginning of their service life up to the time when y must be calculated, in months;

E^*_0 is the weighted average dynamic modulus for a sample tested in the year of construction for the perpetual pavement sections at a frequency of 25 Hz and an average pavement temperature at a depth of 7 cm below the surface, with E^*_0 expressed in MPa;

E^*_1 is the weighted average dynamic modulus for a sample tested after one year freeze-thaw cycles following the year of construction, and E^*_1 is at a frequency of 25 Hz and an average pavement temperature at a depth of 7 cm below the surface, with E^*_0 expressed in MPa;

Temperature is the average temperature of the asphalt in the road at a depth of 7 cm below the surface of the asphalt, in K;

$TSRST_{Bottom\ Layer}$ is the failure temperature for a specimen composed of either the regular SP 25 or SP 25 RBM.

The model is characterized by $R^2 = 77.1\%$ and the adjusted $R^2 = 74.8\ \%$. Table 4-22 lists the ANOVA results for this model.

Table 4-22: ANOVA Table for the Model for Both Perpetual Pavements

ANOVA					
	Degree of Freedom	SS	MS	F	Significance F
Regression	5	11.95	2.39	33.58	7.26E-15
Residual	50	3.56	0.07		
Total	55	15.51			

The P-values for the intercept and independent variables are indicated in Table 4-23.

The effect of the temperature and the dynamic modulus values one year after the year of construction are the independent variables that have the greatest effect on the determination of the 90^{th} percentile for the cumulative tensile strain in the model for both perpetual sections. The residual plots are shown in Figures 4-32 to 4-36.

Table 4-23: P-Value for Various Parameters for Both Perpetual Pavement Model

	P-value
Intercept	0.42
Age	0.02
E*_0	0.02
E*_1	0.007
Temperature	1.06E-05
TSRST_Bottom Layer	0.04

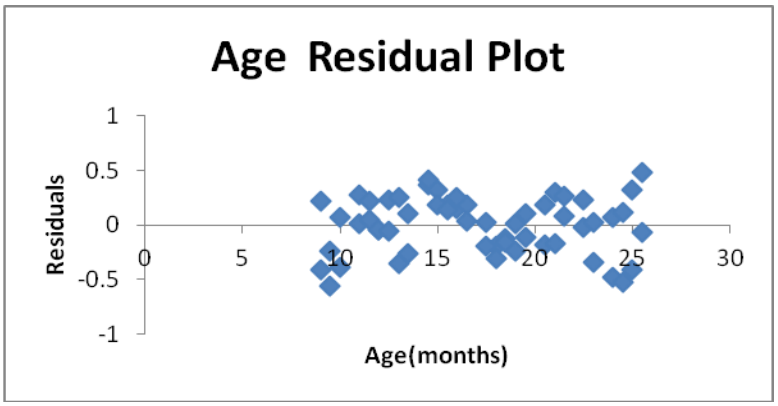

Figure 4-32: Residual Plot for Pavement Age

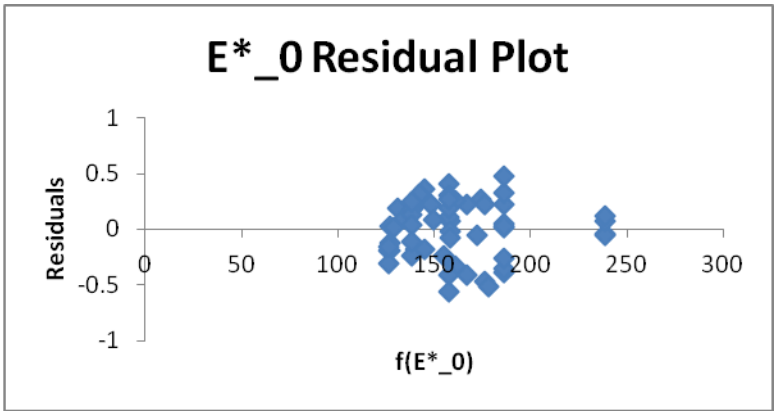

Figure 4-33: Residual Plot for Dynamic Modulus at the Construction Year

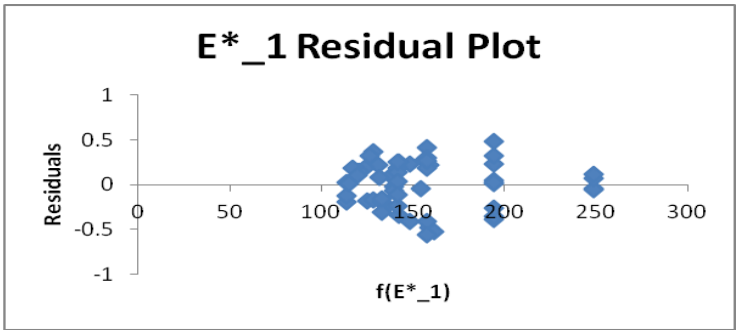

Figure 4-34: Residual Plot for Dynamic Modulus after One Year of Construction

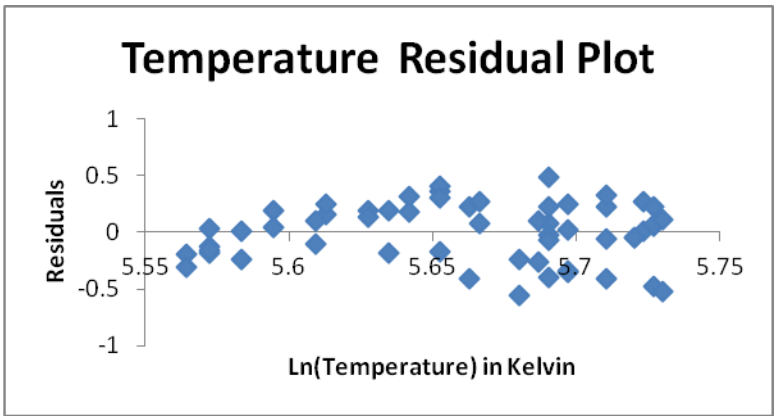

Figure 4-35: Residual Plot for Temperature

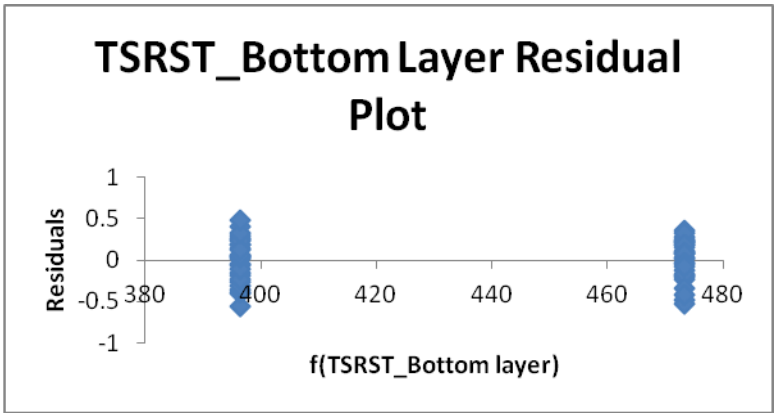

Figure 4-36: Residual Plot for TSRST Failure Temperature

The model was validated through the application of six sets of trials in order to determine ($\hat{Y}$). To evaluate the accuracy of the model, the strain values calculated using the model were compared with those determined from the field data. Figure 4-37 shows the plot that represents the validation of the model. It can be seen that the errors in strain prediction are randomly distributed above and below the line of balance. The model is therefore considered to be neither overpredicting nor underestimating the value of the 90th percentile of the cumulative tensile strain.

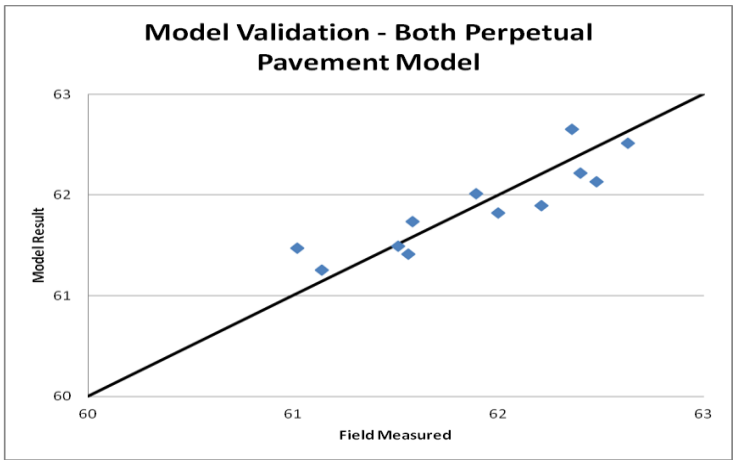

Figure 4-37: Validation of Both Perpetual Pavement Models

4.5.6 Key Findings from Model Development

The models developed are valid for the prediction of the 90th percentile of the cumulative tensile strain within the first two years of the service life of the pavement. Although the models can provide some initial insight into future tensile strain at the bottom of asphalt layers, it is recognized that the limitations of the models are due to the relatively short data collection period compared to the design life of the pavement (20 years for the conventional design and 50 years for the perpetual design). Several trials and combinations of relationships

were investigated, and the models presented in this chapter represent the best fit models. The joint confidence intervals for all the models presented in sections from 4.4.2 to 4.4.5 are presented in Appendix C.

A number of trials were conducted with the goal of generating a general model for predicting the 90^{th} percentile of the cumulative strain for all three pavement designs. Because the strain readings for the perpetual design differed from those for the conventional design, the development of this model was unsuccessful. The trials resulted in inaccurate and unreliable models. Further data collection and monitoring will be required in order to develop a model for a combination of all of the designs.

4.6 Summary and Conclusion

This chapter has described the laboratory testing conducted at the CPATT laboratory for samples collected from the Highway 401 test sections. A summary of the in-situ strain data collected throughout the duration of the study and during the first two years of the service life of the pavement has been presented.

Statistical regression analysis was performed in order to develop linear regression models for the calculation of the 90^{th} percentile of the cumulative tensile strain in the three pavement designs. Similarly, a general linear regression model was also developed in order to calculate the tensile strain in both perpetual sections combined. Based on the P-value of the independent variables in the four models, the general conclusion is that temperature variation and age are the key factors that affect the value of the 90^{th} percentile of cumulative strain. However, the dynamic modulus values at the year of construction and after one year of

freeze-thaw cycles also have a significant impact on the determination of the value of the 90th percentile of the cumulative tensile strain.

The differences between the tensile strain measurements for the perpetual sections and the conventional sections prevented the development of a single general model for the calculation of the 90th percentile of cumulative strain in all three test sections combined. Further data collection and, possibly, additional laboratory tests could possibly lead to a more accurate model.

Chapter 5
Economic Evaluation and Sustainability Assessment

5.1 Introduction

To examine the perpetual pavement design compared to the conventional pavement design from a broader perspective rather than focusing only on the structural assessment of the pavement, an economic evaluation is essential. Such an evaluation assesses the additional costs associated with a high-quality product such as perpetual pavement compared to the cost of constructing conventional pavement. Current economic challenges are forcing decision makers to support a product characterized not only by significant structural capacity but also by a lower cost over both the life cycle. From a taxpayer's point of view, the economic analysis of pavement design constitutes a critical evaluation criterion.

The economic evaluation presented in this thesis was based on construction costs provided by Capital Paving Inc.; the construction costs used are the actual costs of constructing the Highway 401 test sections. The maintenance and rehabilitation costs were estimated based on feedback from contractors and annual reports published by the MTO, which include the average costs of maintenance activities in Ontario [Hein, 2007].

5.2 Economic Analysis

A number of tools are available for conducting an economic analysis. The economic evaluation of pavement design, in particular, is a sophisticated topic for which several methods are appropriate. Uncertainties associated with changes in future maintenance and

rehabilitations costs and changes in discount rates due to a possible future economic crisis increase the complexity of an economic evaluation. The choice of a time window for the Life Cycle Cost Analysis (LCCA) also has a major impact on the outcome of the evaluation.

For this research, the economic analysis was implemented in order to compare the cost of constructing and maintaining the perpetual pavement section with the RBM and the similar costs associated with the conventional pavement section. The difference between the cost of perpetual pavement without the RBM and that of perpetual pavement with the RBM is relatively small. The information currently available with respect to their long-term structural assessment is insufficient to enable the design of significantly different maintenance and rehabilitation programs. As well, the only difference in the costs of constructing the two sections is the cost of the additional 0.8 % of asphalt binder in the RBM layer, which is negligible relative to the total construction costs.

The following is a simplified version of the steps in the economic evaluation undertaken for this study:

1- Determine the construction cost of a unit length (1 km) of both types of pavement design.

2- Design a maintenance and rehabilitation program for both pavement sections based on their structural performance. The time window for the maintenance and rehabilitation program should match the one chosen for the LCCA.

3- Ascertain the costs associated with each type of maintenance and rehabilitation activity.

4- Calculate the net present value (NPV) for both the perpetual and the conventional pavement designs.

5.2.1 Design of Maintenance Programs

The maintenance and rehabilitation program is a key factor in a sound economic evaluation. Preservation has also become more common in Ontario. The calculation of the NPV requires that a reliable and practically acceptable maintenance and rehabilitation program be designed. For this research, the maintenance and rehabilitation program was tailored for the analysis of long-term predicted structural models [El-Hakim, 2013]. A structural evaluation model was created using version 1.003 of the Mechanistic Empirical Pavement Design Guide (MEPDG) software in order to mechanistically evaluate the perpetual pavement section with the RBM as well as the conventional pavement section [El-Hakim, 2012 b]. The MEPDG software is unique because it predicts the performance of the pavement with regard to a number of types of distress in addition to providing roughness measurements. The MEPDG output includes predictions of pavement performance with respect to top-down cracking, bottom-up damage caused by fatigue (alligator) cracking, thermal cracking, rutting, and the International Roughness Index (IRI) values expected throughout the analysis time. An analysis period of 50 years was assumed for the evaluation of both pavement structures

The MEPDG model was created with an input level three. The mechanical and physical properties used in creating the MEPDG models, such as voids in the mineral aggregate (VMA), the percentage of air voids, the percentage of volumetric binder content, and the total unit weight, were based on laboratory tests and a job mix formula (JMF) provided by

Capital Paving Inc. The climate data file used for the model was created from a download of the data monitored in Niagara Falls, New York. At a distance of 160 km, this weather station is the one closest to the location of the project. The approximation of the weather conditions is believed to be acceptable due to the similar climatic characteristics of the two areas.

Based on the MEPDG analysis, bottom-up cracking was predicted to be minimal for the perpetual pavement design, in contrast to that estimated for the conventional design. These results indicate that the actual propagation of bottom-up cracking is less likely to occur in perpetual pavement structures than in conventional asphalt pavement structures. Figure 5-1 shows the results with respect to bottom-up cracking damage. The rate of deterioration in the conventional design signifies that this pavement design will be subject to structural damage and bottom-up cracks over the short term and will require a more intensive and expensive maintenance and rehabilitation program than will the perpetual designs.

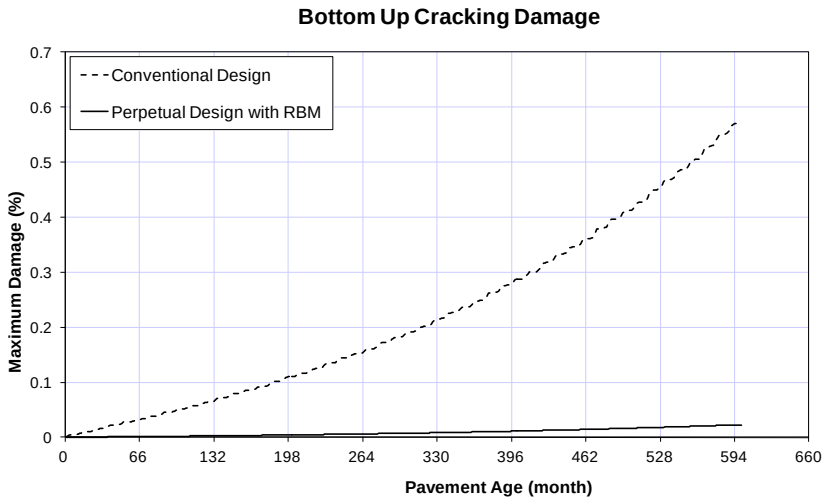

Figure 5-1: Bottom-Up Cracking Damage

Figure 5-2 shows the results of the MEPDG rutting model for the two pavement designs. The perpetual pavement design performs better because it resists rutting throughout the analysis period. Figure 5-2 indicates that the occurrence of base rutting is the same for both conventional and perpetual designs. The main difference in the total rutting predicted is apparent in the asphalt layers, which provide excellent rutting resistance. It can also be observed that, during the first five years, base rutting is the primary type of rutting and is responsible for the greatest contribution to the total rutting. After the fifth year, the rate of increase in the base rutting decreases while the rutting in the asphalt layers maintains a linear trend and then becomes the primary factor contributing to the total overall rutting.

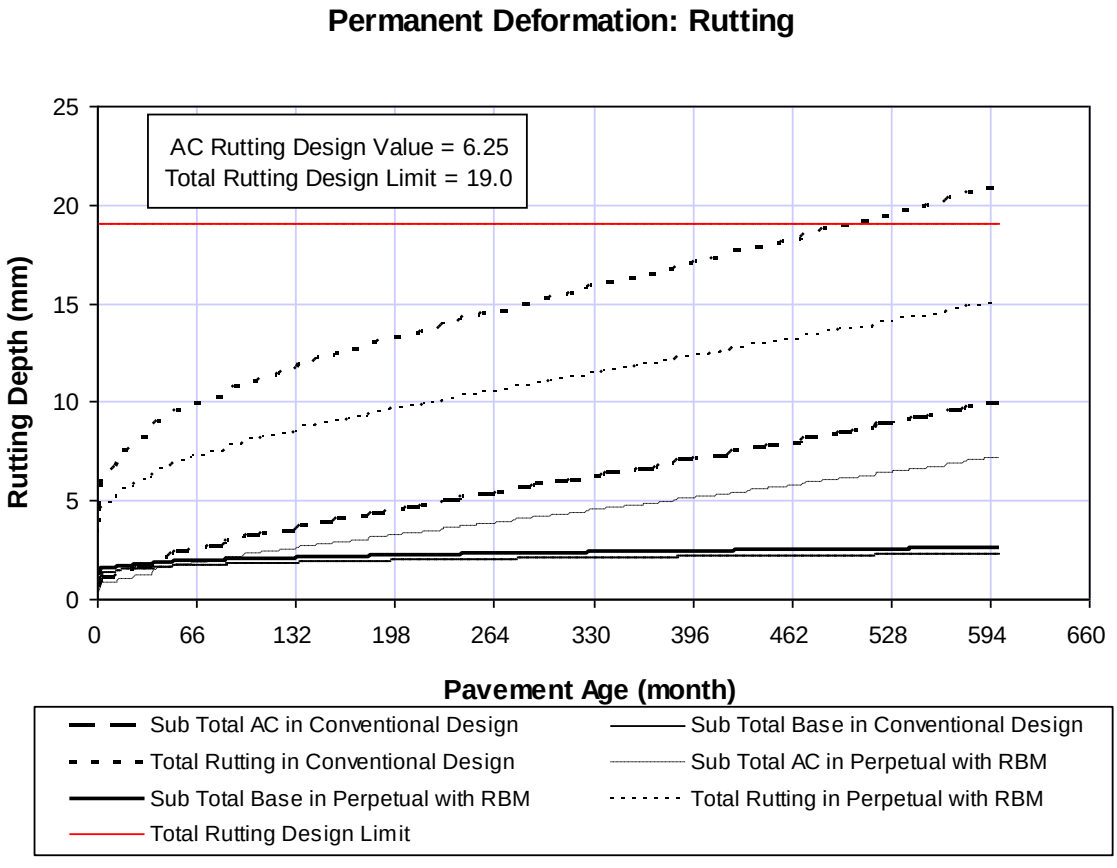

Figure 5-2: Rutting prediction in Conventional and Perpetual Design

Figure 5-3 shows the International Roughness Index (IRI) model results for both pavement designs. The IRI values are shown to be the same immediately following construction. The rate of deterioration in terms of IRI for the conventional asphalt pavement design is slightly higher than in that for the perpetual design. The increase of the IRI can be resolved by milling and overlaying the surface course so that the IRI values remain below the maximum allowable limit.

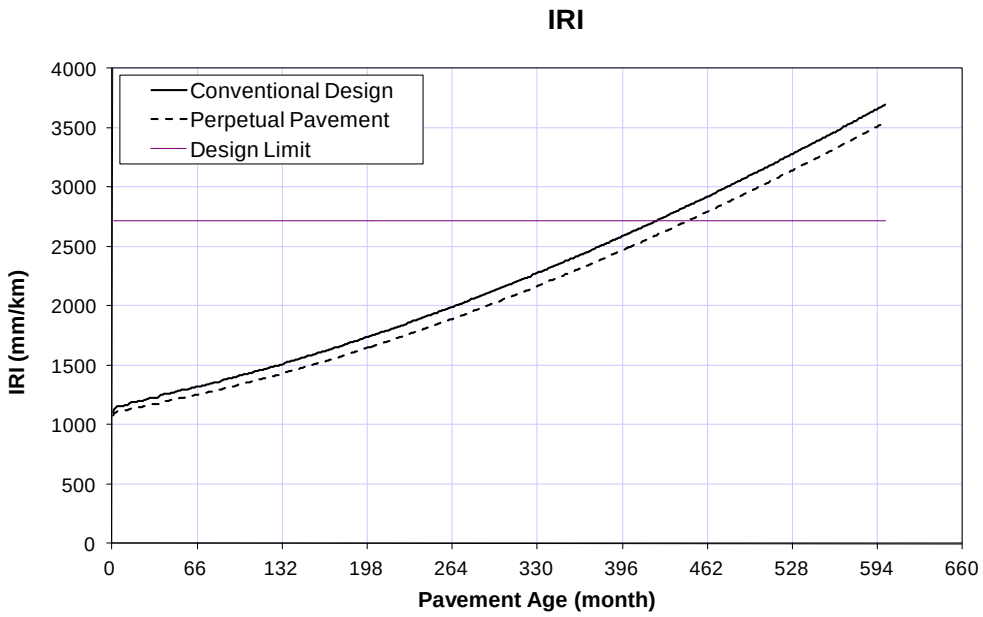

Figure 5-3: International Roughness Index (IRI) Model Results

The maintenance and rehabilitation program for both the perpetual pavement with the RBM and the conventional pavement designs was formulated with consideration of the long-term structural performance predictions using MEPDG and with the guidance of previous LCCA reports published by the MTO and similar other reports by Departments of Transportation (DOTs) and others [Hein, 2007, Smith, 1998, Tighe, 2001]. Tables 5-1 and 5-2 indicate the

proposed maintenance and rehabilitation schedules for the conventional asphalt and the perpetual pavements, respectively [El-Hakim, 2013].

Table 5-1: Maintenance Schedule of Conventional Design

Maintenance Activity	Year
Rout and Crack Sealing (352 m/km)	3
Rout and Crack Sealing (352 m/km)	6
Rout and Crack Sealing (352 m/km)	9
5% Mill and patch 50 mm	9
Rout and Crack Sealing (704 m/km)	12
20% Mill and patch 50 mm	15
Rout and Crack Sealing (704 m/km)	18
Tack Coat	20
Mill 50 mm Asphalt Pavement	20
Superpave 12.5 FC2 - 50 mm	20
Rout and Crack Sealing (352 m/km)	21
Rout and Crack Sealing (352 m/km)	24
Rout and Crack Sealing (352 m/km)	28
20% Mill and patch 50 mm	28
Major Rehabilitation of Pavement	30
Rout and Crack Sealing (352 m/km)	33
Rout and Crack Sealing (352 m/km)	36
Rout and Crack Sealing (352 m/km)	39
5% Mill and patch 50 mm	39
Rout and Crack Sealing (704 m/km)	42
20% Mill and patch 50 mm	45
Rout and Crack Sealing (704 m/km)	48
Tack Coat	50
Mill 50 mm Asphalt Pavement	50
Superpave 12.5 FC2 - 50 mm	50
Rout and Crack Sealing (352 m/km)	51
Rout and Crack Sealing (352 m/km)	54
Rout and Crack Sealing (352 m/km)	58
20% Mill and patch 50 mm	58
Major Rehabilitation of Pavement	60
Rout and Crack Sealing (352 m/km)	63
Rout and Crack Sealing (352 m/km)	66
Rout and Crack Sealing (352 m/km)	69
5% Mill and patch 50 mm	69

Table 5-2: Maintenance Schedule of Perpetual Design

Maintenance Activity	Year
Rout and Crack Sealing (280m/km)	4
Rout and Crack Sealing (280m/km)	8
3% Mill and Patch 40 mm	10
Rout and Crack Sealing (560m/km)	12
15% Mill and patch 40 mm	15
Mill 50mm Asphalt pavement	21
SMA- 50 mm	21
Tack coat	21
Rout and Crack Sealing (280m/km)	24
Rout and Crack Sealing (280m/km)	28
15% Mill and patch 40 mm	32
Rout and Crack Sealing (560m/km)	36
Mill 50mm Asphalt pavement	38
SMA- 50 mm	38
Tack coat	38
Rout and Crack Sealing (280m/km)	42
Rout and Crack Sealing (280m/km)	46
Rout and Crack Sealing (280m/km)	54
Mill 50mm Asphalt pavement	58
SMA- 50 mm	58
Tack coat	58
3% Mill and Patch 40 mm	60
Major Rehabilitation of Pavement	62
15% Mill and patch 40 mm	65
Rout and Crack Sealing (280m/km)	70

Costs for all of the maintenance activities included in the maintenance and rehabilitation programs were either obtained from Capital Paving Inc. or estimated based on average provincial levels as reported by the MTO [Hein, 2007].

5.2.2 Life-Cycle Cost Analysis

The LCCA was performed in order to evaluate the perpetual design with the RBM relative to the conventional design method. The LCCA was based on a long-term structural analysis model implemented using the MEPDG. The regression models developed with respect to the

in situ field strain are valid for a short-term structural evaluation. However, an LCCA requires a long-term structural evaluation so that an adequate maintenance and rehabilitation program can be designed. The results from the MEPDG models were integrated with maintenance and rehabilitation programs designed for similar projects in Ontario and recommended by the MTO. A maintenance and rehabilitation schedule for a 70-year analysis period was designed based on the structural analysis and on the best practices identified by the MTO. The LCCA model was run using the Stantec LCCA program.

It is important to note that the LCCA was performed with the following assumptions:

- The best possible unit cost estimates for pavement material, maintenance and rehabilitation, and labour in Ontario were obtained through the MTO. The final LCCA reports submitted to the MTO in 1998 and 2006 were used for estimating the material, maintenance, and rehabilitation costs [Hein, 2007, Smith, 1998]. However, some unit costs were based on national averages.

- The LCCA evaluation period was 70 years for both pavement design alternatives.

- The assumptions related to preventative maintenance, scheduled maintenance, and/or rehabilitation treatments were based on MTO recommendations.

- Inflation costs per treatment and/or maintenance activities were not applied and were assumed to be constant for different rehabilitation options. This practice is common for LCCA.

- The LCCA was based on 3 % and 4 % discount rates.

- The initial construction costs included the costs of labor and materials associated with the construction of the pavement structure.

- To simplify the LCCA calculation and because of insufficient data, user delay costs during maintenance and rehabilitation activities were not incorporated into the LCCA.

The costs of constructing 1 km of both the conventional and the perpetual pavement designs are summarized in Tables 5-3 and 5-4, respectively.

Table 5-3: Construction Cost of Conventional Pavement Design

Length (m)	(40 mm) SP 12.5 FC2 Density = 2.56 t/m^3	(170mm) SP 19 Density = 2.41 t/m^3	(90 mm) SP 25 Density = 2.34 t/m^3	(200 mm) Granular A Density = 3.12 t/m^3	(200 mm) Granular B Density = 2.05 t/m^3	SUM
1,000	$244,224	$719,024	$279,572	$238,680	$92,250	$1,573,749
1,000	$244,224	$719,024	$279,572	$238,680	$92,250	$1,573,749
					SUM	$3,147,498

Table 5-4: Construction Cost of Perpetual Pavement Design

Length (m)	(40 mm) SP 12.5 FC2 Density = 2.56 t/m^3	(180mm) SP 19 Density = 2.41 t/m^3	(100 mm) SP 25 Density = 2.34 t/m^3	(100 mm) SP 25 RBM Density = 2.44 t/m3	(200 mm) Granular A Density = 3.12 t/m^3	(550 mm) Granular B Density = 2.05 t/m^3	SUM
1,000	$244,224	$761,319	$310,635	356,850	$238,680	$253,688	$2,165,395
1,000	$244,224	$761,319	$310,635	356,850	$238,680	$253,688	$2,165,395
						SUM	$4,330,791

The total NPV of the perpetual pavement was calculated using the 3 % and 4 % percent discount rates, for an analysis period of 70 years. The deterministic NPV results were $5,716,951 and $5,285,569 for 3 % and 4 %, respectively. The LCCA total NPV costs of the

conventional pavement were $6,058,267 and $5,223,858, respectively, for the same discount rates. The LCCA results indicate that the perpetual asphalt pavement is more cost effective over the life cycle. Although the costs of constructing the perpetual pavement design are expected to be 30 % higher than for the conventional design, the overall NPV of the perpetual pavement is lower than that of the conventional design by 5.6 % assuming a 3% discount rate. The NPV of perpetual and conventional designs were marginally similar considering a 4% discount rate.

5.3 Sustainability Assessment

This section presents the overall assessment of perpetual pavement design from sustainability prospective. During the last few decades, the concept of sustainability has gained momentum. Sustainability is defined by the United Nations as "The development that meets the needs of the present without compromising the ability of future generations to meet their own needs" [Brundtland, 1987]. Applying the sustainability definition to the construction field would result in a set of processes by which a profitable and competitive industry delivers buildings, structures and roads which enhances life quality while maximizing the efficient use of natural resources and energy.

One of the key factors enhancing sustainability of roadway construction is increasing pavement durability and lifetime. This philosophy of pavement design is consistent with the perpetual pavement design philosophy which enhances pavement structural capacity to meet a 50 year design life with associated reduced maintenance and rehabilitation activities as compared to the conventional pavement designs.

In short, building a long life perpetual pavement is sustainable as it lasts a long time. Recycling of pavement materials is a major contributing factor in the construction of sustainable roads. The sustainability concept is advanced when natural recourses are managed to fulfill the current needs while ensuring the following generations have sufficient resources to meet their needs too. The recycling of pavement materials contributes to conservation of non-renewable resources [Chan, 2010]. Asphalt is one of the most recycled products on the planet and has been shown to be of high quality [Sanchez, 2012]. RAP is crushed, sieved and used for production of new asphalt mixes. RAP can also be used in granular layers such as the base and subbase under highway shoulders. The benefit of using RAP material in asphalt mixes is not only economic but there are also environmental gains and structural improvements. RAP material has been successfully used for years in Ontario. The addition of RAP increases stiffness to the asphalt mix and reduces permanent deformation (rutting) [Raymond, 2012].

The quantification of pavement sustainability could be implemented using several rating systems. Various green initiatives introduced recently as LEED, Greenroads 1.0, GreenLITES and GreenPave are offering credits to using recycled materials, reducing pollution due to construction activities and introducing innovative designs [Chan, 2010]. The following sections will present Greenroads 1.0 and GreenPave as an example showing the evaluation of perpetual pavement design or long-life pavement designs from sustainability prospective.

5.3.1 Greenroads

Greenroads was developed in 2007 by Martina Soderlund and Professor Stephen Muench at the University of Washington [Muench, 2010]. Greenroads is an assessment program for project level including design and construction of roads [Muench, 2010]. The details about Greenroads are included in a manual that is available online at www.greenroads.us. In order to receive the certification of Greenroads, individual projects should submit the project documents and register in the Greenroads website. Applicable fees are required by Greenroads in order to evaluate the project from a sustainability prospective. There are 11 mandatory credits that must be awarded to all the certified projects. In addition, there are a total of 118 voluntary credits available in Greenroads [Muench, 2010]. The voluntary credits are divided in six categories:

- Environment and Water (21 Credits)
- Access and Equity (30 Credits)
- Construction Activities (14 Credits)
- Materials and Resources (23 Credits)
- Pavement Technologies (20 Credits)
- Custom Credits (10 Credits)

Table 5-5 presents the distribution of credits in the categories of Materials and Resources and the Pavement Technologies.

Table 5-5: Credit Distribution of Greenroads [Muench, 2010]

	Materials & Resources (MR)			
☐	MR-1	Lifecycle Assessment (LCA)	2	Conduct a detailed LCA of the entire project
☐	MR-2	Pavement Reuse	5	Reuse existing pavement sections
☐	MR-3	Earthwork Balance	1	Balance cut/fill quantities
☐	MR-4	Recycled Materials	5	Use recycled materials for new pavement
☐	MR-5	Regional Materials	5	Use regional materials to reduce emissions
☐	MR-6	Energy Efficiency	5	Improve energy efficiency of operational systems
		MR Subtotal:	**23**	
	Pavement Technologies (PT)			
☐	PT-1	Long-Life Pavement	5	Design pavements for long-life
☐	PT-2	Permeable Pavement	3	Use permeable pavement as a LID technique
☐	PT-3	Warm Mix Asphalt	3	Use WMA in place of HMA
☐	PT-4	Cool Pavement	5	Use a surface that retains less heat
☐	PT-5	Quiet Pavement	3	Use a quiet pavement to reduce noise
☐	PT-6	Pavement Performance Tracking	1	Collect performance data as related to construction
		PT Subtotal:	**20**	

The design of long-life pavement is weighted as 5 credits in Greenroads. This represents 25% of the total weight of Pavement Technologies category. In addition, using recycled materials is credited 5 points and the conduction of Life Cycle Assessment is credited 2 points. The distribution of credits in Greenroads reflects encouragement for perpetual pavement designs and the usage of recycled materials.

5.3.2 GreenPave

The MTO is exclusively using the GreenPave rating system to quantify the sustainability of roads and highway projects. GreenPave was developed by the Material Engineering Research Office of MTO. GreenPave was developed with a sole emphasis on local pavement experience and current practices in Ontario. The general trend of pavement design and construction of sustainable pavement practice in Ontario are outlined through the implementation of GreenPave. Consequently, GreenPave is currently recommended by

pavement industry and MTO senior managers. The latest version of GreenPave was developed in 2009 throughout consultation between the MTO and industrial partners [Chan, 2009]. Table 5-6 presents the distribution of credits and credit breakdown for GreenPave. The certification levels are illustrated in Table 5-7.

Table 5-6: Credit Distribution for GreenPave [Kazmierowski, 2012]

Category	Point ID	Description	Maximum Credit
Pavement Technologies	PT-1	Long-life Pavement Designs	3
	PT-2	Permeable Pavements	1
	PT-3	Quiet Pavement	3
	PT-4	Cool Pavements	2
Materials and Resources	MR-1	Recycled Content	6
	MR-2	Reuse of Pavement	3
	MR-3	Local Materials	3
	MR-4	Construction Quality	2
Energy and Atmosphere	EA-1	Reduce Energy Consumption	3
	EA-2	GHG Emission Reduction	2
	EA-3	Improve Rolling Resistance	1
	EA-4	Pollution Reduction	3
Innovation and Design Process	I-1	Innovation in Design	2
	I-2	Exemplary Process	2
Maximum Credits			36

Table 5-7: Levels of Certification in GreenPave

Level	Credits Required
Not Certified	<7
Bronze	7-10
Silver	11-14
Gold	15-19
Trillium	20+

The GreenPave ranking system offers up to three credit points for long life pavement designs and up to six points for using recycled material. Considering only those two aspects would result in achieving up to nine points on the GreenPave ranking system [Chan, 2010]. This would be enough to award a certain project the bronze certification level. Considering the use of local materials, the reuse of asphalt and improving construction quality can easily lead to upgrade the project's certification level to gold certification. The GreenPave ranking system illustrates clearly the current incentive adopted by the MTO towards improving pavement quality to become long life pavements.

5.4 Summary and Conclusion

This chapter has described the economic evaluation of the perpetual pavement design with the RBM and the conventional pavement design. The economic evaluation included the design of a maintenance and rehabilitation program for a 70-year analysis period. The maintenance programs for both pavement designs were based on a long-term structural analysis model developed using MEPDG and the MTO recommendations for highway maintenance.

Based on the LCCA results, the perpetual pavement design is expected to be more financially advantageous than the conventional design. Although the initial construction costs for the perpetual section with the RBM are 30 % higher than those for the conventional design, after a 70-year service life, the NPV of the perpetual design with the RBM is 5.6 % lower compared with that of the conventional design.

The chapter also presented the investigation of perpetual pavement designs and long life pavements from a sustainability perspective. The perpetual pavement designs in this research used recycled materials and based on its expected service life, it would be awarded credits for being both a long life pavement and for recycled content in accordance with the Ontario GreenPave program. The credits reflect that the perpetual pavement design that uses recycled materials contributes to MTO goal of designing and constructing sustainable roads.

Chapter 6
Research Impact on Pavement Engineering

This chapter explains the application of using the models developed based on the in-situ tensile strain collected from the different pavement designs. Furthermore, it provides a context for the future application of the perpetual pavement design.

6.1 Pavement Engineering

The findings of this research are relevant to pavement engineers and designers. The models presented in Chapter Four were developed using data collected from the Highway 401 test sections. Therefore, the developed models are valid for application on roads or projects characterized by similar traffic patterns and the same pavement layer thicknesses. However, the material characterization findings may also be helpful for pavement designers who need to mitigate specific pavement distresses at other various locations. They can potentially use SP 25 RBM at other locations. The findings based on the models developed in Chapter Four can be illustrated as:

1- The perpetual pavement design with the RBM provides benefits in the Southern Ontario environment with very heavy traffic volumes such as the Highway 401 test section.

2- The Traffic at this specific location is approximately 60,000 Average Annual Daily Traffic (AADT) and the truck percentage is approximately 30%. Comparison between the traffic pattern and truck percentage on the Highway 401 sections and various 400 series Highways in Ontario shows that the traffic conditions of the test

sections are similar to several 400 series highways. Thus, this design should be considered elsewhere especially as traffic increases.

3- The thicker structural design of the perpetual pavement design compared to the conventional pavement sections can provide longer life and it will reduce future rehabilitation and maintenance and result potentially in a lower life cycle cost.

4- The material characterization test results showed various benefits. The higher percentage of asphalt binder showed better resistance to low temperature cracking. This mix should be considered for reducing deterioration.

The models developed in this research are valid for most of the 400 series Highways in Southern Ontario. In addition, in Northern Ontario, the asphalt mix characterization findings could be beneficial as the additional asphalt binder could help mitigate bottom up cracking. The traffic loadings on some other 400 series Highways are less than that of the Highway 401 test section. However, the models can still be used taking into consideration the difference in traffic loading. Future research is recommended to calibrate the developed model for highways with different traffic loads and patterns.

Figure 6-1 presents a flow chart explaining how the developed models can improve pavement design for 400 Series Highways in Southern Ontario. The developed models can be used to estimate the fatigue bottom-up cracking resistance in the pavement section prior to construction. The function of the developed models to predict tensile strain at the bottom of asphalt layers can be used to assess the use of various asphalt mixes and study the impact of increasing the percentage of recycled materials. The tensile strain models can also be used to

evaluate the usage of innovative asphalt mixes in perpetual and conventional pavement with Recycled Asphalt Shingles (RAS) mix or the warm mix. The changes in dynamic modulus of that layer will result in changes in the value of tensile strain at the bottom of asphalt layers. Practical examples will be presented in the subsequent sections to evaluate the use of RAS and Warm Mix Asphalt technology (WMA) in the Highway 401 test section from the bottom-up fatigue resistance perspective.

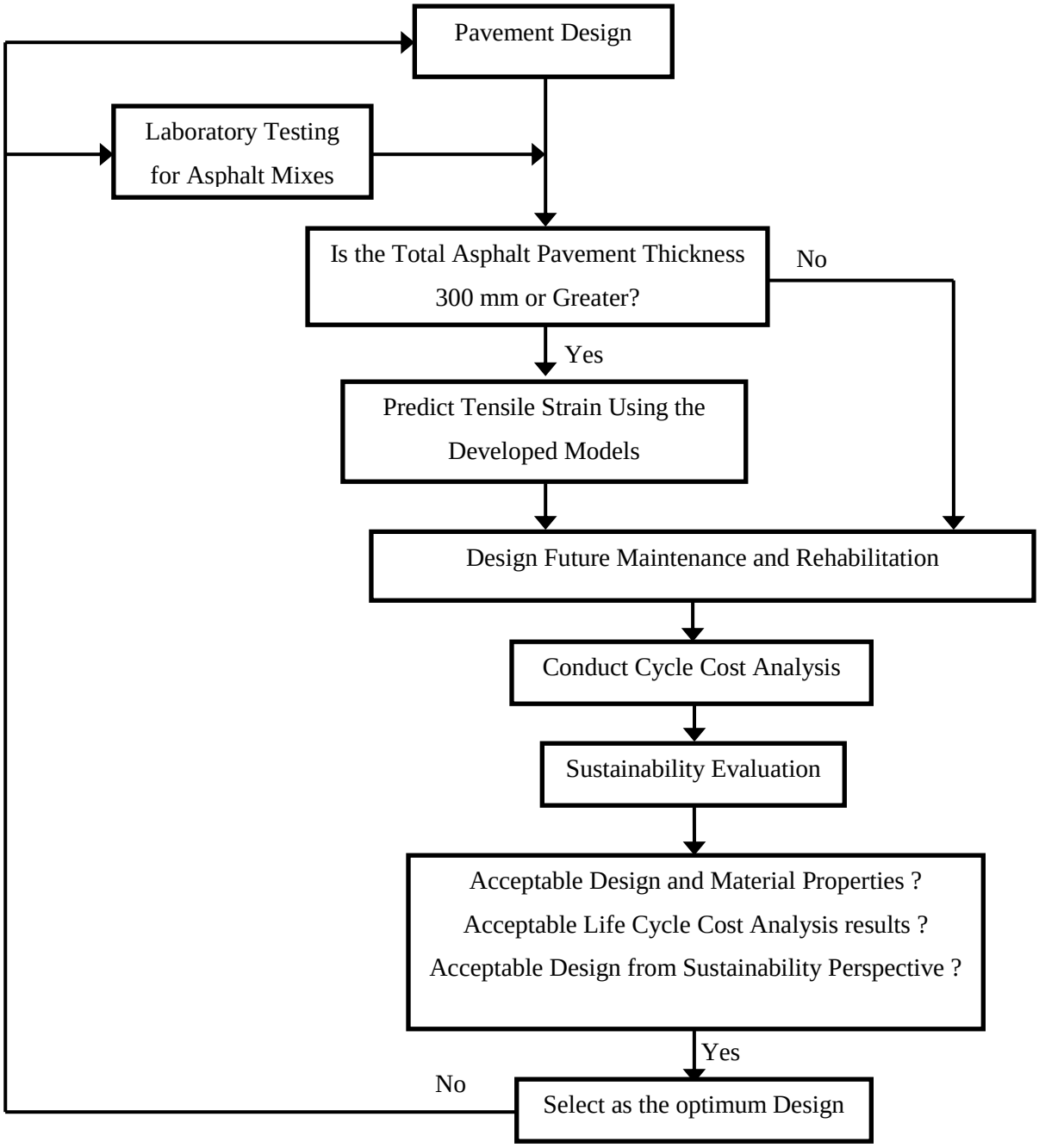

Figure 6-1: Flow Chart for the Application of Tensile Strain Models in Pavement Engineering

6.2 Case Study - RAS

An example for direct application of the models developed using the in-situ tensile strain data collected from the Highway 401 test section is presented in this section. The example will investigate the replacement of the surface asphalt mix and the intermediate asphalt mix with two other mixes. The alternative asphalt mixes which contained RAS were obtained from another research project that was carried out by Ul-Islam in the CPATT laboratory in University of Waterloo in partnership with Miller Group and the Ontario Centres of Excellence (OCE). The research project investigated the impact of adding different percentages of RAP and RAS [Ul-Islam, 2011]. The research work in this project investigated six asphalt mixes. Three asphalt mixes were of SP 12.5 and two were designed as SP 19. The research project included execution of laboratory experimental matrix similar to that executed for the Highway 401 perpetual pavement project. It should be noted that the usage of RAS which is fully recycled and WMA which has lower emissions can also provide credits from the MTO GreenPave program.

The example includes comparing the sections presented in Figure 6-2 and Figure 6-3 if constructed with the same thickness of asphalt layers and subjected to a traffic pattern similar to the Highway 401 section.

The surface asphalt layer in this example was replaced with a material that contains RAS and RAP. In addition, the intermediate asphalt layers were replaced with a material that uses RAS. The modified surface asphalt layer is an SP 12.5 FC2 layer including 3% of RAS and 12% RAP. The modified intermediate layer was designed as SP 19 with a 6% RAS.

Figure 6-2: Pavement One: Perpetual Pavement Section with RBM

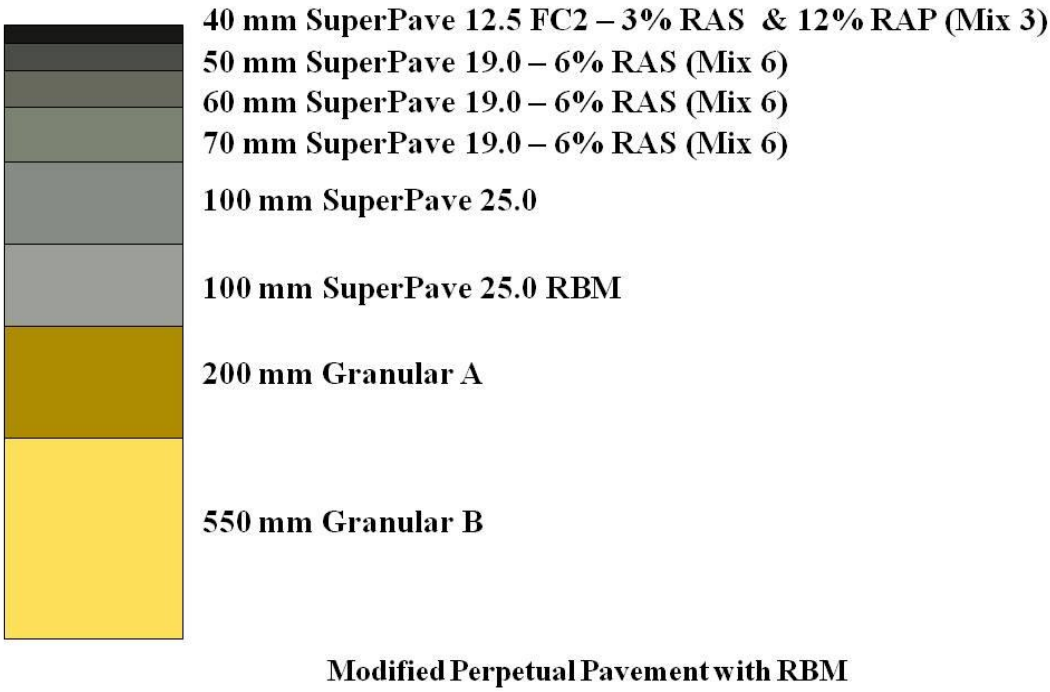

Figure 6-3: Pavement Two: Perpetual Pavement Section with RAS and RAP

The tensile strain model used in this example is that presented in section 4.5.2 for estimating the 90th percentile of the cumulative tensile strain in perpetual pavement. The model is given by the following equation:

$$y = -46.77 - 0.04818 \times age - 0.1346 \times \frac{1000}{\left(E_0^*\right)^{1/5}} + 0.09865 \times \frac{1000}{\left(E_1^*\right)^{0.215}} + 20.5716 \times \ln(Temperature)$$

The definition of the different parameters in the model is similar to that presented in section 4.5.2.

The main difference between the two pavement sections is the value of the weighted average dynamic modulus representing the whole pavement section at the year of construction and after one year of freeze-thaw cycles **(** E_0^* and E_1^* **).**

The dynamic modulus of the modified layers was tested by Ul-Islam in 2011 and the results are included in his MASc thesis [Ul-Islam, 2011]. The results of dynamic modulus of the modified mixes are presented in Table 6-1.

Table 6-1: Dynamic Modulus Results for Alternative Surface and Intermediate Layers

Mix	Frequency (Hz)	Average Dynamic Modulus (MPa)				
		-10ºC	**4.4ºC**	**21.1ºC**	**37.8ºC**	**54.4ºC**
Surface Layer Mix	25	26,599	14,749	7,405	2,345	868
	10	25,392	13,288	6,381	2,159	685
	5	24,125	12,316	5,608	1.892	601
	1	21,045	9,634	4,198	1,423	458
	0.5	19,927	8,721	3,737	1,288	418
	0.1	17,012	6,941	1,316	1,067	356
Intermediate Layer Mix	25	29,006	20,157	7,721	5,558	2,203
	10	27,600	19,557	6,272	4,890	1,822
	5	26,453	18,621	5,619	4,298	1,500
	1	23,787	15,293	4,199	3,211	1,075
	0.5	22,730	13,818	3,790	2,783	988
	0.1	20,136	12,012	2,973	2,169	748

The weighted average of the dynamic modulus was calculated using the results of frequency at 25 Hz. The interpolation between different temperatures was used to calculate the weighted average dynamic modulus at the field temperatures.

The dynamic modulus after one year of freeze-thaw cycles **(**E_1^***)** was not tested in this research project. Therefore, an assumption based on engineering experience was made to estimate the E_1^* for the modified asphalt mixes. The deterioration in dynamic modulus values for Mix 3 and Mix 6 was assumed to take place with the same deterioration rate as the SP 12.5 and SP 19 tested in the Highway 401 project.

The calculation of the 90th percentile of the cumulative tensile strain of the original and modified pavement sections resulted in a direct assessment for the enhancement or deterioration in bottom-up fatigue resistance resulting from using RAS and RAP with certain percentages. The result of this comparison is presented in Figure 6-4.

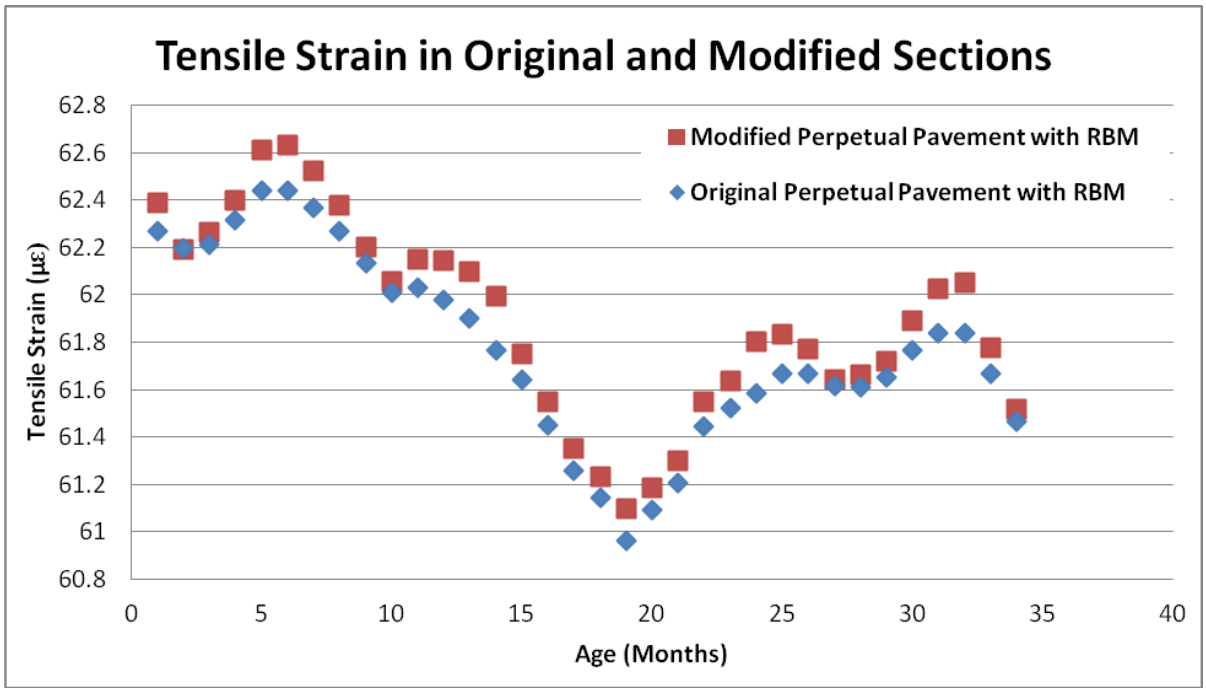

Figure 6-4: Predicted Tensile Strain for the Original and Modified Perpetual Pavement Sections Using the Model

The developed model estimated that the tensile strain at the bottom of asphalt layers will increase if the surface layer constructed including 3% RAS and 12% of RAP and the intermediate layer including 6% of RAS. This result will have a noticeable impact on the LCCA of both designs and the sustainability assessment of both design alternatives.

6.3 Case Study – Warm Mix

The developed models could be used to evaluate the structural impact of using WMA in the construction of perpetual pavements. This case study will assess the impact of replacing the surface asphalt layer in the perpetual pavement section with RBM by a WMA layer. The WMA mix used in this example was tested in CPATT as part of a research project to evaluate WMA in Ramara Township [Tighe, 2006]. The WMA design was recommended as sustainable alternative compared to an HL4 HMA layer which is typically used as surface layer asphalt mix [Tighe, 2006]. Furthermore, it has been shown to have lower emissions as compared to the conventional HMA layer. The dynamic modulus results of the WMA are presented in Table 6-2 [Tighe, 2006].

Table 6-2: Dynamic Modulus Results for WMA

Mix	Frequency (Hz)	Average Dynamic Modulus (MPa)			
		-10ºC	**4.4ºC**	**21.1ºC**	**37.8ºC**
Warm Mix Asphalt	25	18,185	14,511	3,897	1,694
	10	16,677	12,931	2,888	1,145
	5	15,573	11,743	2,282	868
	1	12,864	8,918	1,277	506
	0.5	11,736	7,791	983	419
	0.1	9,188	5,441	604	364

The weighted average of the dynamic modulus was calculated using the results of frequency at 25 Hz. The interpolation between different temperatures was used to calculate the weighted average dynamic modulus at the field temperatures. The calculation of the 90^{th} percentile of the cumulative tensile strain of the perpetual pavement with RBM design and

perpetual pavement with RBM and WMA surface layer was executed. The result of the expected 90th percentile of the two pavement sections is presented in Figure 6-5.

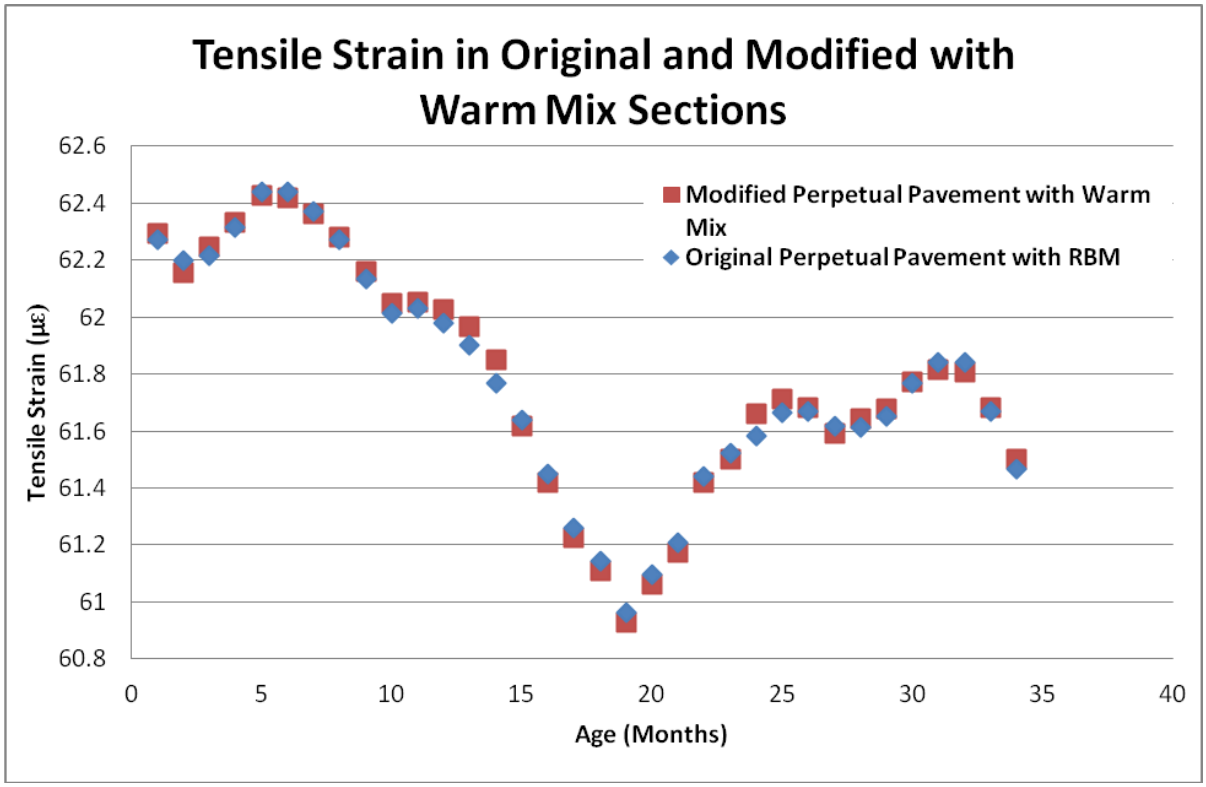

Figure 6-5: Tensile Strain in Perpetual Pavement with RBM and Perpetual Pavement with Warm Mix Asphalt and RBM

The impact of replacing the surface SP 12.5 asphalt layer with the WMA layer on the 90th percentile of cumulative tensile strain is considered insignificant. This conclusion is expected due to the small thickness of the surface layer compared to the total thickness of asphalt layers. Therefore, the impact of changing the surface layer is expected to be limited. Furthermore, the developed model is utilized to calculate the 90th percentile of tensile strain at the bottom of asphalt layers. Thus, the effect of changing the properties of the surface layer is expected to be insignificant especially with the perpetual pavement designs. The result of

this example provides insight and guidance for considering the WMA technology in perpetual pavement designs. However, field research is required to verify the preliminary evaluation that was carried over using the developed model.

6.4 Case Study – In-Situ Strain Prediction

This section presents an example for using the developed models to predict the tensile strain at the bottom of asphalt layers in a different pavement section. The main idea about the use of this model to enhance the in-situ strain prediction is through developing a correction factor between the mechanistic tensile strain and the model predicting the in-situ tensile strain. The mechanistic tensile strain can be calculated using the linear elastic model or software such as WESLEA for Windows, KenPave and ELSYM 5. The ratio between the mechanistic tensile strain and the in-situ tensile strain can be used to correct other mechanistically calculated tensile strains for different pavement deigns. A detailed example will be presented to estimate the in-situ tensile train for a pavement cross section presented in Figure 6-6.

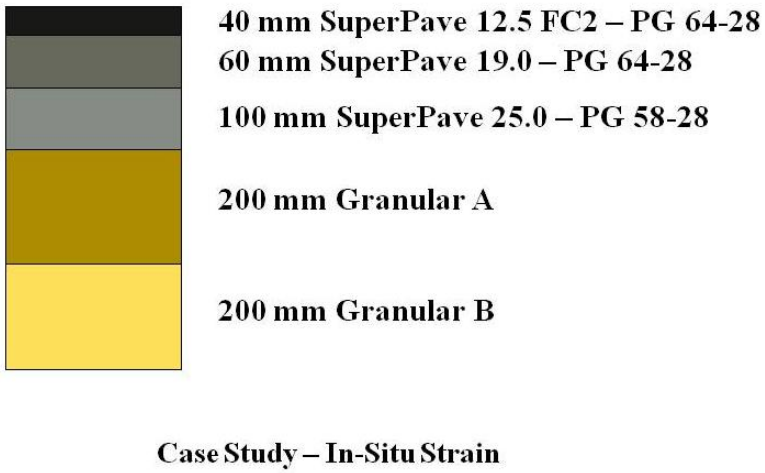

Figure 6-6: Pavement Section for the Case Study

The pavement cross section presented in Figure 6-6 consists of 200 mm thick of asphalt layers. The mechanical properties of the asphalt mixes used to construct this pavement section are assumed to be similar to those of the asphalt mixes used in the construction of the Highway 401 test section. The thickness of asphalt layers in this case study is comparable to that of the conventional pavement section on the Highways 401. Consequently, the prediction of in-situ strain for the section presented in Figure 6-6 will be implemented using a correction factor that is developed from the conventional pavement section of Highway 401.

6.4.1 Calculation of the Correction Factor

The correction factor used in this example is the ratio between the in-situ tensile strain and the mechanistic tensile strain calculated using WESLEA for Windows.

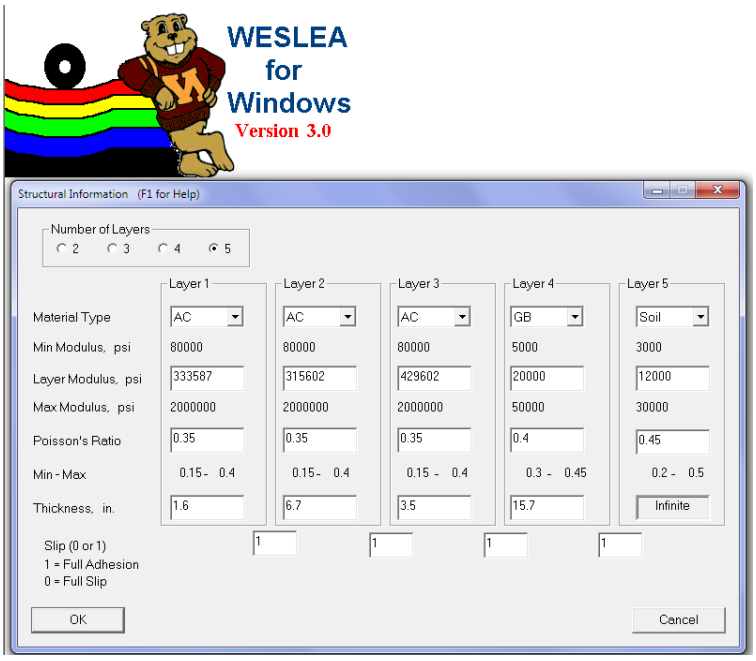

Figure 6-7: Conventional Pavement Inputs for WESLEA

Figure 6-7 presents the inputs for the conventional pavement section of Highway 401. The resilient modulus of different asphalt mixes used in the Highway 401 project was used for the layer's modulus. This assumption was based on research conducted by Minnesota DOT [Timm, 1999]. In addition, the granular base and subbase layers were assumed to have a weighted average layer modulus of 20,000 PSI. Figure 6-8 presents the load configuration for the calculation of the mechanistic tensile strain. The single axle load of 22,000 Lb (100 KN) was used and a tire pressure of 110 PSI was assumed.

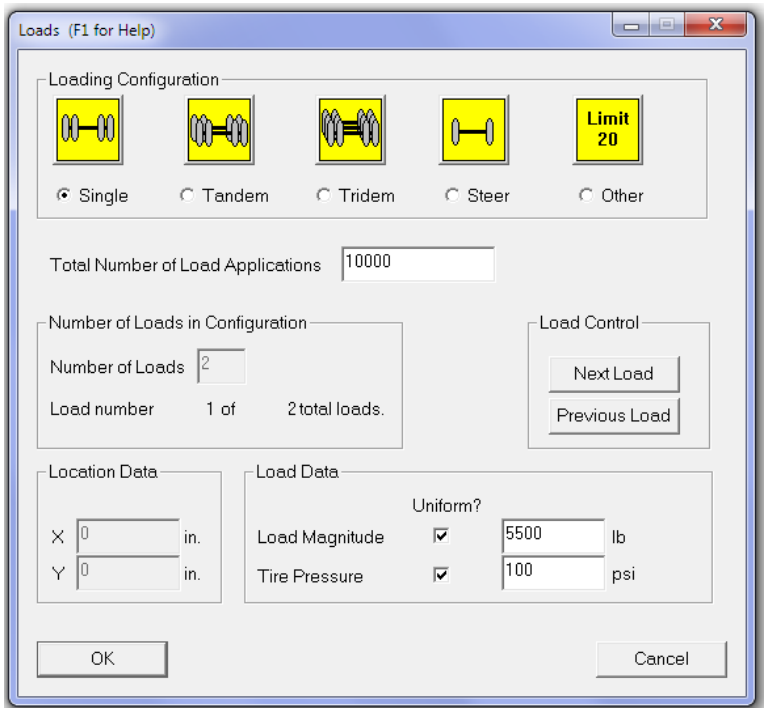

Figure 6-8: Load Configuration for the Mechanistic Calculation of Tensile Strain in Conventional Pavement

The output of the mechanistic tensile strain calculation was the value of 116.74 με. Figure 6-9 shows the output file from WESLEA for Windows.

$$\text{The correction factor is calculated} = \frac{90^{th}\ \text{Percentile of In-Situ Tensile Strain (Model)}}{\text{Mechanistic Tensile Strain (WESLEA)}} \quad (6\text{-}1)$$

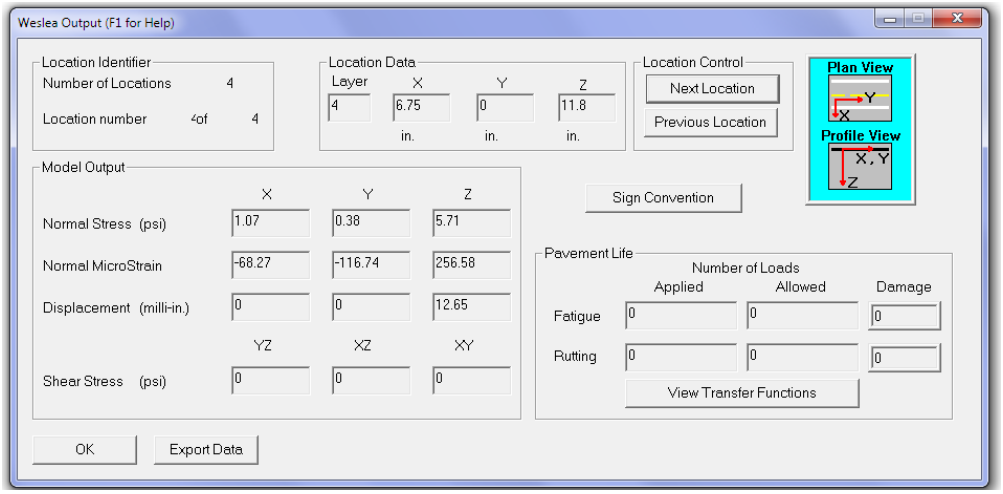

Figure 6-9: Output from WESLEA

The correction factor will vary based on the value of the 90th percentile of the tensile strain of the conventional pavement design. The equation to calculate the 90th percentile of the tensile strain for conventional pavement is presented in section 4.4.4.

$$y = -18.75 + 0.018 \times age - 0.92 \times \frac{1000}{\sqrt{(E_0^*)}} + 0.767 \times \frac{1000}{\sqrt{(E_1^*)}} + 20.24 \times \ln(Temperature) \qquad (6\text{-}2)$$

The direct application of the equation will depend on the pavement age, field temperature and corresponding dynamic modulus value for all asphalt mixes. The calculated 90th percentile of the in-situ tensile strain is presented in Table 6-3.

The calculation of the correction factor can be carried out by applying equation 6-1. The calculated 90th percentile of tensile strain using the developed model is presented in the column entitled "Model" in Table 6-3. The value of the mechanistic tensile strain calculated using WESLEA is 116.74 με. Table 6-4 presents the correction factors corresponding to different temperatures for the conventional pavement section.

Table 6-3: Calculation of the 90th Percentile of Tensile Strain Using the Developed Model

Age (Months)	E*1	E*2	Temp (Kelvin)	MODEL	Actual (Measured)
9	13031	12450	288	94.8	95.0
9.5	10397	10502	293	94.8	94.9
10	9150	9308	296	94.9	94.0
10.5	7711	7699	300	95.1	95.1
11	5552	5287	306	95.5	95.3
11.5	5192	4884	307	95.5	95.9
12	5911	5689	305	95.4	95.8
12.5	6991	6895	302	95.3	95.2
13	8431	8504	298	95.1	95.0
13.5	9510	9710	295	94.9	95.4
14	13031	12450	288	94.9	94.5
14.5	14611	13620	285	94.9	94.8
15	16191	14789	282	94.8	94.7
15.5	18298	16347	278	94.6	94.7
16	21063	18400	274	94.4	94.3
16.5	24794	21172	269	94.2	94.4
17	27779	23389	265	94.0	94.2
17.5	29271	24498	263	93.9	94.0
18	29271	24498	261	93.7	93.5
18.5	29271	24498	263	93.9	93.9
19	27033	22835	266	94.1	94.0
19.5	21810	18954	273	94.5	94.4
20	19571	17291	276	94.6	94.7
20.5	17245	15568	280	94.8	95.0
21	14611	13619	285	95.0	94.6
21.5	12504	12061	289	95.1	95.0
22	10924	10891	292	95.1	95.1
22.5	9150	9308	296	95.1	95.2
23	8431	8504	298	95.2	95.1
23.5	6631	6493	303	95.5	95.5
24	5192	4884	307	95.8	95.6
24.5	4832	4482	308	95.8	95.6
25	6991	6895	302	95.5	95.6
25.5	9150	9308	296	95.2	95.6

Table 6-4: Correction Factor Calculation

MODEL	Correction Factor	MODEL	Correction Factor	MODEL	Correction Factor
94.8	0.812	94.9	0.813	94.8	0.812
94.8	0.812	94.8	0.812	95.0	0.814
94.9	0.813	94.6	0.81	95.1	0.815
95.1	0.815	94.4	0.809	95.1	0.815
95.5	0.818	94.2	0.807	95.1	0.815
95.5	0.818	94.0	0.805	95.2	0.815
95.4	0.817	93.9	0.804	95.5	0.818
95.3	0.816	93.7	0.803	95.8	0.821
95.1	0.815	93.9	0.804	95.8	0.821
94.9	0.813	94.1	0.806	95.5	0.818
94.9	0.813	94.5	0.809	95.2	0.815
		94.6	0.8103		

The mean and standard deviation of correction factors for different temperatures are 0.813 and 0.005 respectively. Thus, the range of the correction factor falls within the boundary between $MEAN_{Correction\ Factor} \pm 3 \times STANDARD\ DEVIATION_{Correction\ Factor}$ with a confidence of 99%. Therefore the correction factor for the mechanistic tensile strain ranges between 0.799 and 0.827.

The mechanistic tensile strain of the case study pavement cross section presented in Figure 6-6 is then calculated. The traffic load used in the mechanistic calculation should represent the expected traffic on the new pavement section. In the case study presented in this thesis, the traffic load used in the mechanistic calculation is assumed similar to that of Highway 401. Similarly, the layer modulus represents the elastic modulus of the asphalt layers that would be used to construct the pavement section. The layer's modulus in this example is assumed as the dynamic modulus result for the mixes used in construction of the Highway 401 test section. The inputs of WESLEA to calculate the mechanistic tensile strain are presented in

Figure 6-10. The calculated mechanistic strain at the bottom of asphalt layers is 188.18 με as shown in Figure 6-11.

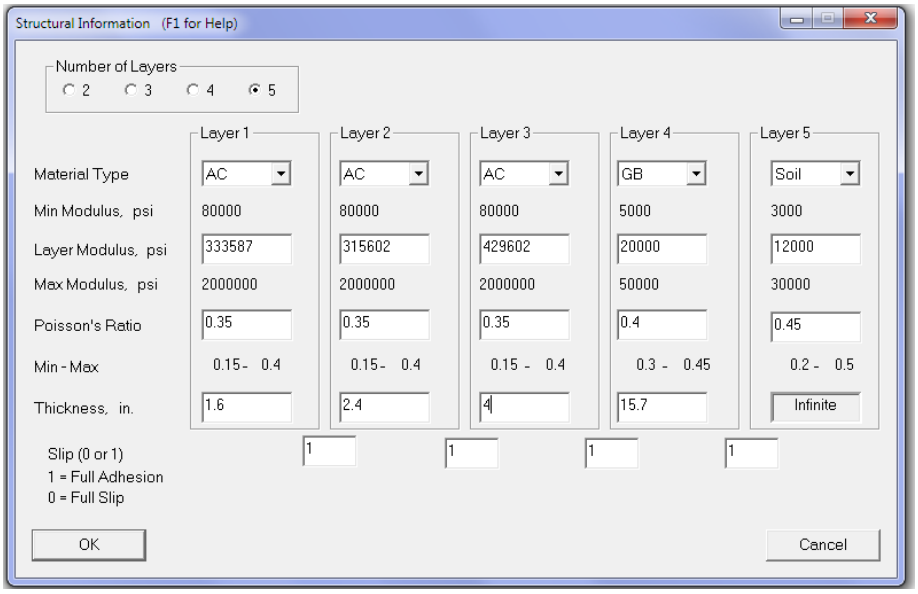

Figure 6-10: Calculation of Mechanistic Strain in the Case Study

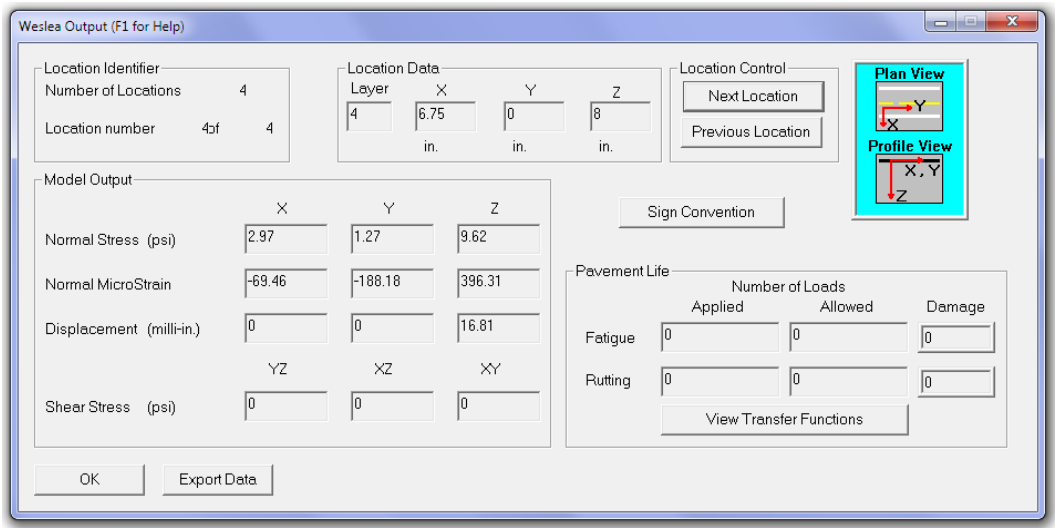

Figure 6-11: Output of WESLEA

The estimated 90th percentile of the in-situ tensile strain is calculated using the calculated mechanistic strain and the correction factor determined using the conventional pavement

model. The following equation illustrates the calculation of estimated 90^{th} percentile of the in-situ tensile strain.

Estimated 90^{th} Percentile of In-Situ Tensile Strain=Mechanistic Strain (WESLEA) X Correction Factor (6-3)

The correction factors calculated and presented in Table 6-4 are noted to depend on the variation in pavement temperature, age and elastic modulus. Therefore, a range of correction factors is recommended for a sensitivity study showing the expected spectrum of the 90^{th} percentile of in-situ tensile strain. The correction factor range is [0.799, 0.827] with a confidence of 99%. Thus, the 90^{th} percentile of the in-situ tensile strain for this case study ranges between 150.3με and 155.6 με.

6.5 Summary

The presented methodologies to apply the developed models to estimate the 90^{th} percentile of in-situ tensile strain are intended to provide insight to the designers and managers on structural changes of the pavement section due to changing pavement thickness and properties of asphalt mixes. Although the developed models have several limitations in the sense they are only applicable to a certain climate region, traffic pattern and thickness, the models can provide guidance for design of several highways in Southern Ontario. In addition, the methodology of assessment outlined can provide valuable insight into pavement performance and ultimately life cycle cost. The proposed applications of the models require future field validation and further research to assess the accuracy and limitations of those applications.

Chapter 7
Conclusions and Recommendations

7.1 Conclusions

The thesis included a structural and economic evaluation of two perpetual pavement designs and a conventional pavement design. In addition, various sustainability aspects and evaluation systems were identified. The two perpetual pavement designs were not identical with the exception of the asphalt cement content in the bottom asphalt layer. One perpetual pavement design did not include a RBM layer while the other section was designed as a perpetual pavement with RBM layer.

The final conclusion of the thesis will summarize the structural and economic evaluation of both designs. The statistical analysis supports the following conclusion and recommendations were presented in previous chapters.

The structural evaluation can be concluded in the following points:

1. The 90^{th} percentile of cumulative tensile strain in perpetual pavement section with RBM is less than that in both the perpetual pavement section without RBM and the conventional section. This indicates that the additional 0.8% asphalt binder provides structural benefits.

2. The comparison between the 90^{th} percentile of tensile strain in perpetual pavement with RBM and the perpetual pavement without RBM layer indicates that the additional binder in the RBM layer resulted in a reduction in the tensile strains at the bottom of asphalt layers. A slight difference between tensile strains in both sections

was noticed through the data collected within the research period. However, the benefits of the additional binder are expected to increase on the medium and long term.

3. Both perpetual pavement structural designs are characterized by small tensile strain year around compared to the conventional pavement designs which is not as thick. This conclusion reflects the ability of perpetual pavement designs to maintain lower tensile strains at the bottom of asphalt layers compared to conventional designs.
4. The monthly tensile strain at the bottom of asphalt layer is sensitive to thickness of asphalt layers, temperature and modulus of elasticity of the different asphalt layers as a representative of the stiffness of asphalt layers.
5. The variation in cumulative tensile strain tends to decrease with the increase of age. At a certain point (around 1.5 to 2 years of service life), the cumulative tensile strain will reach a stable level where the impact of temperature variation on the cumulative tensile strain will level out. The changes in the cumulative tensile strain will reflect the long-term pavement resistance to bottom-up fatigue cracking.

The final conclusions from the economic evaluation can be summarized as follows:

1. The initial construction cost of perpetual pavement design is approximately 30% higher than that of the conventional pavement design.
2. The conventional pavement section would require more frequent maintenance activities compared to that of the perpetual sections. The increase in the number of maintenance activities also results in increases in lane closures, user delay costs

due to lane closures and can result in a direct environmental impact due to the fumes, heat and noise associated with frequent maintenance activities.

3. Although the construction cost of the perpetual pavement design is higher than that of conventional design by 30%, the perpetual pavement design proved to be the most economic alternative compared to the conventional pavement design after a 70-year analysis period of LCCA and especially on high traffic areas. Assuming 3% discount rate, the NPV of the perpetual pavement was 5.6% less than that of the conventional design.

In addition to previously listed specific structural and economic conclusions, other general conclusions could be summarized as follows:

1. Perpetual pavement sections constructed using HMA containing RAP receive sustainability credits in Ontario in accordance with GreenPave.
2. The use of RBM layers in other types of pavements may provide structural benefits.

7.2 Recommendations

This thesis represents the analysis of a research project targeting full evaluation of the benefits of construction of perpetual pavements on a Canadian road network. The general recommendations include recommendations based on the research carried over in this thesis and other recommendations for future research. The following points summarize the recommendations of this thesis.

1. The construction of perpetual pavement sections in provincial highways and on heavy traffic highways provide benefits, especially as they have the potential to resist fatigue cracking and life cycle cost savings.
2. Installation of the RBM layer at the bottom of asphalt layers in perpetual pavement designs reduces stiffness of the bottom asphalt layer and thus enhances resistance to fatigue cracking. The cost associated with the additional binder is negligible compared to the cost of construction of the whole pavement cross section.
3. Regression models introduced in the thesis could be used for calculation of 90^{th} percentile of cumulative tensile strain in perpetual pavements and conventional pavements provided that the pavement cross section is similar to that constructed on Highway 401 and the traffic pattern and volume is relatively close to that on Highway 401.

The recommendations directed towards future research and further investigations are summarized in the following points.

1. Continue data collection for at least 8 years to allow for a full structural evaluation for the first ten years of the service life of perpetual and conventional pavement sections. Further data collection beyond ten years would also be desirable but certainly the first ten years would be very useful.
2. Consider construction of perpetual pavement sections on medium or low traffic volume roads to assess the benefits of constructing perpetual pavement designs on

different categories of traffic loads. Note perpetual pavements could simply be considered as a 20% - 40% increase in asphalt thickness.

3. Conduct further laboratory tests such as measuring rutting depth using the Hamburg Wheel Rut Tester and the four-point fatigue beam testing on the various asphalt mixes. Statistical evaluation for the correlation between in-situ field strain and the different laboratory test results should be undertaken.
4. Evaluation of the vertical compressive strain in both perpetual and conventional pavement designs, as this is another key structural indicator showing the structural capacity of the pavement design.
5. Extending the economic evaluation to include the user delay cost and an economic evaluation related to sustainability.

7.3 Major Contributions

This research project resulted in several major contributions to science. The limitations and uncertainties about in-situ tensile strain at the bottom of asphalt layers in perpetual pavements subjected to cold climate were studied and illuminated in this research project. The main contributions accomplished through this thesis can be summarized in the following points.

1. Investigated the benefits of additional 0.8% binder content to form RBM layer at the bottom of asphalt layers. The evaluation of the benefits was done by comparing the E* results of regular SP 25 and SP 25 RBM mixes at the construction year and how the E* changed after one year of freeze-thaw cycles.

2. Derived relations between several laboratory test results and the in-situ field strain in perpetual and conventional pavement designs.

3. Development of four regression models to accurately calculate the 90^{th} percentile of cumulative in-situ tensile strain. The developed models are valid for perpetual and conventional pavement designs of similar thickness and traffic pattern to that on the Highway 401 project.

4. Execution of economic evaluation through LCCA for a 70-year analysis period to assess the perpetual and conventional pavement designs based on local market costs provided by contractors in Ontario and the MTO.

5. Development of a methodology for assessing the perpetual pavement design in Canada.

References

[AASHTO, 1993] AASHTO TP10-93, “Standard Test Method for Thermal Stress Restrained Specimen Tensile Strength”, American Association of State Highway and Transportation Officials, 444 N Capitol St. NW — Suite 249 — Washington, DC 20001, 1993.

[AASHTO, 2007] AASHTO TP62, “Standard Method of Test for Determining Dynamic modulus of Hot Mix Asphalt (HMA)”, American Association of State Highway and Transportation Officials, 444 N Capitol St. NW — Suite 249 — Washington, DC 20001, 2007.

[AASHTO, 2010] Binder, A. Asphalt. "AASHTO M 320 or AASHTO MP 1a.", Per PC/COT Standard Specifications.

[ASTM, 2007] ASTM Standard D6931, “Standard Test Method for Indirect Tensile (IDT) Strength of Bituminous Mixtures”, ASTM International, West Conshohocken, PA, 2003, DOI: 10.1520/D6931-07, 2007.

[ASTM, 2009 a] ASTM Standard D7369, “Standard Test Method for Determining the Resilient Modulus of Bituminous Mixtures by Indirect Tension Test”, ASTM International, West Conshohocken, PA, 2003, DOI: 10.1520/D7369-09, 2009.

[ASTM, 2009 b] ASTM, “Standard Practice for Preparation of Test Specimens of Bituminous Mixtures by Means of Gyratory Shear Compactor”, ASTM International, West Conshohocken, PA, DOI: 10.1520/D4013-09, 2009.

[Al-Qadi, 2008] Al-Qadi, I.L., Wang, H., Yoo, P., Dessouky, S., "Dynamic Analysis and In-situ Validation of Perpetual Pavement Response to Vehicular Loading", Transportation Research Board Annual Meeting, 2008.

[APA, 2002] Asphalt Pavement Alliance, Perpetual pavements: A synthesis, APA 101, Asphalt Pavement Alliance, 2002.

[Asphalt Institute, 1982] Asphalt-Institute, "Reseach and Development of the Asphalt Institute's Thickness Design Manual (MS-1)", 9th ed. Research Report 82-2ts, Asphalt Institute, Lexington, KY, 1982.

[Asphalt Institute, 1991] Asphalt-Institute, "Thickness Design - Asphalt Pavements for Highways and Streets. Manual Series No.1 (MS-1"), Asphalt Institute, Lexington, KY, 1991.

[Baker, 1903] Baker, I.O., Roads and Pavements, John Wiley and Sons, New York, 1903.

[Baker, 1994] Baker, H., Buth, M., Van Deusen, D., "Minnesota Road Research Project Load Response Instrumentation Installation and Testing Procedures", Report No. MN/PR-94/01, Minnesota Department of Transportation, St. Paul, MN, 1994.

[Battaglia, 2010] Battaglia, I., "Evaluation of a Hot Mix Asphalt Perpetual Pavement", WisDOT, Report No. FEP-01-10, 2010.

[Baus, 2010] Baus, R., Stires, N., "Mechanistic-Empirical Pavement Desig Guide Implementation", FHWA-SC-10-01 Report, University of South Carolina, 2010.

[Brundtland, 1987] Brundtland, Gro Harlem, Report of the World Commission on environment and development:"our common future", United Nations, 1987.

[Boussinesq, 1885] Boussinesq, J., “Application des Potentiels a l’etude de l’equilibre et du Mouvement des Solids Elastiques”, Gauthier-Villars, Paris, 1885.

[Chan, 2009] Chan, S., “MTO Pavement Design and Rehabilitation Manual”, second edition. Chapter 5: Evaluation and Pavement Management. Draft Version. Ministry of Transportation Ontario Material Engineering Research Office, 2009.

[Chan, 2010] Chan, P., Tighe, S., “Quantifying Pavement Sustainability”, Final Report submitted to the Ministry of Transportation of Ontario (MTO), University of Waterloo, Waterloo, Ontario, 2010.

[Crovetti, 2008] Crovetti, J., Titi, H., et al. “Materials Characterization and Analysis of the Marquette Interchange HMA Perpetual Pavement” Project 08-08, Midwest Regional University Transportation Center, University of Wisconsin, Madison, 2008.

[El-Hakim, 2009 a] El-Hakim, M., “Instrumentation and Overall Evaluation of Perpetual and Conventional Flexible Pavement Designs”. MASc Thesis, Department of Civil Engineering, University of Waterloo, Waterloo, Ontario, 2009.

[El-Hakim, 2009 b] El-Hakim M., Tighe S., Galal K., “M-E Performance Evaluation and LCCA of a Conventional Asphalt Pavement and a Perpetual Asphalt Pavement Section”, International Conference on Perpetual Pavements (ICPP), Columbus, Ohio, 2009.

[El-Hakim, 2009 c] El-Hakim, M., Tighe, S., Galal, K., "Performance Prediction and Economic Analysis of Perpetual and Conventional Pavement Designs using Mechanistic Empirical Models", Canadian Technical Asphalt Association (CTAA), Moncton, New Brunswick, 2009.

[El-Hakim, 2010] El-Hakim, M., Norris, J., Tighe, S., "Laboratory Analysis of Asphalt Mixes used in Highway 401 Perpetual Pavement Project", Canadian Technical Asphalt Association (CTAA), Edmonton, Alberta, 2010.

[El-Hakim, 2012 a] El-Hakim, M., Tighe, S., "Evaluation of Environmental Impact on Perpetual and Conventional Pavement Designs: A Canadian Case Study", Transportation Association of Canada (TAC), Fredericton, NB, 2012.

[El-Hakim, 2012 b] El-Hakim, M., Tighe, S., "Sustainability of Perpetual Pavement Designs: A Canadian Prospective", Journal of Transportation Research Record (TRR), Washington DC, 2012.

[El-Hakim, 2013] El-Hakim, M., Tighe, S., "Evaluation of Perpetual Pavement Design Philosophy for Three Traffic Volume Scenarios", Transportation Research Board (TRB), Accepted for presentation in January 2013.

[Gary, 1939] Gray, B.E., "Present Design Practice and Construction Developments in Flexible Pavements," Proceedings, Highway Research Board, Washington, D.C., December 5-8, 1939.

[Gierhart, 2008] Gierhart, D. "Analysis of Oklahoma Mix Designs for the National Center for Asphalt Technology Test Track using the Bailey Method," Transportation Research Board Annual Meeting, Washington D.C., 2008.

[Google Earth, 2008] Google Earth 5.0. (2008, July 18).

[Haas, 1997] Haas, Ralph CG, and Transportation Association of Canada, "Pavement Design and Management Guide", Transportation Association of Canada, 1997.

[Hajek, 2008] Hajek, J., Smith, K., Rao, S., Darter, M.,"Adaptation and Verification of AASHTO Pavement Design Guide for Ontario Conditions", Champaign, Illinois: ERES consultants, 2008.

[Harm, 2001] Harm, E. "Illinois Extended-Life Hot-Mix Asphalt Pavements," Transportation Research Circular, Number 503, pp 108-113, 2001.

[Hein, 2007] Hein, D. & Hajek, J., " Life-cycle cost 2006 update". Toronto: Applied Research Associates, 2001.

[Hornyak, 2007] Hornyak, N. J., Crovetti, J. A., Newman, D. E., & Schabelski, J. P., "Marquette Interchange Perpetual Pavement Instrumentation Project: Phase I Final Report". Milwaukee, Wisconsin: Transportation Research Center - Marquette University, 2007.

[Huang, 1973] Huang, Y., "Critical Tensile Strain in Asphalt Pavements", Transportation Engineering Journal, ASCE, Vol. 99, No. TE3, pp. 553-569, 1973

[Huang, 2004] Huang, Y. H., "Pavement Analysis and Design", Upper Saddle River: Pearson Education Inc., 2004.

[Hubbard, 1910] Hubbard, P., Dust Preventives and Road Binders, John Wiley and Sons, New York, 1910.

[Jones, 1962] Jones, A., "Tables of Stresses in Three-Layer Elastic Systems", Bulletin 342, pp. 176-214, Highway Research Board, 1962.

[Kazmierowski, 2012] Kazmierowski, T., "GreenPave-Ontario's Pavement Sustainability Rating System", Transportation Association of Canada (TAC), New Brunswick, 2012.

[Louliz, 2007] Louliz, A., Al-Qadi, I., Lahouar, S., Freeman, T., “Data Collection and Management of the Instrumented Smart Road Flexible Pavement Sections”, Transportation Research Record , Washington DC, 142-151, 2007.

[Mahoney, 2001] Mahoney, J., “Study of Long-Lasting Pavements in Washington State”, Transportation Research Circular, Number 503, PP 88-95, 2001.

[Merrill, 2006] Merrill, D., Van Dommelen, A., and Gaspar. L., ”A review of practical experience throughout Europe on deterioration in fully-flexible and semi-rigid long-life pavements”, International Journal of Pavement Engineering, Vol. 7, No. 2, pp 101-109, 2006.

[MNDOT, 2001] MNDOT. (2001, February 12). “Minnesota Department of Transportation”, Retrieved July 15, 2009, from About Mn/Road Project: http://www.mrr.dot.state.mn.us/research/Mn/Road_project/AboutMn/Road90.asp

[Mings, 1993] Mings, J., Raad, L., “Uniqueness of Pavement Layer Moduli from Surface Deflection Measurments”, Report No. INE/TRC 93.02, Transportation Research Center, Institute of Northern Engineering, University of Alaska Fairbanks, Alaska, 1993.

[Monismith, 1972] Monismith, C. L., McLean, D. B., “Structural Design Considerations”, Proceedings of the Association of Asphalt Paving Technologists, Vol. 41, 1972.

[Muench, 2010] Muench, Stephen, "Greenroads v1.0 Rating System", University of Washington, 2010.

[NCAT, 2009] NCAT Test Track, Retrieved July 15, 2009, from National Center for Asphalt Technology (NCAT) at Auburn University: http://eng.auburn.edu/research/centers/ncat/facilities/test-track.html

[Newcomb, 2001] Newcomb, D. E., Buncher, M., Huddleston, I. J., "Concepts of perpetual pavements", Transportation Research Circular, 4-11, 2001.

[Newcomb, 2006] Newcomb, D., Hansen, K., "Mix Type Selection for Perpetual Pavements", International Conference on Perpetual Pavements. Columbus, Ohio, 2006.

[Nishizawa, 1997] Nishizawa, T., Shimeno, S., Sekiguchi, M., "Fatigue Analysis of Asphalt Pavements with Thick Asphalt Mixture Layer, Proceedings of the 8th International Conference on Asphalt Pavements, Vol. 2. University of Washington, Seattle, WA, Pp. 969-976, 1997.

[Nunn, 1997] Nunn, M., A. Brown, D. Weston, and J.C. Nicholls. "Design of Long-Life Flexible Pavements for Heavy Traffic", Report No. 250, Transportation Research Laboratory, Berkshire, U.K., 1997.

[Nunn, 2001] Nunn, M., Ferne B., "Design and Assessment of Long-Life Flexible Pavements," Transportation Research Circular, Number 503, pp 32-49, 2001.

[Pave Track, 2009] Pave Track, (2009, June 01). Retrieved July 15, 2009, from Pave Track: http://www.pavetrack.com/index.htm

[Pellinen, 2002] Pellinen, T. K., Witczak, M. W., "Stress dependent master curve construction for dynamic complex modulus" Journal of the Association of Asphalt Paving Technologists 71, 2002.

[Ponniah, 2009] Ponniah, J., Lane, B., Marks, P., Chan, S., "Ontario's Experience in the Construction of Perpetual Pavement Trials", Transportation Association of Canada (TAC), Vancover, British Columbia, 2009.

[Prowell, 2006] Prowell, B., Brown. E., "Methods for Determining the Endurance Limit Using Beam Fatigue Tests", International Conference on Perpetual Pavements (ICPP), Columbus, Ohio, 2006

[Public Roads Administration, 1949] Public Roads Administration, "Highway Practice in the United States of America", Public Roads Administration, Federal Works Agency, Washington, D.C., 1949.

[Raymond, 2012] Raymond, C., "How HMA Helps MTO Meet Its Goal of "the Greenest Roads in North America", Presentation in Ontario Hot Mix Producers Association (OHMPA) Fall Seminars, Toronto, 2012.

[Rolt, 2001] Rolt, J. "Long-Life Pavements," The world Bank Regional Seminar on Innovative Road Rehabilitation and Recycling Technologies, Amman, Jordan, 2000.

[Romanoschi, 2008] Romanoschi, S.A., Gisi, A.J., Portillo, M., Dumitru, C., "The first findings from the Kansas Perpetual Pavements experiment", Transportation Research Board, Washington D.C., 2008.

[Roy, 2008] Roy, F., "From Roads to Rinks: Government Spending on Infrastructure in Canada, 1961 to 2005", Analytical Paper by Statistics Canada, 2008. Retrieved April 25, 2012, from: http://publications.gc.ca/collections/collection_2008/statcan/11-624-M/11-624-MIE2008019.pdf

[Sanchez, 2012] Sanchez, X., Tighe, .S, "Determining Quantity of RAP in HMA in Ontario-Phase 1", Canadian Technical Asphalt Association (CTAA), Vancouver, BC, 2012.

[Schwartz, 2007] Schwartz, C. W., "Implementation of the NCHRP 1-37A Design Guide, Final Report Volume 1: Summary of Findings and Implementation Plan", College Park, Maryland: The University of Maryland, 2007.

[Shenoy, 2002] Shenoy, A. and Romero, P. "A Standardized Procedure for Analysis of the Dynamic Modulus (|E*|) Data to Predict Asphalt Pavement Distresses", Transportation Research Record, Number 1789, P. 173-182, Washington DC, 2002.

[Shook, 1982] Shook, J. F. et al., "Thickness Design of Asphalt Pavements - The Asphalt Institute Method," Proceedings of the 5th International Conference on the Structural Design of Asphalt Pavements, pp. 17-44, 1982.

[Small, 1988] Small, K. A., Winston, C., "Optimal highway durability", The American economic review, 78(3), 560-569, 1988.

[Smith, 1998] Smith, K., "Review of life-cycle costing analysis procedures", Champain, IL: ERES consultants inc., 1998.

[Statistics, Canada 2011] Statistics Canada Agency, "The Canadian Population in 2011: Population Counts and Growth", 2011. Retrieved April 24, 2012, from Statistics Canada: http://www12.statcan.gc.ca/census-recensement/2011/as-sa/98-310-x/98-310-x2011001-eng.pdf

[Thompson, 2006] Thompson, M., Carpenter, S., "Considering Hot-Mix Asphalt Fatigue Endurance Limit in Full-Depth Mechanistic-Empirical Pavement Design", International Conference on Perpetual Pavement (ICPP). Columbus, Ohio, 2006.

[Tighe, 2001] Tighe, S., "Guidelines for Probabilistic Pavement Life Cycle Cost Analysis", Transportation Research Record, 1769:28-38, 2001.

[Tighe, 2006] Tighe, S., ”Evaluation of Warm Asphalt Technology: Ramara Township Trial”, Final Report presented to McAsphalt Industries Ltd., 2006.

[Tighe, 2007] Tighe, S., Falls, L. C., & Dore, G., “Pavement Performance Evaluation of Three Canadian Low-Volume Test Road”, Transportation Research Record , 211-218, 2007.

[Tighe, 2010] Tighe, S., El-Hakim, M., "Canadian Case Study for Perpetual Pavement Design", 11th International Conference on Asphalt Pavements (ISAP), Nagoya, Japan, 2010.

[Tighe, 2012] Tighe, S., and Transportation Association of Canada, “Pavement Asset Design and Management Guide”, Transportation Association of Canada, 2012.

[Timm, 1999] Timm, D., Birgisson, B., Newcomb, D., “Mechanistic-Empirical Flexible Pavement Thickness Design: The Minnesota Method”, Report No. MN/RC-P99-10, Minnesota, 1999.

[Timm, 2003] Timm, D., Newcomb, D., “Calibration of Flexible Pavement Performance”, Transportation Research Record, 134-142, 2003.

[Timm, 2004 a] Timm, D., & Young, J., “The Effects of Load Spectra and Variability on Perpetual Pavement Design”, International Symposium on Design & Construction of Long Lasting Asphalt Pavements, Auburn, AL: International Society for Asphalt Pavements, 2004.

[Timm, 2004 b] Timm, D., Priest, A., McEwen, T., “Design and Instrumentation of the Structural Pavement Experiment at the NCAT Test Track”, NCAT Report NO. 04-01, 2004.

[Timm, 2006] Timm, D., Newcomb, D., "Perpetual Pavement Design for Flexible Pavements in the US", International Journal of Pavement Engineering , 111-119, 2006.

[Timm, 2011] Timm, D., Robbins, M., Huber G., Yang, Y., "Analysis of Perpetual Pavement Experiment Sections in China", Transportation Research Board, Washington DC, 2011

[Transport Canada, 2010] Transport Canada, "Transportation in Canada: An Overview", 2010. Retrieved April 24, 2012, from Transport Canada: http://www.tc.gc.ca/media/documents/policy/overview2010.pdf

[Ul-Islam, 2010] Ul-Islam, R., Tighe, S., Essex, R., "Engineering Recycled Asphalt Shingles into Superpave Mixes: An Ontario Case Study", Canadian Technical Asphalt Association (CTAA), Edmonton, Alberta, 2010.

[Ul-Islam, 2011] Ul-Islam, R., "Performance Evaluation of Recycled Asphalt Shingles (RAS) in Hot Mix Asphalt (HMA): An Ontario Perspective", MASc Thesis, University of Waterloo, 2011.

[Uzarowski, 2008] Uzarowski, L., Moore, G., Gamble, P.,"Innovative, Comprehensive Design and Construction of Perpetual Pavement on the Red Hill Valley Parkway in Hamilton", Transportation Association of Canada, Toronto, Ontario, 2008.

[Uzarowski, 2012] Uzarowski, L., Henderson, V., MacDonald, J., "Pavement and Materials Technology Review for Municipalities-Including a Case Study", Transportation Association of Canada, New Brunswick, 2012.

[Vaziri, 2011] Vaziri, S., "Investigation of Environmental Impact on Piezoelectric Weigh-In-Motion Sensing System", PhD thesis, University of Waterloo, 2011.

[Von Quintus, 2001] VonQuintus, H., "Hot-mix asphalt layer thickness design for longer-life bituminous pavements", Transportation Research Circular, 2001.

[Walubita, 2008] Walubita, L.F., Liu. W., Scullion, T. and Leidy. J., "Modeling Perpetual Pavements Using the Flexible Pavement System (FPS) Software", Transportation Research Board Annual Meeting, Washington D.C., 2008.

[Willis, 2009] Willis, J., "Field-Based Strain Thresholds for Flexible Perpetual Pavement Design". PhD Thesis, Department of Civil Engineering, Auburn University, Auburn, Alabama, 2009.

[Witczak, 2007] Witczak, M., "Specification Criteria for Simple Performance Tests for Rutting", NCHRP report 580, Project 9-19, Transportation Research Board, Washington D.C., 2007.

[Wu, 2004] Wu, Z., Z. Q. Siddique, and A. J. Gisi.,"Kansas Turnpike–An Example of Long Lasting Asphalt Pavement", Proceedings International Symposium on Design and Construction of Long Lasting Asphalt Pavements. National Center for Asphalt Technology, Auburn, AL, pp. 857-876, 2004.

[Yang, 2005] Yang, Y., Gao, X., Lin, W., Timm, D.H., Priest, A.L., G.A. Huber, Andrewski, D.A., "Perpetual Pavement Design in China," International Conference on Perpetual Pavement, Ohio Research Institute for Transportation and the Environment, 2005.

[Yang, 2006] Yang, Y., Gao x., Lin, W. et al. "Perpetual Pavement Design in China", International Conference on Perpetual Pavement, Columbus, Ohio, 2006

[Yoder, 1975] Yoder E., Witczak, M., “Principles of Pavement Design”, Wiley, New York, 1975.

[Zborowski, 2007] Zborowski, A., Kaloush, K., "Predictive equations to evaluate thermal fracture of asphalt rubber mixtures." Road Materials and Pavement Design 8.4: 819-833, 2007.

Appendix A

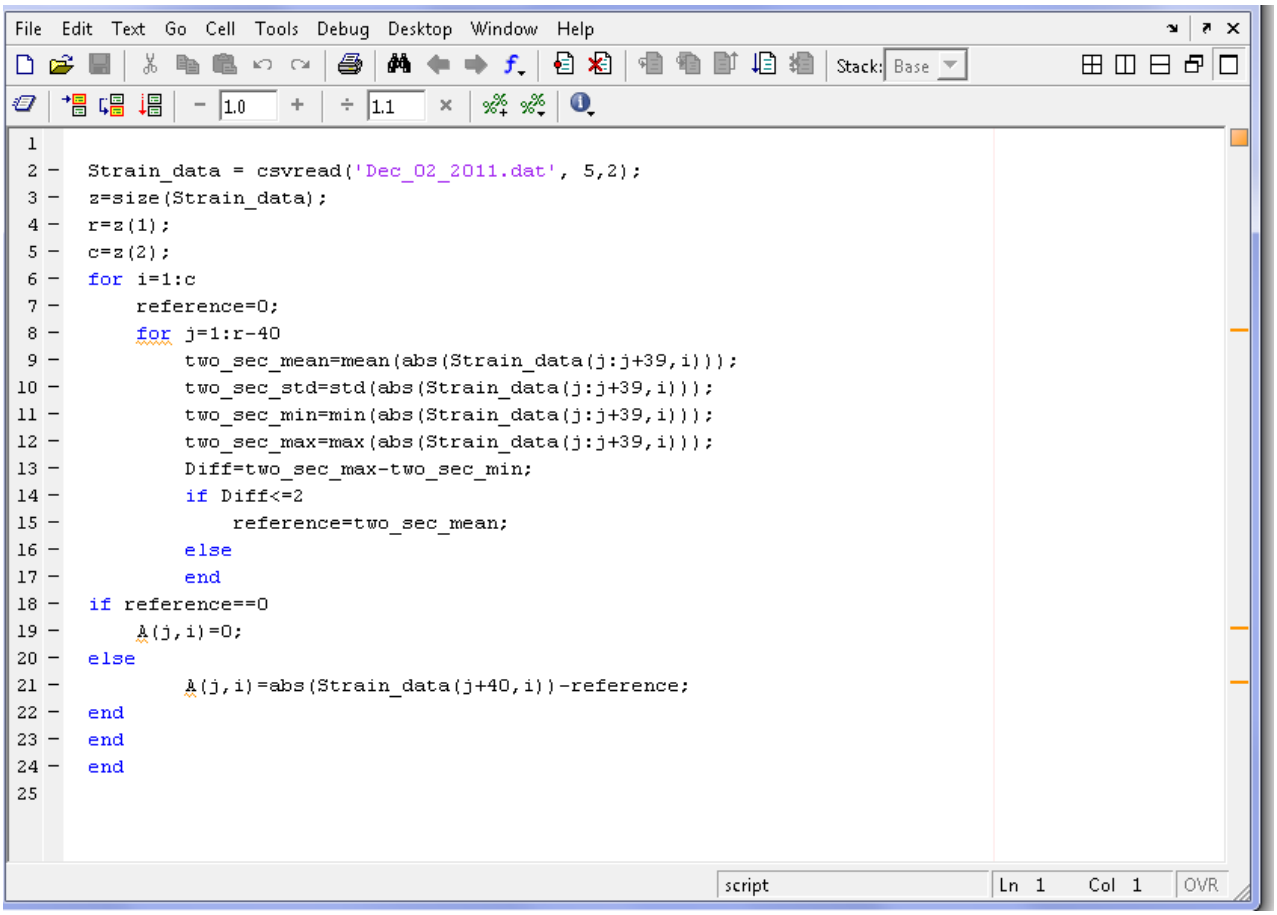
File Edit Text Go Cell Tools Debug Desktop Window Help
Stack: Base
1.0
1.1
Strain_data = csvread('Dec_02_2011.dat', 5,2);
z=size(Strain_data);
r=z(1);
c=z(2);
for i=1:c
reference=0;
for j=1:r-40
two_sec_mean=mean(abs(Strain_data(j:j+39,i)));
two_sec_std=std(abs(Strain_data(j:j+39,i)));
two_sec_min=min(abs(Strain_data(j:j+39,i)));
two_sec_max=max(abs(Strain_data(j:j+39,i)));
Diff=two_sec_max-two_sec_min;
if Diff<=2
reference=two_sec_mean;
else
end
if reference==0
A(j,i)=0;
else
A(j,i)=abs(Strain_data(j+40,i))-reference;
end
end
end
script
Ln 1 Col 1
OVR

Appendix B

Mix Design of SP 12.5

Miller Paving Limited
P.O Box 4080, Markham Industrial Park P.O
Markham, Ontario L3R 9R8
Tel:(905) 475-6660; Fax:(905) 475-4805

SUPERPAVE MIX DESIGN REPORT

CONTRACT NO.	2006-4016	HOT MIX TYPE / USE:	SP12.5FC2 / Surface Course
ITEM NO.:			
PROJECT:	Hwy 401	LOCATION:	Within Contract Limits
TESTING LAB.	Miller Paving Limited	JOB MIX FORMULA NO. :	
LAB MIX NO.	6068A	DATE SAMPLES RECD.	July 5, 2006
MIX SUPPLIER:	Miller Paving Limited	PLANT LOCATION:	GTA & Vicinity Plants
TEST DATA CERTIFIED BY:	[redacted] for Brian Eyers, P. Eng.,	DATE COMPLETED:	August 21, 2006

JOB MIX FORMULA --- GRADATION PERCENT PASSING*

% A.C / Sieve Sizes (mm)	% A.C	53.0	37.5	25.0	19.0	16.0	12.5	9.5	6.7	4.75	2.36	1.18	0.600	0.300	0.150	0.075
Job Mix Formula (JMF)	4.5	100.0	100.0	100.0	100.0	100.0	99.9	85.6	66.2	53.0	35.6	26.1	17.9	10.1	5.4	3.2

Superpave Volumetrics		REQUIRED	SELECTED
N_{des} (% Gmm)		96	96
N_{ini} (% Gmm)		<=89.0	87.8
N_{max} (% Gmm)		<=98.0	97.7
Air Voids (%) @ N_{des}		4.0	4.0
VMA (%)		14.0	14.4
VFA (%)	Minimum	65.0	72.0
	Maximum	75.0	
Dust Proportion	Minimum	0.6	0.77
	Maximum	1.2	
Tensile Strength Ratio, %		80.0% Minimum	83.0
Asphalt Film Thickness		N/A	10.1
Traffic Category		E	E

% CA #1	47.4	% RAP	--
% CA #2	--	%A.C RAP	--
% CA #3	--	Gmb	2.560
% FA #1	31.6		
% FA #2	13.2	Gmm	2.670
% FA #3	7.9		
		Composite Gsb	2.855

ASPHALT CEMENT	
SUPPLIER	AC GRADE
McAsphalt	PG 64-28

ADDITIVE		
SUPPLIER	TYPE	AS % OF Agg
--	Hydrated Lime	1.0

AGGREGATE TYPE	AGGREGATE SOURCE / INVENTORY NO.		AGGREGATE TYPE	AGGREGATE SOURCE / INVENTORY NO.	
COARSE AGG. # 1	DFC CA		FINE AGG. # 2	Unwashed Fines (1/4" minus)	
	MRT	B02-071		MRT	B02-071
COARSE AGG. # 2	--		FINE AGG. # 3	1/4" Chips	
	--	--		MRT	B02-071
COARSE AGG # 3	--		RAP # 1	--	
	--	--		--	--
FINE AGG. # 1	Washed Screenings		RAP # 2	--	
	Fowler/ Brace Bridge	B17-013		--	--

AGG. TYPE	Gsb	Gsa	Abs. (%)	AGGREGATE GRADATION (Sieve Sizes in mm)---- PERCENT PASSING														
				53.0	37.5	25.0	19.0	16.0	12.5	9.5	6.7	4.75	2.36	1.18	0.600	0.300	0.150	0.075
CA #1	2.874	2.910	0.425	100.0	100.0	100.0	100.0	100.0	99.8	69.7	29.5	10.0	6.1	4.9	4.0	2.2	1.0	0.4
CA #2																		
CA #3																		
FA #1	2.817	2.851	0.420	100.0	100.0	100.0	100.0	100.0	100.0	100.0	100	95.7	71.7	52.2	32.9	15.1	5.0	1.7
FA #2	2.864	2.911	0.560	100.0	100.0	100.0	100.0	100.0	100.0	100.0	98	95.9	68.7	48.7	35.3	25.0	17.2	10.5
FA #3	2.886	2.897	0.130	100.0	100.0	100.0	100.0	100.0	100.0	100.0	98.0	69.4	5.5	1.8	1.5	1.4	1.2	1.1

* FINES RETURNED TO MIX (1%)

REMARKS:
1. The pass 4.75mm portion of the blend gradation has been adjusted for fines returned to mix.
2. The specimens were compacted with SGC @ 145 °C (=Recompaction Temp.)
3. No SSD air void correction is required.
4. Weight required for 115 +/-5 mm Height of SGC Specimen = 5000 g
5. Determination of aggregate densities as per LS604/605 Rev.23
6. The absorption of water is <1.0%; hence, no sealing of specimens is required.

REVIEWED BY: _____ DATE _____

The Miller Group
Materials Research Laboratory
Summary of Superpave Properties

Mix Type: Superpave 12.5FC2 **Date:** August 21, 2006
Mix No.: 6068A **Contract No.:** 2006-4016

AC Content (%)	**4.1**	**4.6**	**5.1**	**5.6**
Gmm, Theoritical Maximum Specific Gravity	2.686	2.664	2.641	2.620
Gmb (Measured)	2.545	2.559	2.586	2.593
% Gmm @ Nini	87.0	87.9	89.5	90.9
% Gmm @ Ndes	94.7	96.1	97.9	99.0
Air Voids (%) Ndes	5.3	3.9	2.1	1.0
VMA (%)	14.53	14.49	14.03	14.26
VFA (%)	63.7	72.8	85.2	92.9
Dust Proportion	0.9	0.8	0.7	0.6
Water Absorption %	0.19	0.14	0.06	0.02
Gsb (Composite)	**2.855**			

The Miller Group
Materials Research Laboratory
Summary of Superpave Properties

Mix Type: Superpave 12.5FC2 **Date:** August 21, 2006
Mix No.: 6068A **Contract No.:** 2006-4016

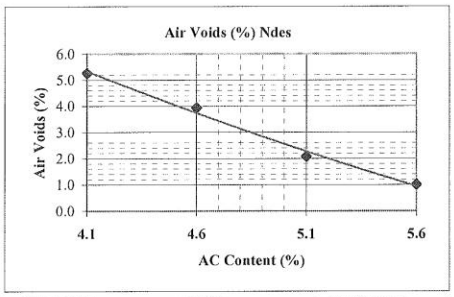

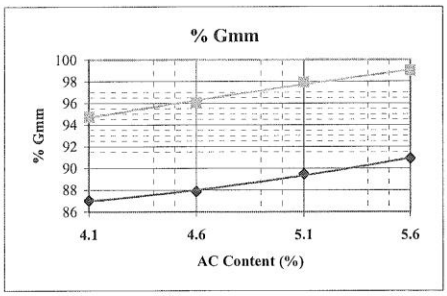

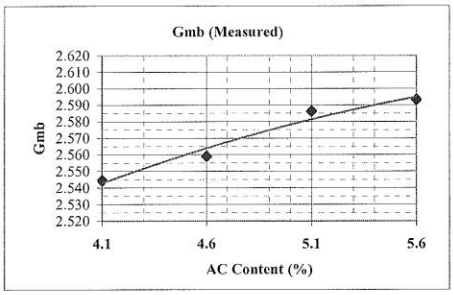

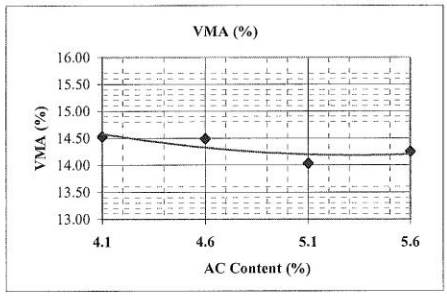

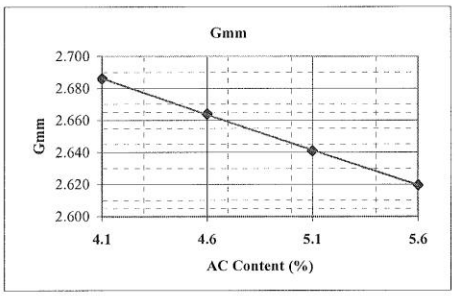

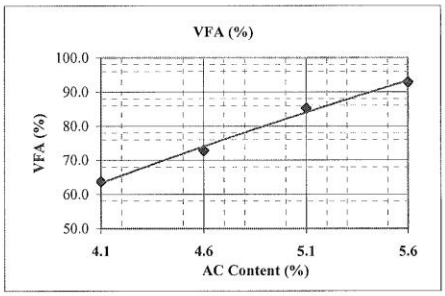

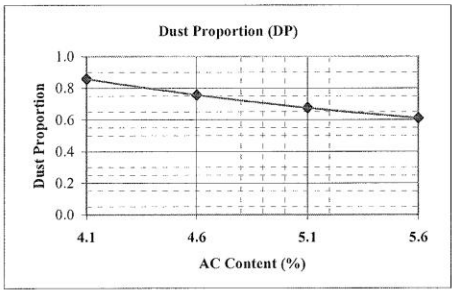

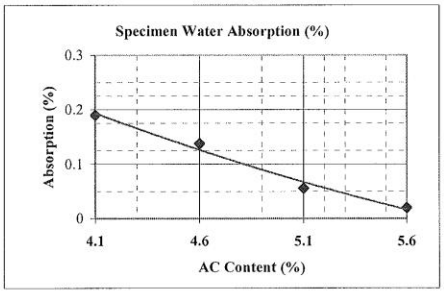

The Miller Group
Materials Research Laboratory

Mix No.: 6068A **Mix Type: Superpave 12.5FC2**

EFFECTIVE SPECIFIC GRAVITIES

Property		1	2
% Asphalt Cement Content	Pb	4.6	5.1
Specific Gravity Of Asphalt Cement	Gb	1.025	1.025
Theoritical Maximum Specific Gravity	Gmm	2.664	2.641
Effective Specific Gravities	Gse	2.887	2.885
Average Effective Specific Gravity		2.886	

THEORETICAL MAXIMUM SPECIFIC GRAVITIES

Property	1	2	3	4
% Asphalt Cement Content	3.6	4.1	5.6	6.1
% Aggregate	96.40	95.90	94.40	93.90
Specific Gravity Of Asphalt Cement	1.025	1.025	1.025	1.025
Effective Specific Gravities	2.886	2.886	2.886	2.886
Theoritical Maximum Specific Gravity	2.709	2.686	2.620	2.598

The Miller Group
Materials Research Laboratory

Superpave BITUMINOUS LABORATORY WORKSHEET

PROJECT NO.:	M600			**DATE:**		August 21, 2006
SUPPLIER	Miller Paving Limited			**MIX TYPE: Superpave 12.5FC2**		
% PASS 4.75mm:	53.0	**Gsb:**	2.855	**% AC:**	4.1	**MIX NO.: 6068A**

PARAMETER	SPECIMEN 1	SPECIMEN 2
A1: MASS OF COMPACTED SPECIMEN IN AIR	5006.5	5004.6
A2: S.D.MASS IN AIR AFTER IMMERSSION IN H_2O	5019.5	5010.6
B1: MASS OF COMPACTED SPECIMEN IN WATEI	3047.4	3048.3
B2: VOLUME (= A2-B1)	1972.1	1962.3
C: BULK REL. DENSITY (= A1/B2), Gmb Measured	2.539	2.550
D: MAX. THEORITICAL DENSITY, Gmm	2.686	

Superpave GYRATORY DENSIFICATION DATA

Mold Diameter, mm 150

GYRATIONS	SPECIMEN 1				SPECIMEN 2			
	HEIGHT (mm)	Gmb - Estimated	Gmb - Corrected	% Gmm	HEIGHT (mm)	Gmb - Estimated	Gmb - Corrected	% Gmm
5	128	2.213	2.267	84.4	125.2	2.262	2.298	85.5
9	124.9	2.268	2.323	86.5	122.3	2.315	2.352	87.6
67	116.3	2.436	2.495	92.9	114.5	2.473	2.513	93.5
125	114.3	2.478	2.539	94.5	112.8	2.510	2.550	94.9

Gyrations	Average % Gmm	Average Air Voids (%)
5	85.0	15.0
9	87.0	13.0
67	93.2	6.8
125	94.7	5.3

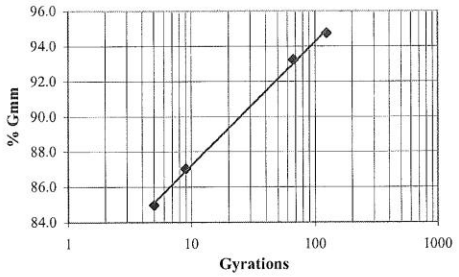

The Miller Group
Materials Research Laboratory

Superpave BITUMINOUS LABORATORY WORKSHEET

PROJECT NO.:	M600			**DATE:**		August 21, 2006
SUPPLIER	Miller Paving Limited			**MIX TYPE: Superpave 12.5FC2**		
% PASS 4.75mm:	53.0	**Gsb:**	2.855	**% AC:**	4.6	**MIX NO.: 6068A**

PARAMETER	SPECIMEN 1	SPECIMEN 2
A1: MASS OF COMPACTED SPECIMEN IN AIR	5005.5	5011.2
A2: S.D.MASS IN AIR AFTER IMMERSSION IN H_2O	5014.3	5016.2
B1: MASS OF COMPACTED SPECIMEN IN WATEI	3054.5	3061.8
B2: VOLUME (= A2-B1)	1959.8	1954.4
C: BULK REL. DENSITY (= A1/B2), Gmb Measured	2.554	2.564
D: MAX. THEORITICAL DENSITY, Gmm	2.664	

Superpave GYRATORY DENSIFICATION DATA

Mold Diameter, mm 150

GYRATIONS	SPECIMEN 1				SPECIMEN 2			
	HEIGHT (mm)	Gmb - Estimated	Gmb - Corrected	% Gmm	HEIGHT (mm)	Gmb - Estimated	Gmb - Corrected	% Gmm
5	127.2	2.227	2.273	85.3	125.4	2.261	2.292	86.0
9	124	2.284	2.332	87.5	122.3	2.318	2.350	88.2
67	115.2	2.458	2.510	94.2	113.9	2.489	2.524	94.7
125	113.2	2.502	2.554	95.9	112.1	2.529	2.564	96.2

Gyrations	Average % Gmm	Average Air Voids (%)
5	85.7	14.3
9	87.9	12.1
67	94.5	5.5
125	96.1	3.9

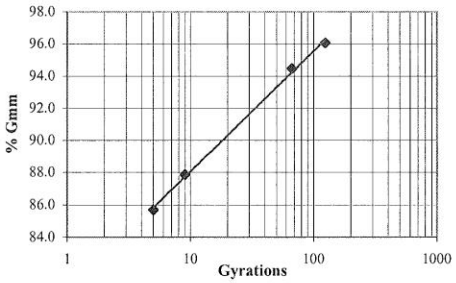

The Miller Group
Materials Research Laboratory

Superpave BITUMINOUS LABORATORY WORKSHEET

PROJECT NO.:	M600			**DATE:**		August 21, 2006
SUPPLIER	Miller Paving Limited			**MIX TYPE: Superpave 12.5FC2**		
% PASS 4.75mm:	53.0	**Gsb:**	2.855	**% AC:**	5.1	**MIX NO.: 6068A**

PARAMETER	SPECIMEN 1	SPECIMEN 2
A1: MASS OF COMPACTED SPECIMEN IN AIR	5017.3	5018.7
A2: S.D.MASS IN AIR AFTER IMMERSSION IN H_2O	5020.0	5021.6
B1: MASS OF COMPACTED SPECIMEN IN WATEI	3080.7	3080.3
B2: VOLUME (= A2-B1)	1939.3	1941.3
C: BULK REL. DENSITY (= A1/B2), Gmb Measured	2.587	2.585
D: MAX. THEORITICAL DENSITY, Gmm	2.641	

Superpave GYRATORY DENSIFICATION DATA

Mold Diameter, mm **150**

GYRATIONS	SPECIMEN 1				SPECIMEN 2			
	HEIGHT (mm)	Gmb - Estimated	Gmb - Corrected	% Gmm	HEIGHT (mm)	Gmb - Estimated	Gmb - Corrected	% Gmm
5	125.1	2.269	2.308	87.4	125.7	2.259	2.301	87.1
9	122	2.327	2.367	89.6	122.6	2.316	2.360	89.3
67	113.4	2.503	2.546	96.4	113.7	2.497	2.544	96.3
125	111.6	2.544	2.587	98.0	111.9	2.538	2.585	97.9

Gyrations	Average % Gmm	Average Air Voids (%)
5	87.3	12.7
9	89.5	10.5
67	96.4	3.6
125	97.9	2.1

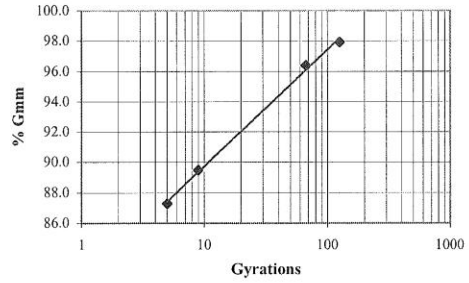

The Miller Group
Materials Research Laboratory

Superpave BITUMINOUS LABORATORY WORKSHEET

PROJECT NO.:	M600			**DATE:**		August 21, 2006
SUPPLIER	Miller Paving Limited			**MIX TYPE: Superpave 12.5FC2**		
% PASS 4.75mm:	53.0	**Gsb:**	2.855	**% AC:**	5.6	**MIX NO.: 6068A**

PARAMETER	SPECIMEN 1	SPECIMEN 2
A1: MASS OF COMPACTED SPECIMEN IN AIR	5012.9	5011.4
A2: S.D.MASS IN AIR AFTER IMMERSSION IN H_2O	5013.8	5012.5
B1: MASS OF COMPACTED SPECIMEN IN WATEI	3085.5	3075.2
B2: VOLUME (= A2-B1)	1928.3	1937.3
C: BULK REL. DENSITY (= A1/B2), Gmb Measured	2.600	2.587
D: MAX. THEORITICAL DENSITY, Gmm	2.620	

Superpave GYRATORY Ddensification DATA

Mold Diameter, mm 150

GYRATIONS	SPECIMEN 1				SPECIMEN 2			
	HEIGHT (mm)	Gmb - Estimated	Gmb - Corrected	% Gmm	HEIGHT (mm)	Gmb - Estimated	Gmb - Corrected	% Gmm
5	124.2	2.284	2.321	88.6	123.6	2.294	2.321	88.6
9	121.1	2.342	2.381	90.9	120.4	2.355	2.383	91.0
67	112.5	2.521	2.563	97.8	112.2	2.527	2.557	97.6
125	110.9	2.558	2.600	99.2	110.9	2.557	2.587	98.7

Gyrations	Average % Gmm	Average Air Voids (%)
5	88.6	11.4
9	90.9	9.1
67	97.7	2.3
125	99.0	1.0

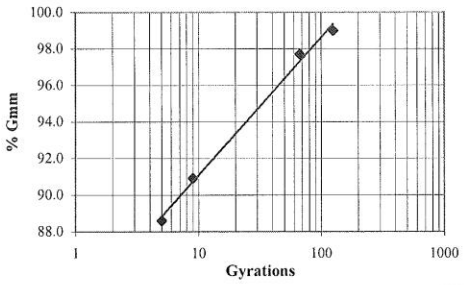

The Miller Group
Materials Research Laboratory

Superpave BITUMINOUS LABORATORY WORKSHEET

Specimens Gyrated to Nmax

PROJECT NO.:	M600			**DATE:**		August 21, 2006
SUPPLIER	Miller Paving Limited			**Mix Type: Superpave 12.5FC2**		
% PASS 4.75mm:	53.0	**Gsb:**	2.855	**% AC:**	4.5	**Mix No.: 6068A**

PARAMETER	SPECIMEN 1	SPECIMEN 2
A1: MASS OF COMPACTED SPECIMEN IN AIR	4999.6	5003.0
A2: S.D.MASS IN AIR AFTER IMMERSSION IN H_2O	5005.0	5006.3
B1: MASS OF COMPACTED SPECIMEN IN WATEI	3091.5	3086.2
B2: VOLUME (= A2-B1)	1913.5	1920.1
C: BULK REL. DENSITY (= A1/B2), Gmb Measured	2.613	2.606
D: MAX. THEORITICAL DENSITY, Gmm	2.670	

Superpave GYRATORY DENSIFICATION DATA

Mold Diameter, mm 150

GYRATIONS	SPECIMEN 1				SPECIMEN 2			
	HEIGHT (mm)	Gmb - Estimated	Gmb - Corrected	% Gmm	HEIGHT (mm)	Gmb - Estimated	Gmb - Corrected	% Gmm
5	124.6	2.270	2.315	86.7	125.3	2.259	2.304	86.3
9	121.6	2.326	2.372	88.8	122.4	2.313	2.359	88.3
125	111.6	2.535	2.585	96.8	112.4	2.518	2.569	96.2
205	110.4	2.562	2.613	97.9	110.8	2.555	2.606	97.6

Gyrations	Average % Gmm	Average Air Voids (%)
5	86.5	13.5
9	88.6	11.4
125	96.5	3.5
205	97.7	2.3

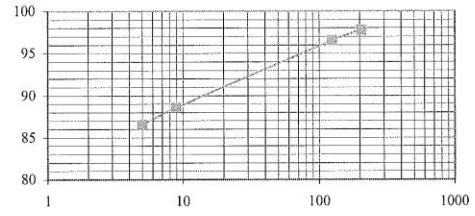

Moisture Susceptibility Test

Bituminous Laboratory Worksheet (AASHTO T283)

Lab (Mix) # 6068A **Mix Type/Use:** SP12.5FC2 **SGC** Baby Pine

Technician: Brian R **Project #** **Date:** August 14, 2006

PG AC GRADE 64-28 **Supplier:** McAsphalt **Antistrip Additive:** Hydrated Lime

SGC Specimen Data

1% Antistripping Additive

Sample ID	**1**	**2**	**6**	**3**	**4**	**5**
D Diameter (mm)	150.0	150.0	150.0	150.0	150.0	150.0
t Thickness (mm)	94.84	94.85	94.78	94.94	94.79	94.78
A Dry Weight in Air (g)	4055.9	4055.9	4055.3	4056.3	4057.8	4057.7
B SSD Weight in Air (g)	4074.3	4074.3	4081.5	4078.0	4081.1	4080.7
C Weight in Water (g)	2436.9	2436.9	2450.9	2439.4	2447.3	2453.1
E (=B-C) Volume (cc)	1637.4	1637.4	1630.6	1638.6	1633.8	1627.6
F (=A/E) **Gmb**, Bulk Sp. Gr.,	2.477	2.477	2.487	2.475	2.484	2.493
G Gmm Max. Sp. Gr.,	2.667	2.667	2.667	2.667	2.667	2.667
H (=100*(G-F)/G), Air Voids (%)	7.1	7.1	6.7	7.2	6.9	6.5
I (=H*E/100), Vol. Of voids (cc)	116.6	116.6	110.1	117.7	112.3	106.2
P Load (N)	20100	20000	21500			

Saturated Specimens	10 minutes		@ 18 mm Hg			
t" Thickness (mm)				94.96	94.74	94.94
B' SSD Wieght (g)				4144.9	4143.6	4137.1
E' (=B'-C') Volume (cc)						
J' (=B'-A) Vol. Of Abs. Water (cc)	-4055.9	-4055.9	-4055.3	88.6	85.8	79.4
% Saturation (=100*J'/I)	-3477.7	-3477.7	-3684.9	75.3	76.4	74.8
P" Load (N)				16000	18900	16250

Indirect Tensile Strength						
S_{td} (=2000P/πtD) Dry Strength	899.5	894.9	962.7			
Stm (=2000P"/πt"D) Wet Strength				715.1	846.7	726.4
TSR (=100*S_{tm}/S_{td})	**Avg. S_{td} (kPa)**	919.0	**Avg. S_{tm} (kPa)**	762.7	*TSR (%) @ 0% Additive*	***83.0***
Visual Stripping (0-5)	0	0	0	0	0	0

Miller Paving Limited
P.O Box 4080, Markham Industrial Park P.O
Markham, Ontario L3R 9R8
Tel:(905) 475-6660; Fax:(905) 475-3755

Superpave Consensus Property Requirement Test Data

Contract No.:	2005-2064	**Contractor**	Miller Paving Ltd	**Contract Location**	Hwy 401 Ajax
Name of Testing Laboratory: Miller Paving Ltd. Markham Lab		**Telephone No.:**	(905)475-6660	**Fax No.:**	(905) 475-3755
Sampled by (PRINT NAME) Bora Hassan		**Sample Type: (Stockpile, Belt etc.,)** Pad (Stockpile)		**Date Sampled : (MM/DD/YY)** 06/13/06	

SUPERPAVE MIX TYPE:

☐ 9.5 ☐ 12.5 ☐ 12.5FC1 ☑ 12.5FC2

☐ 19 ☐ 25 ☐ 37.5

Contains RAP ☐ Yes ☑ No

☑ QC ☐ QA

COARSE AGGREGATE DFC CA

SOURCE NAME: MRT

INVENTORY NUMBER(S) B02-071

FINE AGGREGATE Washed Screenings, Unwashed Fines, 1/4 " Chip

SOURCE NAME: Fowler, MRT, MRT

INVENTORY NUMBER(S) B17-013-02, B02-071, B02-071

DESIGN MIXTURE -- Percent Passing 75 µm sieve

Nominal Maximum Aggregate Size (mm)	9.5	12.5	12.5 FC1	12.5 FC2	19	25	37.5	**Sample Results**	**Meets Specifications (Y/N)**
% Passing 75 µm	2-10	2-10	2-10	2-10	2-8	1-7	0-6	**3.2**	☑ Yes ☐ No

SUPERPAVE AGGREGATE CONSENSUS PROPERTY REQUIREMENTS

Traffic Category	Traffic Level	**Fractured Particles in Coarse Aggregate** ASTM D5821 % minimum		**Sample Results**	**Flat and Elongated** ASTM D4791 %Maximum 5:1	**Sample Results**	**Uncompacted Void Content** of Fine Aggregate AASHTO T304 Method A %minimum		**Sample Results**	**Sand Equivalent** AASHTO T176 Method 2 % minimum	**Sample Results**
		≤ 100 mm	>100 mm				≤ 100 mm	>100 mm			
A		55/-	-/-		--		--	--		40	
B		75/-	50/-		10		40	40		40	
C		85/80	60/-				45[1]	40		45	
D		95/90	80/75				45[1]	40		45	
E	E	100/100	100/100	100/100		1.2	45[1]	45[1]	48.4	50	76.7

Note 1: An Uncompacted Void Content of 43% is acceptable provided that the selected mix satisfies the mix volumetrics specified eslewhere in the Contract Documents.

Issued by:	**Bora Hassan**	[redacted]	**August 21, 2006**
	PRINT NAME	TESTING LABORATORY REPRESENTATIVE SIGNATURE	DATE
Received by:			
	PRINT NAME	MTO REPRESENTATIVE SIGNATURE	DATE

AME Materials Engineering

Superpave Mix Design Report

AME - Materials Engineering, 11 Indell lane, Brampton, Ontario, Canada, L6T 3Y3
Phone: (905) 840-5914; Fax: (905) 840-7859, E-Mail: ame@amecorp.ca

50 BEST EMPLOYERS IN CANADA 2008

LAB MIX NUMBER	30206.01 SP19mm	JOB MIX FORMULA NO.	
CONTRACT NUMBER	Various	HOT MIX TYPE/USE	SP 19mm
HIGHWAY	Various Locations	LOCATION	Capital Paving
TESTING LAB	AME Materials Engineering, Brampton Ont.	DATE SAMPLES REC'D	1-Aug-08
TEST DATA CERTIFIED BY:	[redacted]	DATE COMPLETED	27-Aug-08

Job Mix Formula - Gradation Percent Passing *

% AC	37.5	25	19.0	16.0	12.5	9.5	6.7	4.75	2.36	1.18	600	300	150	75
4.70	100	100.0	96.9	89.3	78.7	66.3		49.6	45.2	28.9	16.7	10.1	6.3	4.4

Traffic Category: E **Gyrations:** N ini: 9 N des: 125 N max: 205

Property	Requirements	Selected
%Gmm @ N des / Va	96.0 / 4.0	96.0 / 4.0
%Gmm @ N ini	89.0 Max	87.3
%Gmm @ N max	98.0 Max	97.2
% VMA (min)	13.0	13.5
% VFA	65-75	70.4
DP	0.6 to 1.2	1.1
TSR	80% Min	99.4

% AGG #1	30.0
% AGG #2	22.0
% AGG #3	40.5
%AGG #4	7.5
% AGG #5	
% AGG #6	-
BRIQ. BRD	2.482
MRD	2.585

% RAP	
% AC RAP	

Consensus Properties

% CR Total	100.0
% CR 2 Face	100.0
% F & E (5:1)	1.4
FAA	48.1
Sand Equiv.	97

ASPHALT CEMENT

SUPPLIER	Grade
Canadian	64-28

ADDITIVE

SUPPLIER	TYPE	AS % of AC
	N/A	

	SOURCE / INVENTORY NUMBER		SOURCE / INVENTORY NUMBER
AGGREGATE #1	19mm Stone / Lafarge Dundas / H03-003	AGGREGATE #4	Screenings / Lafarge Dundas / H03-003
AGGREGATE #2	HL3 Stone / Lafarge Dundas / H03-003	AGGREGATE #5	
AGGREGATE #3	High Stability Sand / Lafarge Dundas / H03-003	RAP	

AGGREGATE DATA	AGG. SPECIFIC GRAVITY	AGG. ABSORP. (%)	AGGREGATE GRADING - PERCENT PASSING												
			37.5	25.0	19.0	16.0	12.5	9.5	4.75	2.36	1.18	600	300	150	75
AGG #1	2.734	1.1		100.0	89.5	63.7	31.4	11.1	2.0	1.5	1.3	1.2	1.0	0.9	0.7
AGG #2	2.729	1.3		100.0	100.0	100.0	95.0	65.8	6.6	2.2	1.7	1.4	1.1	0.9	0.5
AGG #3	2.736	1.1					100.0	100.0	100.0	95.9	58.6	30.0	14.9	6.9	4.0
AGG #4	2.760	0.8					100.0	100.0	84.7	61.2	44.6	34.4	28.5	23.6	17.7
AGG #5															
RAP															
Comb. Gb	2.736														

*JMF Adjusted to Allow for 1.5 % Fines Returned to the Mix

Remarks: Mix Comp Temp=Recomp Temp=145C; Briq. Wt.=4950gms; Abs%<2 no sealing required; AC extraction by Solvent or Ignition; Mix design mixing Temp = 158C

Reviewed By: _____ Date: _____

AMC
Materials Engineering

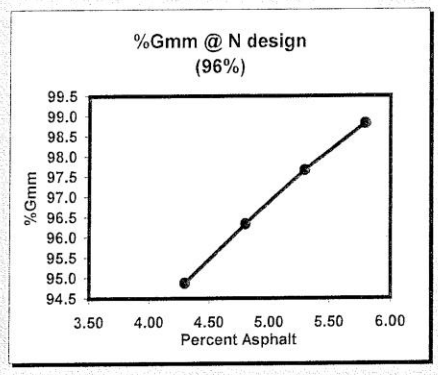

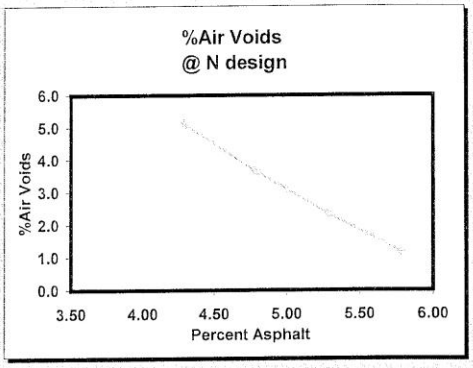

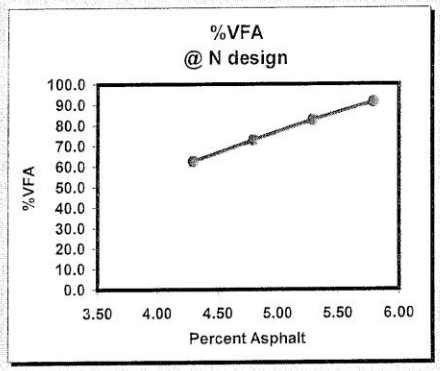

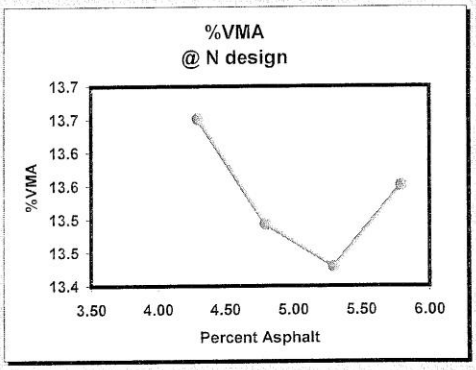

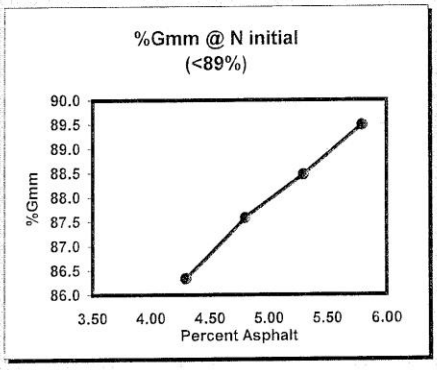

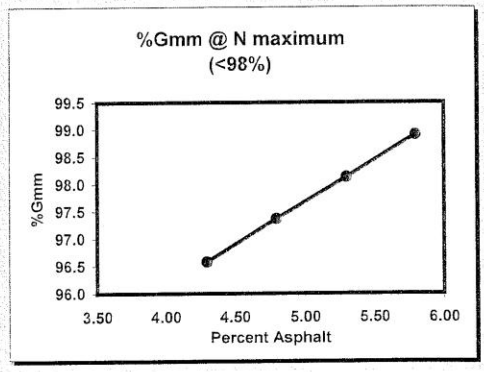

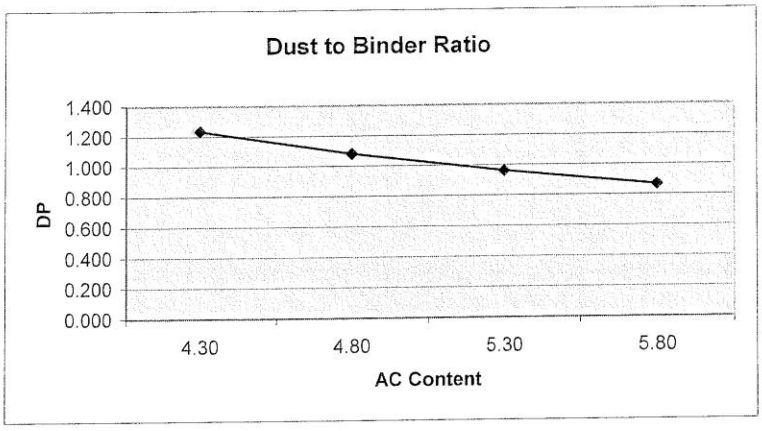
Dust to Binder Ratio
DP
1.400
1.200
1.000
0.800
0.600
0.400
0.200
0.000
4.30
4.80
5.30
5.80
AC Content

SP 19 Design

PROJ.NO.; 30206.01
PROJ NA; Hwy 401 Drumbo Rd
CLIENT; Capital Paving

MIX REF.; 30206.01 SP19mm
MIX TYPE; SP19mm
MTO CONTRACT NO.; 2008-3004

100.00	PARTS	Volume	Mass	S.G	ABS.		
Dundas 19mm		30.0	30.0	2.734	1.07	Gb :	2.736
Dundas HL3		22.1	22.0	2.729	1.29	F. F. RATIO	1.763
Dundas HSS	3.0	40.5	40.5	2.736	1.07	% A.C.:	4.7
Dundas Scr	0.6	7.4	7.5	2.760	0.80	FILM TH;	9.851
	0.0	0.0	0.0	1.000	0.00	SG. OIL	1.03
	0.0	0.0	0.0	1.000	0.00	Est. AC	4.77

Est. P75 : AC Ratio : 1.18

SIEVE SIZE	Dundas 19mm	Dundas HL3	Dundas HSS	Dundas Scr	0	0	AGG. BLEND Volume	Mass
37.5	100.0	100.0	100.0	100.0	100.0	100.0	100.0	100.0
25	100.0	100.0	100.0	100.0	100.0	100.0	100.0	100.0
19.0	89.5	100.0	100.0	100.0	100.0	100.0	96.9	96.9
16.0	63.7	100.0	100.0	100.0	100.0	100.0	89.3	89.3
12.5	31.4	95.0	100.0	100.0	100.0	100.0	78.6	78.7
9.5	11.1	65.8	100.0	100.0	100.0	100.0	66.3	66.3
4.75	2.0	6.6	100.0	84.7	100.0	100.0	49.6	49.6
2.36	1.5	2.2	95.9	61.2	100.0	100.0	45.1	45.2
1.18	1.3	1.7	58.6	44.6	100.0	100.0	28.9	28.9
0.6	1.2	1.4	30.0	34.4	100.0	100.0	16.6	16.7
0.3	1.0	1.1	14.9	28.5	100.0	100.0	10.0	10.1
0.15	0.9	0.9	6.9	23.6	100.0	100.0	6.3	6.3
0.075	0.7	0.5	4.0	17.7	100.0	100.0	4.4	4.4
						FFR;	1.76	
PERCENT BAG HOUSE DUST RET. TO MIX;				1.5		FT.;	9.9	
BAG HOUSE DUST GRADING;			1.18	600	300	150	75	
PERCENT PASSING;			100	99.9	98.2	89.9	81	

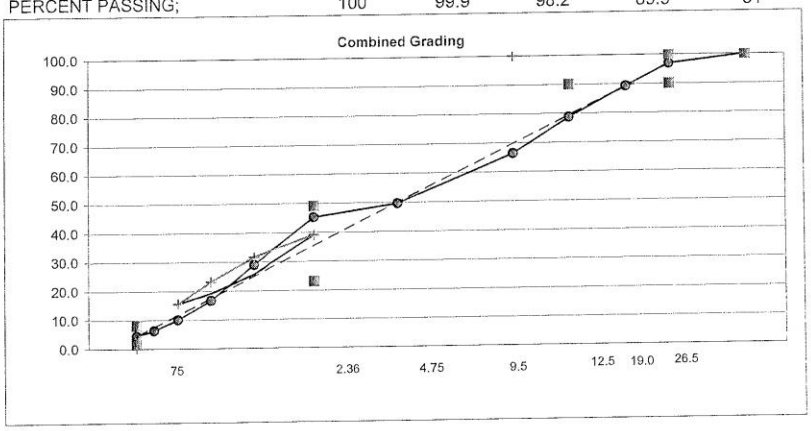

Sample Results

	Sample 1	Sample 2	Sample 3	Sample 4
%Gmm(N-Initial)	86.3	87.6	88.5	89.5
%Gmm(N-Design)	94.9	96.3	97.7	98.8
%Gmm(N-Maximum)	96.6	97.4	98.1	98.9
%Air Voids(N-Design)	5.1	3.7	2.3	1.2
%VMA(N-Design)	13.65	13.49	13.43	13.55
%VFA(N-Design)	62.46	72.77	82.59	91.25

Estimated Results At Target Air Voids (4% at N-Design)

	Sample 1	Sample 2	Sample 3	Sample 4
Pb(Est.)	4.75	4.67	4.63	4.67
%VMA(Est. @ N-Design)	13.43	13.53	13.60	13.83
%VFA(Est. @ N-Design)	70.21	70.43	70.58	71.08
%Gmm(Est. @ N-Initial)	87.45	87.25	86.80	86.67
Pbe	4.01	3.94	3.91	3.95
DP	1.10	1.12	1.13	1.11

AME
Materials Engineering

Bulk

Gmb = (A / (B - C)) * K						
Sample #	A Dry Mass	B SSD Mass	C Mass in H_2O	°C	G_{mb} (Ndes)	Corr. G_{mb} (Nini)
Sample 1a	4903.2	4916.8	2930.9	25	2.469	2.245
Sample 1b	4909.5	4924.9	2935.9	25	2.468	2.248
Sample 1c				25		
Sample 2a	4926.3	4934.0	2951.2	25	2.485	2.259
Sample 2b	4921.9	4930.6	2952.2	25	2.488	2.262
Sample 2c				25		
Sample 3a	4952.9	4955.7	2974.4	25	2.500	2.261
Sample 3b	4950.6	4954.2	2975.9	25	2.502	2.270
Sample 3c				25		
Sample 4a	4968.5	4969.5	2991.9	25	2.512	2.274
Sample 4b	4977.8	4978.7	2995.0	25	2.509	2.274
Sample 4c				25		

Average G_{mb}	(Ndes)	(Nini)
Sample 1 Avg	2.469	2.246
Sample 2 Avg	2.486	2.260
Sample 3 Avg	2.501	2.266
Sample 4 Avg	2.511	2.274

Press the Calculate Button to perform the following:

1. Transfer Gmb @ Ndes to the Property Worksheet
2. Transfer Dry Mass to the Property Worksheet
3. Calculate Gmb @ N-initial

AME Materials Engineering

Superpave Mix Design Report

AME - Materials Engineering, 11 Indell lane, Brampton, Ontario, Canada, L6T 3Y3
Phone: (905) 840-5914; Fax: (905) 840-7859, E-Mail: ame@amecorp.ca

50 BEST EMPLOYERS IN CANADA 2008

LAB MIX NUMBER	30206.01 SP25mm Rap	JOB MIX FORMULA NO.	
CONTRACT NUMBER	Various	HOT MIX TYPE/USE: SP 25mm Rap	ITEM NO.
HIGHWAY	Various Locations	LOCATION: Capital Paving	
TESTING LAB	AME Materials Engineering, Brampton Opt.	DATE SAMPLES REC'D	1-Aug-08
TEST DATA CERTIFIED BY:	[redacted]	DATE COMPLETED	2-Sep-08

Job Mix Formula - Gradation Percent Passing *

% AC	37.5	25	19.0	16.0	12.5	9.5	6.7	4.75	2.36	1.18	600	300	150	75
4.30	100	97.1	89.2	80.9	71.5	62.1		47.3	37.8	23.8	14.2	8.9	5.7	4.0

Traffic Category: E Gyrations: N ini: 9 N des: 125 N max: 205

Property	Requirements	Selected
%Gmm @ N des / Va	96.0 / 4.0	96.0 / 4.0
%Gmm @ N ini	89.0 Max	88.2
%Gmm @ N max	98.0 Max	97.6
% VMA (min)	12.0	12.2
% VFA	65-75	67.3
DP	0.6 to 1.2	1.2
TSR	80% Min	98.4

% AGG #1	14.0
% AGG #2	22.0
% AGG #3	10.0
%AGG #4	29.0
% AGG #5	10.0
% AGG #6	-
BRIQ. BRD	2.511
MRD	2.616

% RAP	15
% AC RAP	4.26%
Consensus Properties	
% CR Total	100.0
% CR 2 Face	100.0
% F & E (5:1)	0.9
FAA	46.2
Sand Equiv.	N/A

ASPHALT CEMENT	
SUPPLIER	Grade
Canadian	58-28

ADDITIVE		
SUPPLIER	TYPE	AS % of AC
	N/A	

	SOURCE / INVENTORY NUMBER		SOURCE / INVENTORY NUMBER
AGGREGATE #1	26.5mm Stone / Lafarge Dundas / H03-003	AGGREGATE #4	High Stability Sand / Lafarge Dundas / H03-003
AGGREGATE #2	19mm Stone / Lafarge Dundas / H03-003	AGGREGATE #5	Chip / Lafarge Dundas Quarry / H03-003
AGGREGATE #3	HL3 Stone / Lafarge Dundas / H03-003	RAP	Capital Paving Yard

AGGREGATE DATA	AGG. SPECIFIC GRAVITY	AGG. ABSORP. (%)	AGGREGATE GRADING - PERCENT PASSING												
			37.5	25.0	19.0	16.0	12.5	9.5	4.75	2.36	1.18	600	300	150	75
AGG #1	2.675	1.2	100.0	74.4	34.4	15.9	6.5	2.5	1.4	1.3	1.1	1.0	0.8	0.6	0.4
AGG #2	2.734	1.1		100.0	89.5	63.7	31.4	11.1	2.0	1.5	1.3	1.2	1.0	0.9	0.7
AGG #3	2.729	1.3		100.0	100.0	100.0	95.0	65.8	6.6	2.2	1.7	1.4	1.1	0.9	0.5
AGG #4	2.736	1.1						100.0	100.0	95.9	58.6	30.0	14.9	6.9	4.0
AGG #5	2.711	1.2						100.0	71.3	16.5	3.0	1.4	1.2	1.0	0.8
RAP	2.830	0.6		100.0	99.5	98.5	95.1	84.4	58.1	42.3	30.4	22.8	17.1	12.4	8.5
Comb. Gb	2.737														

*JMF Adjusted to Allow for 1.5 % Fines Returned to the Mix

Remarks: Mix Comp Temp=Recomp Temp=138C; Briq. Wt.=4925gms; Abs%<2 no sealing required; AC extraction by Solvent or Ignition; Mix design mixing Temp = 151C; Virgin AC=3.66%

Reviewed By: _____ Date: _____

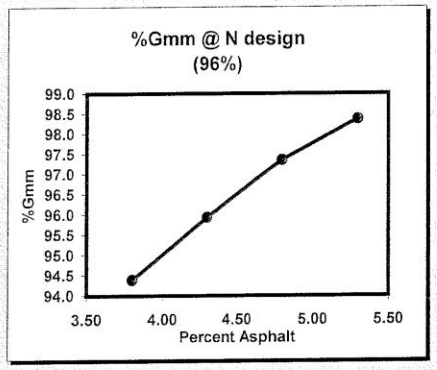
%Gmm @ N design
(96%)
%Gmm
99.0
98.5
98.0
97.5
97.0
96.5
96.0
95.5
95.0
94.5
94.0
3.50
4.00
4.50
5.00
5.50
Percent Asphalt

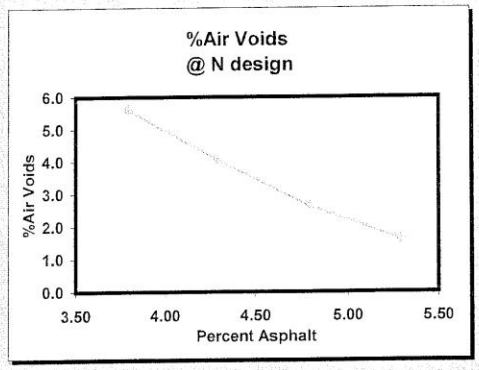
%Air Voids
@ N design
%Air Voids
6.0
5.0
4.0
3.0
2.0
1.0
0.0
3.50
4.00
4.50
5.00
5.50
Percent Asphalt

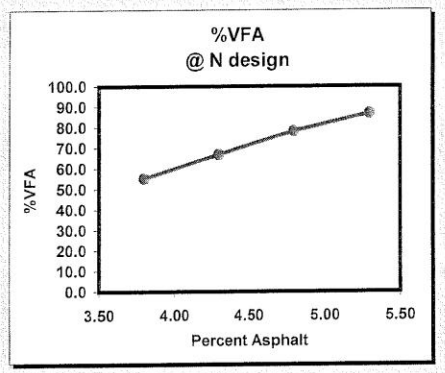
%VFA
@ N design
%VFA
100.0
90.0
80.0
70.0
60.0
50.0
40.0
30.0
20.0
10.0
0.0
3.50
4.00
4.50
5.00
5.50
Percent Asphalt

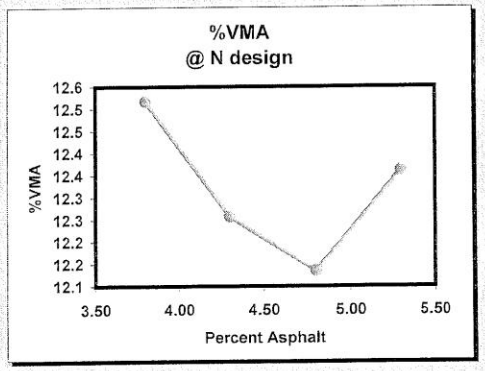
%VMA
@ N design
%VMA
12.6
12.5
12.5
12.4
12.4
12.3
12.3
12.2
12.2
12.1
3.50
4.00
4.50
5.00
5.50
Percent Asphalt

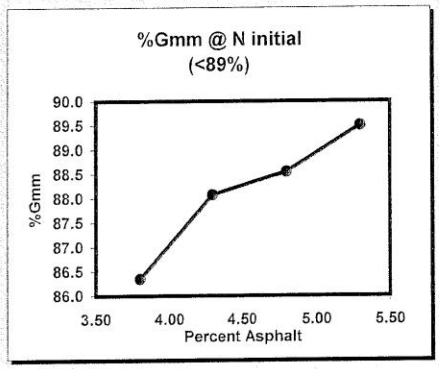
%Gmm @ N initial
(<89%)
%Gmm
90.0
89.5
89.0
88.5
88.0
87.5
87.0
86.5
86.0
3.50
4.00
4.50
5.00
5.50
Percent Asphalt

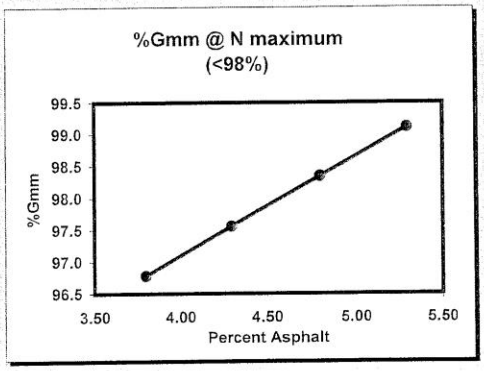
%Gmm @ N maximum
(<98%)
%Gmm
99.5
99.0
98.5
98.0
97.5
97.0
96.5
3.50
4.00
4.50
5.00
5.50
Percent Asphalt

AMC
Materials Engineering

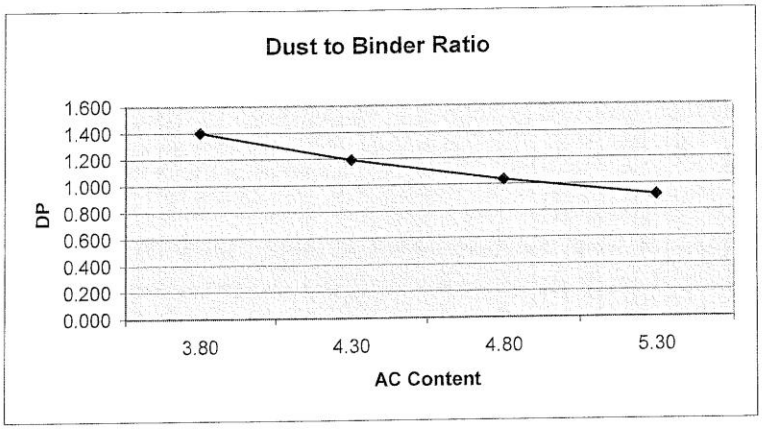

SP 25mm Rap Design

PROJ.NO.; 30206.01
PROJ NA; Hwy 401 Drumbo Rd
CLIENT; Capital Paving

MIX REF.; 30206.01 SP25 Rap
MIX TYPE; SP 25mm Rap
MTO CONTRACT NO.; 2008-3004

100.00	PARTS	% Vol	% Mass	S.G	ABS.		
Dundas 25mm		14.3	14.0	2.675	1.19	Gb :	2.737
Dundas 19mm		22.0	22.0	2.734	1.07	F. F. RATIO	1.664
Dundas HL3		10.0	10.0	2.729	1.29	% A.C.:	4.3
Dundas HSS	3.0	29.1	29.0	2.736	1.07	FILM TH;	10.242
Dundas Chip	1.0	10.1	10.0	2.711	1.21	SG. OIL	1.03
Rap	1.0	14.5	15.0	2.830	0.61	Est. AC	4.10

Combined F & E (%) 0.8
Combined 1 Face Cr 100.0
Combined 2 Face Cr 100.0

Est Dust / AC Ratio : 1.15
Combined FAA :
Combined Sand Eq. :

SIEVE SIZE	Dundas 25mm	Dundas 19mm	Dundas HL3	Dundas HSS	Dundas Chip	Rap	AGG. BLEND Volume	AGG. BLEND Mass	Final Grading Mass
37.5	100.0	100.0	100.0	100.0	100.0	100.0	100.0	100.0	100.0
25	74.4	100.0	100.0	100.0	100.0	100.0	96.4	96.5	97.1
19.0	34.4	89.5	100.0	100.0	100.0	99.5	88.4	88.6	89.2
16.0	15.9	63.7	100.0	100.0	100.0	98.5	80.1	80.3	80.9
12.5	6.5	31.4	95.0	100.0	100.0	95.1	70.8	71.1	71.5
9.5	2.5	11.1	65.8	100.0	100.0	84.4	61.4	61.7	62.1
4.75	1.4	2.0	6.6	100.0	71.3	58.1	46.8	47.0	47.3
2.36	1.3	1.5	2.2	95.9	16.5	42.3	37.4	37.5	37.8
1.18	1.1	1.3	1.7	58.6	3.0	30.4	23.5	23.7	23.8
0.6	1.0	1.2	1.4	30.0	1.4	22.8	14.0	14.1	14.2
0.3	0.8	1.0	1.1	14.9	1.2	17.1	8.7	8.8	8.9
0.15	0.6	0.9	0.9	6.9	1.0	12.4	5.6	5.6	5.7
0.075	0.4	0.7	0.5	4.0	0.8	8.5	3.9	3.9	4.0
						FFR;	1.66		
PERCENT BAG HOUSE DUST RET. TO MIX;				1.5		FT.;	10.2		
BAG HOUSE DUST GRADING;			1.18	600	300	150	75		
PERCENT PASSING;			100	99.9	98.2	89.9	81		

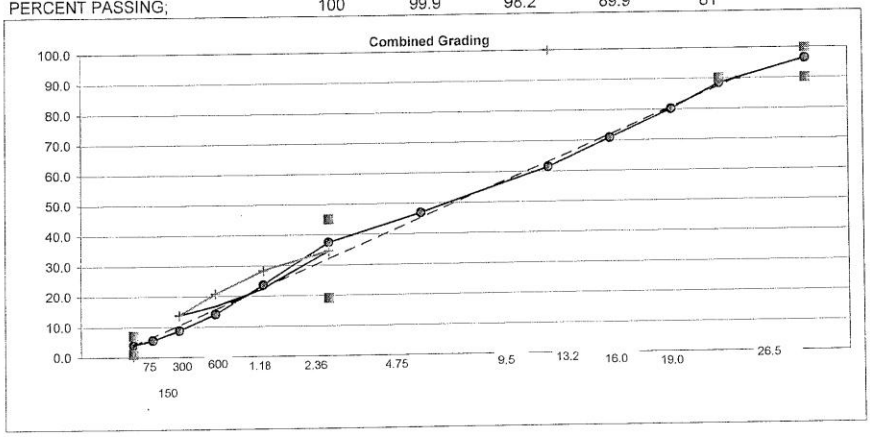

Results

Sample Results

	Sample 1	Sample 2	Sample 3	Sample 4
%Gmm(N-Initial)	86.3	88.1	88.5	89.5
%Gmm(N-Design)	94.4	95.9	97.3	98.4
%Gmm(N-Maximum)	96.8	97.6	98.3	99.1
%Air Voids(N-Design)	5.6	4.1	2.7	1.6
%VMA(N-Design)	12.52	12.26	12.13	12.36
%VFA(N-Design)	55.16	66.76	78.13	86.78

Estimated Results At Target Air Voids (4% at N-Design)

	Sample 1	Sample 2	Sample 3	Sample 4
Pb(Est.)	4.44	4.33	4.26	4.35
%VMA(Est. @ N-Design)	12.19	12.24	12.27	12.60
%VFA(Est. @ N-Design)	67.20	67.33	67.40	68.25
%Gmm(Est. @ N-Initial)	87.96	88.15	87.20	87.13
Pbe	3.50	3.39	3.33	3.43
DP	1.14	1.18	1.20	1.17

Gmb = (A / (B - C)) * K						
Sample #	A Dry Mass	B SSD Mass	C Mass in H_2O	°C	G_{mb} (Ndes)	Corr. G_{mb} (Nini)
Sample 1a	4939.1	4948.4	2965.3	25	2.491	2.276
Sample 1b	4879.1	4899.2	2937.7	25	2.487	2.278
Sample 1c				25		
Sample 2a	4907.4	4916.5	2966.4	25	2.516	2.312
Sample 2b	4898.9	4912.0	2954.3	25	2.502	2.296
Sample 2c				25		
Sample 3a	4922.8	4925.8	2978.7	25	2.528	2.296
Sample 3b	4924.3	4930.8	2979.8	25	2.524	2.300
Sample 3c				25		
Sample 4a	4932.8	4933.7	2985.6	25	2.532	2.301
Sample 4b	4938.7	4939.7	2990.5	25	2.534	2.308
Sample 4c				25		

Average G_{mb}	(Ndes)	(Nini)
Sample 1 Avg	2.489	2.277
Sample 2 Avg	2.509	2.304
Sample 3 Avg	2.526	2.298
Sample 4 Avg	2.533	2.305

Press the Calculate Button to perform the following:

1. Transfer Gmb @ Ndes to the Property Worksheet
2. Transfer Dry Mass to the Property Worksheet
3. Calculate Gmb @ N-initial

Mix Design of SP 25 RBM

AME Materials Engineering

Superpave Mix Design Report

AME - Materials Engineering, 11 Indell lane, Brampton, Ontario, Canada, L6T 3Y3
Phone: (905) 840-5914; Fax: (905) 840-7859, E-Mail: ame@amecorp.ca

BEST EMPLOYERS IN CANADA 2008

LAB MIX NUMBER	30206.01 SP25 RBM	JOB MIX FORMULA NO.	
CONTRACT NUMBER	Various	HOT MIX TYPE/USE: SP25 Rich Bottom Mix	ITEM NO.
HIGHWAY	Various Locations	LOCATION: Capital Paving	
TESTING LAB	AME Materials Engineering, Brampton Ont.	DATE SAMPLES REC'D	1-Aug-08
TEST DATA CERTIFIED BY:	[redacted]	DATE COMPLETED	29-Aug-08

Job Mix Formula - Gradation Percent Passing *

% AC	37.5	25	19.0	16.0	12.5	9.5	6.7	4.75	2.36	1.18	600	300	150	75
5.10	100	97.0	89.3	79.7	68.7	58.4		46.4	42.4	27.2	15.8	9.6	6.1	4.3

Traffic Category: E **Gyrations:** N ini: 9 N des: 125 N max: 205

Property	Requirements	Selected
%Gmm @ N des / Va	96.0 / 4.0	97.6 / 2.4
%Gmm @ N ini	89.0 Max	88.9
%Gmm @ N max	98.0 Max	98.4
% VMA (min)	12.0	12.7
% VFA	65-75	80.9
DP	0.6 to 1.2	1.0
TSR	80% Min	94.5

% AGG #1	12.0
% AGG #2	29.0
% AGG #3	14.0
%AGG #4	37.5
% AGG #5	7.5
% AGG #6	-
BRIQ. BRD	2.512
MRD	2.574

% RAP	-
% AC RAP	-

Consensus Properties

% CR Total	100.0
% CR 2 Face	100.0
% F & E (5:1)	1.3
FAA	47.5
Sand Equiv.	97

ASPHALT CEMENT	
SUPPLIER	Grade
Canadian	58-28

ADDITIVE		
SUPPLIER	TYPE	AS % of AC
	N/A	

	SOURCE / INVENTORY NUMBER		SOURCE / INVENTORY NUMBER
AGGREGATE #1	26.5mm Stone / Lafarge Dundas Quarry / H03-003	AGGREGATE #4	High Stability Sand / Lafarge Dundas Quarry / H03-003
AGGREGATE #2	19mm Stone / Lafarge Dundas Quarry / H03-003	AGGREGATE #5	Screenings / Lafarge Dundas Quarry / H03-003
AGGREGATE #3	HL3 Stone / Lafarge Dundas Quarry / H03-003	RAP	

AGGREGATE DATA	AGG. SPECIFIC GRAVITY	AGG. ABSORP. (%)	AGGREGATE GRADING - PERCENT PASSING												
			37.5	25.0	19.0	16.0	12.5	9.5	4.75	2.36	1.18	600	300	150	75
AGG #1	2.675	1.2	100.0	74.4	34.4	15.9	6.5	2.5	1.4	1.3	1.1	1.0	0.8	0.6	0.4
AGG #2	2.734	1.1		100.0	89.5	63.7	31.4	11.1	2.0	1.5	1.3	1.2	1.0	0.9	0.7
AGG #3	2.729	1.3		100.0	100.0	100.0	95.0	65.8	6.6	2.2	1.7	1.4	1.1	0.9	0.5
AGG #4	2.736	1.1						100.0	100.0	95.9	58.6	30.0	14.9	6.9	4.0
AGG #5	2.760	0.8						100.0	84.7	61.2	44.6	34.4	28.5	23.6	17.7
RAP															
Comb. Gb	2.729														

*JMF Adjusted to Allow for 1.5 % Fines Returned to the Mix

Remarks: **Mix Comp Temp=Recomp Temp=138C; Briq. Wt.=4950gms; Abs%<2 no sealing required; AC extraction by Solvent or Ignition; Mix design mixing Temp = 151C.**

Reviewed By: _____ Date: _____

SP25 and RBM Comparison

PROJ.NO.;	30206.01	MIX REF.;	30206.01 SP25 RBM
PROJ NA;	Hwy 401 Drumbo Rd	MIX TYPE;	SP25 Rich Bottom Mix
CLIENT;	Capital Paving	MTO CONT. NO.;	2008-3004

		Traffic Category		E
ASPHALT CEMENT SOURCE;	Canadian			
ASPHALT CEMENT TYPE;	58-28	Gyrations		
ASPHALT CEMENT SG.;	1.031	N Init	N Des	N Max
Mix Compaction Temperature	138 C	9	125	205

	Design Properties Comparison	
	30206.01 SP25mm	30206.01 SP25 RBM
Design AC Content	4.6	5.1
BULK DENSITY;	2.490	2.512
MAX. RELATIVE DENSITY;	2.594	2.574
AIR VOIDS% @ N Des.;	4.0	2.4
%Gmm @ N Ini.;	87.3	88.9
VMA (%) @ N Des.	13.0	12.7
VFA (%) @ N Des.	69.2	80.9
%Gmm @ N max	97.6	98.4
Dust : AC Ratio	1.2	1.0
Combined Agg Sg:	2.729	2.729

Agg. Blend Percentages	26.5mm Stone	12.0
	19mm Stone	29.0
	HL3 Stone	14.0
	High Stability Sand	37.5
	Screenings	7.5
	BHD	1.5

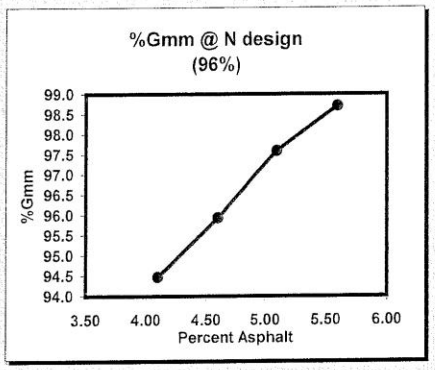
%Gmm @ N design
(96%)
%Gmm
99.0
98.5
98.0
97.5
97.0
96.5
96.0
95.5
95.0
94.5
94.0
3.50
4.00
4.50
5.00
5.50
6.00
Percent Asphalt

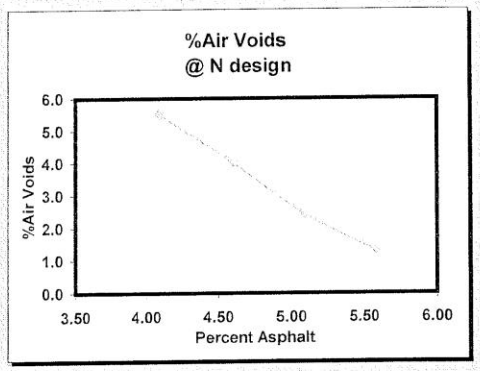
%Air Voids
@ N design
%Air Voids
6.0
5.0
4.0
3.0
2.0
1.0
0.0
3.50
4.00
4.50
5.00
5.50
6.00
Percent Asphalt

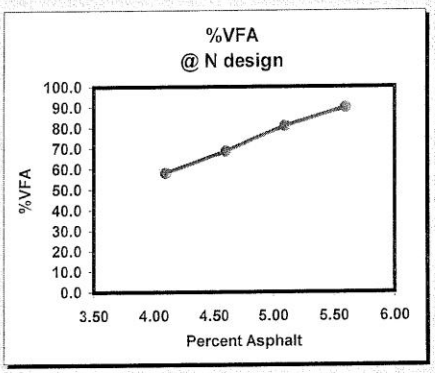
%VFA
@ N design
%VFA
100.0
90.0
80.0
70.0
60.0
50.0
40.0
30.0
20.0
10.0
0.0
3.50
4.00
4.50
5.00
5.50
6.00
Percent Asphalt

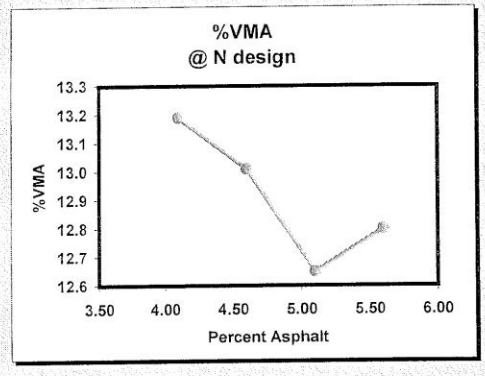
%VMA
@ N design
%VMA
13.3
13.2
13.1
13.0
12.9
12.8
12.7
12.6
3.50
4.00
4.50
5.00
5.50
6.00
Percent Asphalt

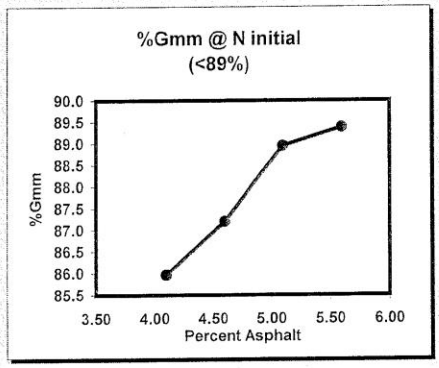
%Gmm @ N initial
(<89%)
%Gmm
90.0
89.5
89.0
88.5
88.0
87.5
87.0
86.5
86.0
85.5
3.50
4.00
4.50
5.00
5.50
6.00
Percent Asphalt

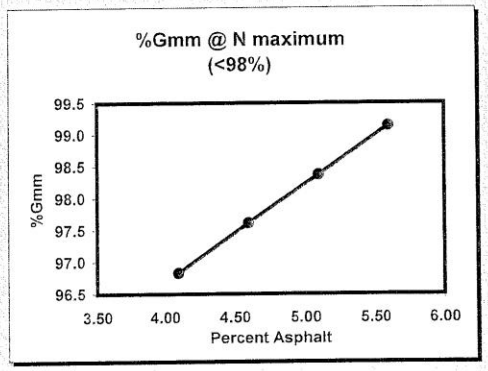
%Gmm @ N maximum
(<98%)
%Gmm
99.5
99.0
98.5
98.0
97.5
97.0
96.5
3.50
4.00
4.50
5.00
5.50
6.00
Percent Asphalt

AMC
Materials Engineering

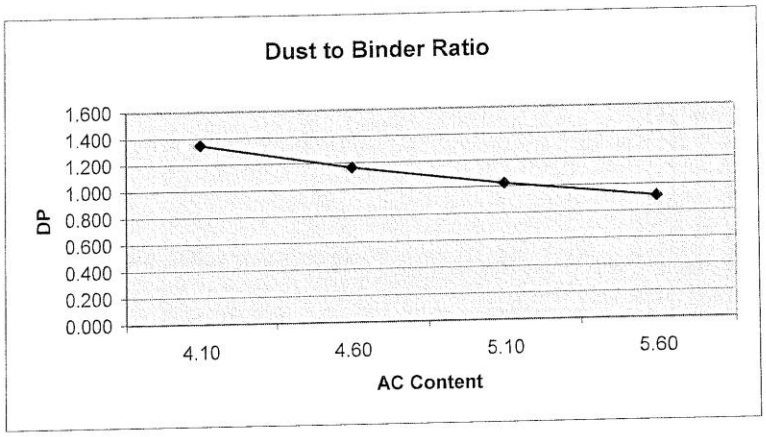

SP 25 Design

PROJ.NO.; 30206.01
PROJ NA; Hwy 401 Drumbo Rd
CLIENT; Capital Paving

MIX REF.; 30206.01 SP25mm
MIX TYPE; SP 25
MTO CONTRACT NO.; 2008-3004

100.00	PARTS	Volume	Mass	S.G	ABS.		
=Summary!m5		12.2	12.0	2.675	1.19	Gb :	2.729
=Summary!n5		28.9	29.0	2.734	1.07	F. F. RATIO	1.749
Dundas HL3		14.0	14.0	2.729	1.29	Tr % A.C.:	4.6
Dundas HSS	3.0	37.4	37.5	2.736	1.07	FILM TH;	9.985
	0.6	7.5	7.5	2.760	0.80	SG. OIL	1.03
	0.0	0.0	0.0	1.000	0.00	Est. AC	4.55

Est. Dust / AC Ratio : 1.17

						AGG. BLEND		
SIEVE SIZE	Dundas 26.5mm	Dundas 19mm	Dundas HL3	Dundas HSS	Dundas Scr	0	Volume	Mass
37.5	100.0	100.0	100.0	100.0	100.0	100.0	100.0	100.0
25	74.4	100.0	100.0	100.0	100.0	100.0	96.9	97.0
19.0	34.4	89.5	100.0	100.0	100.0	100.0	89.1	89.3
16.0	15.9	63.7	100.0	100.0	100.0	100.0	79.6	79.7
12.5	6.5	31.4	95.0	100.0	100.0	100.0	68.5	68.7
9.5	2.5	11.1	65.8	100.0	100.0	100.0	58.3	58.4
4.75	1.4	2.0	6.6	100.0	84.7	100.0	46.2	46.4
2.36	1.3	1.5	2.2	95.9	61.2	100.0	42.2	42.4
1.18	1.1	1.3	1.7	58.6	44.6	100.0	27.1	27.2
0.6	1.0	1.2	1.4	30.0	34.4	100.0	15.7	15.8
0.3	0.8	1.0	1.1	14.9	28.5	100.0	9.6	9.6
0.15	0.6	0.9	0.9	6.9	23.6	100.0	6.1	6.1
0.075	0.4	0.7	0.5	4.0	17.7	100.0	4.3	4.3
						FFR;	1.75	
PERCENT BAG HOUSE DUST RET. TO MIX;				1.5		FT.;	10.0	
BAG HOUSE DUST GRADING;			1.18	600	300	150	75	
PERCENT PASSING;			100	99.9	98.2	89.9	81	

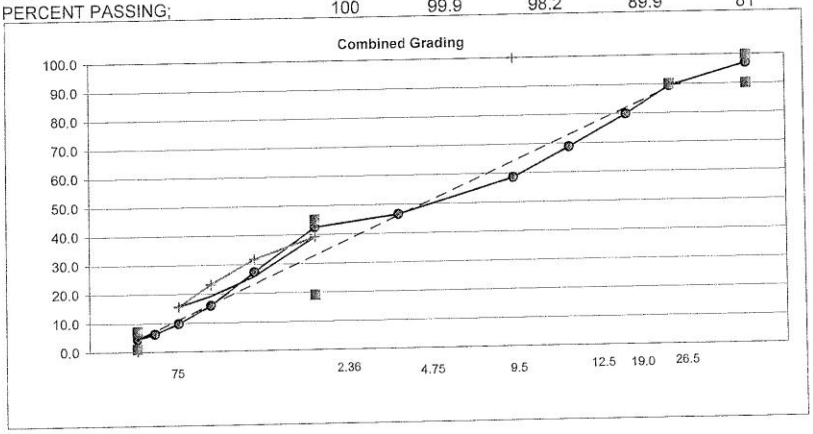

Sample Results

	Sample 1	Sample 2	Sample 3	Sample 4
%Gmm(N-Initial)	86.0	87.2	88.9	89.4
%Gmm(N-Design)	94.5	95.9	97.6	98.7
%Gmm(N-Maximum)	96.8	97.6	98.4	99.1
%Air Voids(N-Design)	5.5	4.1	2.4	1.3
%VMA(N-Design)	13.19	13.01	12.65	12.80
%VFA(N-Design)	58.06	68.72	80.93	89.87

Estimated Results At Target Air Voids (4% at N-Design)

	Sample 1	Sample 2	Sample 3	Sample 4
Pb(Est.)	4.71	4.63	4.46	4.52
%VMA(Est. @ N-Design)	12.88	13.00	12.81	13.07
%VFA(Est. @ N-Design)	68.95	69.22	68.77	69.39
%Gmm(Est. @ N-Initial)	87.49	87.27	87.35	86.67
Pbe	3.81	3.73	3.57	3.63
DP	1.13	1.15	1.20	1.19

Gmb = (A / (B - C)) * K						
Sample #	A Dry Mass	B SSD Mass	C Mass in H_2O	°C	G_{mb} (Ndes)	Corr. G_{mb} (Nini)
Sample 1a	4900.1	4918.1	2935.7	25	2.472	2.249
Sample 1b	4895.6	4914.4	2931.5	25	2.469	2.247
Sample 1c				25		
Sample 2a	4914.2	4920.5	2948.8	25	2.492	2.270
Sample 2b	4912.6	4922.8	2945.5	25	2.484	2.254
Sample 2c				25		
Sample 3a	4945.5	4951.2	2982.9	25	2.513	2.298
Sample 3b	4875.6	4882.2	2940.7	25	2.511	2.281
Sample 3c				25		
Sample 4a	4924.5	4926.2	2974.0	25	2.523	2.294
Sample 4b	4940.7	4943.4	2982.2	25	2.519	2.272
Sample 4c				25		

Average G_{mb}	(Ndes)	(Nini)
Sample 1 Avg	2.470	2.248
Sample 2 Avg	2.488	2.262
Sample 3 Avg	2.512	2.289
Sample 4 Avg	2.521	2.283

Press the Calculate Button to perform the following:

1. Transfer Gmb @ Ndes to the Property Worksheet
2. Transfer Dry Mass to the Property Worksheet
3. Calculate Gmb @ N-initial

Appendix C

Joint Confidence Intervals for Perpetual Pavement with RBM Model

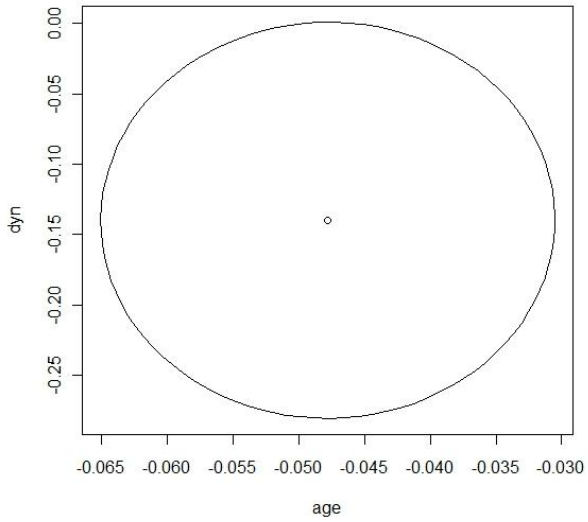

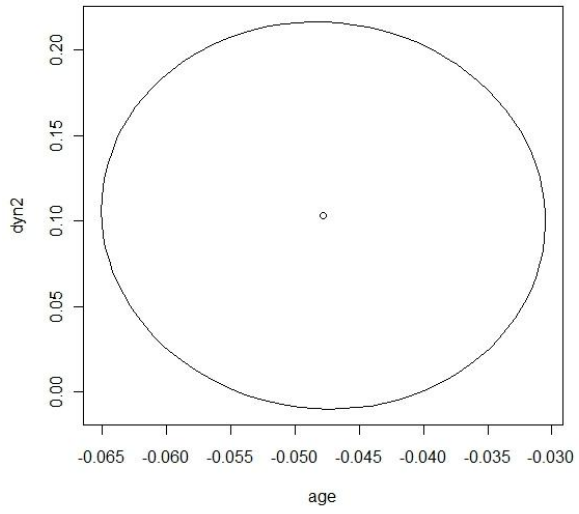

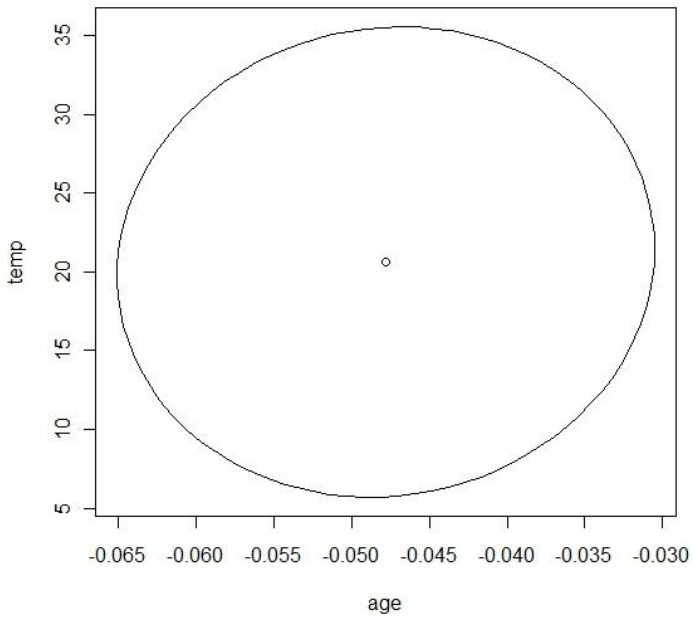
temp
35
30
25
20
15
10
5
-0.065
-0.060
-0.055
-0.050
-0.045
-0.040
-0.035
-0.030
age

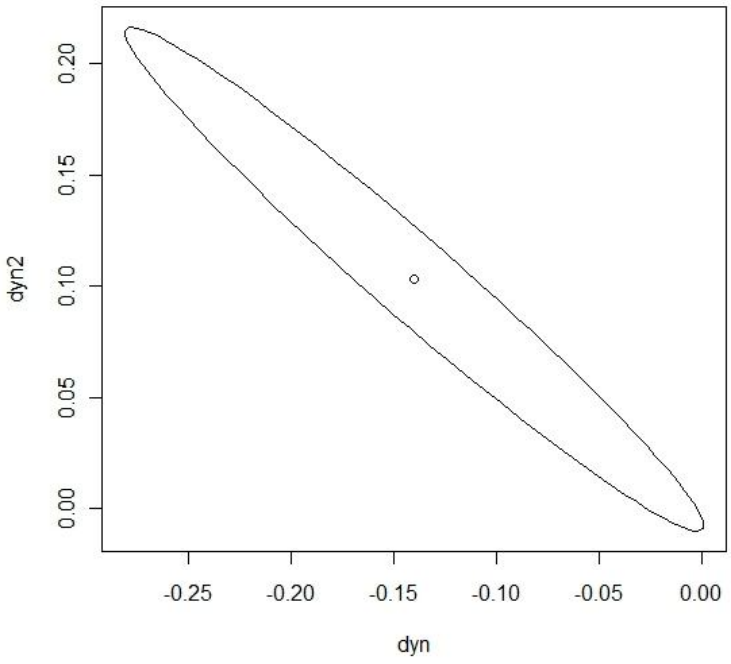
dyn2
0.20
0.15
0.10
0.05
0.00
-0.25
-0.20
-0.15
-0.10
-0.05
0.00
dyn

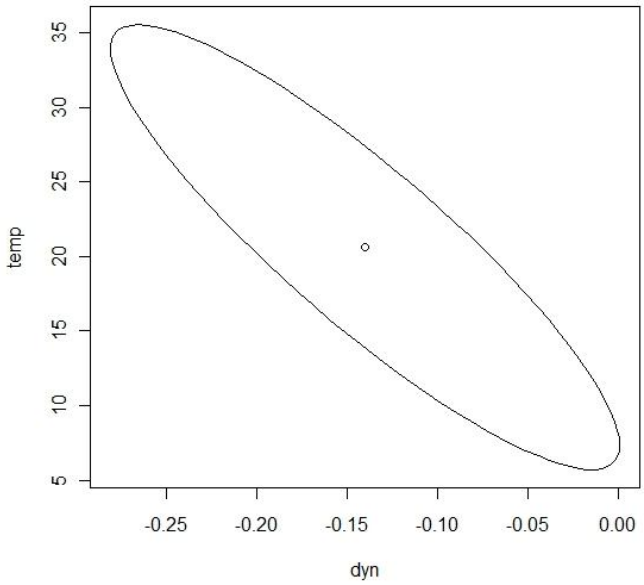
temp
35
30
25
20
15
10
5
-0.25
-0.20
-0.15
-0.10
-0.05
0.00
dyn

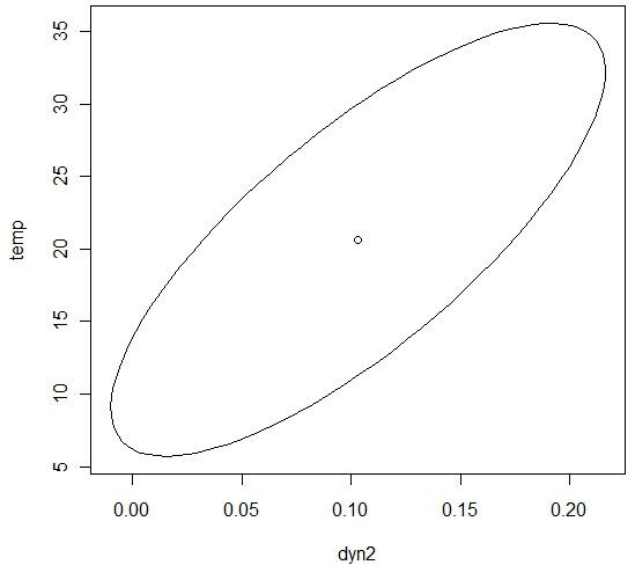
temp
35
30
25
20
15
10
5
0.00
0.05
0.10
0.15
0.20
dyn2

Joint Confidence Intervals for Perpetual Pavement without RBM Model

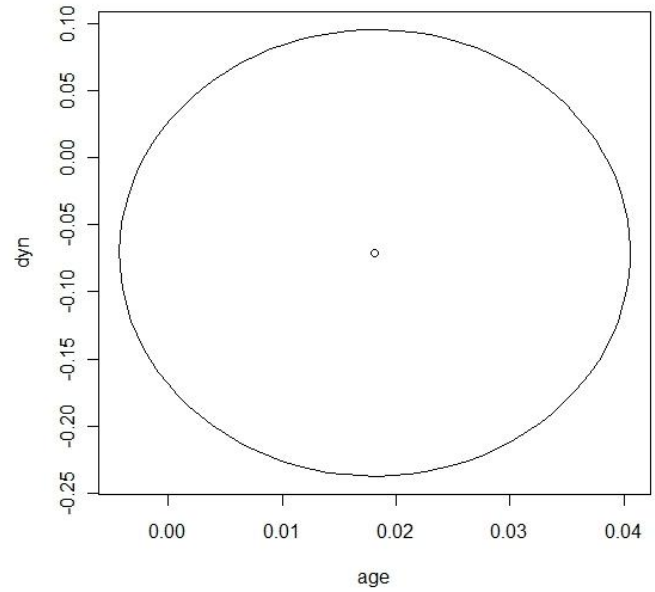

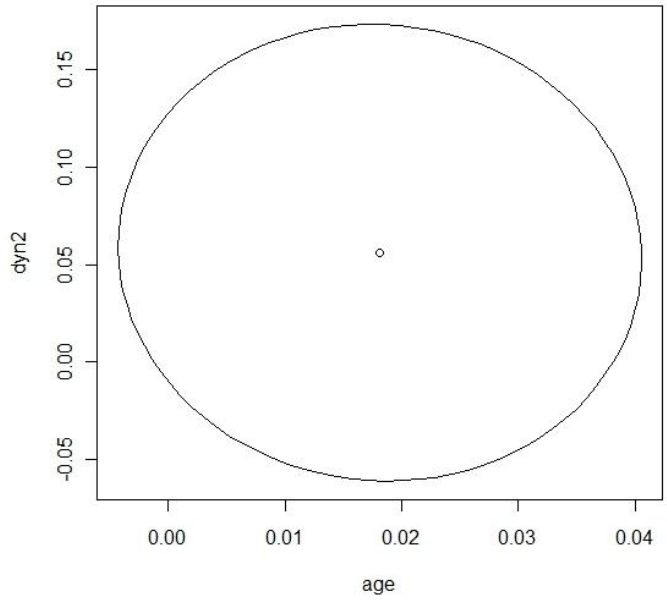

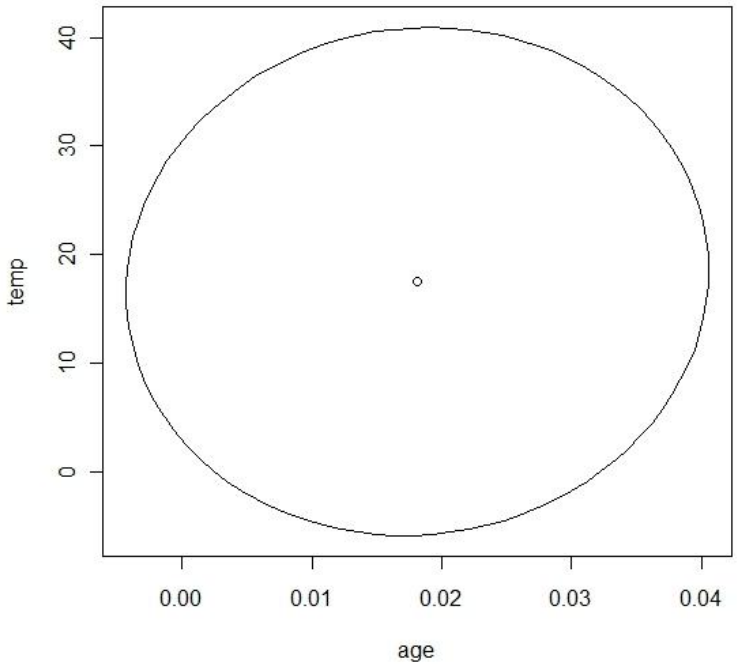
temp
40
30
20
10
0
0.00
0.01
0.02
0.03
0.04
age

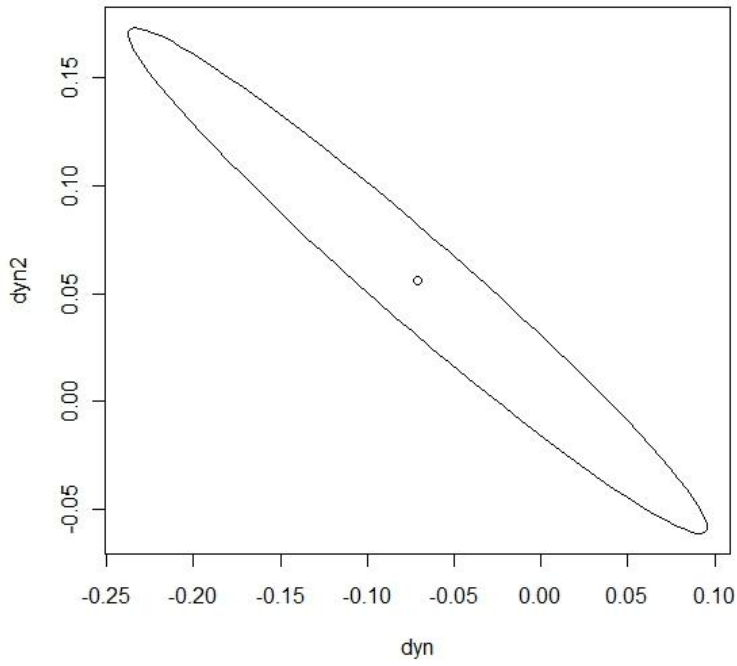
dyn2
0.15
0.10
0.05
0.00
-0.05
-0.25
-0.20
-0.15
-0.10
-0.05
0.00
0.05
0.10
dyn

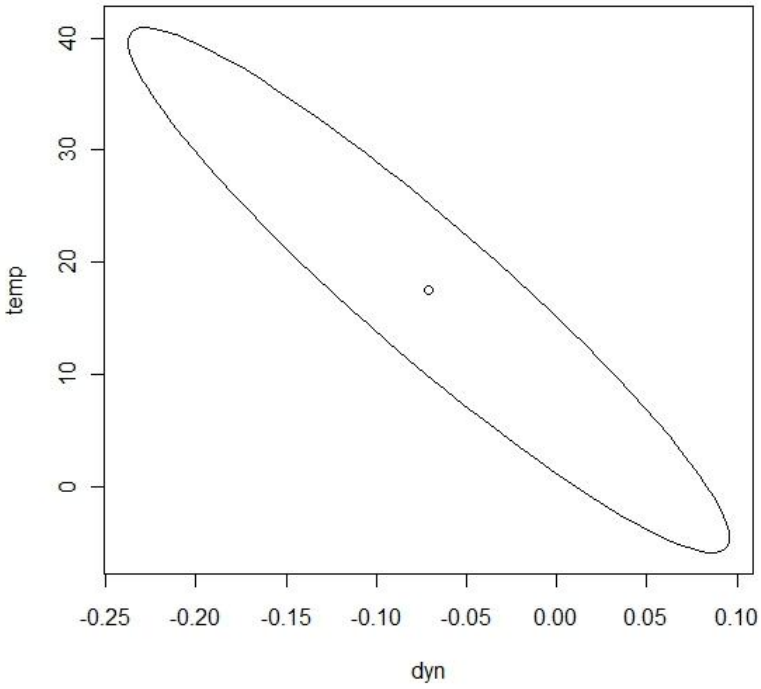
temp
40
30
20
10
0
-0.25
-0.20
-0.15
-0.10
-0.05
0.00
0.05
0.10
dyn

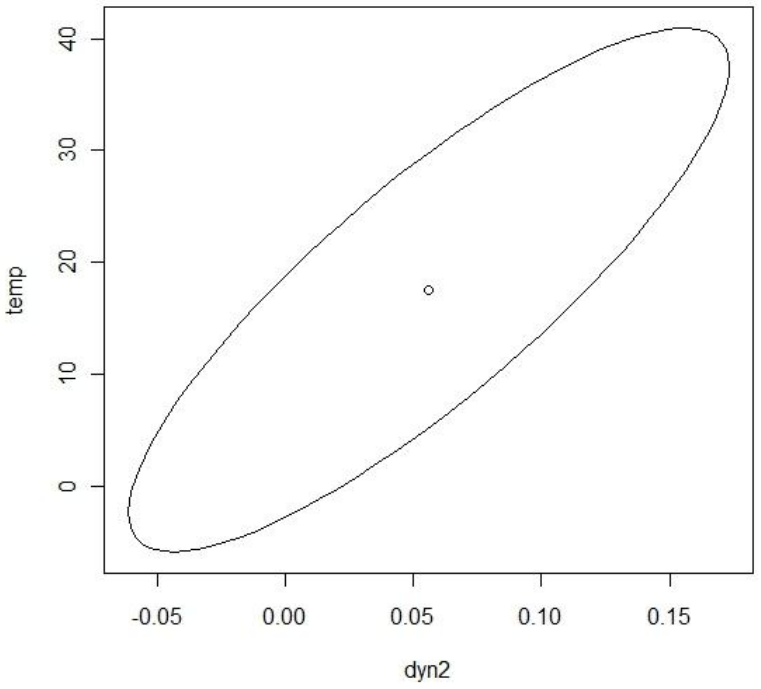
temp
40
30
20
10
0
-0.05
0.00
0.05
0.10
0.15
dyn2

Joint Confidence Intervals for Conventional Pavement

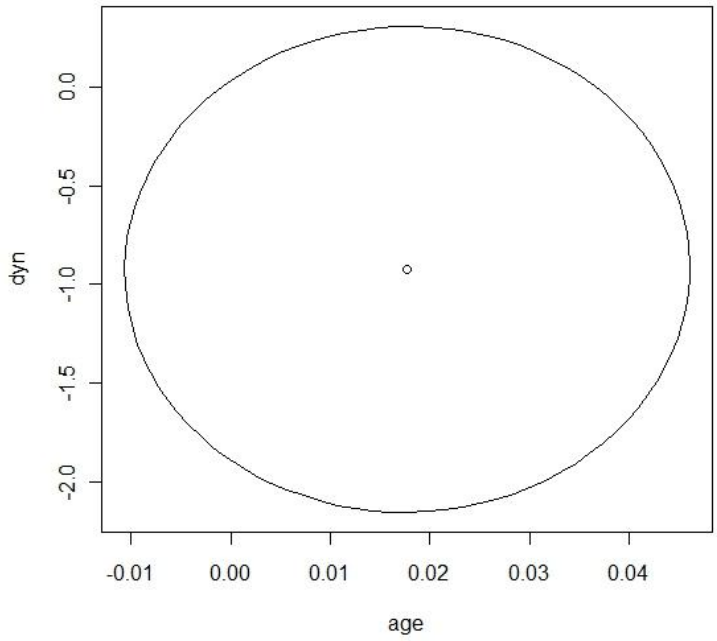

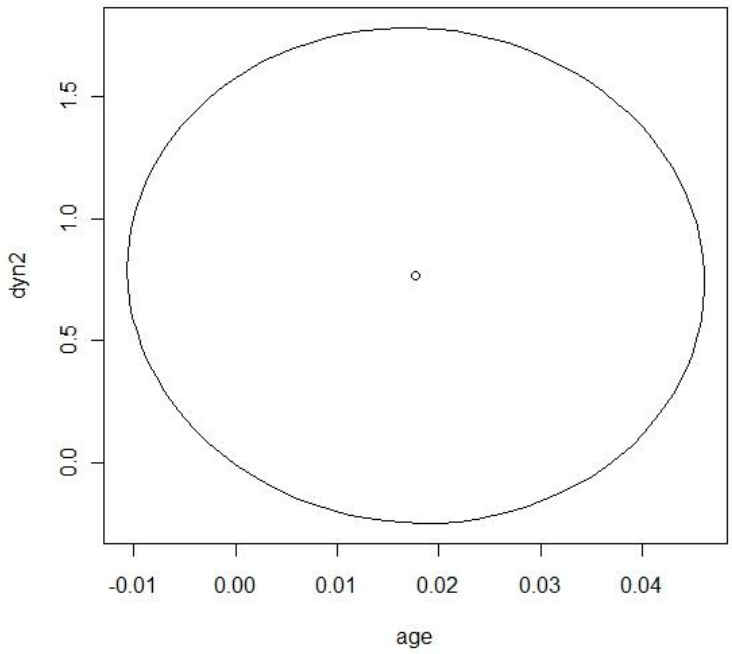

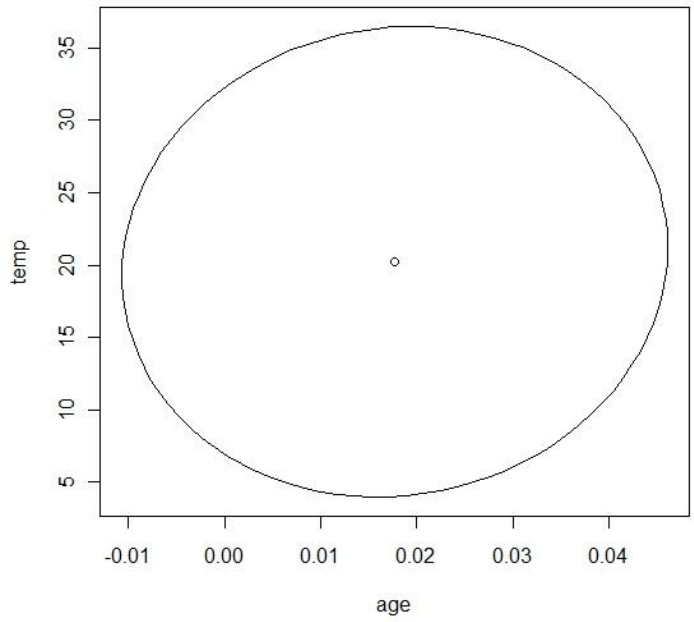
temp
35
30
25
20
15
10
5
-0.01
0.00
0.01
0.02
0.03
0.04
age

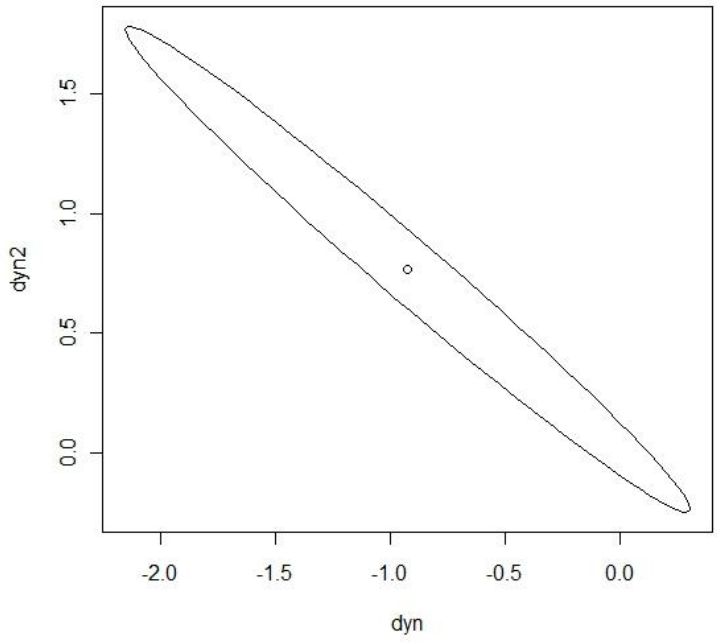
dyn2
1.5
1.0
0.5
0.0
-2.0
-1.5
-1.0
-0.5
0.0
dyn

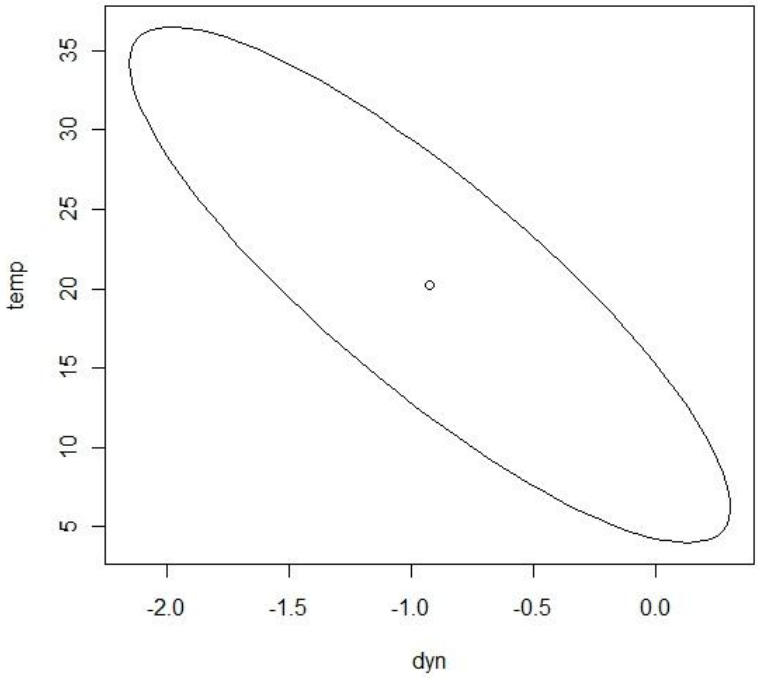
temp
35
30
25
20
15
10
5
-2.0
-1.5
-1.0
-0.5
0.0
dyn

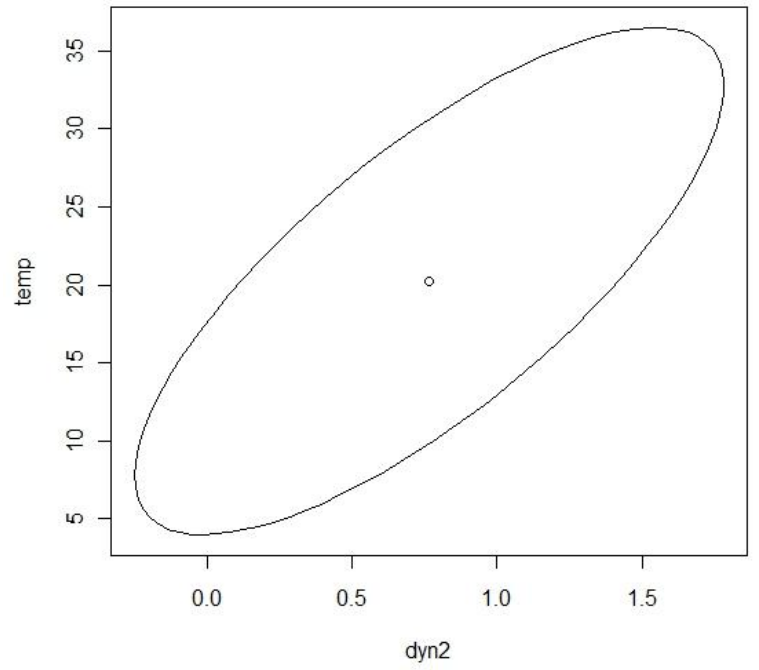
temp
35
30
25
20
15
10
5
0.0
0.5
1.0
1.5
dyn2

Joint Confidence Intervals for Both Perpetual Pavement Model

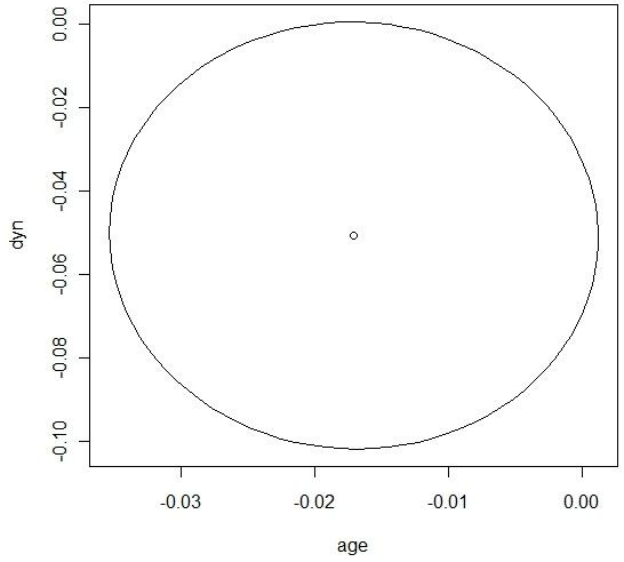

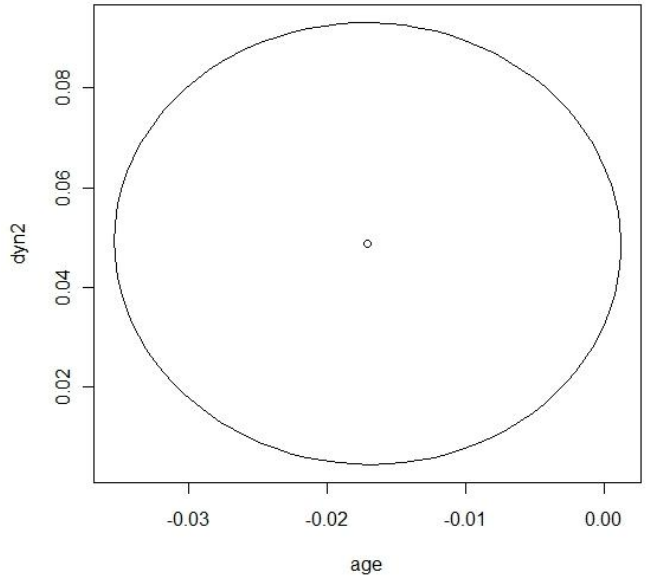

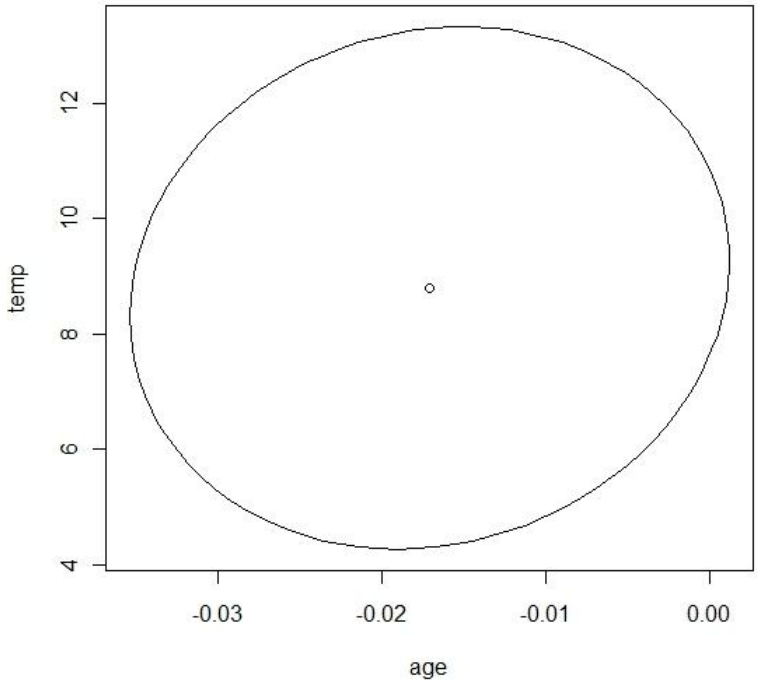
temp
12
10
8
6
4
-0.03
-0.02
-0.01
0.00
age

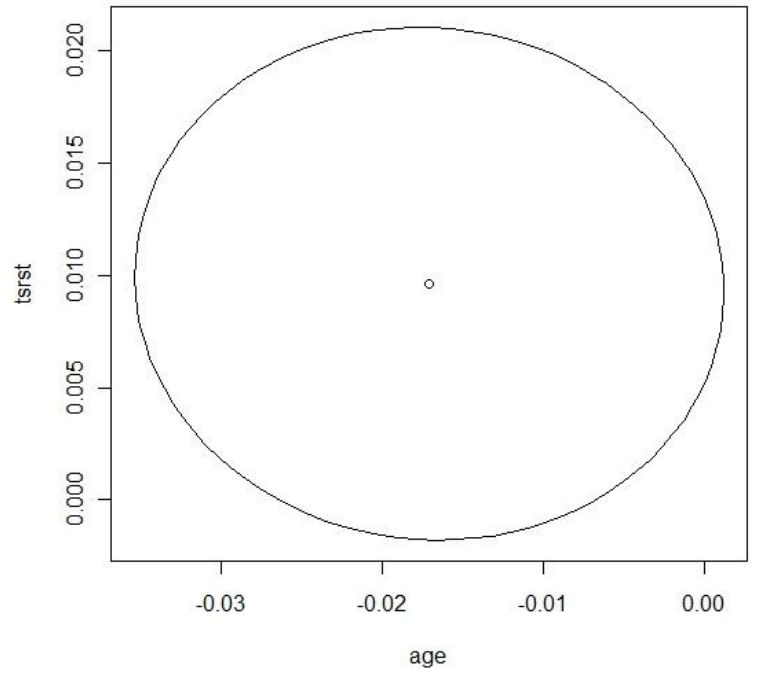
tsrst
0.020
0.015
0.010
0.005
0.000
-0.03
-0.02
-0.01
0.00
age

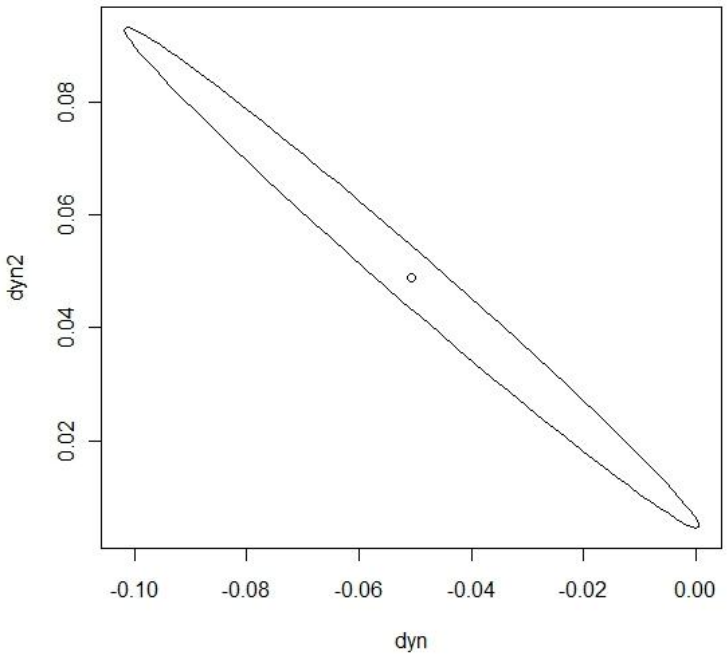
dyn2
0.02
0.04
0.06
0.08
-0.10
-0.08
-0.06
-0.04
-0.02
0.00
dyn

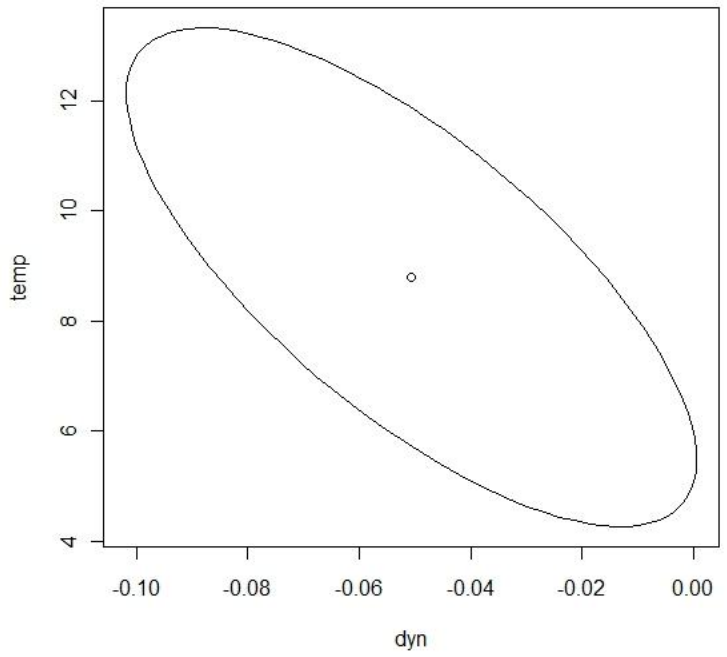
temp
4
6
8
10
12
-0.10
-0.08
-0.06
-0.04
-0.02
0.00
dyn

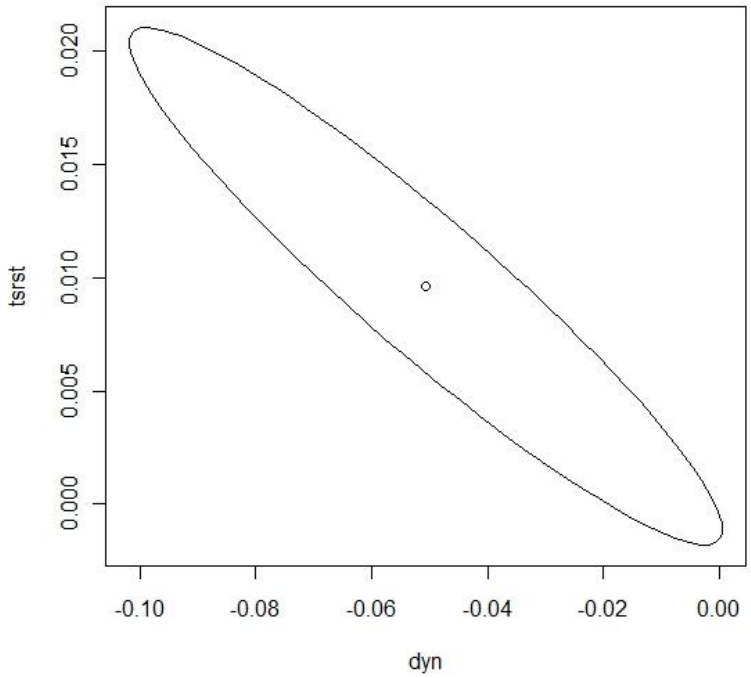
tsrst
0.000
0.005
0.010
0.015
0.020
-0.10
-0.08
-0.06
-0.04
-0.02
0.00
dyn

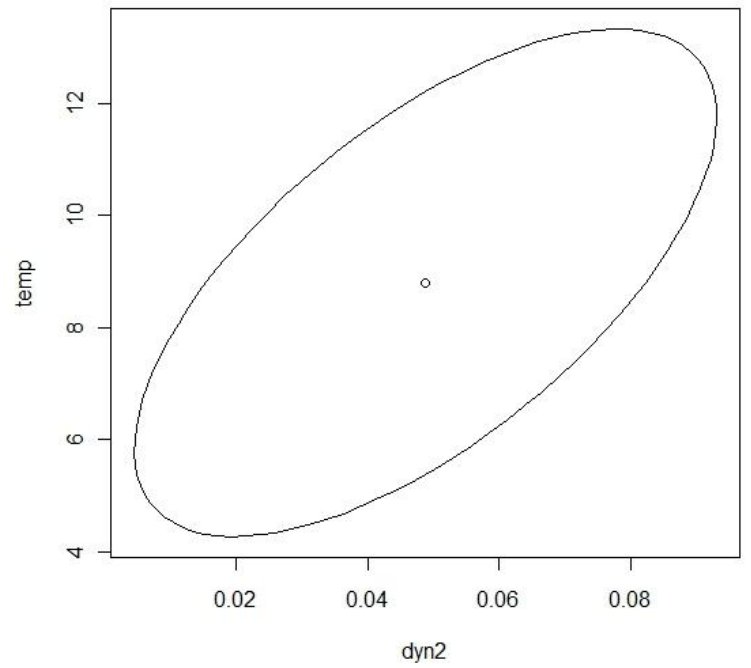
temp
4
6
8
10
12
0.02
0.04
0.06
0.08
dyn2

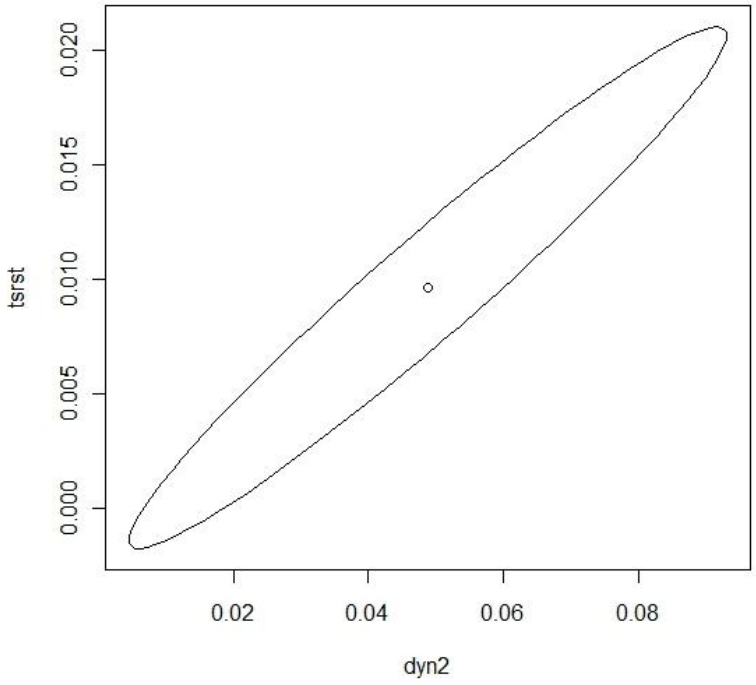
tsrst
0.000
0.005
0.010
0.015
0.020
0.02
0.04
0.06
0.08
dyn2

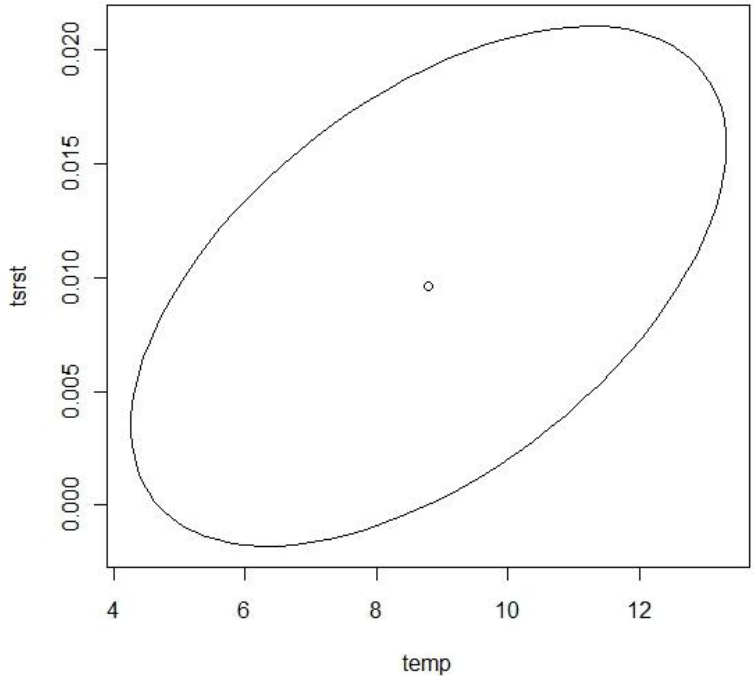
tsrst
0.000
0.005
0.010
0.015
0.020
4
6
8
10
12
temp